Phylogenetic relationships of fossil and Recent opsariichthines (Pisces, Cypriniformes, Cyprinidae)

化石および現生ハス類（コイ科）の系統関係

February 2014

Shinya	MIYATA
宮田	真也

Phylogenetic relationships of fossil and Recent opsariichthines (Pisces, Cypriniformes, Cyprinidae)

化石および現生ハス類（コイ科）の系統関係

February 2014

Waseda University

Graduate School of Creative Science and Engineering
Major in Earth Sciences, Resources and Environmental Engineering
Research on paleontology

Shinya	MIYATA
宮田	真也

Contents

Abstract

In Chapter 1, the osteology and phylogeny of Recent opsariichthines, which are the endemic cyprind fishes of East Asia, are presented. The osteological characters within Recent opsariichthines are systematically described in detail and illustrated five genera nine species selected in this study are as follows: *Zacco platypus* (Temminck and Schlegel, 1846), *Nipponocypris temminckii* (Temminck and Schlegel, 1846), *N. sieboldii* (Temminck and Schlegel, 1846), *N. koreanus* (Kim, Oh and Hosoya, 2005), *Parazacco spilurus* (Günther, 1868), *Candidia barbatu*s (Regan, 1908), *Opsariichthys uncirostris* (Temminck et Schlegel, 1846), *O. bidens* Günther, 1873, and *O. evolans* (Jordan and Evermann, 1902). The phylogenetic interrelationship within opsariichthines based on morphology is discussed in this chapter. Results and discussions are presented as follows: the opsariichthines divaricates off three clades, *Parazacco*, *Zacco* + *Opsariichthys*, and *Candidia* +*Nipponocypri*s; the genus *Prazacco* is the most basal group within opsariichthines, and the sister group of the other opsariichthines; the genus *Nipponocypris* is not assigned to *Candidia*, and is distinguished from the genus *Candidia* by evidence of phylogenetic characterizations; and *Opsariichthys* forms the paraphyletic group, because the morphological characters of *O. evolans* converges with *Zacco*. It reflects that the feeding habits of *O. evolans* is closely similar to *Zacco*.

In Chapter 2, fossils of "*Zacco*" collected from the Middle Pleistocene Nogami Formation, Oita Prefecture, Northern Kyushu, Japan, which have been recognized as *Zacco* cf. *Z. temminckii*, are systematically described. In addition, the fossil specimens are examined by cladistic analysis with Recent opsariichthines, and discussed phylogenetic relationships between fossil and Recent opsariichthines. Results suggest that the genus "*Zacco*" from the Nogami Formation can be assigned to the genus *Nipponocypris* and regarded as the first fossil record of the genus. It indicates that divergence time of *N. koreanus*s is earlier than the Middle Pleistocene, and the genus *Nipponocypris* appeared in East Asia by Middle Pleistocne at the latest.

In Chapter 3, a biogeographic analysis of opsariichthines fishes is examined, and the origin and distribution of *Nipponocypris temminckii* are discussed based on the results of the previous Chapters. Its results suggest that *N. temminckii* expanded the distribution between the Korean peninsula and Japanese Islands when Korean peninsula and Japanese Islands ware connected by a land bridge, and the genus *Nipponocypris* has been endemic to Japan and Korea at least since Middle Pleistocene time. Finally, the results and discussions in this thesis are summarized, and future prospects are presented.

Key words: Cyprinidae, opsariichthines, *Nipponocypris*, osteology, phylogeny, Kyushu, East Asia, Nogami Formation, Middle Pleistocene, land bridge.

Chapter 1: Osteology and phylogeny of Recent opsariichthines (Cyprinidae)

Introduction

The Recent Cyprinidae is the most diversified and species-rich freshwater fish family, occurring in North America (northern Canada to southern Mexico), Eurasia, and Africa. About 210 genera and about 2420 species in this family are known (Nelson, 2006). Among them, about 1200 species are known from Asia (Bănărescu and Coad, 1991; Rainboth, 1991), and therefore, we can recognize that Asia is the most diversified area of cyprinid fishes.

The opsariichthine group (Chen, 1982) is the one of the common Asian endemic cyprinid fishes. The group dwells in China, Vietnam, Korea, eastern Russia, Taiwan Island, and Japan, and consists of following five genera: *Zacco* Jordan and Evermann, 1902, *Opsariichthys* Bleeker, 1863, *Parazacco* Chen, 1982, *Candidia* Jordan and Richardson, 1909, and *Nipponocypris* Chen et al., 2008, which is treated as *Zacco* by Chen (1982) and other ichthyologists (see, Chen et al., 2008).

Meanwhile, the fossils of opsariichthines are known from China and Japan. For example, *Zacco honggangensis* Li and Wang, 1981 occurs in the Buxin Formation (Eocene), China (Wang et al., 1981); *Zacco* sp. is known from Ishikawa prefecture, Japan, probably derived from the Eozen Formation (Miocene); and *Z. temminckii* or *Z.* cf. *Z. temminckii* are known from the Nogami Formation (Middle Pleistocene), Oita prefecture has been reported.

After these discoveries, studies of taxonomy or molecular phylogeny of Recent opsariichthines have been remarkably increased (e.g. Chen et al., 2008; Hosoya et al., 2003; Kim et al., 2006; Tang et al., 2010, 2013a, b).

Hosoya et al. (2003) demonstrated that Japanese "*Zacco*" *temminckii* and divided into two species, "*Zacco*" *temminckii* and "*Zacco*" *sieboldii*, based on the detailed diagnostic characters such as the number of the anal fin rays, the coloration of the anterior margin of the pectoral and the pelvic fins, and the number of lateral line scales. As the same way, Kim et al (2006) divided "*Zacco*" *temminckii* of southern Korea into two species, "*Zacco*" *temminckii* and "*Zacco*" *koreanus* based on the color of the upper margin of the eyes and the anterorateral part of the body, and the number of scales above the lateral line to the dorsal fin origin. Moreover, Chen et al. (2008) suggested that *Zacco platypus* was closely related the genus *Opsariichthys*, and "*Z.*" *sieboldii*, "*Z.*" *temminckii* and "*Z.*" *koreanus*, froming the monophyletic group and closer to the genera

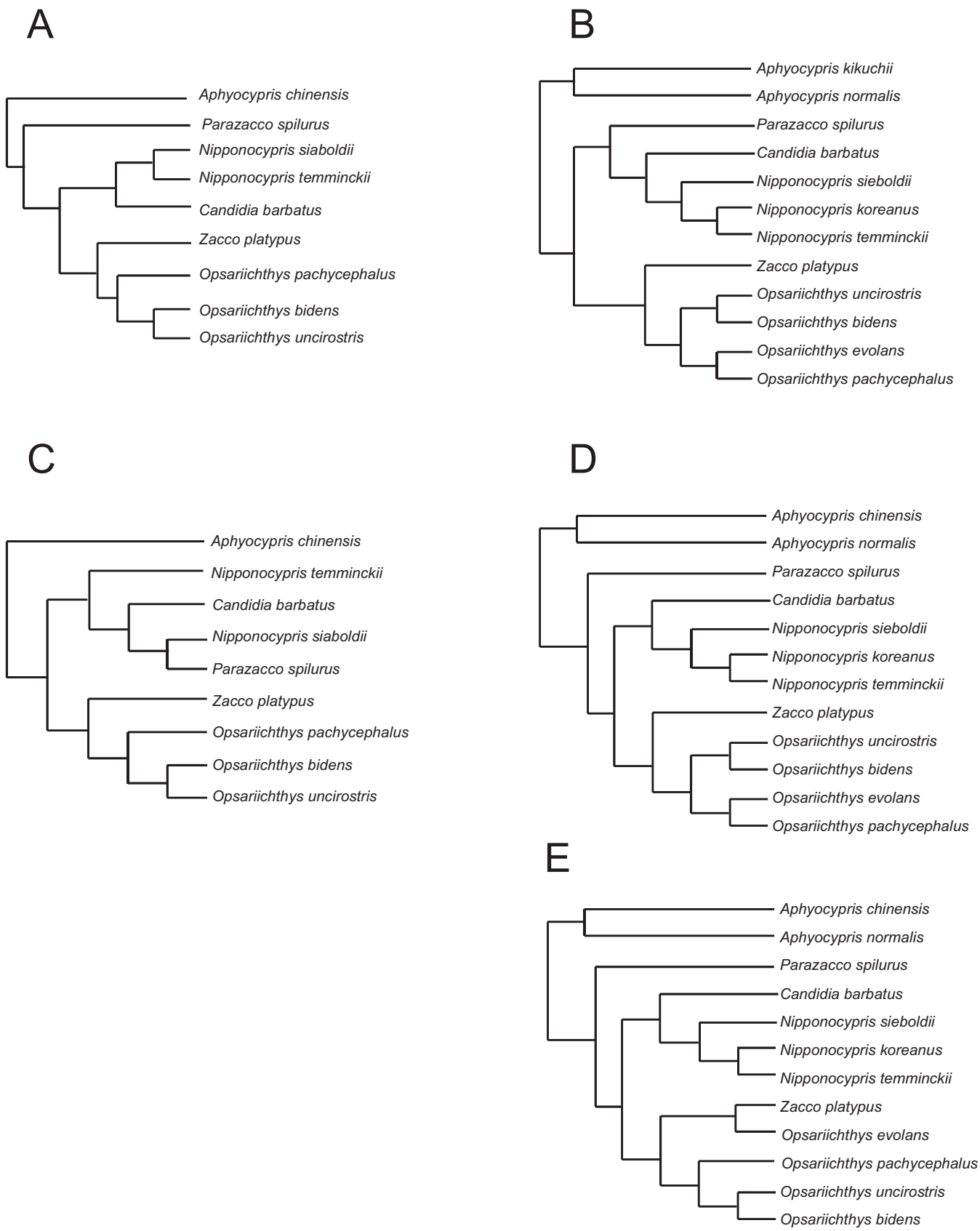

Fig. 1. Previously published opsariichthines phylogenies based on molecular data. (A) Phylogenetic tree based on mtDNA cytochrome b (cyt b) sequence (modified from Wang et al., 2007). (B) Phylogenetic tree of based on complete mtDNA D-roop sequence (modified from Chen et al., 2008). (C and D) Phylogenetic tree based on cyt b, cytochrome c oxidase (COI) I, 3 of recombination activating gene 1 (RAG 1) and rhodopsin (rh) sequence (C: modified from Tang et al,. 2010; D: modified from Tang et al., 2013b). E: Phylogenetic tree based on morphology in the present study.

Candidia and *Parazacco* than *Z. platypus*. In other words, the genus *Zacco* is a paraphyletic group. Thus, Chen et al. (2008) advocated the new genus *Nipponocypris* for "*Z.*" *sieboldii*, "*Z.*" *temminckii* and "*Z.*" *koreanus*. As the result of molecular phylogenetic study of Tang et al (2010), *Candidia*, *Parazacco* and *Nipponocypris* are polyphyletic, but low bootstrap support. In Tang et al. (2013a, b), the genus *Opsariichthys* and *Nipponocypris* form a monophyletic group, and the genus *Parazacco* is the basal taxon for opsariichthines.

However, the evidence of the morphological phylogenetic characterization of opsariichthines has not been clarified. In addition, it is necessary to study or revise the taxonomy about the fossil taxa in opsariichthine group, because the study about Recent opsariichthines are increased rapidly as mentioned above recently.

The osteology of Recent opsariichthines has been little examined, although osteological data is necessary to study for fossil taxa. There are few examples, Hows (1980, 1982) described some osteological characters of *O. bidens* and *Z. platypus*, and compared with *Luciosoma*, *Barilius* and *Engraulicypris*. Asiwa and Hosoya (1998) described *O. pachycephalus* Günther, 1868 and discussed systematic relationship for this species. The other species of Recent opsariichthines are examined fragmentally, or there is no osteological study.

The osteological study of Recent opsariichthines is necessary to understand the phylogenetic relationships of fossil and Recent species in this group. Here, in this Chapter, osteology of nine opsariichthine species are described and illustrated and cladistic analysis of ten species including previous study carried out.

Material and Method

Taxa selection

The specimens used in the present study are deposited at Kitakyushu Museum of Natural History and Human History (KMNH).

The following nine species in five genera of opsariichthines fishes are selected to this study:

Zacco platypus (Temminck and Schlegel, 1846), (Oita Prefecture, Japan, KMNH VR 100,128, SL 104.0 mm ; KMNH VR 100,129, SL 101.0 mm ; KMNH VR 100,130, SL 91.0 mm).

Nipponocypris temminckii (Temminck and Schlegel, 1846), (Oita Prefecture, Japan, KMNH VR 100, 134, SL 103.2 mm ; KMNH VR 100,135, SL 101.4 mm; KMNH VR

100,136，SL 80.7 mm).

Nipponocypris sieboldii (Temminck and Schlegel, 1846) , (Okayama, Japan，KMNH VR 100,138，SL 92.7 mm; KMNH VR 100,139，SL 90.8 mm; KMNH VR 100,140，SL 100.9 mm).

Nipponocypris koreanus (Kim, Oh and Hosoya, 2005)，(Korea，KMNH VR 100,141，SL 84.1 mm ; KMNH VR 100,142，SL 87.4 mm; KMNH VR 100,143，SL 101.0 mm, KMNH VR 100,144，SL 95.0 mm).

Parazacco spilurus (Günther，1868), (Guangdong，China, KMNH VR 100,145，SL 79.5mm ; KMNH VR 100,146，SL 87.7 mm; KMNH VR 100,147，SL 107.0mm).

*Candidia barbatu*s (Regan, 1908)，(Kaohsiung, Taiwan，KMNH VR 100, 131，SL 84.9 mm; KMNH VR 100, 132，SL 91.6 mm; KMNH VR 100, 133, SL 88.3 mm) .

Opsariichthys uncirostris (Temminck et Schlegel, 1846) , (Siga, Japan, KMNH VR 100, 148, SL 204.7mm; KMNH VR 100, 149, SL 196.0 mm; KMNH VR 100, 150, SL 191.8 mm) .

Opsariichthys bidens Günther，1873 (China，KMNH VR 100, 151，SL 102 mm; KMNH VR 100, 152，SL 79.5 mm).

Opsariichthys evolans (Jordan and Evermann，1902) (Taiwan，KMNH VR 100, 155，SL 73.7 mm; KMNH VR 100, 156，SL 86.5 mm; KMNH VR 100, 157，SL 70.1 mm).

Preparation

The examined specimens were cleared and double - stained using the methods described by Kawamura and Hosoya (1991) with slight modifications. The cleared and stained specimens were dissected following the method by Ridewood (1905) and taken photos by Nikon Digital Camera. Each part of the skeleton was drawn on the photo using a graphics tablet-screen hybrid and a personal computer with observation of the specimen under a microscope.

Osteological Terminology.

Names of skull bones and the anterior part of vertebrae follow Britz and Conway (2009), Chen et al. (1984), Dahdul et al. (2010), Harrington (1955) and Uyeno and Sakamoto (2005) , and caudal bones follow Fujita (1999).

Cladistic analysis

A cladistic analysis of the data matrix of Appendix 1 (summarized in Table 1) was carried out using PAUP* (v. 4.0 Beta, Windows Swofford 2003), Mesquite (v. 2.75

Windows, Maddison and Maddison, 2011) and MS – Excel. The characters of the number 5–9, 20, 27–28, 30, 32, and 35–36 are from Dai and Yang (2003), characters of the number 31 and 32 are Dai et al. (2005), and character of number 39 are from Cavender and Coburan (1991). The osteological characters of *O. pachycephalus* Günther, 1868 are from Asiwa and Hosoya (1998) and the examination of additional specimens (KMNH VR 100, 153, SL 102.0 mm; KMNH VR 100, 154, SL 110.0 mm).

. The number of vertebrae and an external morphological data are from Hosoya et al. (2003), Kim et al. (2006), and Chen et al. (1998, 2008, 2009, 2011). The characters were optimized to the tree using the ACCTRAN option.

Osteological description of opsariichthines

Neurocranium (Plate1 – 1 – Plate 2 – 9)

The neurocranium is grouped into four regions as follows: ethmoid region (olfactory region of Harrington, 1955); orbital region; otic region; and occipital region (e.g. Harringron, 1955)

Ethmoid region: The region occupy anterior part of neurocranium and is composed of prevomer, preethmoid, supuraethmoid, ethmoid, kinethmoid and lateral ethmoid.

The **prevomer**, viewed in its entirety only from below, is a horizontal, thin, flat and platelike bone underlying the ethmoid, and suturing with the anterior end of the parasphenoid ventrally. The anterior margin is concave, and connects to preethmoids on its anterolateral sides.

The **preethmoid** is a pair of small and rounded bone. It is laying anterior end of ethmoid region.

The **ethmoid** lies on medially at the anterior area of ethmoid region. It contact with preethmoids anteriorly, with prevomer ventrally, with supuraethmoid dorsally, and with lateral ethmoid posteriorly.

The **supuraethmoid** is a quadrilateral, thin, flat, horizontal, and plate like bone and its anterior margin is concave. The posterior margin of this bone is connected with the anterior ends of the frontals.

The **kinethmoid** is a small median bone that lies between the processes of premaxila.

The **lateral ethmoid** forms the anterior margin of the orbit. The ventral part is thickened which contacts with the endopterygoid, and anteroventral region laterally contacts with the first infraorbital.

Orbital region: Orbital region is composeed of frontal, pterosphenoid, orbitsphenoid

and parasphenoid.

The frontal is a paired, broad and plate-like bone, and it forms the roof of the neurocranium anterodorsally. The pair of bones connects with each other by suture. There is a supuraorbital canal. The anterior ends of the frontals connect with the posterior part of the supuraethmoid. The posterolateral sides connect with the pterotic and autosphenotic. The posterior ends connect with the parietals by suture. , The lateral margin (orbital margin) of the frontal is convex in *O. uncirostris* and *O. bidens*, has a notch in *N. temminckii*, and is smooth in other species .

The **pterosphenoid** is paired bone, which elongates laterally. It connects with each other at the anteromedially and with the autosphenotic and prootic posteriorly, and the frontal dorsally.

The **orbitsphenoid** lies anterior to the pterosphenoids. The dorsal part expands laterally. The ventral part, interorbital septum is thin and plane, it connects with the parasphenoid.

The **parasphenoid** forms the dorsomedial part of the oral cavity. Its long and thin shaped, and extends to the basioccipital. At the posterior part of the orbital cavity, the parasphenoid wing is developed dorsolaterally and connects with the prootic. In only the genus *Opsariichthys*, there is a groove at the ventral side of the parasphenoid.

Otic region: The otic region is composed of the parietal, autosphenotics, prootics, pterotics, epiotics, and intercalar.

The **autosphenotic** lies on the anterodorsal area of the otic region. There is a projection on its anterolateral face, which is directed ventrally. It contacts with the pterosphenoid and the frontal dorsally, and with the prootic ventrally.

The **parietal** forms the dorsoanterior part of the otic region. It's a paired bone and connects each other by sutures. In only *O. uncirostris*, the posterior margin concaves arc like shaped anteriolly. There is a lateral line canal and its lateral side connects with the lateral line of the posttemporal. The lateral line canals of parietals contact each other in *C. barabatus*, do not connect each other and its length is shorter than the half of the width of the parietal in *Z. platypus*, and do not contact other and its length is longer than the half of the width of the parietal in the other species. The posterior margins of parietals connect with the anterior margin of epiotics and the supuraoccipital by sutures.

The **prootics** lies ventral to the autosphenotic. The trigemino–facialis chamber presents at the anterior part of the prootic. Its lateral side is short column shaped, and possesses foramen for the trigeminal nerve and foramen for the facial nerve. The posterior parts of the prootics connect with exoccipital dorsally, and with basioccipital ventrally.

The **pterotics** forms the dorsolateral sides of the otic region. The lateral line sensory canal runs through its posterior end. The pterotic spine is developed ventrally at the posterolateral part of the pterotic. The pterotic is anteriorly in contact with the frontal, anteroventrally with the autosphenotic, and posteriorly with the exoccipital and epiotic.

The **epiotic** is a pair bone and lies on the posterodorsal part of otic region. It articulates with the supuratemporal and the pterotic ventrolaterally, and with the exoccipital posteroventrally.

The **intercalar** is a small, thin and plate element. In *Zacco* and *Opsariichthys*, there is the projection at the posterior end, and in the other species, there is no projection. The intercalar connects with the pterotic and exoccipital.

Occipital region: The region occupies the posterior part of the neurocranium and consists of the supraoccipital, exoccipital and basioccipital.

The **supraoccipital** forms the postero–medial end of the cranial roof. The supraoccipital is characterized by having the dorsoposterior extension of the supraoccipital crest. Its anterior edge is overlapped by the pair of parietal. The lateral sides contact with the pair of epiotic, and the ventral side contact with the pair of exocipital.

A pair of **exoccipital** is located at the posterior center of the occipital region. The foramen magnum (fm) is located just below the supraoccipital crest. The exoccipital exhibits a large foramen on its lateral surface.

The **basioccipital** is located at the posteroventral portion of the neurocranium. It articulates with the first centrum at the articulation facet for the first centrum. On the ventral part of the basioccipital elongates psteriorly. Its middle part project ovoid in shape laterally.

Sensory canal bones (Plate1 – 1 – Plate 3 – 9)

Sensory canal bones consist of nasal, infraorbitals, supraorbital, and supratemporal (posttemporal with fused lateral extrascapular of Harrington, 1955).

The **nasal** is a pair of tube – shaped bones, but in *N. sieboldii*, it is triangular. It situated at the anterior part of frontals.

The **supraorbita**l is a pair of thin and elongate bone, and forms the dorsal margin of the orbit. The medial margin of the supraorbital turns downward in *Z. platypus* and *O. evolans*, is strongly convexed in *O. uncirostris* and *O. bidens*, is slightly convexed in *N. temminckii*,, and, is long, ovoid shaped, and smoothly sweeping in the other species.

The **infraorbitals** are a thin and flat plate bones forming the ventral margin of the orbit, and are composed of five bones. The first infraorbital (lachrymal) is a pentagonal

bone having the straight infraorbital canal with two or three pores. The posterior margin of the first infraorbital is stolongly concaved in the genus *Opsariichthys* excluding *O. evolans*, is snicked in the genus *Parazacco*, and is slightly sweeping or smooth in the other species .

The second infraorbital is elongated and rectangular in almost species., It shape is wide and flat in *O. uncirostris* and *O. bidens*, the anterior half of the second infraorbital is gradually narrow from its anterior end to its posterior end in *Z. platypus* and *O. pachycephalis*, and is remains almost as wide as its posterior half in the other specie.

The third infraorbital is flat, elongated and rectangular in shape, and is almost as wide as the fourth infraorbital. In *O. uncirostris* and *O. bidens*, the third infraorbital is a wide plate.

The width of the fourth infraorbital is the almost same width the third infraorbital in *Parazacco* and all species of *Nipponocypris*, and it is abruptly widened below its middle point in all species of *Opsariichthys*, and it is gradually widened from its anterior end to its posterior end in *Z. platypus* and *Candidia*. The posterodorsal margin of the fourth infraorbital is U – shaped in *N. sieboldii*, *N. koreanus*, and *O. pachycephalus*, and L – shaped in *Z. platypus*, *N. temminckii*, and *Candidia barbatus*, and straight in the other species.

The fifth infraorbital is the smallest bone in the infraorbital series. It is almost quadrangular in *Candidia*, *Parazacco* and all species of *Nipponocypris*, is tubular in *O. uncirostris*, *O. bidens*, and *O. evolans*, and is tubular or triangular in *O. pachychephalus* and *Z. platypus*. There is a projection at the posterior or antiror margin of them in *Parazacco* and all species of *Nipponocypris* In *Candidia*, the fifth infraorbital is wide plate.

The **supratemporal** is the tube – shaped and very small bone, and located on the posterodorsal corner of the otic region of the neurocranium. The bone connects with the temporal canal of the pterotic and the supratemporal canal of the parietal.

Jaw bones (Plate4 – 1 – Plate 5 – 9)

Jaw bones are composed of following elements: premaxilla, maxilla, dentary, anguloarticular and retroarticular.

The **premaxilla** is located in the anterior part of the upper jaw and forms the upper rim of the gape. Anteriorly, it expands dorsoventrally to form a prominent ascending process. The anterior edge of ascending process of *O. uncirostri*s and *O. bidens* is grooved, and is smooth in the others. The anteroventral margin of the premaxilla is rounded in *P.*

spilurus, and is strongly convex ventrally in *O. uncirostris* and *O. bidens*.

The **maxilla** is located in the posterior part of the upper jaw and not forms the upper rim of the gape. The anterior part forms the articulation with three processes protruding in various directions: the neurocranial condyle (nc) dorsally, premaxillary wing (pmw) medially, and palatinal wing (plw) laterally. The neurocranial condyle is situated at the dorsal part of the articulation. The neurocranial condyle is bulbous in *Parazacco*, *Z. platypus* and *O. evolans*, oosphere shaped in *Nipponocypris*, and rounded tetragonal in *O. uncirostris*, *Opsariichthys bidens*.

Between the premaxillary wing and the palatinal wing, the anterior part of the premaxilla is wedged. The premaxillary wing is rounded triangular shape in *Z. platypus*, *O. evolans*, and almost tongue - shaped in other species. The palatinal wing is elongated tongue – shaped in *O. uncirostris* and *O. bidens,* and rounded triangular shape in other species. The post dorsal process on the maxilla is trapezoidal shaped in *Parazacco* and *Candidia*, triangular in *Z. platypus*, *O. evolans* and all species of *Nipponocypris* , and linearly – extended *O. pachycephalus*, *O. uncirostris* and *bidens*.

The posterior end of the maxilla is a quadrilateral plate and connects with the posterior end of the premaxilla.

The **dentary** forms the lower rim of the gape. In *Z. platypus* and *O. evolans* the dorsal margin of dentary turns downward and in other species, it is straight or slightly curved ventrally. The anterior end of the dentary is constricted in *Parazacco*, *Z. platypus*, *O. pachycephalus* and *O. evolans*., hooked in *O. uncirostris* and *O. bidens*, and not constricted and not hooked in *Candidia*, and all species of *Nipponocypris*. On lateral side along the ventral margin, there is a perforated bony tubule enclosing the mandibular lateral-line canal. There are two pores laterally opened in *Z. platypus* and *O. evolans*. there are three to four pores laterally opened in *O. pachycephalus* and *N. sieboldii*,. In *O. bidens*, *O. pachychelus*, *Candidia* ,and *Parazacco*, the pores are almost ventrally opened, there are two pores in *Candidia*,and three pores in the others. In *N. temminckii* and *O. uncirostris* pores postoroventrally opened, and there are three pores in *N. temminckii* and three are four pores in *O. uncirostris*. The posterior part of dentary sends dorsally a flat, broad, ascending process. The posterior margin of ascending process contacts with the anterior margin of anguloarticular in *O*. uncirostris and *O. bidens*.

The anguloarticular is almost allow shaped, and the anterior half is inserted in the dentary fossa. In internal side the meckelian cartilage lies down and extends anteriorly into the dentary fossa. In posterior part, the saddle-like suspensorial articulation facet (sat), which connects with quadrate presents on the dorsoposterior facet area of the bone.

The **retroarticular** is the smallest bone in the jaws, located at the posteroventral corner of the lower jaw, and attached to the ventral part of the anguloarticular.

Opercular Bones (Plate6 – 1 – Plate 7 – 9)

Opercular bones are composed of opercle, subopercle, preopercle, and interopercle.

The **opercle** is a thin, plate – like and trapezoid bone that articulates with the hyomandibular at the suspensorium articulation socket (sas) anteriorly. The dorsal margin is concave and ventral margin is convex. The posterior marigin of the opercle is convex or straight in *Z. platypus* and,the genus *Opsariichthys*, and concave in *Parazacco*, *Candidia* and the genus *Nipponocypris*. The opeculer canal is present on the anterodorsal part of the opercle in *N. temminckii*, and *N. koreanus*, but it is absent in other species.

The **subopercle** is the most interior bone in the opercular series. It gradually narrows to a point behind, and a knife like shaped. The anterodorsal corner of subopercle projects anterodorsally.

The **preopercle** is L – shaped with the preopercular – mandibular laterosensory canal in the bony tube. It underlies the posterior end of quadrate. Preopercle overlies the hind the ends of symplectic, the interhyal, the upper lateral surface of the interopercle the lower posterolateral surface of the hyomandibular, and the anterior edge of the opercle.

The **interopercle** is a knife-like shaped bone and has the incurved upper edge. It is in turn overlapped anterolaterally by the preopercle

Suspensorium (Plate6 – 1 – Plate 7 – 9)

The suspensorium is composed of autopalatine, endopterygoid, ectopterygoid, metapterygoid, quadrate, symplectic, and hyomandibular. The metapterygoid, quadrate, and symplectic make the quadrate – pterygoid fenestra (qpf) (Greenwood et al., 1966).

The **autopalatine** is situated at the anteriormost part of the suspensorium and continues posteriorly to the ectopterygoid. The anterior end of autopalatine is trifurcate. The lateral arm of the triforaction articulates with the lateral surface of articulation of the maxilla. The dorsal and interior arms receive to the lateral surface of the preethmoid.

The **endopterygoid** is a thin bone. The anterior part is saddle – shaped and thickened, and articulated to the posterior end of the autopalatine.

The ectopterygoid is a thin and membraneous bone.

The **metapterygoid** is a thin and plate like bone with sturts on the central region. It is H-shaped and its posterior and ventral margins are strongly concaved in the genus *Opsariichthys* exclude *O. evolans*, and is almost quadrilateral and the posterior margin of

metapterygoid is slightly concave in all the other species. The ventral margin of the metapterigoid is slightly concave in *Z. platypus*, *O. evolans* and the genus *Nipponocypris*, and slightly convex in *Candidia* and *Parazacco*.

The **quadrate** is a fanlike bone situated at the anteroventral corner of the suspensorium, and articulates with the angular by the articulation facet for mandibule (fmd). The dorsal part of the quadrate strongly projects posterodorsally. The dorsal-medial surface of the quadrate is a strong U – shaped, and upper arm of them is slightly constricted and the same in length of the lower arm in *O. uncirostris* and *O. bidens*. In the other species the dorsal – medial surface of them is a L shaped or weakly U – shaped.

The **symplectic** is a rod-shaped bone and fits in the groove on the dorso-mesial surface of the posterior projection of the quadrate. The symplectic does not contact with the ventral margin of the metapterygoid.

The **hyomandibular** is situated at the postero-dorsal part of the suspensorium, and is divided into three portions: the articulation head, the arm rim, and the flange zone. The articulation head is the dorsal part of the bone, that has three condyles: the anterior condyle of hyomandibular for neurocranium (acn); the posterior condyle of hyomandibular for neurocranium (pen); and the posteriormost opercular condyle (oc). The anterior and posterior condyles of hyomandibular for neurocranium articulate with the lateral otic region of the neurocranium. The opercular condyle articulates with the suspensorium articulation socket of the opercle.

Branchial arch (Plate8 – 1 – Plate 8 – 9)

The branchial arch is composed of the basihyal, basibranchial, hypobranchial, ceratobranchial, epibranchial, and infrapharyngobranchial (pharyngobranchial of Harrington, 1955).

The **basihyal** is a slender bone and located at the anterior most in the branchial arch. The basihyal is curved ventraly. The posterior end connects with the anterior basibranchial.

There are three **basibranchials**. These are thin and cylindrical shaped. The first basibranchial is the shortest in the three. The second and third basibranchials are similar in length and about twice as long as the first one.

There are three pairs of the **hypobranchials** adjacent respectively to the first to the third basibranchials. The first and second hypobranchials are small bony fragment shaped and the third one is thin arched .

There are five pairs of the **ceratobranchials**. The ceratobranchials are rod – like bones,

and the longest in the branchial arche elements. These decrease slightly in length and width posteriorly. The first to third ceratobranchials articulate anteriorly with hypobranchials, but the fourth ceratobranchial does not articulate anteriorly with hypobranchials. The fifth ceratobranchials (pharyngeal bones) are crescent shape with pharyngeal teeth. The dental formula is three row 2.3.4 – 4.3.2 in *Z. platypus*, 1.4.5 – 4.4.1 in *O. evolans*, 2.4.4 – 4.4.2 in *O. uncirostris*, 1.4.5 – 5.4.1 or 0 in *O. bidens*, 1.4.4 – 4.1.1 in *C. barbatus*, 2.4.5 – 5.4.2 in *N. temminckii*, 2.3.4 – 4.3.2 in *N. sieboldii*, 2.4.4 – 4.4.2 in *N. koreanus* and two row 3.5 – 5.3 in *P. spilurus*. The anterior branch of the pharyngeal bone is longer than its posterior branch in *O. uncirostris* and *O. bidens*, but it is almost the same as the posterior branch in the other species.

There are four **epibranchials**, and decrease in size posteriorly. The ceratobranchials articulate anteriorly with ceratobranchials. The lavatory process presents at the middle part of the third and the fourth epibranchials

There are two pairs of **infrapharyngobranchials**. The infrapharyngobranchials are rounded trapezoidal shape and small bone.

Hyoid Arch

The hyoid arch is composed of hypohyal, anterior ceratohyal (ceratohyal of Harrington, 1955), posterior ceratohyal (epihyal of Harrington, 1955), interhyal, branchiostegal, and urohyal.

The **hypohyal** is located at the anteriormost part of the hyoid arch, and composed of the lower hypohyal (ventral hypohyal of Britz and Conway, 2009) and the upper hypohyal (dorsal hypohyal of Britz and Conway, 2009). The lower hypohyal is a thick V-shaped bone. Its ventral limb articulates with the upper hypohyal, and its dorsal limb articulates with the ceratohyal. The upper hypohyal is a curved subcylindrical bone, and smaller than the lower hypohyal. The anterior end of the upper hypohyal is articulated with the lower hypohyal, and the posterior ends of these are articulated with the anterior ceratohyal.

The **anterior ceratohyal** is very broad lateroposteriorly, and thick at the dorsal part. In the anterior end of the anterior ceratohyal terminates in two heads, and the fenstra on the ceratohyal (fch) is opened. The dorsal head articulates with the upper hypohyal and the ventral head articulates with the lower hypohyal. The insection of the ventral margin at the anterior part of the anterior ceratohyal is articulated with the anterior end of the first branchiostegal. In the posterior end, the anterior ceratohyal connects with the posterior ceratohyal.

The **posterior ceratohyal** is a rounded and trianguloid bone. The dorsal part of the posterior ceratohyal is thick. The posterior end articulates with the interhyal on the articulation facet for the interhyal.

The **interhyal** is the smallest in the hyoid arch. The interhyal is a long and thin bone in *O. uncirostris* and *O. bidens*, and a short column bone in other species.

Three **branchiostegal** rays of similar length and thickness are present. These branchiostegal rays are boomerang or arch shaped bones. The anteriormost one articulates on the insection of the ventral margin at the anterior part of the anterior ceratohyal. The middle one attaches to the external surface of the posteroventral corner of the anterior ccratohyal. The posteriormost one attaches to the external surface of the anteroventral corner of the posterior ceratohyal.

The **urohyal** is located under the medial line of the branchial archs. It is ventrally flanged with a dorsally directed wing-like thin process extending along the midline of the bone. The anterior end of the urohyal divides dichotomously and attaches to the lower hypohyals. The wing-like process of the posterior margin of the urohyal is snicked at the ventral part in *P. spilurus*, *Z. platypus* and *O. evolans*, smoothness in *C. barbatus* and the genus *Nipponocypris*. The ventral franged part of the urohyal is comparatively narrow in *O. uncirostris* and *O. bidens*.

Vertebrae (Plate12 – 1 – Plate 12 – 9)

Vertebrae are composed of abdominal vertebrae and caudal vertebrae, and total number is than 41. There are 22 abdominal vertebrae + 19 caudal vertebrae in *Z. platypus*, 19 + 22 in *O. evolans*, 23 + 21 in *O. uncirostris*, 21 + 20 in *O. bidens*, 21 + 22 in *P. spilurus*, 22 + 19 in *C. barbatus*, 21 + 23 in *N. temminckii*, 21 + 21 *N. sieboldii*, and 23 + 21 in *N. koreanus*. The first vertebra articulates with the articuration facet for the first centrum of the basioccipital. Each abdominal vertebra bears a paire of **parapophyses**, which attaches near the ventral part of each centrum. The first to fourth parapophyses are deformed for elements of Weberian osicles. The parapophyses which posterior to the fourth one is short and nub, and articulate with the rib laterally. The last three parapophyses are fused with each other.

The rib is arch shaped, and thickened at the lateral margin. The medial side is wide, and ventral end is spireing. It articulates with posterior to the forth parapophyses exclusive of last three parapophyses. The last three ribs are intermuscular bones like shaped, and not articulate with the parapophysis.

The **Weberian ossicles** consist of specialized the first to the fourth abdominal vertebrae

and associated elements (parapophysis, supuraneurals, neural arch and spine, and ribs, claustrum, intercalarium, scaphium, tripus, and os suspensorium).

The **claustrum** is the pair of bone that sits anterior edge of the second supraneural and the medial side of the scaphium.

The **intercalarium** is small and curved bone, and posterior end is spireing. Its element elongates to the upper part of the neural arch 3.

The **scaphium** is rhomboid-shaped bone with the projection. Its projection spires posterodorsally, and elongates to the boundary between the supraneural 2 bone and the third neural arch.

The **tripus** is sickle-shaped bone, which posteriormost tip curves medially, and elongates to the under the fifth centrum. Its anterior end attaches to the centrum 3. The dorsal face of tripus exhibits Y-shaped runnel.

The **fourth parapophysis** is fused with the fourth rib, and branched. The tip of the dorsal branch is blunt, but it is tipped in *Parazacco*. The medial branch, the **os suspensorium** spires and contacts with the one.

The **second supraneural** is rounded and trapezoidal shaped. Its dorsal margin is concave.

The **third supraneural** is comb shaped at the dorsal margin. In *N. sieboldii*, its anterodorsal margin is projected anteriorly. .

The **third neural arch** is comb-shaped. There is a fenestra laterally at the middle part. Their dorsal margins is triangular shape, and connects with the supuraneural 2 bone anterodorsally, with the supuraneural 3 bone posterodorsally, and the fourth neural arch posteriolly.

The **fourth neural arch** is about half the length of the fifth one. It connects with the supuraneural 2 bone and the neural arch at the anterior part.

The **first parapophysis** is shorter than the second one. The first and second parapophyses extend laterally, and theirs head is spireing.

Caudal fin skeleton (Plate13 – 1 – Plate 13 – 9)

The caudal fin skeleton is composed of following six elements: preuralcentrum, pleurostyle, epural, uroneural, hypural, and parhypural.

The **first ural vertebra (u1)** is fused with the first preural centrum (pu1). There is the **neural spine of preural centrum 1**, which is short, wide, and spires. The second and third neural spines of preural centra are long and thin spines with the wing, which are projected at the lower part in *N. sieboldii*, the wing of the neural spine of the preural

centrum 2 and 3 do not extend over the middle of the neural spine of the preural centrum, or reach to the middle in *P. spilurus*. The wing of second neural spines of preural centrum do not extend over the middle of the neural spine of the preural centrum, or reach to the middle, but the wing of the third one extends over the middle of the neural spine of the preural centrum in *C. barbatus*. In the other species, the second and third neural spines of preural centra extends over the middle of the neural spine of the preural centrum.

A pair of first **uroneurals** is fused with the first ural vertebra and the first preural centrum, and makes the pleurostyle.

A pair of second uroneurals is long and thin. These locate at about the upper part of the pleurostyle.

The **epural** is the rod like bone, which is located between pleurostyle and the neural spine of the second preural centrum.

There are six **hypurals**. The first to third hypurals are almost the same length. The fourth to sixth hypurals are inserted into the pleurostyle, and become progressively shorter. The first hypural is about three times wider than the second one in *Z. platypus*, *O. uncirostris*, *C. barbatus*, and *N. sieboldii*, and about twice wider than the second one in the other species. The second hypural is fused with the first ural vertebra and the first preural centrum. The width of the second hypural is almost same as the third one. The third hypural articulates with the first ural vertebra and the first preural centrum at the anterior part. The fourth hypural is wide and the same width as the first one. The fifth and sixth hypurals are short, thin, and rod like bones. The sixth hypural is the smallest in the hypural series.

The **perhypural** is fused with the first hypural, and articulated with the fused hypural 1 + 2. There is the hypurapophysis at the base of perhypural.

The haemal spine of preural centrum 2 is articulated (not fused) with the second ural vertebra. The all the rest haemal spines of preural centra are fused with centrum.

Intermuscular Bones (Plate14 – 1 – Plate 14 – 9)

The intermuscular bones are composed of epipleural, epineural, and supraneural bones.

The **epipleural** lies the posteriormost of the rib series to the neural spine of the preural centrum 4 or 5. The some elements are long and thin bones at the anterior section, are three-pronged at the periphery of anal fin base, and are not branched at the posterior section.

The **epineural** lies between rearward of the cranium and the neural spine of the preural

centrum 4 or 5. It is a long, thin, and three-pronged elements. These branches elongates to anteriorly, posteriorly, and medially. The elements at the posterior section divides dichotomously.

There are a plates or needle-shaped **supraneurals** at between the Weberian apparatus and the first proximal pterigiophores of the dorsal fin. These elements do not contact with each other, and located at between each neural spines. The first one (the fourth supraneurals) is a plate and quadrangle like in the genus *Nipponocypris*, *Candidia*, *Opsariichthys*, and *Zacco*. The anterior margin of the fourth supraneural is snicked in *P. spilurus*,. In posterior supuraneurals decrease slightly in length and width posteriorly., There are 8 supuraneurals in the genus *Nipponocypris*, 5 – 6 supuraneurals in *Z. platypus*, *O. uncirostris* and *O. evolans*, 6 – 7 supuraneurals in *C. barbatus*, *O. bidens* , and 9 supuraneurals in *P. spilurus*.

Dorsal fin and its skeleton (Plate15 – 1 – Plate 15 – 9)

The dorsal fin is located in the middle of the body, with its origin posterior to the pelvic insertion. The dorsal fin base is shorter than that of the anal fin base. There are three unbranched dorsal fin rays. The first one is vestigial. The third one is extremely long, and the length is about twice the length of the second one. There are seven dorsal branched fin rays. The last one is branched for two at the anterior end.

These **fin rays** are supported by pterygiophores (proximal, median, and distal pterygiophores) and stay.

The **proximal pterigiophores** are elongated bone with wings. The first one is the large bony plate and divides dichotomously. The dorsal margin of the first proximal pterigiophore contacts with the first and the second unbranched dorsal fin rays.

The **median pterygiophores** are small and a drum like bone, and are located in between the third or later of the proximal pterigiophores and the distal pterigiophores. The last one articulates with the stay ventrally, and articulates with the distal pterygyophore dorsally.

The **distal pterygiophores** are small bone and rounded at the both ends, and wedged in the anterior end of the soft fin rays.

Anal fin and its skeleton (Plate15 – 1 – Plate 15 – 9)

The anal fin is suspended from the haemal spines of the anterior part of caudal vertebrae. Its origin is behind the posterior end of the dorsal fin base. The anal fin composed of 11 fin rays (iii, 8) in *O. bidens*. 12 fin rays (iii, 9) in *N. sieboldii*, *C. barbatus*, *Z.*

platypus, *O. evolans*, and *O. uncirostris*, 13 fin lays (iii, 10) in *N. temminckii* and *N. koreanus*, and 14 fin rays (iii, 11) in *P. spilurus*.

These **fin rays** are supported by the pterygiophores (proximal, median, and distal pterygiophores). The proximal pterigiophores is elongated bone with wings. The first proximal pterigiophore supports for the first and second anal fin rays. There are 10 proximal pterygiophores in the genus *Opsariichthys*, *Z. platypus*, *N. sieboldii*, and *C. barbatus*. 11 proximal pterygiophores in *N. temminckii* and *N. koreanus*, and 12 proximal pterygiophores in *P. spilurus*.

The **median pterygiophores** are small and a drum like bones, and are located in between the forth or later of the proximal pterigiophores and distal pterigiophores. The last one is articulated with the stay ventrally, and articulated with the distal pterygyophore dorsally

The **distal pterygiophores** are a small bones and rounded at the both ends, and wedged in the anterior end of soft fin rays.

Pectral girdle (Plate16 – 1 – Plate 16 – 9)

The pectoral girdle is composed of posttemporal, spracleithrum, cleithrum, scapula, coracoid, postcleithrum, pectral radial, and, distal radial.

The **posttemporal** is located on the upper most of the pectral girdle. The dorsal part of them spires and it articulates with the posterolateral corner of the neurocranium dorsally. The sensory canal on the posttemporal contacts with the supuratemporal and the sensory canal of the spracleithrum.

The **spracleithrum** is the thin and long bone, which located under the posttemporal. The dorsal part is a hook-like projection, which articulates dorsally with the ventral part of the posttemporal. In the posterior part, the sensory canal on the spracleithrum is present, and connects with the sensory canal on the supuratemporal at the dorsal part.

The **cleithrum** is the largest element of the pectoral girdle, and forms main portion of anterior margin of the pectral girdle. It is a L-shaped, and its ventral part is flanged. The anterodorsal margin of the lower part projects upward in *Z. platypus* and *O. evolans*, and smooth in the other species. The cleithrum articulates with the medial face of the supracleithrum dorsally, with the postcleithrum posteriorly, with the mesocoracoid medially, and with the scapula and coracoid posteroventrally.

The **scapula** is the short column element and lies between the cleithrum and the coracoid as a bridge. It has scapula foramen (sf) at its center at the lateral side of the middle part. The scapula articulates with the medial face of the cleithrum dorsally, with the

coracoid and mesocoracoid ventrally, and with the first pectoral radial posteroventrally.

The **coracoid** forms ventral portion of anterior margin of pectral girdle. The anterodorsal part, it connects with cleithrum and forms ellipsoidal fenestra. The coracoid articulates with the second pectral radial posterodorsally end, and with mesocoracoid and scapura posterodorsally.

The **mesocoracoid** is a slender cylindrical bone. The dorsal end is attached to the median face of the cleithrum, and the ventral end is attached to the scapula and the coracoid. The mesocoracoid forms a bridge between the cleithrum and the coracoid.

The **postcleithrum** is a long, thin and gradual S-shaped element, and both ends spires sharply. It attaches to the posteromedial face of the cleithrum.

There are three to four pectral radial, and these are thin element. The posterior end articulates with a small-grained **distal radial**.

Pelvic Girdle (Plate17 – 1 – Plate 17 – 9)

The pelvic fin is composed of 9 segmented fin rays with one unsegmented and short fin lay, and is located in the middle of the ventral margin of the body.

The pelvic girdle is composed of basipterygouim and three pelvic radial.

The **basipterygouim** divides dichotomously at the anterior part. There is the elongated articular process at the posterior part of them, and it articulates with companion of the basipterygouim.

The **pelvic radials** are located at the posterior end of the basipterygouim, and are wedged in the pelvic fin rays. The medial side one is coronoid shaped, and two others are sclerite shaped.

Result and discussion

The cladistic analysis using the branch–and–bound search option resulted in one parsimonious tree (length = 93, CI =0.70, RI =0.73, RC =0.51). The parsimonious tree is shown in Figure 2 with apomorphic states of each clades and bootstrap values (%) based on 1000 replicates. The character matrix is shown in Table 2.

The 14 characters following below were placed at node of the opsariichthines, which separates from its outgroup the genus *Aphyocyprs* (boot strap = 100); the width of the supraorbital is narrower than the half of the length (character number 4 [status 1]); the sensory canal on the lacrimal curved (5 [1]); the third infraorbital is almost as wide as the fourth (8 [1]); the posterodorsal margin of the fourth infraorbital bone has a nub (10

Table 1: Character list of in this study to be used for the constructing the cladogram of Recent opsariichthines.

Character No.	Character and status.	Reference	CI	RI	RC	HI
1	The sensory canals of parietals: (0) does not tangent to the edge of the other one, and its length is longer than the half the width of the parietal; (1) does not tangent to the edge of the other one, and its length is shorter than the half the width; (2) the sensory canals of the parietals contact each other		1.00	0/0	0/0	0.00
2	The posterior lateral margin of the frontal: (0) smooth; (1) convex; (2) notched.		1.00	1.00	1.00	0.00
3	The intercalar: (0) not has a projection; (1) has a projection.		0.33	0.33	0.11	0.67
4	The width of supraorbital: (0) the almost the same width as half of the length of these; (1); narrower than half of the length of these.		0.50	0.67	0.33	0.50
5	The sensory canal on the lacrimal: (0) straight; (1) curved.	Dai and Yang (2003)	1.00	1.00	1.00	0.00
6	The pores of the sensory canalon the lacrimal: (0) 2 pores; (1) 3 pores .	Dai and Yang (2003)	0.50	0.00	0.00	0.50
7	The anterior half of the second infraorbital: (0) remains as wide as its posterior half of these; (1) gradually narrows from its anterior end to its posterior end.	Dai and Yang (2003)	0.50	0.00	0.00	0.50
8	The third infraorbital: (0) significantly wider than the fourth; (1) almost as wide as the fourth.	Dai and Yang (2003)	1.00	1.00	1.00	0.00
9	The width of the fourth infraorbital (0) remains the same width or the half of the width of the fourth infraorbital; (1) abruptly widens below at its middle point; (2) gradually widens from its anterior end to its posterior end.		0.67	0.75	0.50	0.33
10	The posterodorsal margin of the fourth infraorbitals bone (0)not has a nub; (1) has a nob.		0.33	0.60	0.20	0.67
11	The posterior margin of the fourth infraorbital bone is (0) straight ; (1) L – shaped; (2) U– shaped.		0.40	0.25	0.10	0.60
12	The fifth infraorbitals bone: (0) absent; (1) approximately quadrangle; (2) approximately triangle; (3) tube shaped .		1.00	1.00	1.00	0.00
13	The width of the fifth infraorbitals bone: (0) narrower than the length of these; (1) about the same as the length of theese; (2) wider than the length of theese.		0.67	0.67	0.44	0.33
14	The fifth infraorbital bone: (0) has a projections; (1) has a projections .		0.50	0.67	0.33	0.50
15	The pores of the dentary sensory canals opedned (0) laterally; (1) ventrally; (2) posteroventrally .		0.33	0.00	0.00	0.67

Continued

Character No.	Character and status.	Reference	CI	RI	RC	HI
16	The anterior end of the dentary: (0) constricted; (1) hooked; (2) not constricted.		1.00	1.00	1.00	0.00
17	The dorsal margin of the dentary: (0) straight; (1) downward.		1.00	1.00	1.00	0.00
18	The post - dorsal process of the maxilla: (0) a trapezoidal shaped; (1)a triangular shaped; (2) dorsally – convexed or straight, and that the dorsal margin of these elongate to the posterior part.		0.67	0.80	0.53	0.33
19	The ventral margin of the premaxilla: (0) straight; (1) convex.		1.00	1.00	1.00	0.00
20	The posterior margin of the opercule: (0) concave; (1) convex or straight.	Dai and Yang (2003)	1.00	1.00	1.00	0.00
21	The quadrate - pterygoid fenestra: (0) absent; (1) present.		1.00	1.00	1.00	0.00
22	The metapterygoid: (0) not constricted; (1) constricted to the H-shaped.		1.00	1.00	1.00	0.00
23	The quadrate: (0) snicked to a V-shaped; (1) snicked to a L -shaped or weakly U shaped, and the upper arm of them is shorter than the lower arm ; (2) a strong U-shaped, and the upper arm is the same length of lower		1.00	1.00	1.00	0.00
24	The symplectic: (0) contacts with the ventral margin of the metapterygoid; (1) not contacts with the ventral margin of the metapterygoid.		1.00	1.00	1.00	0.00
25	The posterior margin of the urohyal: (0) smooth; (1) snicked.		0.50	0.50	0.25	0.50
26	The urohyal: (0) slender; (1) the posterior region is wider than the anterior one in the ventral view.		0.50	0.75	0.38	0.50
27	The pharyngeal tooth: (0) 2 rows; (1) 3 rows	Dai and Yang (2003)	1.00	1.00	1.00	0.00
28	The anterior branch of the pharyngeal bone: (0) as long as its posterior branch; (1) longer than its posterior branch	Dai and Yang (2003)	1.00	1.00	1.00	0.00
29	The maximum number of the vertebrae: (0) less than 40; (1) 40-43 or less; (2) more than 44		0.67	0.75	0.50	0.33
30	The end of the dorsal branch of the parapophysis of the 4th vertebra: (0) tipped; (1) blunt ; (2) shovel-shaped.	Dai and Yang (2003)	0.50	0.67	0.33	0.50

Continued

Character No.	Character and status.	Reference	CI	RI	RC	HI
31	The fouth supraneural bone: (0) convex ventrally or sigmoid; (1) snicked at the anterior margin; (2) almost quadrangular	Dai et al. (2005)	1.00	1.00	1.00	0.00
32	The maximum number of the supraneural bones: (0) more than 8; (1) 7 ; (2) 6.	Dai et al. (2005)	0.50	0.50	0.25	0.50
33	The number of the proximal pterygiophores of the anal fin: (0) 9; (1); 10; (2) 11; (3); 12.		1.00	1.00	1.00	0.00
34	The wing of the neural spine of the preural centrum 2: (0)do not extend over the middle of the neural spine of the preural centrum 2, or reach to the middle; (1)extends over the middle of the neural spine of the preural centrum 2; (2) projected at the base;(3)extends to the top of the neural spine of the preural centrum 2		0.67	0.67	0.44	0.33
35	The wing of the neural spine of the preural centrum 3: (0) do not extend over the middle of the neural spine of the preural centrum 3, or reach to the middle; (1) extends over the middle of the neural spine of the preural centrum 3 ;(3) extends to the top of the neural spine of the preural centrum 3		1.00	1.00	1.00	0.00
36	The anterodorsal margin of the cleithrum: (0) straight; (1) comvex.	Dai and Yang, (2003)	1.00	1.00	1.00	0.00
37	The maximum number of the lateral line scale: (0) less than 40; (1) 40-50 or less; (2) more than 51		0.50	0.50	0.25	0.50
38	The lateral line scales: (0) complete; (1) incomplete.		1.00	0/0	0/0	0.00
39	The maxillary barbels: (0) present; (1) absent.	Cavender and Coburn (1992)	1.00	0/0	0/0	0.00
40	The ventral keel: (0) run on the pelvic fin base to anus; (1) absent on the anterior half region from the pelvic fin base to the anus; (2) absent or indistinct.		1.00	1.00	1.00	0.00
41	The vertical stripes: (0) absent or blurred; (1) an irregular pattern and black; (2) a bandlike and black,		1.00	1.00	1.00	0.00
42	The crossband of the body: (0) absent; (1) a bandlike; (2)an irregular pattern and blue		0.67	0.67	0.44	0.33
43	The pectoral fins color: (0) transparent or lightness yellow; (1) yellow, and orange or red at the margin; (2) highly-yellow.		1.00	1.00	1.00	0.00

Table 2. Character matrix of this study, which used for constructing the cladogram of Recent opsariichthines.

	1	2	3	4	5	6	7	8	9	10	11	12	13	14	15	16	17	18	19	20	21	22
Aphyocypris normalis	0	0	0	0	0	0	0	0	0	0	0	0	0	0	0	0	0	0	0	0	0	0
Aphyocypris chinensis	0	0	1	0	0	0	0	0	0	0	0	0	0	0	0	0	0	0	0	0	0	0
Zacco platypus	1	0	0	1	1	0	1	1	2	1	1	2,3	0	0	0	0	1	1	0	1	1	0
Nipponocypris temminckii	0	1	0	1	1	0	0	1	0	1	1	1	1	1	2	2	0	1	0	0	1	0
Nipponocypris sieboldii	0	0	0	1	1	0	0	1	0	1	2	1	1	1	0	2	0	1	0	0	1	0
Nipponocypris koreanus	0	0	0	1	1	1	0	1	0	1	2	1	1	1	1	2	0	1	0	0	1	0
Candidia barbatus	2	0	0	1	1	1	0	1	2	1	1	1	2	0	1	2	0	0	0	0	1	0
Opsariichthys evolans	0	0	1	1	1	0	0	1	1	0	0	3	0	0	0	0	1	0	0	1	1	0
Opsariichthys pachycephalus	0	0	0	1	1	0	1	1	1	0	2	2, 3	0	0	0	0	0	2	0	1	1	1
Opsariichthys uncirostris	0	2	1	0	1	0	0	1	1	0	0	3	0	0	2	1	0	2	1	1	1	1
Opsariichthys bidans	0	2	1	1	1	1, 0	0	1	1	0	0	3	0	0	1	1	0	2	1	1	1	1
Parazacco spilurus	0	0	0	1	1	0	0	1	0	1	0	1	1	1	1	0	0	0	0	0	1	0

	23	24	25	26	27	28	29	30	31	32	33	34	35	36	37	38	39	40	41	42	43
Aphyocypris normalis	0	0	0	0	0	0	0	0	0	0	0	0	0	0	0	0	1	0	0	0	0
Aphyocypris chinensis	1	0	0	0	0	0	0	0	0	0	0	0	0	0	0	1	1	0	0	0	0
Zacco platypus	1	1	1	1	1	0	1	1	2	2	1	1	1	1	1	0	1	2	0	2	1
Nipponocypris temminckii	1	1	0	1	1	0	2	1	2	0	2	1	1	0	2	0	1	2	2	0	2
Nipponocypris sieboldii	1	1	0	1	1	0	1	1	2	0	1	2	2	0	2	0	1	2	2	0	1
Nipponocypris koreanus	1	1	0	1	1	0	2	1	2	0	2	1	1	0	2	0	1	2	2	0	1
Candidia barbatus	1	1	0	1	1	0	1	1	2	1	1	0	1	0	2	0	0	1	2	0	1
Opsariichthys evolans	1	1	1	1	1	0	1	0	2	2	1	1	1	1	1	0	1	2	0	1	1
Opsariichthys pachycephalus	1	1	0	0	1	0	1	1	2	1	1	1	1	0	1	0	1	2	0	1	1
Opsariichthys uncirostris	2	1	0	0	1	1	2	1	2	2	1	1	1	0	2	0	1	2	0	2	1
Opsariichthys bidans	2	1	0	0	1	1	2	1	2	1	1	1	1	0	1	0	1	2	0	1	1
Parazacco spilurus	1	1	1	1	0	0	1	0	1	0	3	0	0	0	1	0	1	0	1	0	0

[1]); the fifth infraorbital bone is approximately quadrangle (12 [1]); the width of the fifth infraorbital bone is about the same as the length (13 [1]); the pores of sensory canal of the dentary opens laterally (15 [1]); The quadrate-pterygoid fenestra is present (21 [1]); the symplectic doesn't contact with the ventral margin of the metapterygoid (24 [1]); the posterior region of the urohyal is wider than the anterior one in the ventral view (26 [1]); the maximum number of the vertebrae is more than 40 (29 [1]); the fourth supraneural bone is snicked at the anterior margin (31 [1]); there are ten anal fin proximal pterygiophores (33 [1]); and there are more than 40 lateral line scales (37 [1]). Within opsariichthines divaricates off three clades, *Parazacco*, *Zacco* + *Opsariichthys*, and *Candidia* +*Nipponocypris*.

Relationship of the genus *Parazacco*

In molecular phylogenetic studies of Wang et al. (2007) and Tang et al. (2013a, b), *Parazacco* forms a sister group of the clade of *Nipponocypris* + *Candidia* and the clade of *Zacco* and *Opsariichthys* (Fig. 1A, D). In the molecular phylogenetic trees of Chen et al. (2008), *Parazacco* forms a monophyletic group with *Candidia* and *Nipponocypris* and is located at the basal position in this clade (Fig. 1B).

In this phylogenetic study based on morphology, *Parazacco* forms a sister group of the other opsariichthines (*Zacco*, *Opsariichthys*, *Candidia*, and *Nipponocypris*) (Fig. 1E). The opsariichthines expects for *Parazacco* has eight synapomorphies as follows: the pharyngeal tooth are three rows (27 [1]); the end of the dorsal branch of the parapaphysis of the fourth vertebra is blunt (30 [1]); the fourth supraneural bone is almost quadrangular (31 [2]); the maximum number of the supraneural bones is 7 (32 [1]); the wing of the neural spine of the preural centrum 2 extends over the middle of the neural spine of the preural centrum 2 (34 [1]); the wing of the neural spine of the preural centrum 3 extends over the middle of neural spine of the preural centrum 3 (35 [1]); the ventral keel is absent or indistinct (40 [2]); and the color of pectoral fin is yellow and orange or red at the margin (43 [1]).

On the other hand, *Parazacco* does not have these synapomorphies, and has four autapomorphies as follows: the fifth infraorbitals bone has a projections (14 [1]); the posterior margin of the urohyal is snicked (25 [1]); there are 12 anal fin proximal pterygiophores (33 [3]); and the vertical stripes are irregular pattern and black (41 [1]).

Thus, the present study concludes that the genus *Prazacco* is the most basal taxa within opsariichthines, and the sister group of the other opsariichthines. Its supports Wang et al. (2007) and Tang et al. (2013a, b) based on molecular analysis.

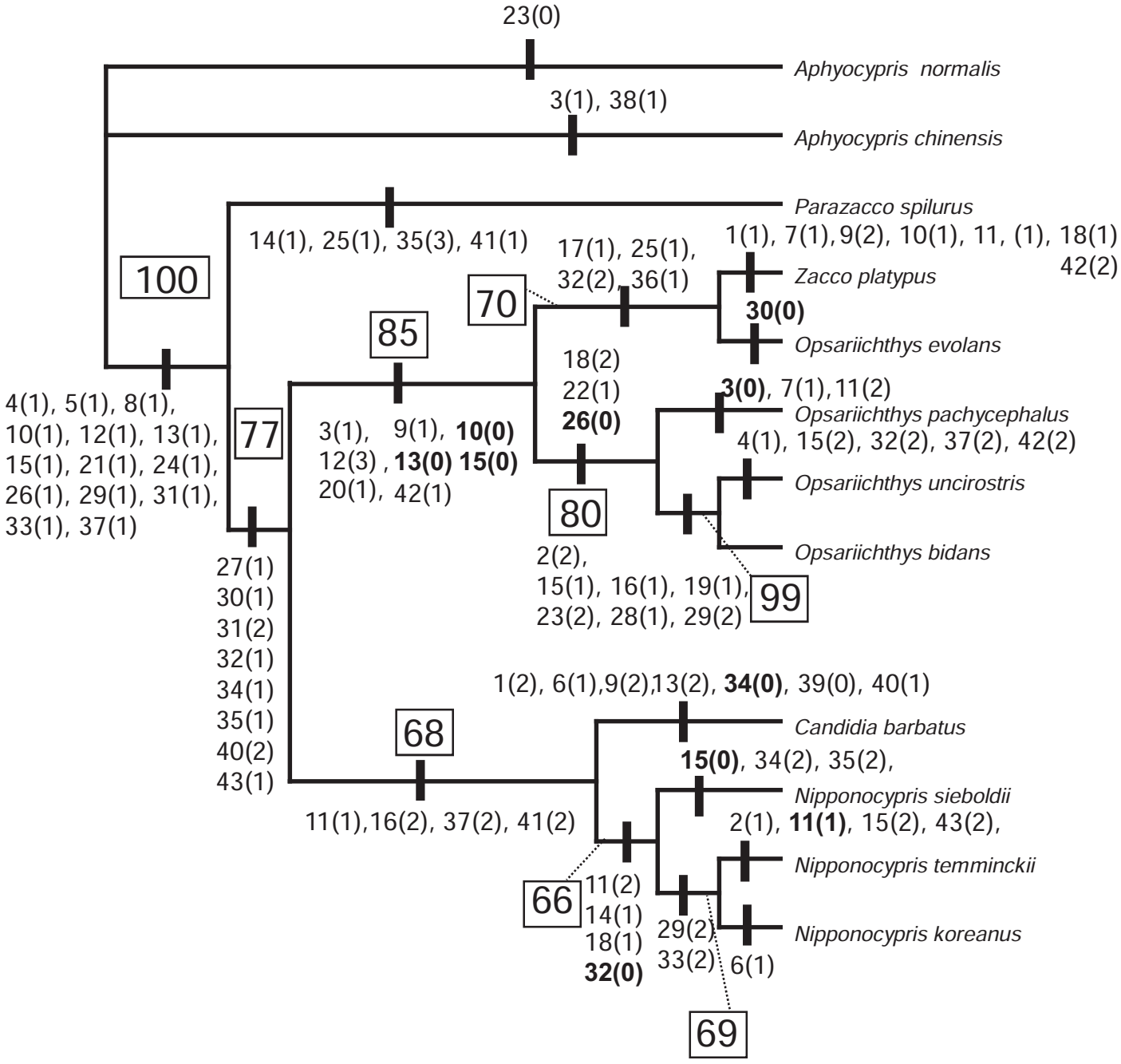

Fig.2. Cladogram of opsariichthines. Two species of *Aphyocyprs* designated as outgroup, and all 43 characters are unordered. Number of boldface represents reversed characters. Figure in box represents bootstrap values after 1000 replications.

Relationship of *Candidia* and *Nipponocypris*

The clade of the genus *Candidia* + *Nipponocypris* forms a monophyletic group supported by following combination of four characters: the posterior margin of the fourth infraorbital bone is L-shaped (11 [1]); the anterior end of dentary is not constricted (16 [2]); the maximum number of the lateral line scale is more than 51 (37 [2]); and the vertical stripes are bandlike and black (41 [2]).

The genus *Nipponocypris* forms a monophyletic group and is distinguished from the genus *Candidia* supported by combination of follows as four characters; the posterior margin of the fourth infraorbitals bone is U-shaped (11 [2]); the fifth infraorbital bone has a projection (14[1]); the post-dorsal process of the maxilla is a triangle shaped (18[1]); and the maximum number of the supraneural bones is 8 (32 [0]). The character of number 32 is reversed character.

Within the clade of the genus *Nipponocypris*, *N. sieboldii* is at the basal position in this clade, and has three autapomorphies as follows: pores of the sensory canals of the dentary are opened laterally (15 [0]); the wings of the neural spines of the preural centrum 2 and 3 are projected at the base (34[2], 35[2]). The character of number 5 is reversed character.

N. temminckii and *N. koreanus* has two synapomorphies as follows: the maximum number of the vertebrae is 43 (29 [2]); and there are 11 anal fin proximal pterygiophores (33 [2]). *N. temminckii* is distinguished from *N. koreanus* by combination of the following five characters: the posterior lateral margin of the frontal is notched (2 [1]); the posterior margin of the fourth infraorbital bone is L-shaped (11 [1]); the pore of the sensory canals of the dentary are opened posteroventrally (15 [2]); and the color of pectoral fins is highly - colored yellow (43 [2]). The characters of number 43 and 2 are unique for *N. temminckii*.

Thus, three species of the genus *Nipponocypris* form a monophyletic group, and are distinguished by these characters. This supports the previous molecular phylogenetic studies.

Wang et al. (2007) concluded that *Candidia* is the only available name for the clade of *C. barbatus*, *N. temminckii*, and *N. sieboldii*. In Hosoya (2013) suggested, *N. temminckii* and *N. sieboldii* assigned for the genus *Candidia*, in other words the genus *Nipponocypris* is synonymized for *Candidia* based on the result of molecular phylogenetic study of Chen et al. (2008), which is *Parazacco*, *Candndia*, and *Nipponocypris* form a monophyletic group. Chen et al. (2011) treated "*N. temminckii*" and "*N. sieboldii*" as the

genus *Candidia*.

As previously mentioned, in the present phylogenetic analysis based on morphology results that the genus *Nipponocypris* is distinguished from *Candidia*. In addition, the *Candidia* has seven autapomorphis as follows: the sensory canals of the parietals contact each other (1 [2]); the sense canal on the lacrimal has three pores (6 [1]); the fourth infraorbital is gradually widened from its anterior end to its posterior end (9 [2]); the width of the fifth infraorbital bone is larger than its length (13 [2]); the wing of the neural spine of the preural centrum 2 do not extend over the middle of the neural spine of the preural centrum 2, or extend to the middle (34 [0]); the maxillary barbels are present (39[0]); the ventral keel is absent on the anterior half region from the pelvic fin base to the anus (40[1]).

Thus, the present study concluded the genus *Nipponocypris* not assigned to *Candidia*, and is distinguished from the genus *Candidia* by evidence of those of characteristics of this clade .

Relationship of *Opsariichthys* and *Zacco*

The genera *Opsariichthys* and *Zacco* form a monophyletic group supported by many previous molecular studies (e.g. Wang et al. 2007; Chen et al., 2008, 2009; Fang et al., 2009; Tang et al., 2010; Tang et al ., 2013a, b).

In the present study, these two genera form a monophyletic group, which is supported by eight synapomorphies as follows: the intercalar has the projection (9 [1]); the fourth infraorbital abruptly widens below its middle point (9 [1]); The posterodorsal margin of the fourth infraorbitals does not have a nub (10 [0]); the fifth infraorbital bone forms a tube shaped (12 [3]); The width of fifth infraorbital bone is slender than the length of them (13 [0]); The pores of the sensory canals of the dentary are opened laterally (15 [0]); the posterior margin of the opercular is convex (20 [1]); and the crossband of the body is a band-like (42 [1]). The characters of number 10, 13, and 15 are reversed characters. This clade divides to two groups *Zacco* + *O. evolans* clade and *O. pachycephalus* + *O. uncirostris* + *O. bidens*, and it suggested the genus *Opsariichthys* forms a paraphyletic group.

The phylogenetic relationships of the genus *Opsariichthys* and *Zacco* based on molecular phylogenetic analysis has been discussed in some previous studies (e.g. Chen et al., 2008; Tang et al., 2013b). Their studies demonstrated the genus *Opsariichthys* forms a monophyletic group, and the closer relationship of *O. evolans* being closer to *O. pachycephalus* than the genus *Zacco*.

Fig. 3

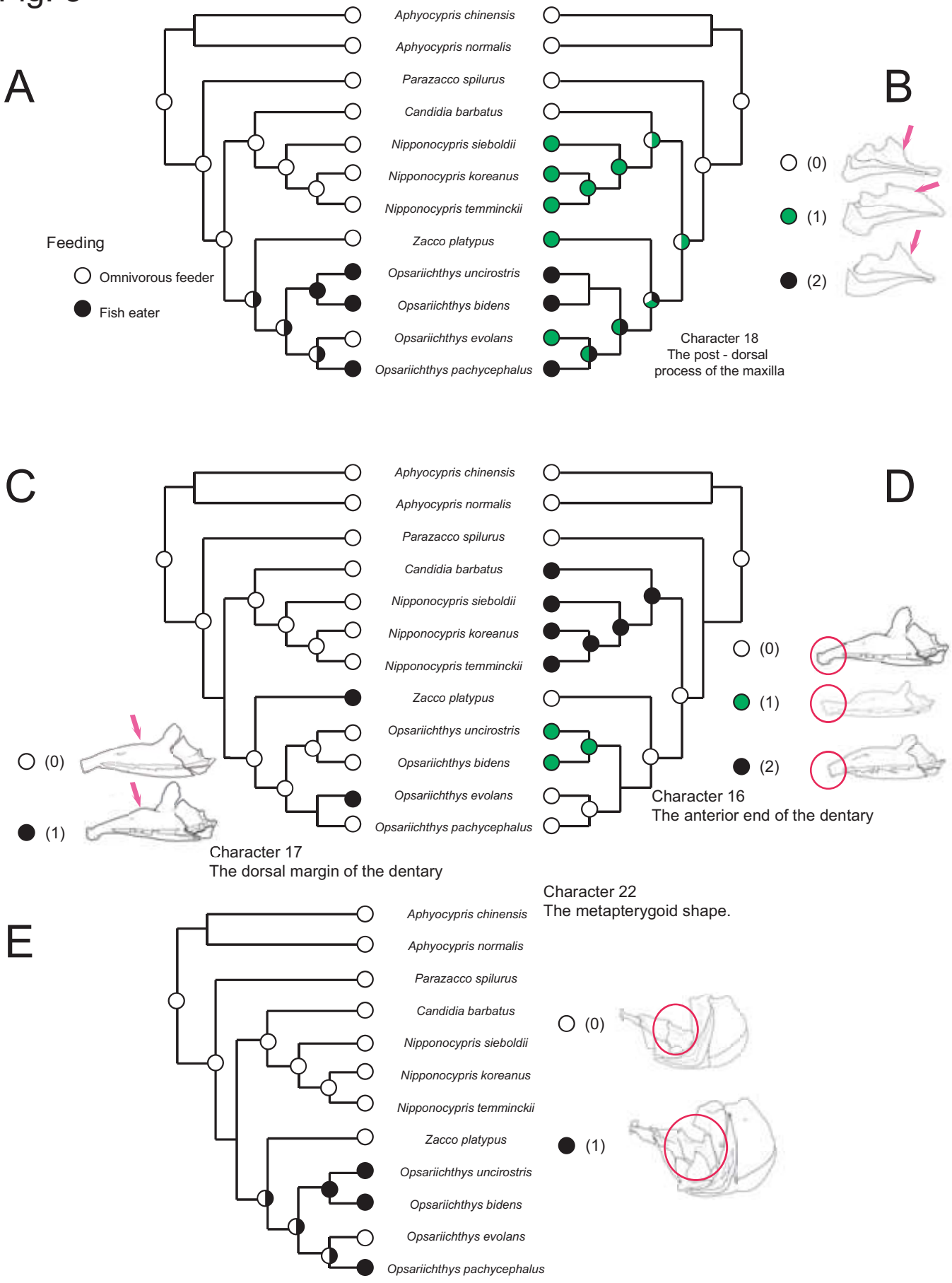

Fig.3. The feeding habits and the feeding characters trait evolution within opsariichthines. The phylogenetic tree from Tang et al. (2013b). The datas of the feeding habits are based on Chen and Chang (2005), Hosoya (2013), and Morimune et al. (2003). A: Feeding habits; B: Character 18, the shape of the post - dorsal process of the maxilla; C: Character 17, the dorsal margin of the dentary; D: Character 16, the anterior end of the dentary; E: Character 22, the shape of the

In the present study, based on morphological data, the clade of *O. pachycephalus* + *O. uncirostris* + *O. bidens* has three synapomorphies: the post-dorsal process of the maxilla is dorsally-convexed or straight, and that the dorsal margin elongates to the posterior part (18 [2]); the metapterygoid constricts to H-shaped (22 [1]); and the urohyal is slender in the ventral view (26 [0]). The character of number 26 is reversed character.

Z. platypus + *O. evolans* forms a monophyletic group supported by four synapomorphies as follows: the dorsal margin of the dentary is downloaded (17 [1]); the posterior margin of the urohyal is snicked (25 [1]); the maximum number of the supraneural bones is 6 (32 [2]); and the anterodorsal margin of the cleithrum is convex (36 [1]). *O. evolans* does not have synapomorphies of the other species of *Opsariichthys*.

Thus, the present morophological phylogenetic study suggests the closer relationship of *O. evolans* with the genus *Zacco* than the other species of the genus *Opsariichthys*. In the molecular phylogenetic analysis of Chen et al. (2008) and Tang et al. (2013b), *O. evolans* has closer relationships with *O. pachychpharus* than *Zacco*, and the genus *Opsariichthys* forms a monophyletic group.

The feeding habit of the genus *Opsariichthys* expect *O. evolans* is carnivorous, especially yet adult one is fish-eater (e.g. Hosoya, 2013; Morimune 2003). *O. evolans*, and fishes of the genus *Parazacco*, *Zacco*, *Candidia*, and *Nipponocypris* are omnivorous (Chen and Chang, 2005; Hosoya, 2013; Morimune, 2003).

The oral region is the one of the part, which associated with the feeding behavior (e.g. Sibbing, 1991). Here, in this study, traced the evolution of the feeding habitat and the jaws and metapterygoid characters on the phylogenetic tree, using the parsimony algorithm implemented in Mesquite Version2.73. The tree based on the molecular phylogenetic tree of Tang et al. (2013b) is similar to the present study (Fig. 3), because the following discussion avoids for begging the question by the present phylogenetic study.

In the post dorsal process of the maxilla, trapezoidal or triangle shaped type (*Zacco*, *Nipponocypris*, *Candidia*, *Parazacco*, and *O. evolans*) is omnivorous behavior. Dorsally-convexed or straight, and the dorsal margin elongating to posterior part type (*O. uncirostris*, *O. bidens*, and *O. pachycephalus*) are fish eating behavior (fig. 3B).

The downward the dorsal margin of the dentary type are only *Zacco* and *O. evolans*. This two species are regarded as a herbivory-omnivorous habit species by previous studies (e.g. Chen and Chang, 2005; Hosoya, 2013; Morimune, 2003). The straight dorsal margin of the dentary type is omnivorous habit or carnivorous-omnivorous habit or and fish eating habit (fig. 3D).

In the hookced type dentary species are only *O. uncirostris* and *O. bidens*. These spe-

cies are storongry fish eater habit (e.g. Morumune, 2003; Hosoya, 2013). In the other types of the dentary are omnivorous habit expect for *O*. *pachycephalus*. *Opsariichthys pachycephalus* is not hooked type, in spite of the species is fish eater (Fig. 3C). Morimune et al. (2003) suggested that *O*. *pachycephalus* adapts not enough for fish eating habit based on body size and intestine morphology.

The metapterygoid is the one of the related characters of attaching the adductor mandiburae muscle A1 for the pisucicous habit (Asiwa and Hosoya, 1998; Gosline, 1973; Hows, 1980). The H-saped metapterygoid species (*O*. *uncirostris*, *O*. *bidens*, and *O*. *pachycephalus*) are fish eating behavior. The unconstricted metapterygoid species are omnivorous habit (fig. 3E).

Thus, the present study demonstrates that the morphology of the metapterygoid and jaw bones in opsariichthines strongly reflects of the feeding habitat. In addition, *O*. *evolans* bears a genetic relationship to *Opsariichthys* than *Zacco*, but morphological characters converge with *Zacco*, because the feeding habit of *O*. *evolans* is closely similar to *Zacco* .

Chapter 2

The genus *Nipponocypris* (Pisces: Cyprinidae) from the Nogami Formation (Middle Pleistocene) in the southern part of the Kusu basin, Oita, Japan.

Introduction

The Middle Pleistocene Nogami Formation of Oita Prefecture, Northern Kyushu, Japan is lacustrine deposits, and yields many complete fossils of freshwater fishes, which belong to Salmonidae (*Oncorhyncus* cf. *O. masou* or *O. rhodums* or sp), Gobiidae (*Rhinogobius giurinus* and *R. brumous*), and Cyprinidae (*Zacco*. cf. *Z. temminckii*, *Hemibarbus barbus* or *Hemibarbus* sp., and *Acheilognathus lanceolata*) (e.g., Uyeno et al., 1975, 2000; Takahashi and Okumura, 1998; Yabumoto, 1987). These specimens are very important for paleontologists and ichthyologists to provide an information of the freshwater fish fauna of the East Asia at the Quaternary, because the Quaternary deposits in the East Asia yield almost fragmentary bones and detached pharyngeal teeth (Chang and Chen, 2008). However, there is no detailed comparative osteology about Recent and fossil taxa, and the phylogeny of the freshwater fishes from the Nogami Formation.

Among the above-mentioned fishes from the Nogami Formation, the genus *Zacco* (Cyprinidae), which is a member of opsariichthines, studies of the taxonomy and molecular phylogeny have been rapidly increased as mentioned in the Chapter 1(e.g., Chen et al., 2008; Hosoya et al., 2003; Kim et al., 2006; Tang et al., 2010, 2013a,b). Therefore, it is necessary to study taxonomy and phylogeny about the fossil species.

In the present Chapter, the fossil opsariichthines is described from the Nogami Formation of the Middle Pleistocene, Oita Prefecture, Japan and its phylogenetic position within the recent opsariichthine group is discussed.

Geological setting

The southern part of the Kusu basin, Oita Prefecture of Northern Kyushu, Japan belongs to the Hohi volcanic zone, and consists of volcanic rocks and lacustrine deposits (Fig. 1). Stratigraphic, sedimentologic, volcanic, paleontologic, and paleoecologic investigations have been conducted since 1950's (e.g., Hayashi, 1959; Iwauchi, 1998; Iwauchi and Hase, 1987; Kamata and Muraoka, 1982; Julius et al., 2006; Ishihara et al., 2010; Suto, 1953a, b).

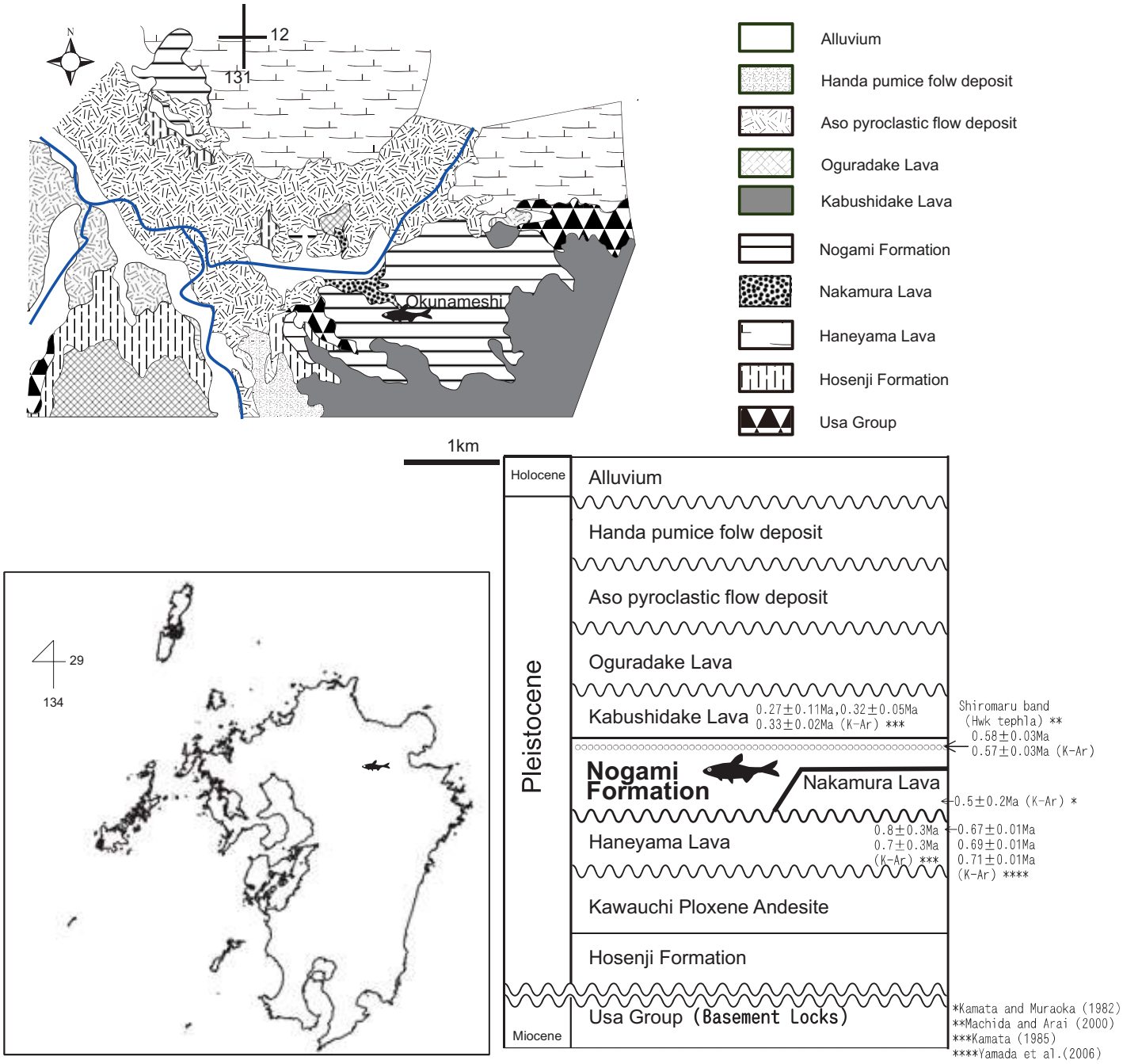

Figure 1. Locality maps of the fossil fish. A, Geological map of Nogami area, southern part of Kusu basin (modified from Iwauchi and Hase, 1987). Fish symbol indicates the locality of Nipponocypris sp. B, Stratigraphic sequence of Late Cenozoic formations in the southern part of Kusu basin (modified from Iwauchi and Hase, 1987. Radiometric age from Kamata and Muraoka, 1982, Kamata, 1985; Iwauchi and Hase, 1987, Machida and Arai, 2000; Yamada et al., 2006).

The lower part of the Nogami Formation that fossils are yielding is mainly composed of lacustrine diatomaceous beds with the Nakamura Lava that inflowed into the paleo-lake (Iwauchi and Hase, 1987). The Nogami formation yields well-preserved fossils of frogs (Nokariya and Kitabayashi 1987), plants (e.g. Iwauchi and Hase, 1987), diatoms (e.g. Julius, et al., 2006) and freshwater fishes (e.g. Uyeno et al. 1975; 2000).

The age of Nogami Formation is the Middle Pleistocene, which is supported as follows: the K-Ar age of the Haneyama Lava that is covered by the Nogami Formation (e.g. 0.8±0.3Ma, 0.7±0.3Ma: Kamata and Muraoka, 1982; 0.67±0.01Ma, 0.69±0.01Ma, 0.71±0.01Ma: Yamada et al., 2006,); the K-Ar age of the Kabushidake Lava that covers the Nogami Formation (0.27±0.11Ma, 0.32±0.05Ma, 0.33±0.02Ma: Kamata, 1985); and the K-Ar age of the Hiwaku (Hwk) tepla (Shiromaru band of Iwauchi and Hase, 1987), which is within the Nogami Formation (0.58±0.03Ma, 0.57±0.03Ma; Machida and Arai, 2000; fig. 1).

Material and Methods

Counts and Measurements.—Standard length measurements were done for the estimated tip of the snout to the posterior end of the hypural along the midline of the body. Fin ray counts were made according to Chen (1998) and vertebral counts were made according to Uyeno (1984).

Osteological Terminology.—Names of skull bones and the anterior part of vertebrae follow Britz and Conway (2009), Chen et al. (1984), Dahdul, et al. (2010), Harrington (1955), Uyeno and Sakamoto (2000), and Witszman (1962), and caudal bones follow Fujita (1999).

Comparative materials. The depository of the specimens of the Recent opsariichthines examined is the Kitakyushu Museum of Natural History and Human History, Kitakyushu, Fukuoka Prefecture, Kyushu Islands, Japan, with the prefix KMNH. These specimens were transported and stained by the method of modified from Kawamura and Hosoya (1991): *Zacco platypus* (Temminck and Schlegel, 1846), (Oita Prefecture, Japan, KMNH VR 100,128, SL 104.0 mm; KMNH VR 100,129, SL 101.0 mm; KMNH VR 100,130, SL 91.0 mm). *Nipponocypris temminckii* (Temminck and Schlegel, 1846), (Oita Prefecture, Japan, KMNH VR 100, 134, SL 103.2 mm ; KMNH VR 100,135, SL 101.4 mm; KMNH VR 100,136, SL 80.7 mm). *Nipponocypris sieboldii* (Temminck and Schlegel, 1846) , (Okayama, Japan, KMNH VR 100,138, SL 92.7 mm;

KMNH VR 100,139, SL 90.8 mm; KMNH VR 100,140, SL 100.9 mm). *Nipponocypris koreanus* (Kim, Oh and Hosoya, 2005), (Korea, KMNH VR 100,141, SL 84.1 mm ; KMNH VR 100,142, SL 87.4 mm; KMNH VR 100,143, SL 101.0 mm, KMNH VR 100,144, SL 95.0 mm). *Parazacco spilurus* (Günther, 1868), (Guangdong, China, KMNH VR 100,145, SL 79.5mm ; KMNH VR 100,146, SL 87.7 mm; KMNH VR 100,147, SL 107.0mm). *Candidia barbatu*s (Regan, 1908), (Kaohsiung, Taiwan, KMNH VR 100, 131, SL 84.9 mm; KMNH VR 100, 132, SL 91.6 mm; KMNH VR 100, 133, SL 88.3 mm). *Opsariichthys uncirostris* (Temminck et Schlegel, 1846) , (Siga, Japan, KMNH VR 100, 148, SL 204.7mm; KMNH VR 100, 149, SL 196.0 mm; KMNH VR 100, 150, SL 191.8 mm). *Opsariichthys bidens* Günther, 1873 (China, KMNH VR 100, 151, SL 102 mm; KMNH VR 100, 152, SL 79.5 mm).*Opsariichthys evolans* (Jordan and Evermann, 1902) (Taiwan, KMNH VR 100, 155, SL 73.7 mm; KMNH VR 100, 156, SL 86.5 mm; KMNH VR 100, 157, SL 70.1 mm).

Systematic description

Order Cypriniformes Bleeker, 1859

Family Cyprinidae Cuvier, 1817

Opsariichthine sensu Chen, 1982

Genus *Nipponocypris* Chen et al., 2008

Nipponocypris sp.

Material—KMNH (Kitakyushu Museum of Natural History and Human History) VP 102. 036 (SL 114 mm), KMNH VP 102. 028 (SL 107mm), KMNH VP 102, 034 (SL 111.4 mm), , KMNH VP 102. 062 (SL 136.5mm), NSM (National Science Museum, Tsukuba) No3-A (SL 158 mm), and NSM, XXX (HL 24.1mm+)

Locality and Horizon. —All specimens were in phosphorite nodule, which discovered from the Nogami Formation (Middle Pleistocene) at the quarry of Hakusan Kogyo Campany, Okunameshi area, Kokonoe town, Oita Prefecture, Northern Kyusyu, Japan (fig. 1).

Description

Skull (Figs. 2 – 6). The skull is almost preserved in all specimens, especially KMNH VP 102, 036, KMNH VP 102, 042 and NSM, XXX are almost completely preserved. Kiethmoid, ethmoid, preethmoid and prevomer are fragmentary and not clearly visible.

The Supraethmoid is a thin sheet and located in the anterior margin of the frontals (KMNH VP 102, 042). The lateral ethomoid, which is well observable in KMNH VP

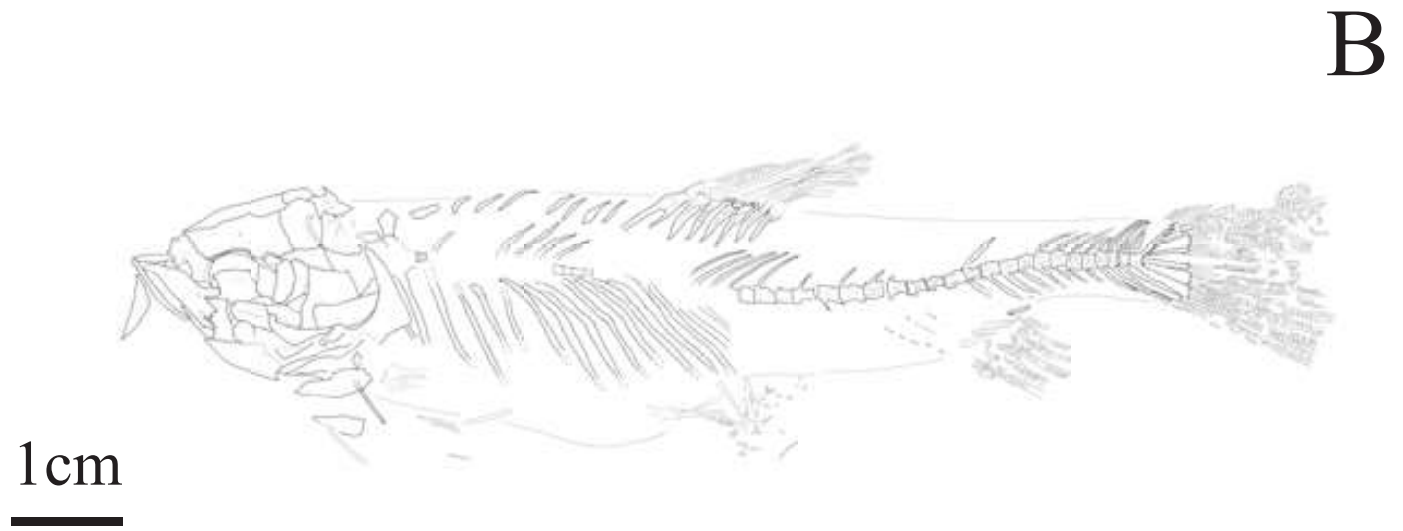

Figure 2. *Nipponocypris* sp. A. photo of, KMNH VP 102, 036. B. line drawing of A.

Figure 3 (next page). *Nipponocypris* sp. skull in lateral view. A. photo of, KMNH VP 102, 036. B. line drawing of A. Abbreviations: ACH, anterior ceratohyal; ANG, anguloarticular; BRA, branchiostegal rays; CLE, cleithrum; CRA; coracoid; DEN, dentary; ETH LAT, lateral ethmoid; EPO, epiotic ; FRO, frontal; IOP, interopercle; IO4, 4th infraorbital; MET, metapterygoid; OP, opercle; PAR, parietal; PCL, postcleithrum; PCH, posterior ceratohyal; PMX, premaxilla; PTO, pterotic; SOC, supraoc-cipital; SOP, subopercle; SRPE, supraethmoid .

Fig. 3

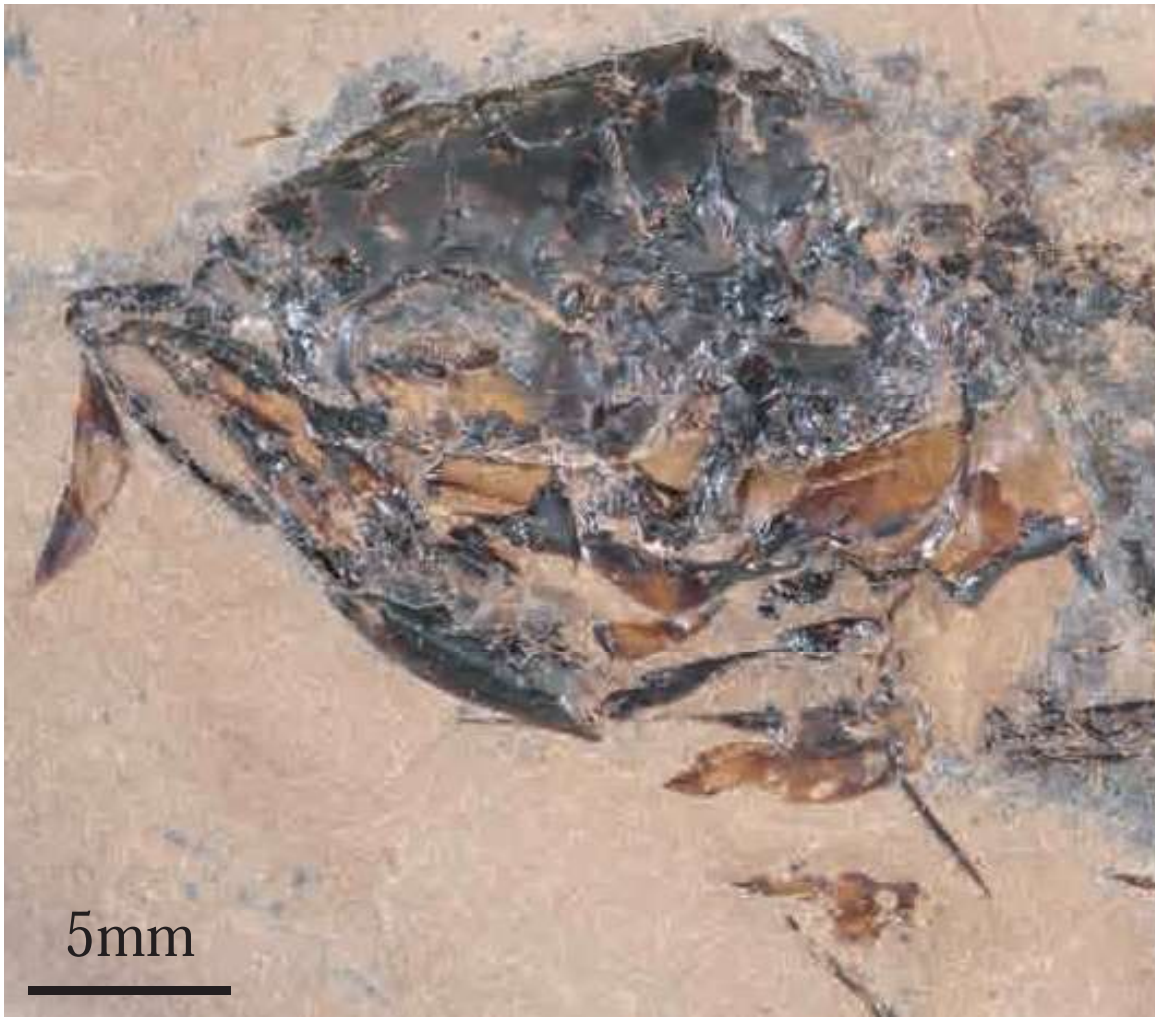
A
5mm

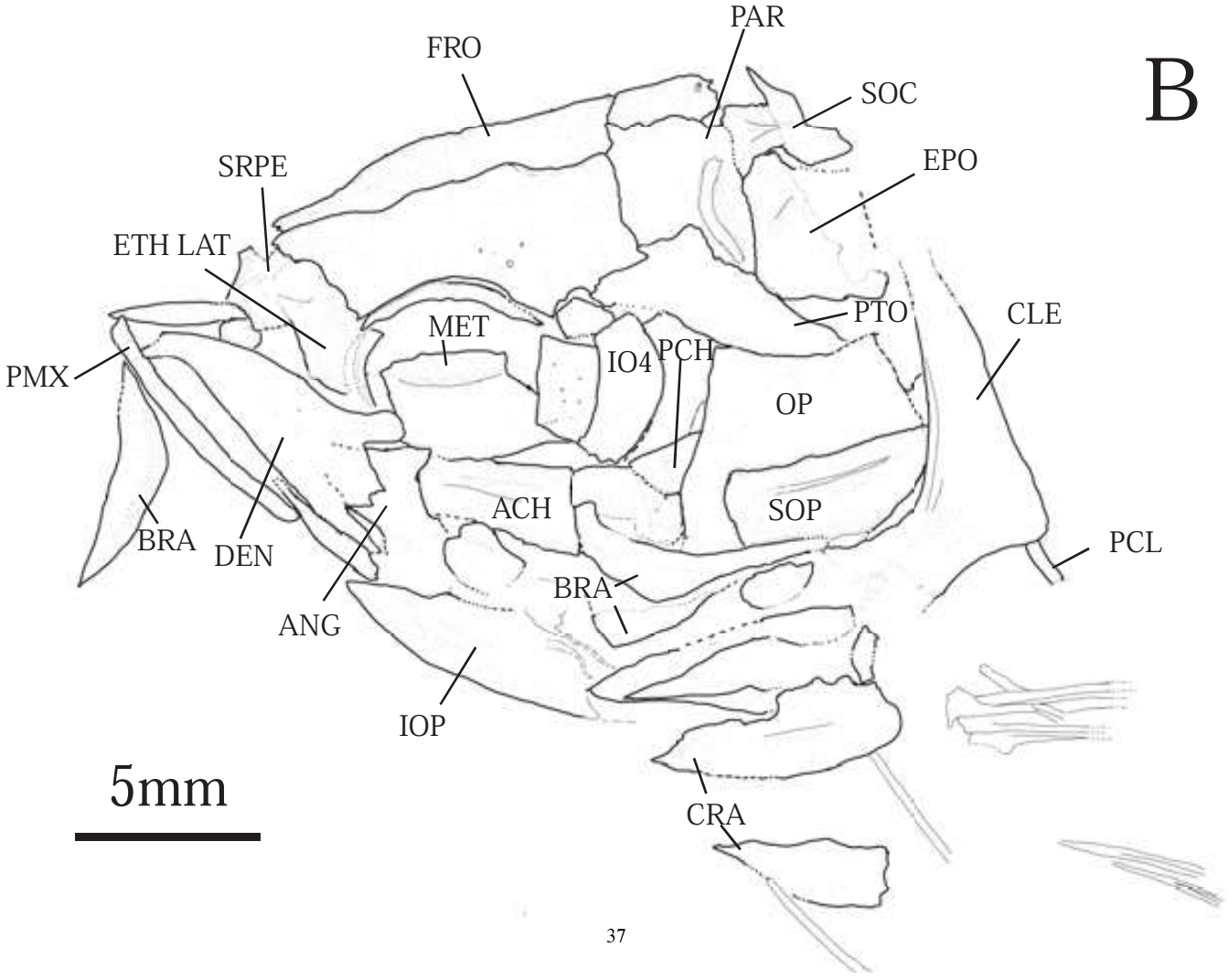
B
PAR
FRO
SOC
SRPE
EPO
ETH LAT
PTO
CLE
MET
IO4
PCH
PMX
OP
ACH
SOP
BRA
DEN
PCL
BRA
ANG
IOP
5mm
CRA

102, 036 and KMNH VP 102, 042. It contacts the anterolateral margin of the frontal and, sticks out sideways. The frontal is a large, elongate bone that forms the dorsal roof of the orbit, and there is a notch at the posterior lateral margin of the frontal in KMNH VP 102, 036 (figs. 2, 3).

The parietal is almost a square in shape and there is a sensory canal. The sensory canal does not reach to the medial edge of the parietal, and the length is longer than the half of the width of the parietal (KMNH VP 102, 036, NSM No XXX). The supraoccipital connects with the posterior margin of the frontal, and has a crest on its dorsal medial surface (NSM, XX).

Other bones of the otic region (e.g. prootic, autosphenotic.) and the occipital region (e.g. exooccipital, basioccipital.) are not clearly visible, because these are fragmentary or covered by the opercular bone and the shoulder girdle.

Infraorbital bones (Fig. 6). The infraorbital bones are partially preserved in KMNH VP 102, 028, NSM, No 03-A and NSM, XXX. The first infraorbital (= lachrymal by Harrington, 1955) is preserved on KMNH VP, 102, 034, NSM, No 03-A and MNHXXX. It's about a pentagon-shaped and a large flat bone. The sensory canal runs along the middle of the bone and slightly curved in KMNH VP 102, 028. The second infraorbital is observable in KMNH 102, 042 and KMNH 102, 034, whose width is almost the same as the third one, and a sensory canal runs close on the middle. The third and fourth infraorbitals are preserved in KMNH 102, 042 and KMNH 102, 028, whose width is the same size each other, and the length of the third one is slightly longer than the fourth one. The posterodorsal corner of the fourth infraorbital has the small projection which is L-shaped. The sensory canal runs along the dorsal margin of the third and fourth infraorbitals. The fifth infraorbital is not preserved.

Jaws (Figs. 3, 5, 7). The jaw bones are well preserved in KMNH VP 102, 036, KMNH VP 102, 042 and NSM, XXX. The anteroventral margin of the maxilla is rounded in KMNH VP 102, 042. The posterior margin of the post-dorsal process on the maxilla is triangular, slightly convex such as the genus *Zacco* or *Nipponocypris* in KMNH VP 102, 042 and NSM, XXX. The premaxilla is located at the anterior to maxilla. The anterior end of the premaxilla is process which stretching to the dorsal in KMNH VP 102, 042. The dentary is a large, deep bone, and the mandibular sensory canal runs at the ventral part. The flat coronoid process is present and it inclines about 45 degrees dorsally. The oral margin of the dentary is slightly convex. The anguloarticular is located behind the

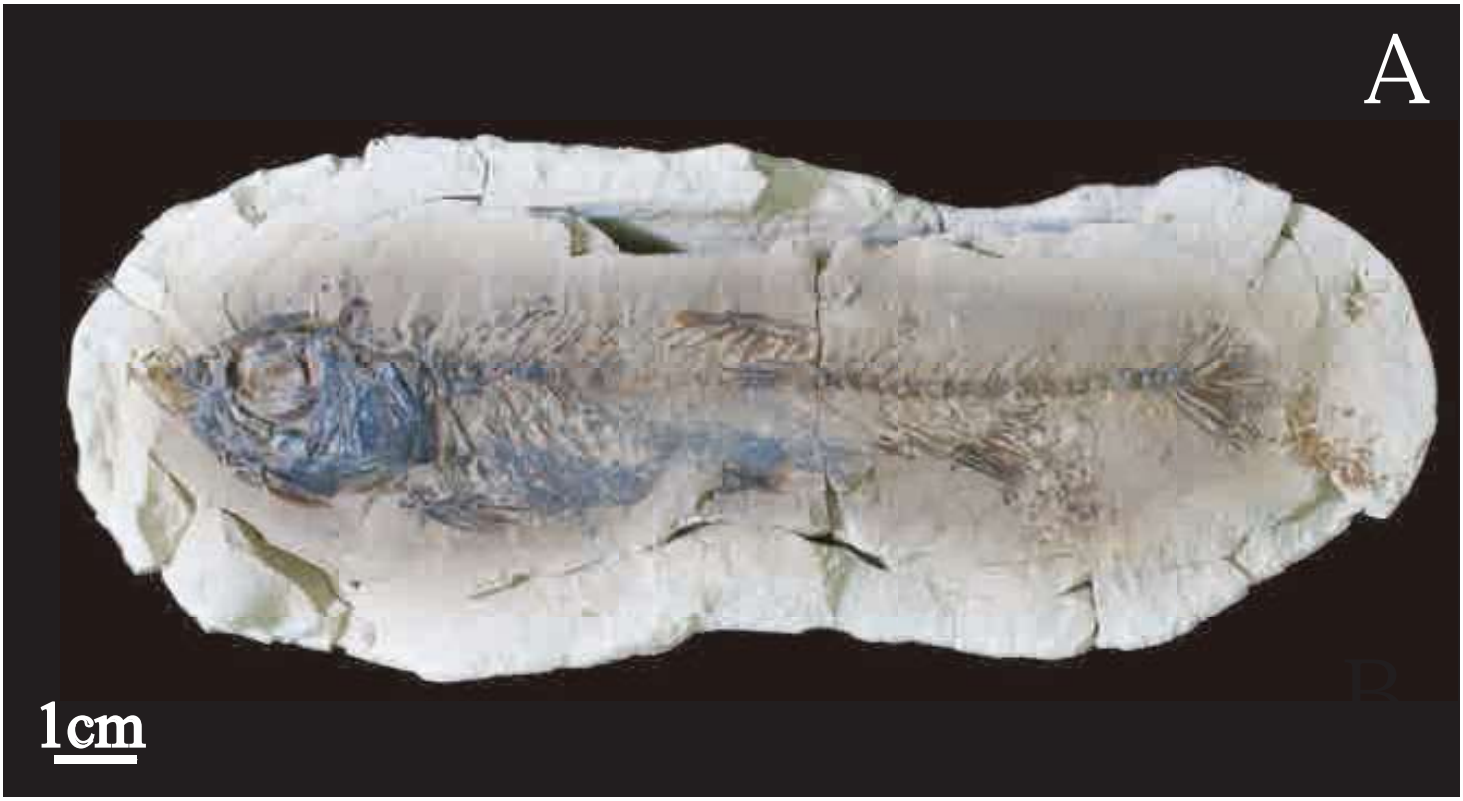

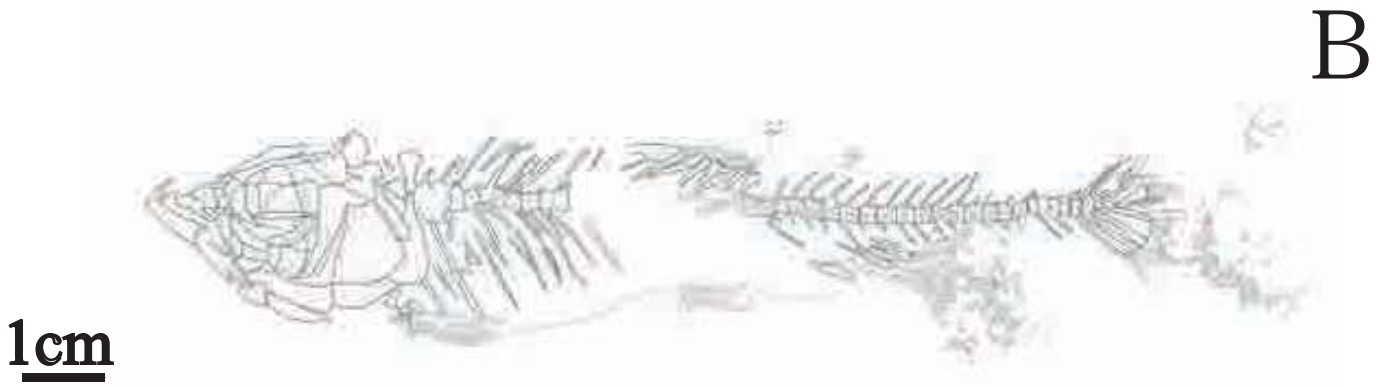

Figure 4. *Nipponocypris* sp. A. photo of, KMNH VP 102, 042. B. line drawing of A.

Figure 5 (next page). *Nipponocypris* sp. skull in lateral view. A. photo of, KMNH VP 102, 042. B. line drawing of A. Abbreviations: ANG, anguloarticular; BRA, branchiostegal rays; CHY, ceratohyal; CLE, cleithrum; DEN, dentary; ECT, ectopterygoid; ETH, eth-moid; ETH LAT, lateral ethmoid; EPO, epiotic; FRO, frontal; HYO, hyomandibular; IOP, interopercle; IO2, 2nd infraorbital; IO3; 3rd infraorbital; IO4, 4th infraorbital; MAX, maxilla; MET, metapterygoid; OP, opercle; P, autopalatine; PAR, parietal; PARA, parasphenoid; PCL, postcleithrum; PMX, premaxilla; POP, preopercle; PTO, pterotic; Q, quadrate; RET, retroar-ticular; R4+OS, rib4+os suspensorium; RD, pectral radial; SC; scapula; SCL, supracleithrum; SN3, supraneural 3 bone; SOP, subopercle.

Fig. 5

A


5mm

B

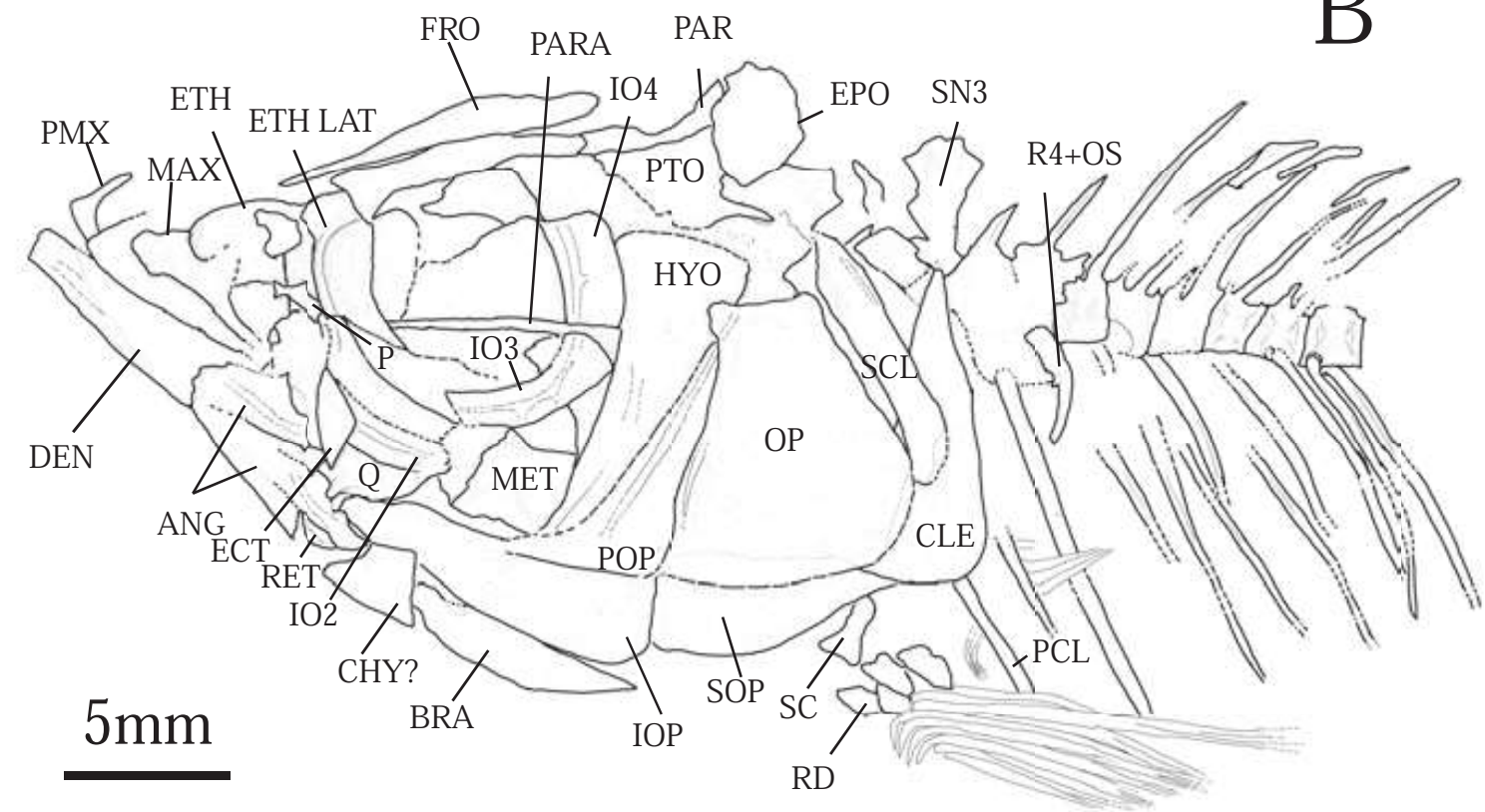
FRO
PARA
PAR
IO4
EPO
SN3
ETH
ETH LAT
PMX
MAX
PTO
R4+OS
HYO
P
IO3
SCL
DEN
OP
Q
MET
ANG
ECT
CLE
POP
RET
IO2
PCL
CHY?
SOP
SC
BRA
IOP
RD
5mm

dentary, and its dorsal margin is almost triangular. The suspensorial articulation facet is present at the posterior part of the anguloarticular. The sensory canal runs along the ventral part of the anguloarticular. The small retroarticular contacts with the ventral surface of the anguloarticular in KMNH VP 102, 042 and NSM, XXX.

Opercular series (Fig. 5). The opercle is a large and trapezoidal shaped, and the posterior margin is concave. Its anterodorsal corner is slightly projected anteriorly and the opercular canal is present. In KMNH VP 102, 042, the preopercle is marginally observable. The preoperculomandibular sensory canal is preserved, and it is enclosed in the bony tube and reaches to the opercular canal.

The interopercle is almost the same size as the subopercle. The bone is narrow at its anterior end and gradually widens posteriorly. Its dorsal margin is concave and ventral margin is slightly convex on KMNH VP 102, 042 and NSM, XXX. The subopercle is a knife-like shaped and gradually narrows posteriorly.

Suspensorium (Fig. 5). The suspensorium series bones are preserved in KMNH VP 102, 042, and in the other specimens, the bones are fragmental or covered by other bones. The posterior margin of the autopalatine articulates with the endopterygoid in KMNH VP 102, 042. The endopterygoid is a large and flat bone. Its anterior margin is saddle-shaped and thick, and articulates with the autopalatine in KMNH VP 102, 042. The ectopterygoid is a thin and oval-shaped bone in KMNH VP 102, 042. The metapterygoid is a broad and flat plate with a strut along its dorsal margin. The quadrate is shallow, and consists of the fan-like part and the thick ventral projection (articulation feacet for the mandibular). The projection articulates with the suspensorial articulation facet of the anguloarticular in NSM XXX. The synpmplectic is not able to be observed, because of fragmentary or covered with the operculer bones. The hyomandibular is barely observable in KMNH VP 102, 042, and almost of these are covered by the opercular bones or the infraorbital bones. The elongated opening of the hyomandibular branch of the facial nerve is present in the lower portion of the strut.

Hyoid arch (Fig. 6). The upper and lower hypohyals are fragmentally preserved in NSM. XXX.

The anterior and posterior ceratohyals are partially preserved in KMNH VP 102, 036 and NSM. XXX. The anterior one is a thick bone that is narrow anterior and expanded posterior area, and it is convex at the ventral margin. The posterior one is narrow against

the posterior. There are three branchiostegals, which are flat and boomerang like curvetuare.

Pharyngeal bone and teeth (fig. 6). The pharyngeal bone and teeth are observed in only NSM XXX, and in the other specimens, these are covered by the opecular series bones. In NSM XXX, only one pharyngeal tooth is preserved, which is conical shaped. There is a cycloid vestige of the pharyngeal tooth on the pharyngeal bone. This shows that dental formula is 5, 4, and 2 or 3.

Vertebrae (Figs. 2 – 5) In the present study, the estimated number of vertebrae based on the number of neural spines, haemal spines and ribs, although some abdominal and caudal vertebrae are missing. There are about 23 – 24 abdominal vertebrae, 19 – 20 caudal vertebrae, and the total number of vertebrae are about 42 – 44 . The first to fourth abdominal vertebrae relates to Weberian ossicle. The first vertebra is not visible. The Weberian apparatus is not well preserved. The upper part of supernural 3 bone is comb-like shaped and connects with the dorsal margin of the neural arch of the third and fourth vertebrae. The neural spine of the fourth vertebra is shorter than the fifth. The supraneural 4 bone is located between the supuraneural 3 bone and the neural spine of the fifth vertebra, and do not contact each other (KMNH VP 012, 036). There are 15 to 16 pairs of ribs in total in KMNH VP 012, 036 and No. 03-A. The Other ribs are elongate, arch-like shaped, and reaching to the abdominal edge. The dorsal margin of the neural spine of the third vertebra turns downward (KMNH VP 012, 042).

Figure 6. *Nipponocypris* sp. skull in lateral view. A. photo of NSM, XXX. B. line drawing of A. Abbreviations: ACH, anterior ceratohyal; ANG, anguloarticular; BRA, branchiostegal rays; CLE, cleithrum; DEN, dentary; EB5, 5th ceratobranchial; ETH LAT, lateral ethmoid; FRO, frontal; IOP, interopercle; IO1, 1st infraorbital; MAX, maxilla; MET, metapterygoid; OP, opercle; PAR, parietal; PCL, postcleithrum; PCH, posterior ceratohyal; pt; pharyngeal teeth; Q, quadrate; RD, pectral radial; RET, retroarticular; SC; scapula; SCL, supracleithrum; SN3, supraneural 3 bone; SN4, supraneural 4 bone; SOC, supraoccipital.

Fig. 6

A

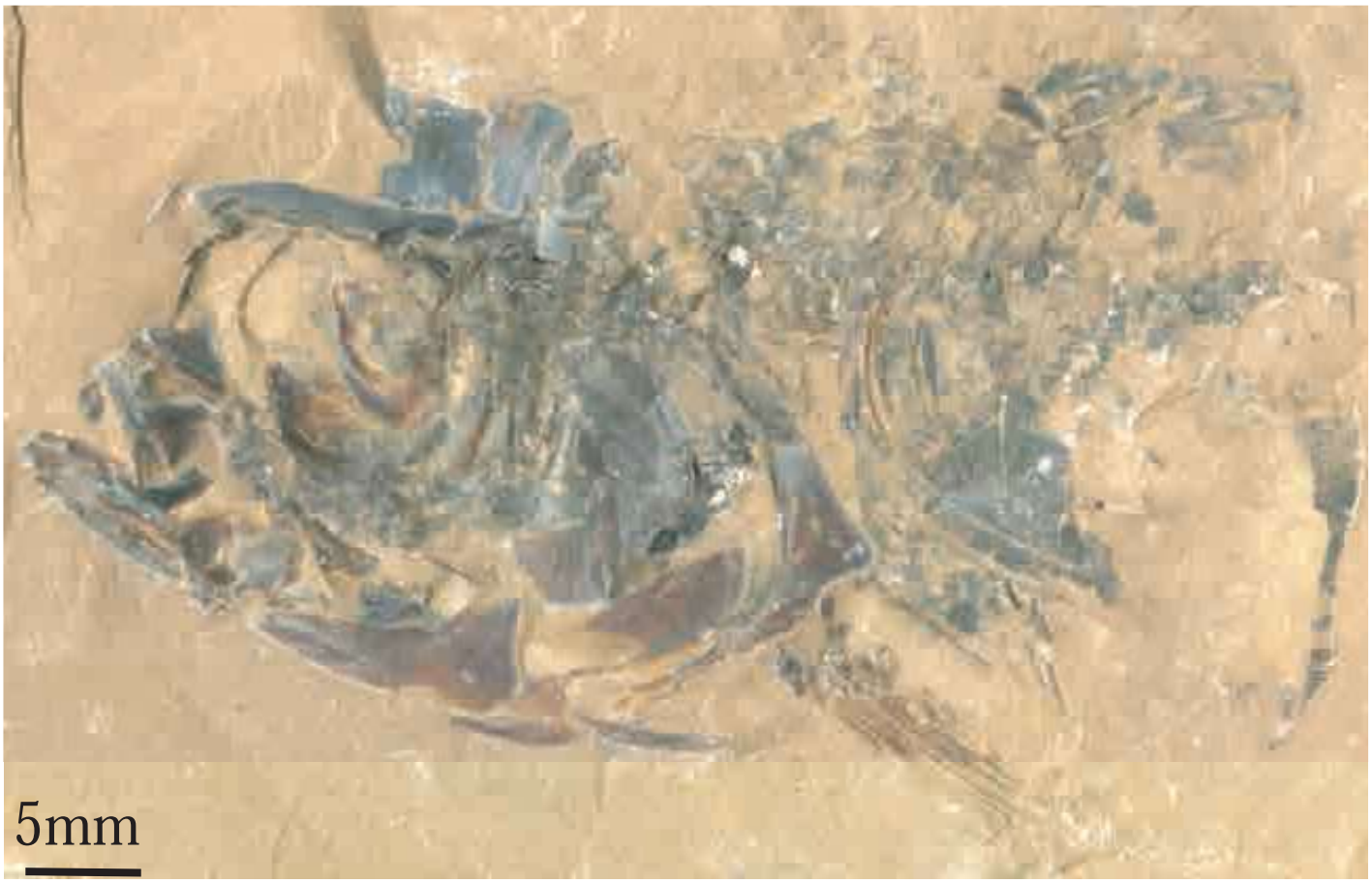
5mm

B

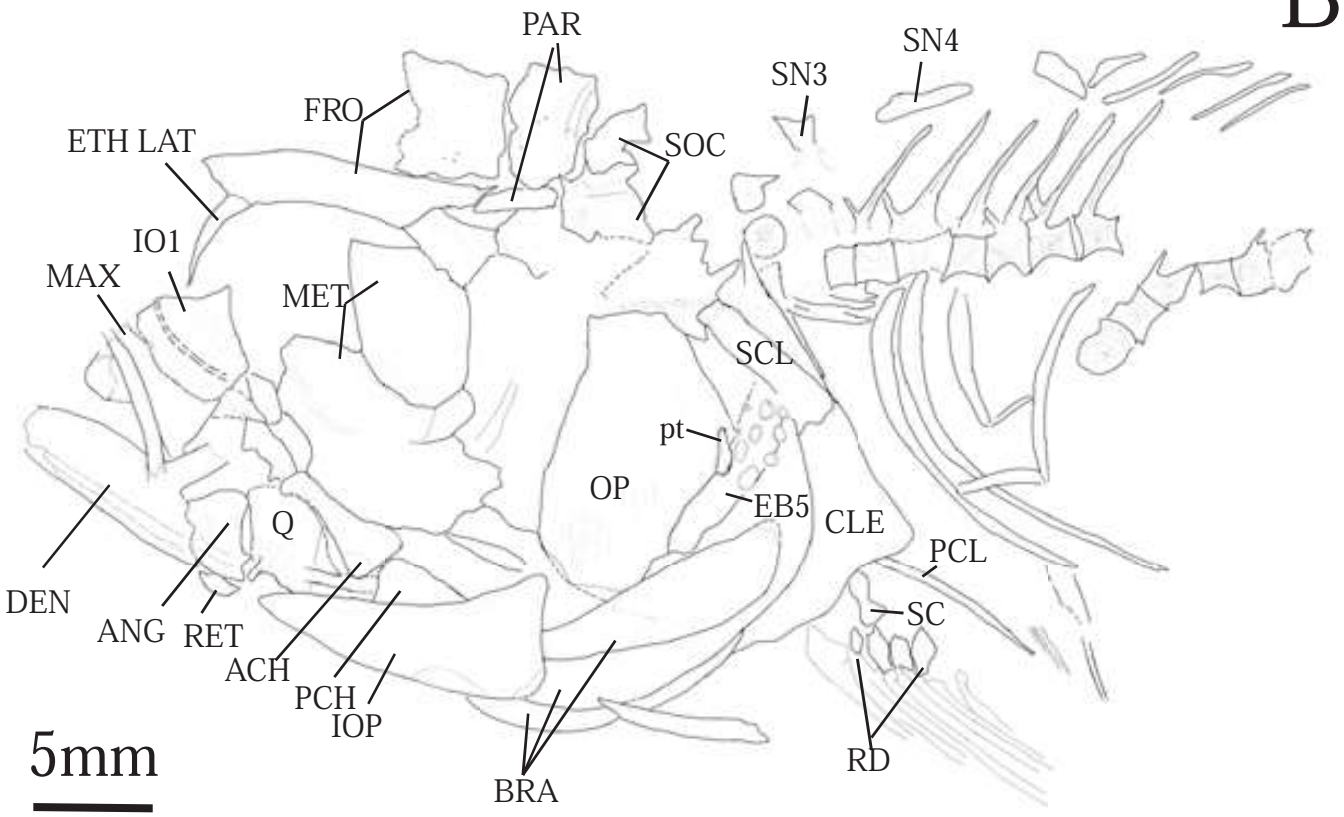
PAR
SN4
SN3
FRO
ETH LAT
SOC
IO1
MAX
MET
SCL
pt
OP
EB5
CLE
Q
PCL
DEN
SC
ANG
RET
ACH
PCH
IOP
RD
BRA
5mm

Caudal fin skeleton (Fig. 7) —The first uroneural is fused with preural centrum 1 and ural centrum 1 to form the pleurostyle. The pleurostyle is stout and straight. The hypural 1 is the largest of hypural series, and its posterior margin is about 1.3 times that of the parhypural. The hypural 2 is fused with the preural centrum 1 and ural centrum 1, and is the same size as the hypural 3. A large gap exists between hypurals 2 and 3. The hypural 3 is articulated with the preural centrum 1 and ural centrum 1. The hypural 4 is spread posterior area, fan like shaped, and its width at the posterior margin is almost the same as the hypural 1. The hypural 5 is almost the same width as the hypural 3, and is almost the same length as half of the hypural 3. The hypural 6 is the smallest in hypural series, which is well observed in KMNH VP103, 028 and KMNH VP103, 036. A single long, narrow epural is present and does not reach to the neural spine of the first preuralcentrum that is especially observed in NSM No. 03-A and KMNH VP103, 028. The neural spine of the first preuralcentra is sharp and is shorter than one-third the length of the neural spine of the second preuralcentrum. The neural spines of the second and third preuralcentra are almost the same size, and the wings of these extend to the top of the neural spines. The haemal spines of the second and third preuralcentra are almost the same length. The posterior margin of the haemal spine of the second preuralcentrum is about twice that of the third.

Intermuscular bones (Fig. 8) Eight supuraneural bones are located between the dorsal fin skeleton and the supuranerural 3 bones. Supuraneural 4 – 11 bones are not contacted with each neural spine. The anteriomrmost supuraneural (supuraneural 4 bone) is the largest, a thin sheet and apporoximately rectangle. The fifth to eleventh are small and thin in the series. There are numerous epipleural and epineural. These are hair-thin and almost of these divide dichotomously.

Figure 7. Caudal fin skeleton of *Nipponocypris* sp. A. photo of, KMNH VP 102, 036. B. line drawing of A. Abbreviations: hpu2, haemal spine of the second preural centrum; hpu3, haemal spine of the third preural centrum; npu1, neural spine of first preural centrum; npu2, neural spine of the second preural centrum; npu3, neural spine of the third preural centrum; pp, hypurapophysis; pu1+u1, first preuralcentrum+first ural vertebra; pu2, second preuralcentrum; pu3, third ural vertebra; pu4, fourth ural vertebra.

Fig. 7

A

2 mm

B

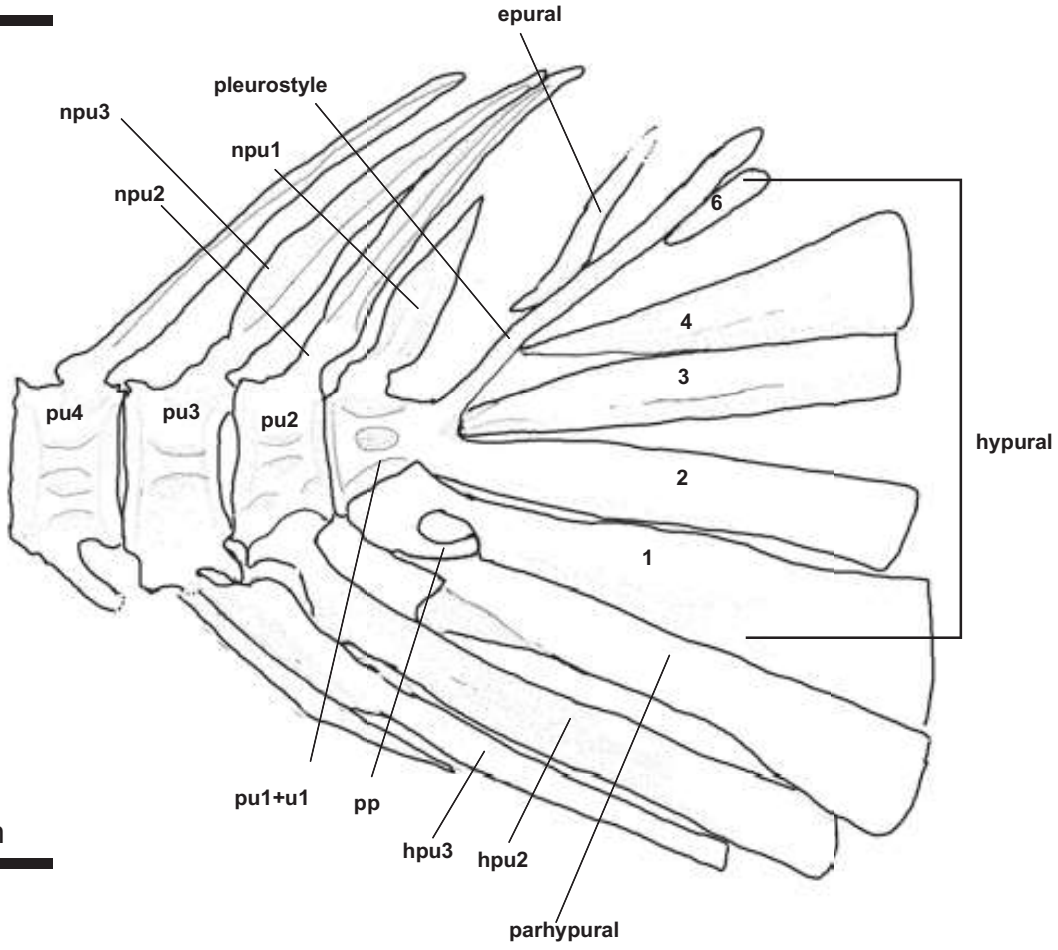

2 mm

Figure 8. Supuraneural bones of *Nipponocypris* sp. A. photo of, KMNH VP 102, 036. B. line drawing of A.

Dorsal fin and Skeleton (Figs. 2, 4). The dorsal fin is located in the middle of the body, with its origin approximately posterior to the pelvic insertion. The length of the dorsal fin base is shorter than that of the anal fin. In KMNH VP, 102, 036, there are three unbranched and unsegmented dorsal fin rays, and are seven branched dorsal fin rays. The first dorsal fin ray is short. In KMNH VP, 102, 036, KMNH VP, 102, 028, KMNH VP, 102, 042 and No. 03A, the proximal pterygiophores are preserved. The first one forms a large bony plate with struts along the anterior and posterior margines, and divides dichotomously. The other proximal pterygiophores are shorter than the first one, and have median struts with developed anterior and posterior wings. The posterior and median pterygiophores are drum-like shaped.

Anal fin and Skeleton (Figs. 2, 4, and 9) The anal fin is well preserved in NSM No, 03-A. It is suspended under the haemal spines of the anterior caudal vertebrae. Its origin is well behind the posterior end of the dorsal fin base. The proximal pterygiophores are slight, and have median struts with anterior and posterior wings. The posterior and median pterygiophores are drum-like shaped. Anal fin rays are fragmented and not clearly visible. However, it is estimated that the number of anal fin rays are 13, because the number of anal proximal pterygiophores are 11 based on comparison with moderm species, which have 13 anal fin rays (e.g. *Nipponocypris temminckii* and *N. koreanus*).

Shoulder Girdle (Fig. 5). The postcleithrum is fragmentary and not clearly visible. The supracleithrum is well observable in KMNH VP 102, 042 and KMNH VP 102, 028, which is slender and slightly thick along the posterior margin. The sensory canal runs along the posterior upper edge of the supracleithrum. The cleithrum is L-shaped, and the anterior margin of its upper arm is thick. The posteroventral margin of the cleithrum is concave. The coracoid is thin and the ventral margin is convex, and the posterior margin is slightly thick and connects with the scapula. The mesocoracoid is observable in only KMNH VP 102, 062, whose reedy bone and gradually thinner dorsally, and attached to the cleithrum at the dorsal margin. The postcleithrum is long, thin and slightly sigmoidal. The scapula is short, stout, and attached to the cleithrum at the dorsal part. Four pectral radials are preserved between the coracoid and pectoral fin rays in KMNH VP 102, 042. There are 14 or 15 pectoral fin rays in KMNH VP, 102, 028, KMNH VP, 102, 042, and NSM No. 03-A

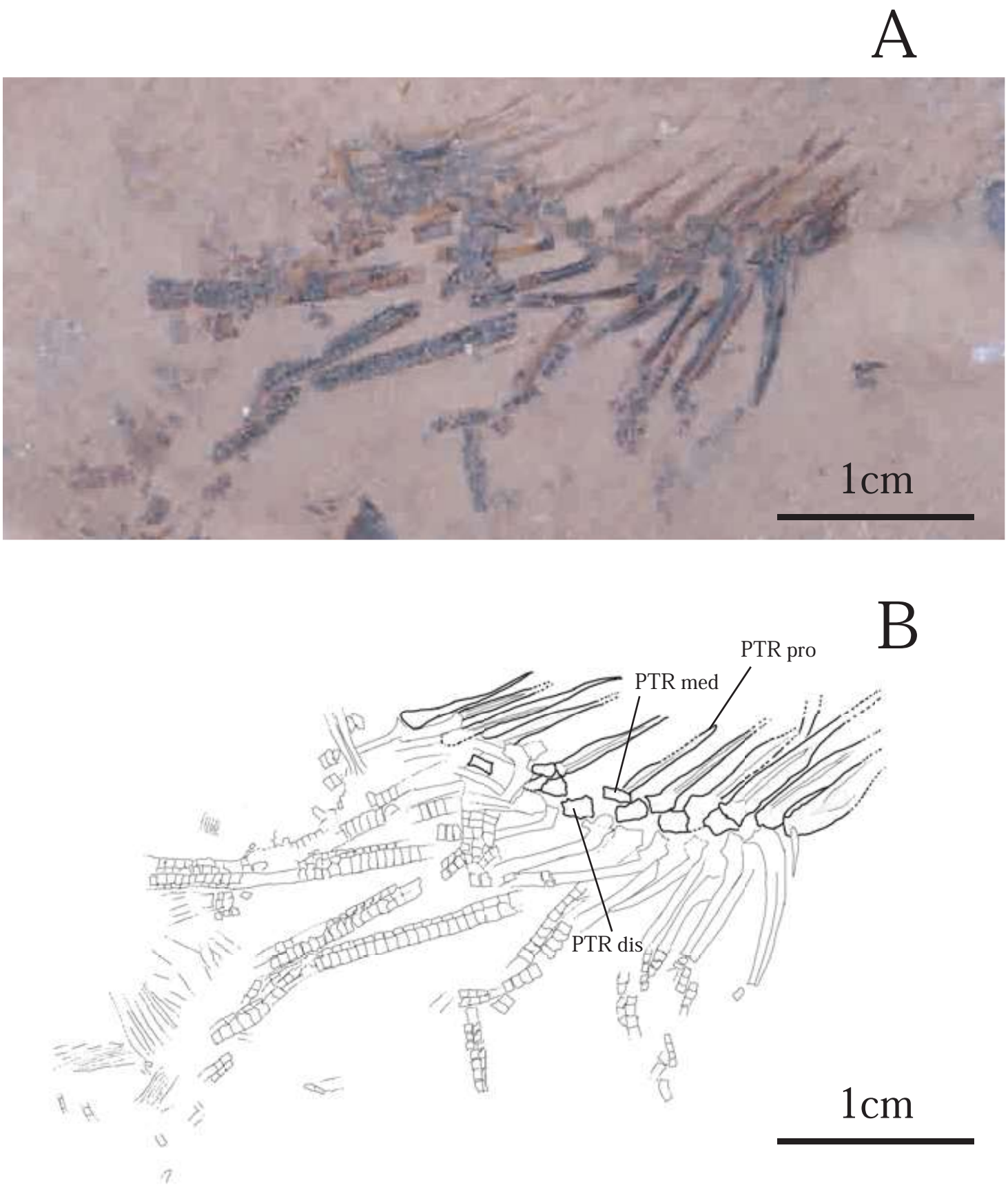

Figure 9. Anal fin skeleton of *Nipponocypris* sp. A. photo of, NSM. No. 03 - A. B. line drawing of A. Abbreviations: PTR dis, distal pterygiophore; PTR med, median pterygiophore; PTR pro, proximal pterigiophore.

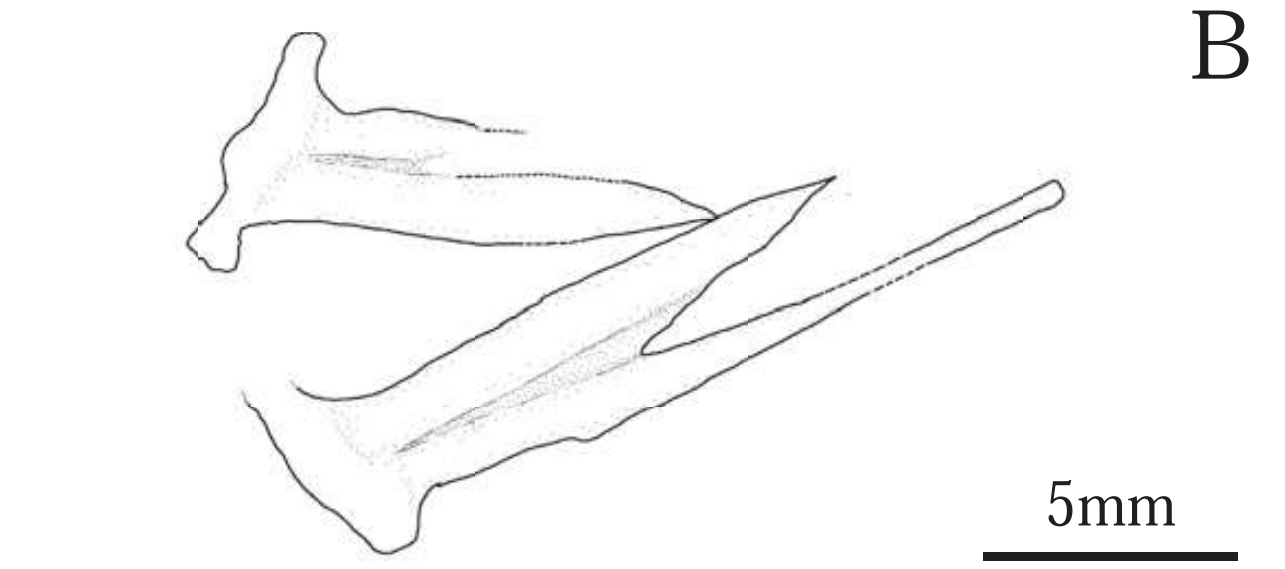

Figure 10. Pelvic girdle of *Nipponocypris* sp. A. photo of, KMNH VP 102, 062. B. line drawing of A.

Pelvic girdle (Fig. 10) The pelvic fin is located in the middle of the ventral margin of the body and its insertion is approximately anterior to the origin of the dorsal fin base. There are ten ventral fin rays in NSM No. 03-A and KMNH VP 102, 028, although almost of these are fragmented. The basipterygium is bifurcated and forms the external deep wing and the internal shallow wing with trough-like depression at the ventral view of KMNH VP 102, 062. The anterior ends of both wings are apart and the bifurcation reaches beyond the two-thirds point of the bone. The posterior part is thick, and has projections reaching internally.

Discussion

Phylogenetic relationship of *Nipponocypris* sp.

In the present study, the opsariichthines fossils from Kusu basin is assigned to a member of the family Cyprinidae based on toothless jaws, the short anteriorly curved ribs of the fourth vertebra, having the upper jaw bordered only by the premaxilla, and presence of pharyngeal teeth (see Cavender and Coburn 1992; Chen et al. 1984; Nelson 2006).

The fossils have been identified as *Zacco temminckii* or *Zacco* cf. *Zacco temminckii* by Uyeno et al. (1975, 2000), because the dorsal fin origin is slightly posterior to the pelvic insertion, eight dorsal fin rays, 46 vertebrae, and 10 – 11 anal fin rays. The genus *Zacco* is a cyprinid fishes, established by Jordan and Evermann (1902). The diagnostic characters of *Zacco* are following combination of characters: dorsal fin rays iii, 7; anal fin rays iii, 9 – 10; pharyngeal tooth two or three rows; the mouse located on the anterior extremity of the head; the pelvic fin inserted below the origin of dorsal fin base or little posterior of dorsal fin base; and others (see Jordan and Evermann, 1903; Yang and Huang, 1964; Chen and Chu, 1998).

The present fossil specimens are included within the genus *Zacco* defined by Jordan and Everman (1902) based on following characters: the dorsal fin origin slightly posterior to the pelvic insertion; ten dorsal fin rays (iii, 7); 13 anal fin rays; pharyngeal tooth three rows; and the mouse located anterior extremity of the head.

Zacco temminckii was divided three species, *Z. temminckii*, *Z. sieboldii* and *Z. koreanus* by Hosoya et al. (2003) and Kim et al., (2006). Chen et al. (2008) changed so called "*Zacco temminckii*", "*Z. sieboldii*" and "*Z. koreanus*" into the genus *Nipponocypris*, because the molecular phylogenetic study supported that *Zacco* forms

Table 1. Character matrix from Chapter 1 in this study with the data of *Nipponocyprii* sp. used for constructing the cladograms of opsariichthines.

	1	2	3	4	5	6	7	8	9	10	11	12	13	14	15	16	17	18	19	20	21	22
Aphyocypris normalis	0	0	0	0	0	0	0	0	0	0	0	0	0	0	0	0	0	0	0	0	0	0
Aphyocypris chinensis	0	0	1	0	0	0	0	0	0	0	0	0	0	0	0	0	0	0	0	0	0	0
Zacco platypus	1	0	0	1	1	0	1	1	2	1	1	2,3	0	0	0	0	1	1	0	1	1	0
Nipponocypris temminckii	0	1	0	1	1	0	0	1	0	1	1	1	1	1	2	2	0	1	0	0	1	0
Nipponocypris sieboldii	0	0	0	1	1	0	0	1	0	1	2	1	1	1	0	2	0	1	0	0	1	0
Nipponocypris koreanus	0	0	0	1	1	1	0	1	0	1	2	1	1	1	1	2	0	1	0	0	1	0
Candidia barbatus	2	0	0	1	1	1	0	1	2	1	1	1	2	0	1	2	0	0	0	0	1	0
Opsariichthys evolans	0	0	1	1	1	0	0	1	1	0	0	3	0	0	0	0	1	0	0	1	1	0
Opsariichthys pachycephalus	0	0	0	1	1	0	1	1	1	0	2	2,3	0	0	0	0	0	2	0	1	1	1
Opsariichthys uncirostris	0	2	1	0	1	0	0	1	1	0	0	3	0	0	2	1	0	2	1	1	1	1
Opsariichthys bidans	0	2	1	1	1	1, 0	0	1	1	0	0	3	0	0	1	1	0	2	1	1	1	1
Parazacco spilurus	0	0	0	1	1	0	0	1	0	1	0	1	1	1	1	0	0	0	0	0	1	0
Nipponocypris sp.	0	1	?	?	1	?	0	1	0	1	1	?	?	?	?	2	0	1	0	0	?	0

	23	24	25	26	27	28	29	30	31	32	33	34	35	36	37	38	39	40	41	42	43
Aphyocypris normalis	0	0	0	0	0	0	0	0	0	0	0	0	0	0	0	0	1	0	0	0	0
Aphyocypris chinensis	1	0	0	0	0	0	0	0	0	0	0	0	0	0	0	1	1	0	0	0	0
Zacco platypus	1	1	1	1	1	0	1	1	2	2	1	1	1	1	1	0	1	2	0	2	1
Nipponocypris temminckii	1	1	0	1	1	0	2	1	2	0	2	1	1	0	2	0	1	2	2	0	2
Nipponocypris sieboldii	1	1	0	1	1	0	1	1	2	0	1	2	2	0	2	0	1	2	2	0	1
Nipponocypris koreanus	1	1	0	1	1	0	2	1	2	0	2	1	1	0	2	0	1	2	2	0	1
Candidia barbatus	1	1	0	1	1	0	1	1	2	1	1	0	1	0	2	0	0	1	2	0	1
Opsariichthys evolans	1	1	1	1	1	0	1	0	2	2	1	1	1	1	1	0	1	2	0	1	1
Opsariichthys pachycephalus	1	1	0	0	1	0	1	1	2	1	1	1	1	0	1	0	1	2	0	1	1
Opsariichthys uncirostris	2	1	0	0	1	1	2	1	2	2	1	1	1	0	2	0	1	2	0	2	1
Opsariichthys bidans	2	1	0	0	1	1	2	1	2	1	1	1	1	0	1	0	1	2	0	1	1
Parazacco spilurus	1	1	1	1	0	0	1	0	1	0	3	0	0	0	1	0	1	0	1	0	0
Nipponocypris sp.	?	?	?	?	1	0	2	?	2	0	2	3	3	0	?	?	?	?	?	?	?

Fig. 11

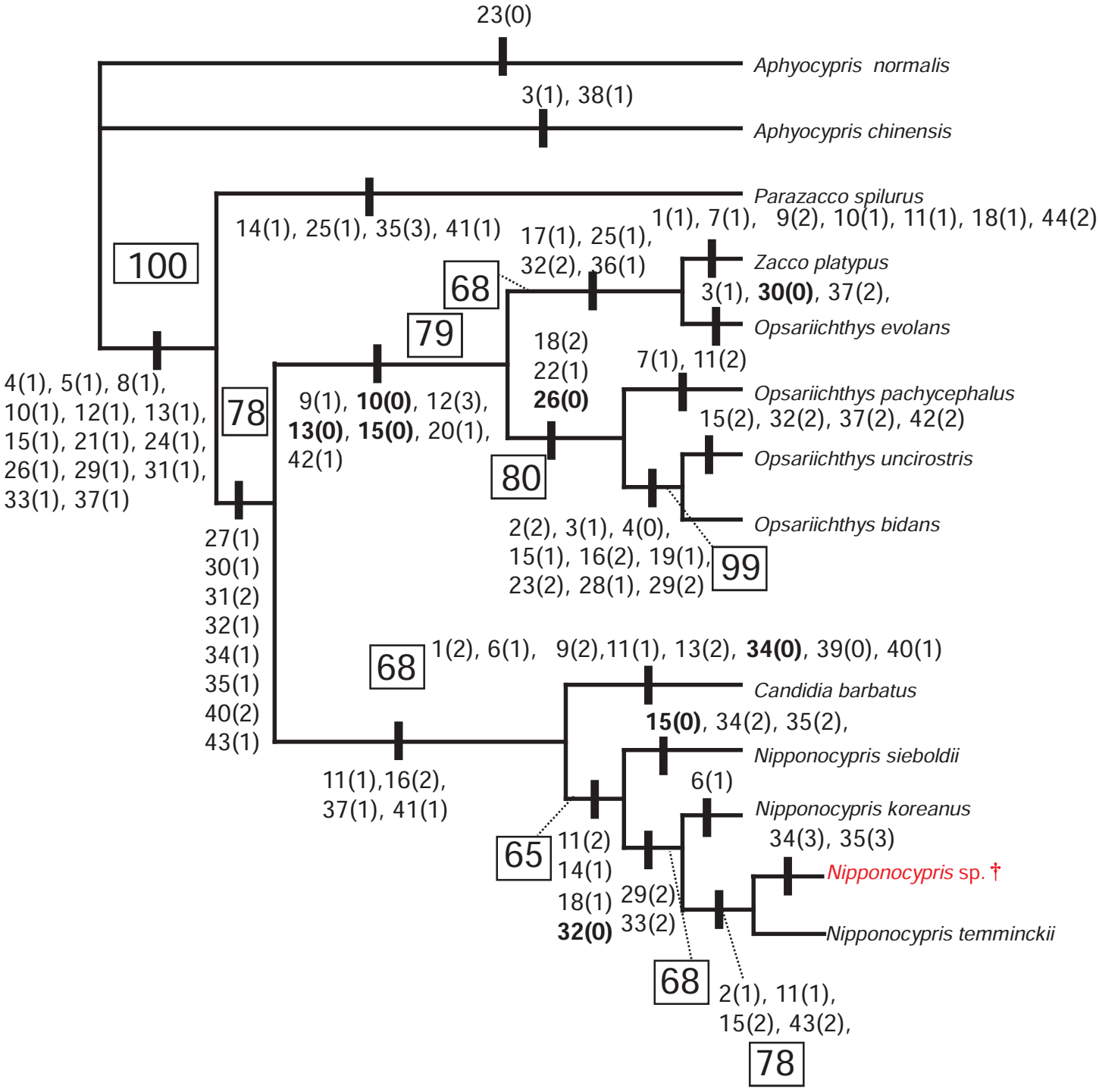

Figure 11. The single most parsimonious tree (length 95, CI =0.71, RI =0.74, RC =0.52) resulting from the character matrix of Table 1. Numbers to the right of the branches are the apomorphic states of each clades. Numbers to the box of branches are bootstrap values (%) based on 1,000 replicates

the paraphyletic group. The diagnostic characters of *Nipponocypris* are following combination of characters: dorsal fin rays iii, 7 – 9; anal fin rays iii, 8 – 10; pharyngeal tooth three rows (1 – 2, 3 – 4, 5 - 5, 2– 4, 1 – 2); and some external characters (Chen et al., 2008). In addition, the numbers of vertebrae of *Nipponocypris* are 42 – 45 (see Hosoya et al., 2003; Kim et al., 2006). Thus, in the present study, the present fossil specimens are included in the genus *Nipponocypris* based on the characters noted above them.

There have been few studies of morphological phylogenetic analysis of this group utilizing cladistic methods, although there are some molecular phylogenetic studies in the opsariichthines. The morphological phylogenetic analysis in the opsariichthines was discussed in the Chapter 1 in the present study.

A cladistic analysis of the data matrix of the Chapter 1 in this study with the data set of the present fossil species, *Nipponocypris*. sp. was carried out using PAUP* (v. 4.0 Beta, Windows Swofford 2003), Mesquite (v. 2.75 Windows, Maddison and Maddison, 2011) and MS – Excel.

Analysis of PAUP using the branch-and-bound search option resulted in one parsimonious tree (length 95, CI =0.71, RI =0.74, RC =0.52).

About 44% of the 43 data for *Nipponocypris* sp. are designated as question marks in the matrix. The characters were optimized to the tree using the ACCTRAN option. The parsimonious tree is shown in Fig. 11 with apomorphic states of each clades and boot strap values (%) for 1,000 replicates.

The clade of *Nipponocypris* + *Candida* is supported by four synapomorphies (the dorsal margin of the fourth infraorbitals bone is L shaped (11[1]); the anterior end of the dentary is not constricted (16[2]); the maximum number of the lateral line scales are 40 – 50 (37[1]); and the vertical stripes are bandlike and black (41[1])).

The clade of *Nipponocypris* forms monophyletic group, which supported by four synapomorphies (the dorsal margin of the fourth infraorbital bone is U shaped (11[2]); the fifth infraorbital bone has a projections (14[1]); the post - dorsal process on the maxilla is triangular (18[1]); and the maximum number of the supraneural bones is more than eight (32[0])).

The species of *N. koreanus* + *N. temminckii* + *N*. sp. have two synapomorphies (the maximum number of vertebrae are more than 44 (29[2]); and the number of the proximal pterygiophores of the anal fin is 11 (33[2])).

N. temminckii + *N*. sp. have four synapomorphies (the posterior lateral margin of the frontal is notched (2[1]); the dorsal margin of the fourth infraorbital bone is L shaped

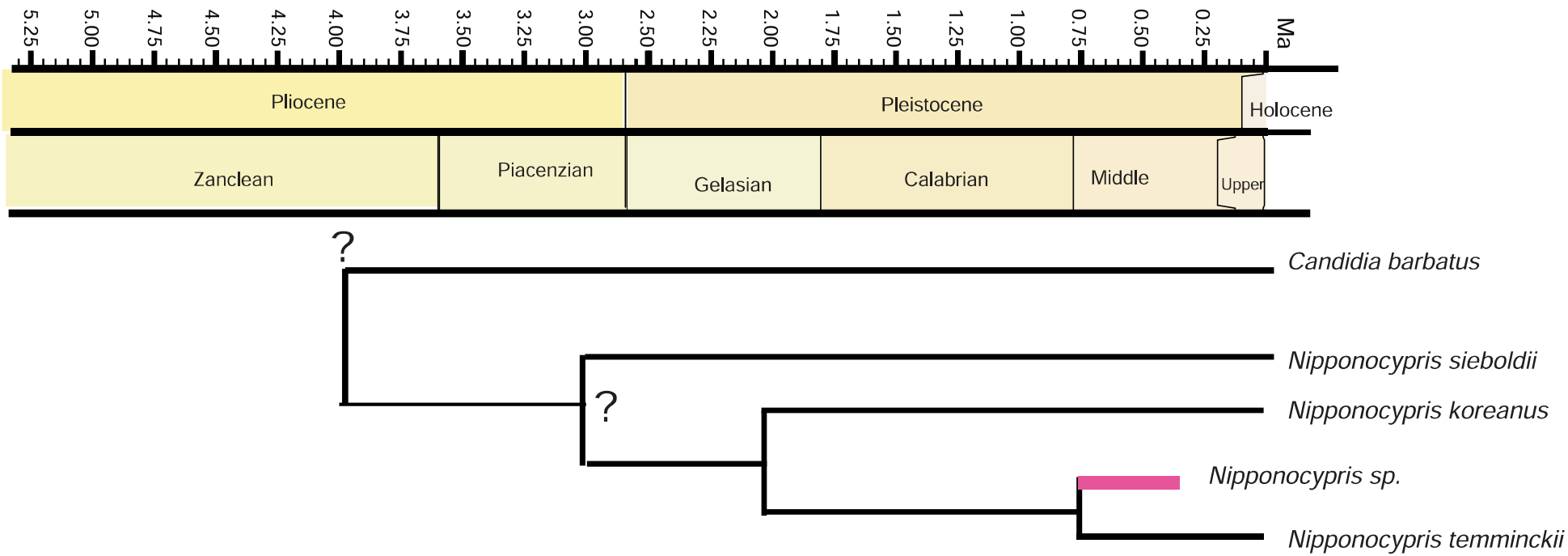

Figure 12. Phylogenetic relathionsip of the genus *Nipponocypris*. The divergence times of *Candidia barbatus* and *Nipponocypris sieboldii* are unknown. *Nipponocypris* sp. form the Middle Pleistocene Nogami Formation indicates that divergence time of *N. koreanus* is earlier than the Middle Pleistocene.

11[1]; the pores of the sensory canal of the dentary open posteroventral (15[2]); and the pectoral fins color is highly-colored yellow (43[2])), although the character states in the characters of numbers 15 and 43 are unknown in *N*. sp..

In addition to the characters mentioned above, this fossil species is distinguished from *N*. *temminckii* and the other species by the following combination of the characters; the wings of NPU2 and 3 are developed (34[3]; 35[3]); the notch at the frontal margin is weaker than that of *N*. *temmincki* (2[1]); and the shape of the dentary resembles *N*. *sieboldii* than *N*. *temminckii* and *N*. *koreanus* (see, figs 3, 5, 7, Plate 5).

On the other hand, the fossil species, *Zacco honggangensis* from the Buxin Formation, Sanshui Basin, China is related to *Z*. *platypus* with almost the same numbers of vertebrae and fin rays (Wang et al., 1981). *Zacco*. sp from the Eozen Formation in Ishikawa Prefecture is similar to *Z*. *platyps* with the shape of the dentary and the number of vertebrae. Therefore, it is possible that these fossils are closer *Zacco* than *Nipponocypris*.

As a result, the cladistic analysis and comparisons with the Recent species in the present study demonstrate that the fossil species, *Nipponocypris* sp. from Kusu basin is the first record of the genus *Nipponocypris* from the Cenozoic of East Asia and a sister species of *N*. *temminckii* (i.e., it is the stem taxon of *N*. *temminckii*).

Divergence time of the genus *Nipponocypris*

The divergence time of the genus *Nipponocypris* is uncertain, although it estimated by several previous molecular phylogenetic studies. In Lee et al. (1989), the estimated divergence time of *N*. *temminckii* (*Zacco temminckii* MM Type in Lee et al. 1989) from *N*. *koreanus* (*Zacco temminckii* MS Type in Lee et al. 1989) was 2.1Ma. Its estimation of divergence times was based on the general rate for mitochondrial genes (2% nucleotide substitution per million years) by Brown et al. (1979). Min and Yang (1991) estimated that the divergence of lineages *Nipponocypris* (*Zacco temminckii* group in Min and Yang, 1991) from *Candidia* took place 2.5Ma. This estimates based on Nei's (1972) genetic distance coefficients (D values) and Nei's protein calibrations (Nei, 1975). In Okazaki et al. (1991), the divergence time of *Nipponocypris sieboldii* (*Zacco temminckii* Type A in Okazaki et al. 1991) from *N*. *temminckii* (*Zacco temminckii* Type B in Okazaki et al. 1991) was 3Ma, it based on the Nei's formula (1975). Wu et al. (2007) hypothesized that the estimation for divergence times of mitochondrial D-loop

sequences was 6% per million years, and estimated that separation between *Candidia* and *Nipponocypris* (*Zacco temminckii* complex in Wu et al. 2007) was 0.75 Ma. Chen et al. (2011) hypothesized that the earliest possible divergence time of *Candidia* lineages was between 5 and 3 Ma. This estimates based on the Taiwan Island was lifted above sea level (Chemenda et al. 2001).

However, the molecular clock should not be applied to the estimation of divergence times, because evolutionary rates are never constant (Thorne and Kishino, 2002). Okazaki et al. (1991) remarked that the fossil record is important to set up a standard molecular clock for cyprinid fishes. Recently, molecular geneticists have suggested that the fossil record is important for molecular phylogenetic studies to calibrate divergence time (e.g. Thorne and Kishino, 2002; Inoue et al., 2010).

The fossil-bearing strata, the Nogami Formation, deposited the Middle Pleistocene based on the radiometric age of the basement igneous rock, and the Hiwaku Tephra in the uppermost part of the Nogami Formation as mentioned above. The results of the cladstic analysis in the present study suggest that the fossil species, *Nipponocypris* sp. from Kusu basin is the sister species of *N. temminckii*. If the fossil species, *Nipponocypris* sp. is the ancestor of *N. temminckii*, the appearance of the origin of *N. temminckii* is nearly Middle Pleistocene time. In addition, the line of evidence for this fossil suggests that the divergence time of *N. koreanus* is earlier than the *Nipponocypris* sp. (Fig. 12), which means the divergence time of *N. koreanus* is earlier than the Middle Pleistocene. It provides the first evidence of the divergence time of *N. temminckii* from *N. koreanus*. In addition, the *Nipponocypris* sp. from the Nogami Formation indicates that the genus *Nipponocypris* appeared in East Asia by the Middle Pleistocene at the latest.

Chapter 3

The Comment on paleobiogeography of the genus *Nipponocypris.* Summary, general overview and future research

Introduction

The Cyprinidae is the most diversified and species-rich freshwater fish family. It is one of good model creatures for comprehending the evolutionary history deriving the distribution and diversification of species (Zardoya and Doadrio, 1991). Because, the distribution and diversification patterns of the freshwater fishes relate in any way to geological history. For example, the changing freshwater system caused as the result of continental drift, uplift, sea level change, and the rest.

The opsariichthine group (Chen, 1982) is one of endemic cyprinid fishes in the East Asia, and has an interesting pattern of distribution. The group dwells in the continental area of Eastern Asia (China, Vietnam, Korea), and the Islands of Japan and Taiwan.

In Chapter 2, the fossil opsariichthines was described from the Nogami Formation of the Middle Pleistocene, Oita Prefecture, Japan, and discussed its phylogenetic position within the Recent opsariichthine group. It concluded that opsariichthines from the Nogami Formation is a member of the genus of *Nipponocypris*, and the divergence time of *N. koreanus* is earlier than the Middle Pleistocene.

The distribution of the Recent *Nipponocypris* shows the interesting pattern, which is restricted in the Southwest Japan and the Korean peninsula. However, there are no examinations of the biogeographic analysis of the genus *Nipponocypris*. The present Chapter examines biogeographic analysis of opsariichthine fishes based on the results and discussions of previous Chapters, and discusses the origin of distributions of the genus *Nipponocypris*. Moreover the results and discussions in this thesis are summarized, and future prospects are presented

Material and method

The present study traced the distribution pattern on a phylogenetic tree, using the parsimony algorithm implemented in Mesquite Ver. 2.73 (Maddison and Maddison,

2011). The phylogenetic tree is based on previous morphological phylogenetic analysis in Chapter 2.

The general distribution data of Recent opsariichthin fishes are based on Chen and Chu (1998), Chen and Chang (2005), Chen et al. (2008, 2009, 2011), Hosoya (2003, 2013), Kim et al. (2006), and Kottelat (2001). The present study zones the distribution range of opsariichthines into six regions and coding as follows: Southeastern China [0]; Northeastern China [1]; Taiwan [2]; Korea [3]; Japan [4]; and Southeastern Asia [5].

Result

Tracing on the distributional range on the cladogram of fossil and Recent opsariichthines is shown in Figure 1. The distributional area of the common ancestor of opsariichthines is estimated to be Southeastern China.

Within the clade of *Opsariichthys* + *Zacco*, the distribution ranges of *Zacco platypus* are Japanese Archipelago, Korean Peninsula, Northeastern to Southeastern China and Vietnam (Chen and Chu, 1998; Hosoya, 2013; Kottelat, 2001). *Opsariichthys bidens* is distributed in Korean Peninsula Northeastern to Southeastern China, and Vietnam (Chen and Chu, 1998), and *O. evolans* ranges Southeastern China and Taiwan Island (Chen and Chang, 2005; Chen et al. 2009). *O. uncirostris* is endemic to Japan (Hosoya, 2013), and *O. pachycephalus* is endemic to Taiwan (Chen and Chu, 1998; Chen and Chang, 2005; Chen et al. 2009). In this analysis, the distribution ranges of the ancestor of these species are reconstructed as being Southeastern China.

Within the clade of *Candidia* + *Nipponocypris, Candida* is endemic to Taiwan Island (Chen and Chu, 1998; Chen and Chang, 2005; Chen et al., 2008, 2011). The distribution ranges of *N. temminckii* are Japanese Archipelago and Korean Peninsula (Hosoya et al., 2003; Hosoya, 2013; Kim et al., 2006). *N. sieboldii* is endemic to Japan (Hosoya et al., 2003; Hosoya, 2013; Kim et al., 2006), and *N. koreanus* is endemic to Korean Peninsula (Kim et al., 2006). The result of the biogeographic analysis suggests that the origin of *Candidia* + *Nipponocypris* group is Taiwan, Southeastern China, or Japan.

Discussion

The origin of the distributions of *Nipponocypris temminckii*

The distribution of *Nipponocypris temminckii* shows an interesting pattern. *Nipponocypris temminckii* is distributed in the Southwest Japan and the southern part of

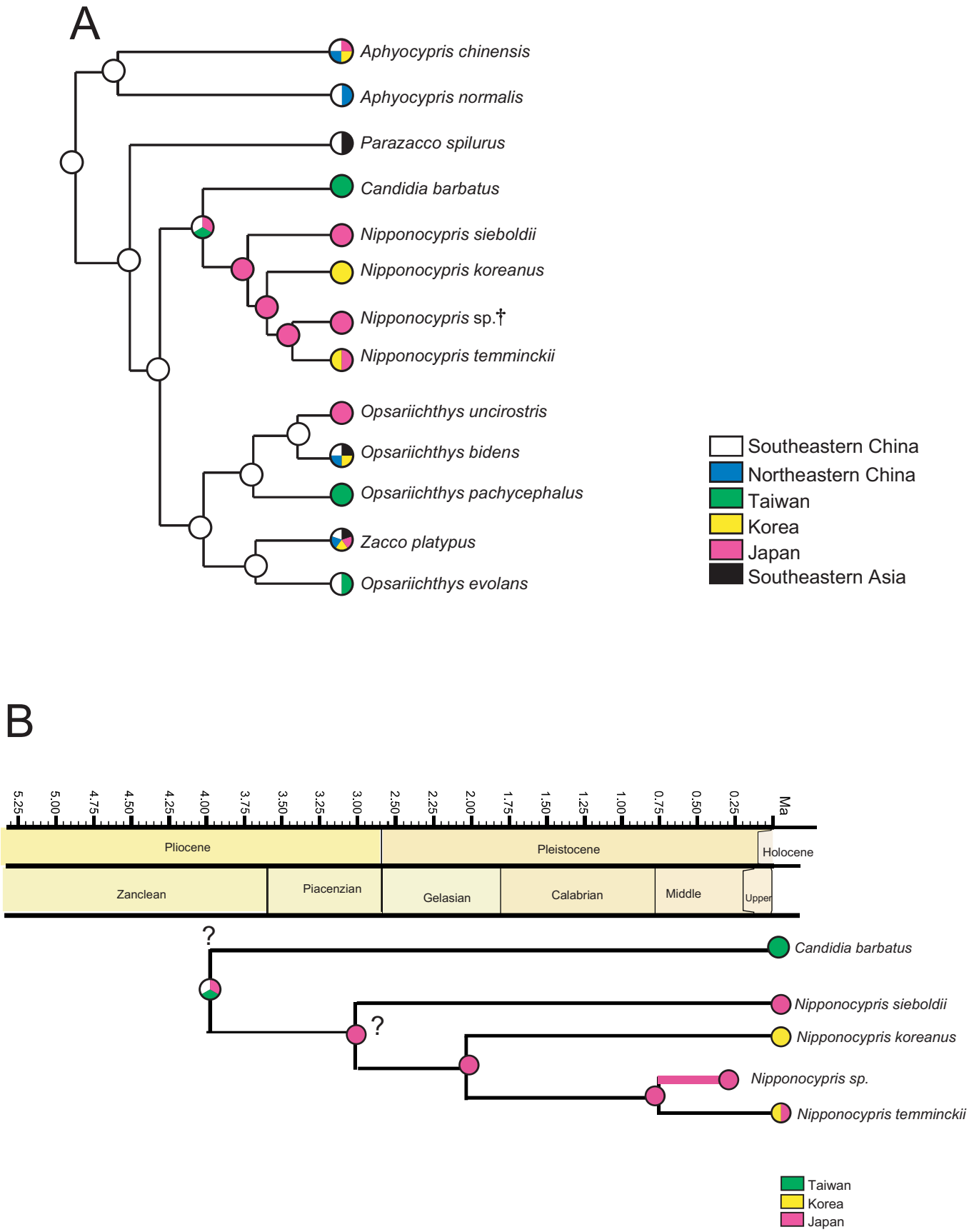

Figure 1. A: The biogeographic evolution within opsariichthines. The distribution data from Chen (1998), Chen and Zang, (2005) Hosoya et al. (2003, 2013), Kim et al. (2006), Chen et al. (2008); B: Phylogenetic relathionsip of the genus *Nipponocypris*. The divergence times of *Candidia barbatus* and *Nipponocypris sieboldii* are unknown. *Nipponocypris* sp. form the Middle Pleistocene Nogami Formation indicates that divergence time of *N. koreanus* is earlier than the Middle Pleistocene.

the Korean peninsula (Hosoya, 2003, 2013, Kim et al., 2006). Hence, it is possible that when the Korean peninsula was connected to the SW Japan, *N. temminckii* or their ancestor expanded the distribution after radiating from *Npponocypris* sp.(Fig. 2).

When the Nogami formation deposited or later (i.e., the Marine Isotope Stage (MIS) 16 (0.63Ma), 12 (0.43Ma), 10 (0.36－0.34Ma), 6 (0.13Ma), and 2 (0.02Ma)), the sea level significantly falled in the Japan sea (East sea) isolated from the Pacific Ocean based on the analysis of the ODP cores (Tada 1991). If the Japanese Islands connected to the East Asian Continent by land bridges, the sea-level fall of these stages were probably caused. Within these particular Marine Isotope Stages, MIS 16, 12, 10, 6, and 2 remain possible strongly that the land bridge was formed between the Japanese Islands and the adjacent Continent, and it was easy for terrestrial animals to move between the Japanese archipelago and the adjacent Continent of the East Asia. This hypothesis is supported by the following paleontological and geological data: The first occurrence of *Stegodon orientaris* in the Japanese Islands is stage 15.5. It suggests that *S. orientaris* immigrated to the Japanese Islands from the southeast area of the Asian Continent using the land bridge existing between the Japanese Islands and the Asian mainland at the stage16 (Konishi and Yoshikawa, 1999; Yoshikawa et al., 2007; fig13); the first occurrence of *Palaeoxodon naumanni* is stage 11 or somewhat later. It suggests that *P. naumanni* immigrated to The Japanese Islands from northern area of the Asian Continent using the land bridge at the stage 12 (Konishi and Yoshikawa, 1999; Yoshikawa et al., 2007; fig13); and in the cores of ODP site 797 (Tada et al., 1992), relatively-thick dark layers indicative of euxinic condition of deep sea water are better developed at the horizons correlative with the MIS 16, 12 and 2. It suggests that the Japan Sea (East Sea) isolated from the Yellow Sea and East China Sea, and increase in the flow of freshwater into the Japan Sea (Konishi and Yoshikawa, 1999; Tada et al., 1992; Tada, 1991; Yoshikawa et al., 2007). Thus, these stages are best timing for *Nipponocypris temminckii* or its ancestor to expand of the distribution between the Korean peninsula and the Japanese Islands. Possibly, stage 10, 8, and 6 were also best timing for to expand of the distribution between the Japanese Islands and the Korean peninsula.

Nipponocypris sp. is the first fossil species of the genus described from the East Asia, although it is necessary to find new specimens for detailed paleobiological implications. Furthermore, these discoveries demonstrate that this genus of the cyprinid fishes has dwelled in and has been endemic to Japan and Korea at least since Middle Pleistocene time.

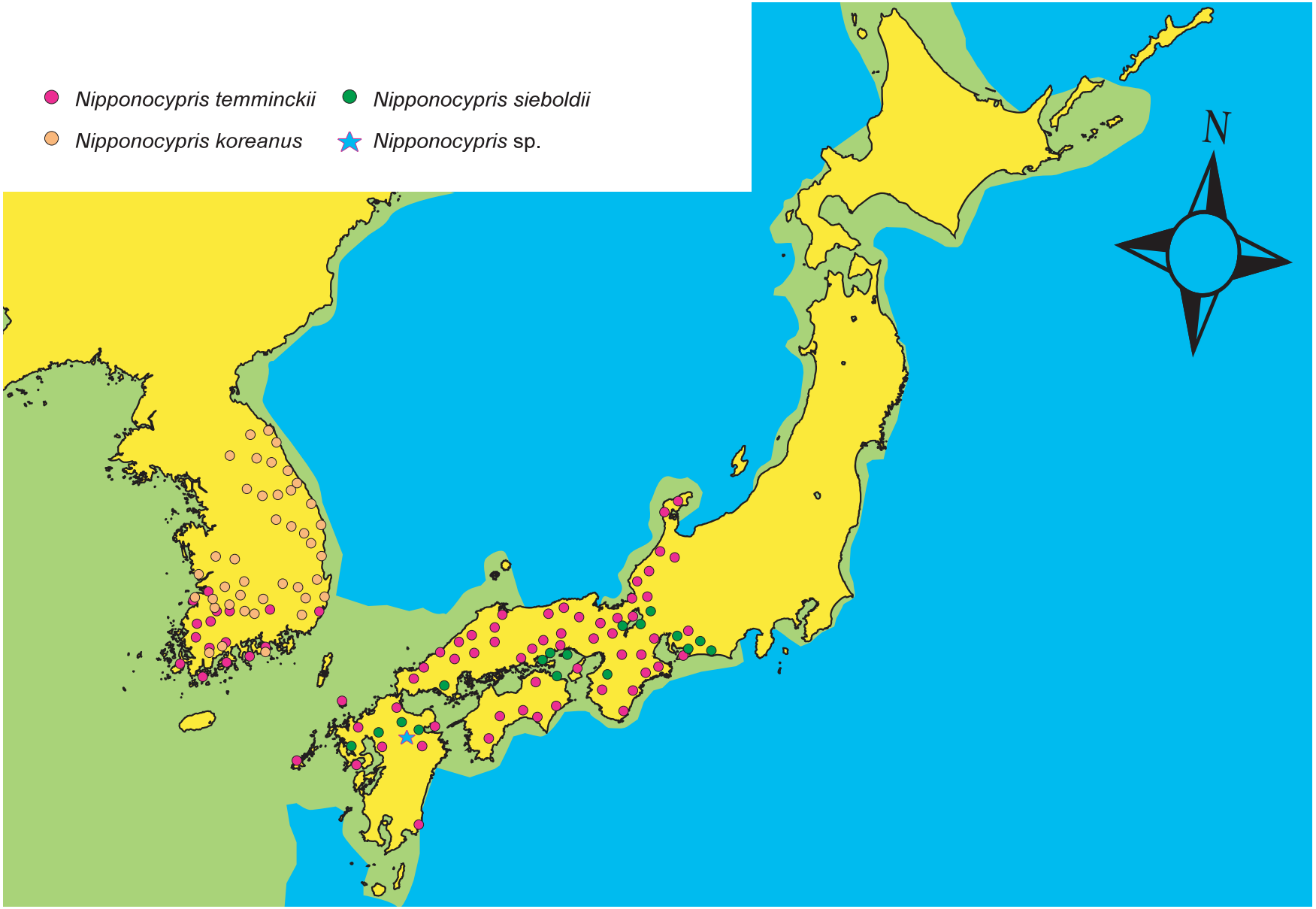

Figure 2. The paleomap in East Asia at the MIS 16 and 12 (modified from Konishi and Yoshikawa,1998, Yoshikawa et al., 2007) with protting the distribution of the fossil and Recent *Nipponocypris* (Hosoya et al., 2003; Kim et al,. 2005). The star mak is Kusu basin, which fossil occurence.

Summary, general overview and future research

In the Chapter 1 of the present study, the osteological and phylogenetic study of Recent opsariichthynes clarified as follows: the genus *Parazacco* is the most basal group within opsariichthynes and it is the sister group of the other opsariichthynes; the genus *Nipponocypris* forms monophyletic group and it is distinguished from the genus of *Candidia*; the genus *Opsariichthys* forms a paraphyletic group, and morophological phylogenetic data suggests that the relationship of *O. evolans* is closer *Z. platypus* than the other *Opsariichthys.* Because the morphological characters of *O. evolans* converges with *Zacco*. It reflects that the feeding habits of *O. evolans* are closely similar to *Zacco.*

In the Chapter 2, the fossils of "*Zacco*" collected from the Middle Pleistocene Nogami Formation, Oita Prefecture, Northern Kyushu, Japan was assigned to the genus *Nipponocypris* based on the osteological and phylogenetic data of the Chapter 1, and regarded as the first fossil record of the genus *Nipponocypris*. These discoveries demonstrate that divergence time of *N. koreanus* is earlier than the Middle Pleistocene, and the genus *Nipponocypris* appeared in East Asia by the Middle Pleistocene at the latest.

In the Chapter 3, the paleobiogeography of the genus *Nipponocypris* was discussed based on the phylogenetic data of the Chapter 2. This chapter refers about the potential that the origin of distribution of *Nipponocypris temminckii* is related glacio-eustatic sea-level change at the Quaternary, although it is necessary to find new fossil specimens for detailed paleobiological implications.

In the Nogami Formation, other freshwater fishes occurred as follows (Fig. 3): Salmonidae (*Oncorhyncus* cf. *O. masou*, or *O. rhodums* or sp.), Gobiidae (*Rhinogobius giurinus* and *R. brumous*), and Cyprinidae (*Hemibarbus barbus* or *Hemibarbus* sp., and *Acheilognathus lanceolata*), but phylogenetic relationships among these fossils and related Recent species are uncertain.

In the future research, it is necessary to make an osteological comparison between fossil specimens and Recent species, and to analyze cladistics, such as this study as the basis of discussion. These accumulations will clarify the freshwater fish fauna in the East Asia at the Quaternary, and clarify the evolution and paleobiogeographic patterns of freshwater fishes of the East Asia.

Recently, some molecular phylogenetic studies use the fossil record to constrain the divergence time estimations of Recent species (e.g. Nakatani et al., 2011; Wang et al.,

2007). Thorne and Kishino (2002) and Inoue et al. (2010) suggest that the fossil record is important for molecular studies to estimate of species divergence times.

Thus, such as the present paleoichthyological study provides a chronological basis for the molecular phylogenetic studies, and integrate paleoichthyology and molecular phylogeny might be going to make a huge contribution to the evolutionally and phylogenetic studies of fishes.

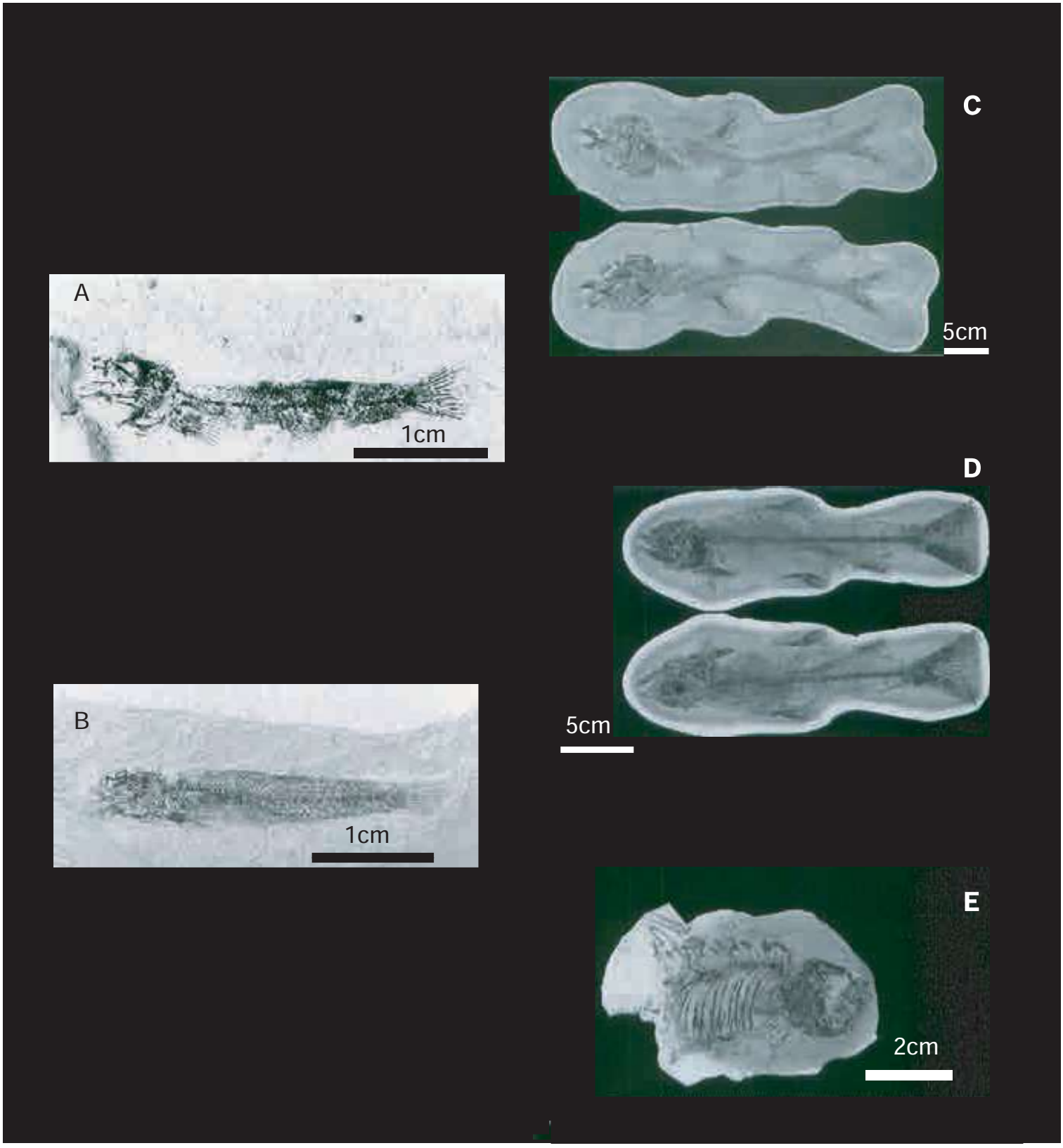

Figure 3. Photographs of the fossil fresh water fishes from the Middle Pleistocene Nogami Formation, Kusu Basin, Oita Prefecture, Japan (Yabumoto, 1987; Uyeno et al., 2000).

A. *Rhinogobius giurinus* (Rutter) from the Middle Pleistocene Nogami Formation. KMNH VP 100, 118 (from Yabumoto, 1987); B. *Rhinogobius brunneus* (Temminck and Schlegel). KMNH VP 100, 125 (from Yabumoto, 1987); C. *Hemibarbus* sp. (intermediate *H. barbus*×*H.* l*abeo*). KMNH VP 102, 064 (from Uyeno et al., 2000); D. *Oncorhynchus masou* subsp. KMNH VP 102, 026 (from Uyeno et al., 2000); E. *Acheilognathus* sp. KMNH VP 102, 044 (from Uyeno et al., 2000).

Acknowledgments

This doctoral thesis is submitted under my name. However, its completion would never have been possible without the support and guidance of many affiliated people.

I wish to express my sincerest appreciation to the members of my doctoral committee for their guidance and encouragement. I am greatly indebted to Professor Hiromichi Hirano (Waseda University), for his time, patience and suggestions throughout this study. He has taught me much about paleontology, stratigraphy, paleoenvironmentology, and all the rest since I was an undergraduate student (Unfortunately, he has been ill since May 2013. I wish for his recovery as soon as possible).

I am also thankful to Associate Professor Tohru Ohta (Waseda University) helped me with a constructive suggestions and comments in my studies. He took on the task of my chief examiner and kindly helped a set of procedures for my degree. My gratitude is expressed to Drs. Yoshitaka Yabumoto (Kitakyushu Museum of Natural History and Human History) and Teruya Uyeno (National Museum of Nature and Science, Tokyo) have supported me in paleoichthylogical investigation, looked over carefully my manuscript of this thesis, giving me valuable encouragement and guidance. Without their aid in the preparation of the manuscript, my difficulties with English could not have been overcome. And they have given me their knowledge of the enthusiasm for ichthyology and paleoichthlogy since I started studying the paleoichthyology at the master's course.

I am grateful to Professors Hideo Takagi (Waseda University), Yoshihide Ogasawara (Waseda University), and Ren Hirayama (Waseda University), for giving me valuable suggestions and comments. They have taught me much about the importance and interests of Earth Science and field work since I was an undergraduate student. I also deeply thank to Dr. Akinori Takahashi (Waseda University) looked over carefully my manuscript and gave me valuable advices. Without his support, my difficulties in English could not have been overcome.

I wish to thank the following people for the loan of specimens and the helps in field work: Dr. Makoto Manabe (National Museum of Nature and Science) for helping me in examining specimens of the National Museum of Nature and Science, Tokyo. Professor Tokuji Mitsugi (The Factory of Education and Welfare Science of Oita University) and the staff of Hakusan Kogyo Company, Oita for their help and support to my field work in Oita prefecture.

My considerable appreciation is expressed to the following for collecting and sending

fresh specimens for the skeletal preparations: KATSUAYU Company (Tokushima), Aqua Shop Ishi–to-izumi (pet shop, Suginami, Tokyo), Sanei Tansuigyo Company (Hyogo), Ichigaya Fish Center (Tokyo), and Sato Craft (Okayama) .Without their help, I could not collect and study about the Recent species.

I also deeply thank to Research Associates Dr. Mizuki Murakami (Waseda University) and Mr. Seike Kazuma (Waseda University), graduate and undergraduate students of Hirano Laboratory, and all of the staff of the Department of Earth Sciences, School of Education, Waseda University for their valuable discussions, supports, and warm encouragement.

References

Ashiwa, H. and Hosoya, K., 1998: Osteology of *Zacco pachycephalus*, sensu Jordan & Evermann (1903), with special reference to its systematic position. *Environmental Biology of Fishes*, vol. 52, p. 163–171.

Bănărescu, P. and Coad, B. W. 1991: Cyprinids of Eurasia. *In*, Winfield, I. J. and Nelson, J. S. *eds*., *Cyprinid Fishes: Systematics, Biology and Exploitation*, p. 127–155. Chapman & Hall, London.

Bleeker, P., 1859: Conspectus systematis Cyprinorum. Natuurkundig *Tijdschrift voor Nederlands-Indië*, vol. 20, p. 421–441.

Britz, R. and Conway, K. W. 2009: Osteology of *Paedocypris*, a miniature and highly developmentally truncated fish (Teleostei: Ostariophysi: Cyprinidae) . *Journal of Morphology*, vol. 270, p. 389–412.

Brown, W. M., George, M. and Willson, A. C., 1979: Rapid evolution of animal mitochondrial DNA. *Proceedings of the National Academy of Sciences*, vol. 76, p. 1967–1971.

Cavender, T. M. and Coburn, M. M., 1992: Phylogenetic relationships of North American Cyprinidae. *In*, Mayden R. L. ed., *Systematics, Historical Ecology and North American Freshwater Fishes*, p. 293–327. Stanford University Press, Stanford.

Chang, M. M. and Chen, G., 2008: Fossil Cypriniformes from China and its adjacent areas and their palaeobiogeographical implications. *Geological Society, London, Special Publications*, vol. 295, 337–350.

Chemenda, A. I., Yang, R. K., Stephan, J. F., Konstantinovskaya, E. A., and Ivanov, G. M., 2001: New results from physical modelling of arc-continent collision in Taiwan: evolutionary model. *Tectonophysics*, vol. 333, p.159–178.

Chen, X. L., Yue, P. Q. and Lin. R. D. 1984: Major groups within the family Cyprinidae and their phylogenetic relationships. *Acta Zootaxonomica Sinica*, vol. 9, p. 424–440. (*in Chinese with English abstract*).

Chen, I. S., Wu, J. H. and Hsu, C. H. 2008: The taxonomy and phylogeny of *Candidia* (Teleostei: Cyprinidae) from Taiwan, with description of a new species and comment on a new genus. *The Raffles Bulletin of Zoology*, vol. 19, p. 203–214.

Chen, I. S., Wu, J. H. and Huang, S. P. 2009: The taxonomy and phylogeny of the cyprinid genus *Opsariichthys* Bleeker (Teleostei: Cyprinidae) from Taiwan, with description of a new species. *Environmental Biology of Fishes*, vol. 86, p. 165–183.

Chen, F. W., Chia, H. H., Sin, C. L. and Hurng, Y. W. 2011: Systematics and

phylogeography of the Taiwanese endemic minnow *Candidia barbatus* (Pisces: Cyprinidae) based on DNA sequence, allozymic, and morphological analyses. *Zoological Journal of the Linnean Society*, vol. 161, p. 613–632.

Chen I. S. and Chang Y. C., 2005: *A photographic guide to the inlandwater fishes of Taiwan. Vol. I. Cypriniformes*, 284p. The Sueichan Press, Keelung.

Chen, I. Y., 1982: A revision of opsariichthine cyprinid fishes. *Oceanologi et Limnologia Sinica* vol. 13, p. 293–298. (*in Chinese with English abstract*).

Chen, Y. and Chu, X., 1998: Danioninae. *In*, Chu, X. and Chen, Y. ed., *The Fishes of Yunnan, China. I. Cyprinidae*, p. 19–41. Science Press, Beijiang.

Cuvier, G., 1817: *Le Règne Animal, Tome 2*, 532 p. Deterville, Paris.

Dai, Y. G. and Yang, J. X., 2003: Phylogeny and Zoogeography of the Cyprinid Hemicultrine Group (Cyprinidae: Cultrinae). *Zoological Studies*, vol.42, p. 73–92.

Dai, Y. G., Yang, J. X. and Chen Y. R., 2005: Phylogeny and Zoogeography of the Subfamily Cultrinae (Cyprinidae). *Acta Zootaxonomica Sinica*, vol.30, p. 213–233.

Dahdul, W. M., Lundberg, J. G., Midford, P. E., Balhoff, J. P., Lapp, H., Vision, T. J., Haendel, M. A., Westerfield, M. and Mabee, P. M., 2010: The teleost anatomy ontology: anatomical representation for the genomics age. *Systematic Biology*, vol. 59, p. 369–383.

Fang, F., M. Norén, M., Liao, T.Y., Källersjö, M., and Kullander, S.O., 2009: Molecular phylogenetic interrelationships of the south Asian cyprinid genera *Danio*, *Devario* and *Microrasbora* (Teleostei, Cyprinidae, Danioninae). *Zoologica Scripta*, vol. 38, p. 237–256.

Fujita, K., 1990: *The Caudal Skeleton of Teleostean Fishes*. Tokai University Press, Tokyo.

Gosline, W. A., 1973: Considerations regarding the phylogeny of cypriniform fishes, with special reference to structures associated with feeding. Copeia, vol. 1973, p. 761–776.

Günther, A., 1868: *Catalogue of the fishes in British Museum*, vol. 7, British Museum, London.

Günther, A., 1873: Report on a collection of fishes from China. *Annals and Magazine of Natural Histo*ry (Series 4), vol. 12, p. 239–250.

Greenwood, P. H., Rosen, D. E., Weitzman, S. H. and Myers, G. S., 1966. Phyletic studies of teleostean fishes, with a provisional classification of living forms. *Bulletin of the American Museum of Natural History*, vol. 131, p. 341–455.

Harrington, R.W., 1955: The osteocranium of American cyprinid fish *Notropis*

bifrenatus, with an annotated synonymy of teleost skull bones. *Copeia*, vol. 1995 p. 267–290.

Hayashi, Y., 1959: On the Non-marine Diatomite in Central Kyushu, Japan. *Journal of Geolical Society of Japan*, vol. 65, p. 519–587. (*in Japanese with English abstract*).

Hosoya, K .,H, Ashiwa., M, Watanabe, K, Mizuguti and T, Okazaki, 2003: *Zacoo sieboldii*, a species distinct from *Z. temminkii* (Cyprinidae). *Ichthyological Research*, vol. 50, p. 1—8.

Hosoya, K., 2013: Cyprinidae. *In*, Nakabo T. ed., *Fishes of Japan with pictoral keys to the species*. p 308–327, 1813–1819. Tokai University Press, Tokyo (*in Japanese*).

Hows, D. J., 1980: The anatomy, phylogeny and classification of bariliine cyprinid fishes. *Bulletin of the British Museum Natural History*, vol. 37, p. 129–198.

Hows, D. J., 1983: Additional notes on bariliine cyprinid fishes. *Bulletin of the British Museum Natural History*, vol. 45, p. 95–101.

Inoue, J., Donoghue, P. C. and Yang, Z. 2010: The Impact of the Representation of Fossil Calibrations on Bayesian Estimation of Species Divergence Times. *Systematic Biology*, vol. 59, p. 74–89.

Iwauchi, A. and Hase, Y., 1987: Late Cenozoic vegetation and paleoenvironment of northern and central Kyushu, Japan, Part 3 Southern part of Kusu Basin (Lower and Middle Pleistocene). *Journal of Geolical Society of Japan*, vol. 65, p. 469–489. (*in Japanese with English abstract*).

Iwauchi, A., 1998: Late Cenozoic vegetational and climatic changes in Kyushu, Japan. *Palaeogeography, Palaeoclimatology, Palaeoecology*, vol. 108, p. 229–280.

Ishihara, Y., Nkao, C., Sasaki, Y. and Yumi, M., 2010: Sediment-gravity flow deposits in lacustrine laminated diatomite: an example of the Pleistocene Nogami Formation. *The bulletin of Central Research Institute, Fukuoka University. Series C, Science and technology*, vol. 2, p. 19–33. (*in Japanese with English abstract*).

Jullis, L. M., Curtin, M and Tanaka, H., 2006: *Stephanodiscus kusuensis*, sp. nov. a new Pleistocene diatom from southern Japan. *Phycological Research* , vol. 54, p. 294–301.

Jordan, D. S. and Evermann, B. W., 1902: Note on a collection of fishes from the island of Formosa. *Proceedings of the National Museum*, vol. 25, p. 315–368.

Jordan. D. S. and Richardson, R. E., 1909: A catalog of the fishes of the island of Formosa, or Taiwan, based on the collections of Dr Hans Sauter. *Memories of the Carnegie Museum*, vol. 4, p. 159–204.

Kamata, H., 1985: Stratigraphy and eruption age of the volcanic rocks in the west of

Miyanoharu area, Kumamoto Prefecture-age and distribution of the volcanic activity of central-north Kyushu, Japan. *The Journal of the Geological Society of Japan*,vol. 91, p. 289–303 (in Japanese with English abstract).

Kamata, H. and Muraoka, H., 1982: K– Ar ages of the volcanic rocks in the central part of Oita Prefecture, southwestern Japan. *Bulletin of the Geological Survey of Japan*, vol. 33, p. 561–567. (*in Japanese with English abstract*).

Kawamura, K. and Hosoya, K., 1991: A modified staining technique for making a transport fish – skeletal specimen. *Bulletin of National Research Institute of Aquaculture*, no. 20, 11 – 18.

Kim, I. S., Oh, M. K. and Hosoya, K. 2005: A new species of cyprinid fish, *Zacco koreanus* with redescription of *Z. temminkii* (Cyprinidae) from Korea. *Korean Jurnal of Ichtyology*, vol. 17 p. 1–7.

Konishi, S. and Yoshikawa, S., 1999 Immigration times of the two proboscidean species, *Stegodon orientalis* and *Palaeoloxodon naumanni*, into the Japanese Islands and the formation of land bridge. *Earth Science* (*Chikyu Kagaku*), vol. 53, p. 125 – 134 (in Japanese with English abstract).

Kottelat, M., 2001: *Freshwater fishes of northern Vietnam*. 123p. World Bank, Washington, DC.

Lee, H. Y., Yang, S. Y., Chang, C. S., and Park C. S., Evolutionary Study on The Dark Chub (*Zacco temminckii*) VIII. Mitochondrial DAN Analysis of The Subfamily Danioninae (Pisces, Cyprinidae). *Korean Journal of Genetics*, vol. 11, p. 175– 187 (in Korean with English abstract).

Maddison, W. and Maddison, D., 2011: Mesquite: a modular system for evolutionary analysis, version 2.75 (software) http://mesquiteproject.org.

Min, M. S and Yang S. Y., 1991: Systematic study on the genus *Zacco* (Pisces, Cyprinidae), 2; Phylogenetic relationships of the genera *Zacco* and *Candidia*. *Korean Journal of Zoology*, vol. 34, p. 571– 584 (in Korean with English abstract).

Morimune, T., Ashiwa, H. and Hosoya, K., 2006: Comparison of the intestines of species in the cyprinid genera *Opsariichthys* and *Zacco*. Bulletin of the Biogeographical Society of Japan, vol. 61, p. 99 – 108.

Nakajima, T. 1975: A Fossil Cyprinid Fish preserved in Seison–kaku, Kanazawa City. *Earth Science*, vol. 29, p. 192–195. (*in Japanese with English abstract*).

Nakatani, M., Miya, M., Mabuchi, K., Saitoh, K. and Nishida, M., 2011: Evolutionary history of Otophysi (Teleostei), a major clade of the modern freshwater fishes: Pangaean origin and Mesozoic radiation. *BMC evolutionary biology*, vol. 11, 177.

Nei, M., 1972: Genetic distance between populations. *American naturalis*, vol. 106, p. 283 – 292.

Nei, M., 1975: *Molecular population genetics and evolution*, 288p. North-Holland, Amsterdam.

Nelson, J. S. 2006: *Fishes of the world. 4th Edition*, 601p. John Wiley Hoboken, New Jersey.

Okazaki, T., Watanabe, K., Mizuguchi, K., and Hosoya, K., 1991: Genetic differentiation between two types of dark chub, *Zacco temminckii*, in Japan. *Jpnese Journal of Ichthyology*, vol.38, p. 133–140

Regan, C. T., 1908: Description of new freshwater fishes from Lake Candidius, Formosa, collected by Dr. A. Moltrecht. *Annals and Magazine of Natural History*, vol. 8, p. 358–360.

Regan, C. T. 1911: The classification of the teleostean fishes of the order Ostariophysi: I. Cyprinoidea. *Annals and Magazine of Natural History*, vol. 8, p. 13–32.

Ridewood, W. G., 1905: On the cranial osteology of the fishes of the families Elopidae and Albulidae with remarks on the morphology of the skull in lower teleostean fishes generally. *Proceedings of the Zoological Society of London*, vol. 2, p. 35–81.

Shuto, T., 1953a: Younger Cenozoic History of Oita District, Kyushu (I). *Journal of Geolical Society of Japan*, vol. 59, p. 225–240. (*in Japanese*).

Shuto, T., 1953b: Younger Cenozoic History of Oita District, Kyushu (□). *Journal of Geolical Society of Japan*, vol. 59, p. 372–383. (*in Japanese with English abstract*).

Sibbing, F. A., 1992: Food capture and oral processing. *In*, Mayden R. L. ed., Systematics, *His torical Ecology and North American Freshwater Fishes*, p. 377–412. Stanford University Press, Stanford.

Swofford, D. L., 2003: *Phylogenetic Analysis Using Parsimony. Version 4.0 Beta*. Sinauer Associates, Sunderland, Massachusetts.

Takahashi, S and Okumura, S., 1996: Some Fish Fossils from the Nogami Formation of the Kusu Basin, Oita Prefecture. *The journal of the Society of Earthscientists and Amateurs of Japan*, vol. 45, p. 199 – 208. (*in Japanese*).

Tada, R., 1991: Accumulation rhythms and ocean fluctuations observed in Sea of Japan sediment. *Chikyu monthly*, vol. 13, p. 606 – 612(*in Japanese*).

Tada, R., Koizumi, 1., Cramp, A. and Rahman, A., 1992: Correlation of dark and light layers, and the origin of their cyclicity in the Quaternary sediments from the Japan Sea. *Proceedings of the Ocean Drilling Program, Scientific Results, Part 1*, vol.127/128, p. 577-601.

Tang, K. L., Agnew, M. K., Chen. W. J., Hirt, M. V., Sado, T., Schneider, L. M., Freyhof, J., Sulaiman, Z., Swartz, E., Vidthayanon, C., Miya, M., Saitoh, K., Simons, A. M., Wood, R. M. and Mayden, R. L. 2010: Systematics of the subfamily Danioninae (Teleostei: Cypriniformes: Cyprinidae). *Molecular Phylogenetics and Evolution*, vol. 57, p. 189–214.

Tang, K. L., Lumbantobing, D. N. and Mayden, R. L., 2013a : The hylogenetic Placement of *Oxygaster* van Hasselt, 1823 (Teleostei: Cypriniformes: Cyprinidae) and the Taxonomic Status of the Family Group Name Oxygastrinae Bleeker, 1860. *Copeia*, vol. 2013, p. 13–22.

Tang, K. L., Agnew, M. K., Chen. W. J., Hirt, M. V., Lumbantobing, D. N. Raley, M. E., Sado, T., Teoh, V. H., Yang, L., Bart, H. L., Harris, P. M., He, S., Miya, M., Saitoh, K., Simons, A. M., Wood, R. M. and Mayden, R. L., 2013b: Limits and phylogenetic relationships of East Asian fishes in the subfamily Oxygastrinae (Teleostei: Cypriniformes: Cyprinidae). *Zootaxa*, vol. 3681, p. 101–135.

Temminck, G. J and Schlegel, H., 1846: Pisces in Siebold's Fauna Japonica. Lugduni Batavorum, Leiden.

Thorne, J. L and Kishino, H. 2005: Estimation of divergence times frommolecular sequence data. *In*: Nielsen R. ed., *Statistical methods in molecular evolution*, p. 233–256. Springer-Verlag, New York.

Uyeno, T., 1984: Characters and methods of measuring and counting. *In*, Masuda, H. K., Amaoka, K., Araga, C., Uyeno, T. and Yoshino, T. *eds*., *The Fishes of the Japanese Archipelago*, p. xii–xvi. Tokai Univ Press, Tokyo.

Uyeno, T., Kimura, S. and Hasegawa Y., 1975: Freshwater fishes from Late Cenozoic depositsvin KusuvBasin, Oita Prefecture, Japan. *Memoirs of the National Science Museum*. vol. 8, p. 57–66. (*in Japanese*).

Uyeno, T., Yabumoto, Y., Kitabayashi, E., Aoki, T. and Tomida, Y., 2000: Paleoichthyological Survey of a Middle Pleistocene Lacustrine Bed in the Kusu Basin, Oita Prefecture, Kyushu, Japan. *Memoirs of the National Science Museum*. vol. 32, p. 55–75. (*in Japanese*).

Uyeno, T. and Sakamoto, K., 2005: *Pictorial guidebook to fish taxonomy. 2nd Edition*, 159p. Tokai University Press, Kanagawa, Japan.

Wang, J., Li, G. and Wang, J., 1981: The early Tertiary fossil fishes From San Shui and its adjacent basin, Guangdong. *Paleontology of Sinica,* vol.160, p. 1–100 (*in Chinese with English summary*).

Wang, X., Li, J., & He, S. (2007). Molecular evidence for the monophyly of East Asian

groups of Cyprinidae (Teleostei: Cypriniformes) derived from the nuclear recombination activating gene 2 sequences. *Molecular phylogenetics and evolution*, vol. 42, p. 157–170.

Weitzman S. H., 1962: The osteology of *Brycon meeki*, a generalizedcharacid fish, with an osteological definition of the family. *Stanford Ichthyolgical Bulletin*, vol. 8, p. 1–77.

Yamada, K., Tagami, T. and Kamata, H. 2006: K–Ar geochronology of rhyolitic rocks in the Hohi volcanic zone, central Kyushu, Japan. *Journal of Asian Earth Sciences*, vol. 27, p. 430–436.

Yabumoto, Y., 1987: Pleistocene gobiid fishes of the genus *Rhinogobius* from Kusu Basin, Oita Prefecture, Japan. *Bulletin of the Kitakyushu museum of natural history*, vol. 7, p. 111 – 119.

Yoshikawa, S., Kawamura, S. and Taruno, H., 2007: Land bridge formation and proboscidean immigration into the Japanese Islands during the Quaternary. *Journal of Geosciences, Osaka City University*, vol. 50, p. 1 – 6.

Zardoya, R. and Doadrio, I., 1999: Molecular Evidence on the Evolutionary and Biogeographical Patterns of European Cyprinids. Journal of Molecular Evolution, vol. 49, p. 227 – 237.

Appendix 1: Definitions of Characters used in Cladistic Analysis

Character 1

The sensory canal of the parietals.—Character states: (0) not tangent to the edge of the other one, and its length is longer than the half the width of the parietal in the genus *Nipponocypris* (Plates 1–2 to 1–4), *Opsariichthys* (Plates 1–6 to 1–8), and *Parazacco* (Plates 1–9); (1) not tangent to the edge of the other one, and its length is shorter than the half the width in *Zacco platypus* (Plate 1–1); (2) contacts with each other in *Candidia barbatus* (Plate 1–5).

Character 2

The posterior lateral margin of the frontal.—Character states: (0) smooth (e.g. *Z. platypus*, Plate 1–1; *C. barbatus*, Plate 1–5); (1) convex in *O. uncirostris* and *O. biden*s (Plates 1–7 to 1–8); (2) notched in *N. temminckii* and *Nipponocypris* sp. (Plate 1–2, Chapter 2–Figure 3).

Character 3

The intercalar.—Character states: (0) not has a projection in the genera *Nipponocypris* (Plates 1–2 to 1–4), *Candidia* (Plate 1–5), and *Parazacco* (Plates 1–9); (1) has a projection in *Z. platypus* (Plates 1–1, 2–1), *O. evolans*, *O. uncirostris*, and *O. bidens* (Plates 1–6 to 1–8, 2–6 to 2–8).

Character 4

The width of supraorbital.—Character states: (0) almost the same width as half the length of these in *O. uncirostris* (Plates 1–7, 2–7); (1) narrower than half the length of these (e.g. the genus *Parazacco*, Plates 1–9, 2–9).

Character 5

The sensory canal on the lacrimal.—Character states: (0) straight; (1) curved in all of opsariichthin fishes (Plates 3–1 to 9) (modified from Dai and Yang, 2003; character no. 9).

Character 6

The pores of the sensory canal on the lacrimal.—Character states: (0) 2 pores (e.g. *Z*. *platypus*, Plate 3-1); (1) has 3 pores in *N*. *koreanus* (Plate 3–4) and *Candidia* (Plate 3–5) (modified from Dai and Yang, 2003; character no. 11).

Character 7

The anterior half of the second infraorbital.—Character states: (0) remains as wide as its posterior half of these (e.g. *N*. *koreanus*, Plate 3–4; *O*. *uncirostris*, Plate 3–7); (1) gradually narrows from its anterior end to its posterior end (e.g. *Z*. *platypus*, Plate 3-1) (Dai and Yang, 2003; character no. 12).

Character 8

The third infraorbital.—Character states: (0) significantly wider than the fourth; (1) almost as wide as the fourth in all of opsariichthine fishes (Plates 3–1 to 9) (modified from Dai and Yang, 2003; character no. 13).

Character 9

The width of the fourth infraorbital.—Character states: (0) remains the same width in the genera *Nipponocypris* (Plate 3–2 to 3–4) and *Parazacco* (Plate 3–9); (1) abruptly widens below at its middle point in the genus *Opsariichthys* (Plates 3–6 to 3–8); (2) gradually widens from its anterior end to its posterior end in *Candidia* (Plate 3–5) and *Z*. *platypus* (Plate 3–1).

Character 10

The posterodorsal margin of the fourth infraorbitals bone.—Character states: (0) not has a nub in the genus *Opsariichthys* (Plates 3–6 to 3–8); (1) has a nob (e. g. the genus *Nipponocypris*, Plates 3–2 to 3–4).

Character 11

The posterior margin of the fourth infraorbital bone.—Character states: (0) straight (e.g. *O*. *uncirostris*, Plate 3–7); (1) L – shaped (e.g. *Candidia*, Plate 3–5); (2) U– shaped in *N*. *sieboldii* and *N*. *koreanus* (Plates 3–3 and 3–4).

Character 12

The fifth infraorbitals bone.—Character states: (0) absent; (1) approximately quadrangle; (2) approximately triangle; (3) tube shaped in the genus *Opsariichthys* (Plates 3–6 to 3–8).

Character 13

The width of the fifth infraorbitals bone.—Character states: (0) narrower than the length of these in the genus *Opsariichthys* (Plates 3–6 to 3–8) and *Z. platypus* (Plate 3–1); (1) approximately the same as the length of these in the genus *Nipponocypris* (Plate 3–2 to 3–4) and *Parazacco* (Plate 3–9); (2) wider than the length of these in *Candidia barbatus* (Plate 3–5).

Character 14

The fifth infraorbital bone.—Character states: (0) not has a projection (e.g. the genus *Opsariichthys*, Plates 3–6 to 3–8); (1) has a projection (e.g. the genus *Nipponocypris*, Plates 3–2 to 3–4).

Character 15

The pores of the dentary sensory canals are opedned.—Character states: (0) laterally (e.g. *Z. platypus*, Plate 5 – 1; *N. sieboldii* Plate 5 – 3); (1) ventrally (e.g. *N. koreanus*, Plate 5 – 4); (2) posteroventrally in *N. temminckii* (Plate 5 – 7) and *O. uncirostris* (Plate 5 – 7).

Character 16

The anterior end of the dentary.—Character states: (0) constricted in *Z. platypus* (Plate 5 – 1), *O.* evolans (Plate 5 – 6), and *Parazacco* (Plate 5–9) and ; (1) hooked in *O. uncirostris* (Plate 5 – 7) and *O. bidens* (Plate 5 – 8); (2) not constricted in the genus *Nipponocypris* (Plates 5–2 to 5–4).

Character 17

The dorsal margin of the dentary.—Character states: (0) straight (e.g. the genus *Nipponocypris*, Plates 5–2 to 5–4); (1) downward in *Z. platypus* (Plate 5 – 1) and *O.* evolans (Plate 5 – 6).

Character 18

The post–dorsal process of the maxilla.—Character states: (0) a trapezoidal shaped in *Candidia barbatus* (Plate 4 – 5) and *Parazacco spilurus* (Plate 4 – 9); (1) a triangular shaped (e.g. the genus *Nipponocypris*, Plates 4 – 2 to 4 – 4), *O*. evolans, Plate 5 – 6); (2) dorsally – convex or straight, and that the dorsal margin of these elongates to the posterior part in *O*. *uncirostris* and *O*. *bidens* (Plates 4 – 7 to 4 – 8).

Character 19

The ventral margin of the premaxilla.—Character states: (0) straight (e.g. *Z*. *platypus*,Plate 5 – 1); (1) convex in *O*. *uncirostris* and *O*. *bidens* (Plates 4 – 7 to 4 – 8).

Character 20

The posterior margin of the opercule.—Character states: (0) concave (e.g. *Parazacco spilurus*, Plates 6 – 9 and 7 – 9); (1) convex or straight in *Z*. *platypus* (Plates 6 – 1 and 7 – 1) and the genus *Opsariichthys* (Plates 6 – 6 to 6 – 8, Plates 7 – 6 to 7 – 8) (modified from Dai and Yang, 2003; character no. 21).

Character 21

The quadrate – pterygoid fenestra (Greenwood et al., 1966).—Character states: (0) absent; (1) presents in all of opsariichthine fishes (Plates 6 – 1 to 7 – 9).

Character 22

The metapterygoid.—Character states: (0) not constricted (e.g. *Z*. *platypus*, Plates 6 – 1 and 7 – 1); (1) constricted to the H – shaped in *O*. *uncirostris* and *O*. *bidens* (Plates 6 – 7 to 6 – 8, Plates 7 – 7 to 7 – 8).

Character 23

The quadrate.—Character states: (0) snicked to a V – shaped; (1) snicked to a L – shaped or weakly U shaped, and the upper arm of the quadrate is shorter than the lower arm (e.g. *Z*. *platypus*, Plates 6 – 1 and 7 – 1); (2) snicked a strong U – shaped, the upper arm of the quadrate elongates, and the length of the upper arm is the same size in length of the lower arm in *O*. *uncirostris* and *O*. *bidens* (Plates 6 – 7 to 6 – 8, Plates 7 – 7 to 7 – 8).

Character 24

The symplectic.—Character states: (0) contacts with the ventral margin of the metapterygoid; (1) not contacts with the ventral margin of the metapterygoid in all of opsariichthine fishes (Plates 6 – 1 to 7 – 9).

Character 25

The posterior margin of the urohyal.—Character states: (0) smooth (e.g. *Candidia barbatus* Plate 9 – 5); (1) snicked in *Z*. *platypus* (Plates 9 – 1), *O*. *evolans* (Plates9 – 6) and *Parazacco spilurus* (Plate 9– 9).

Character 26

The urohyal.—Character states: (0) slender at the ventral view in *O*. *uncirostris* and *O*. *bidens* (Plates 9 – 7 to 9 – 9); (1) the posterior region is wider than the anterior one in the ventral view (e.g. *Parazacco spilurus*, Plates 9 – 9).

Character 27

The pharyngeal tooth.—Character states: (0) 2 rows in *Parazacco spilurus* (Plates 8 – 9); (1) 3 rows (e.g. *Z*. *platypus*, Plates 8 –1) (modified from Dai and Yang, 2003; character no. 24).

Character 28

The anterior branch of the pharyngeal bone.—Character states: (0) as long as its posterior branch (e.g. *Candidia barbatus* Plate 8 – 5); (1) longer than its posterior branch in *O*. *uncirostris* and *O*. *bidens* (Plates 8–7 to 8–8) (Dai and Yang, 2003; character no. 26).

Character 29

The maximum number of the vertebrae.—Character states: (0) less than 40; (1) 40-43 or less (e.g. *O*. *pachycephalus*, see Chen et al., 2009); (2) more than 44 (e.g. *N*. *temminckii* and *N*. *koreanus*, Hosoya et al., 2003; Kim et al., 2006)

Character 30

The end of the dorsal branch of the parapophysis of the 4th vertebra.—Character states: (0) tipped (e.g. *Parazacco spilurus*, Plate 12 – 9); (1) blunt (e.g. *O. bidens*, Plate 12 – 8) (modified from Dai and Yang, 2003; character no. 42).

Character 31

The fouth supraneural bone.—Character states: (0) convex ventrally or sigmoid; (1) snicked at the anterior margin in *Parazacco spilurus* (Plate 14 – 9); (2) approximately quadrangle (e.g. the genus *Nipponocypris*, Plates 14 – 2 to 14 – 4) (modified from Dai et al. 2005; character no. 56).

Character 32

The maximum number of the supraneural bones.—Character states: (0) more than 8 in the genus *Nipponocypris* (Plates 14 – 2 to 14 – 4) and *Parazacco spilurus* (Plate 14 – 9); (1) 7 (e.g.*O. bidens* Plate 14 – 5); (2) 6 (e.g. *Z. platypus*, Plates 14 – 1) (modified from Dai et al. 2005; character no. 57).

Character 33

The number of the proximal pterygiophores of the anal fin.—Character states: (0) 9; (1); 10 (e.g. the genus *Opsariichthys*, Plates 15 – 6 to 15 – 8); (2) 11 in *N. temminckii* (Plate 15 – 2) and *N. koreanus* (Plates 15 – 4); (3); 12 in *Parazacco spilurus* (Plate 15 – 9).

Character 34

The wing of the neural spine of the preural centrum 2.—Character states: (0) do not extend over the middle of the neural spine of the preural centrum 2, or reach to the middle in *Candidia barbatus* (Plate 13 – 5) and *Parazacco spilurus* (Plate 13 – 9); (1) extends over the middle of the neural spine of the preural centrum 2 (e.g. *N. temminckii*, Plate 13 – 2); (2) projected at the base in *N. sieboldii* (Plate 13 – 3); (3) extends to the top of the neural spine of the preural centrum 2 in *Nipponocypris* sp.(Chapter 2 – Figure 7)

Character 35

The wing of the neural spine of the preural centrum 3.—Character states: (0) do not extend over the middle of the neural spine of the preural centrum 3, or reach to the middle in *Parazacco spilurus* (Plate 13 – 9); (1) extends over the middle of the neural

spine of the preural centrum 3 (e.g. *Z. platypus*, Plate 13 – 1); (2) projected at the base in *N. sieboldii* (Plate 13 – 3); (3) extends to the top at the neural spine of the preural centrum 3 in *Nipponocypris* sp.(Chapter 2 – Figure 7).

Character 36

The anterodorsal margin of the cleithrum.—Character states: (0) straight (e.g. the genus *Nipponocypris*, Plates 15 – 2 to 15 – 4); (1) convex in *Z. platypus* (Plate 16 – 1) and *O. evolans* (Plate 13 – 6) (Dai and Yang, 2003; character no. 30).

Character 37

The maximum number of the lateral line scale.—Character states: (0) less than 40 in the genus *Aphyocypris* see (Chen and Chu, 1998); (1) 40-50 or less (e.g. *O. evolans*, see Chen et al., 2009); (2) more than 51 (e.g. the genus *Nipponocypris*, see Hosoya et al., 2003; Kim et al., 2006)

Character 38

The lateral line scales.—Character states: (0) complete in *Aphyocypris normalis* and all of opsariichthines (see Chen and Chu, 1998; Chen et al., 2009; Hosoya, 2013; Kim et al., 2006;); (1) incomplete in *Aphyocypris chinensis* (see Chen and Chu, 1998, Fig. 27).

Character 39

The maxillary barbels. —Character states: (0) present in *Candidia barbatus* (e.g. Chen and Chu, 1998, Fig. 12); (1) absent (e.g. the genus *Nipponocypris*, Hosoya et al., 2003, figs. 1 and 3; Kim et al., 2006 figs. 1 and 2). (Cavender and Coburn, 1992; character no. 41)

Character 40

The ventral keel. —Character states: (0) run on the pelvic fin base to anus; (1) absent on the anterior half region from the pelvic fin base to the anus in ; (2) absent or indistinct (e.g. the genus *Nipponocypris*, see Chen et al., 2008).

Character 41

The vertical stripes. —Character states: (0) absent or blurred; (1) an irregular pattern and black in *Parazacco spilurus* (see Chen et al., 2008, Fig. 2); (2) a bandlike and black in the genera and *Nipponocypris* and *Candidia* (see Chen et al., 2008).

Character 42

The crossband of the body. —Character states: (0) absent; (1) a bandlike (e.g. *O. pachycephalus*, see Chen et al., 2009, Fig. 4); (2) an irregular pattern and blue (e.g. *Z. platypus*, see Chen and Chang, 2005)

Character 43

The color of pectoral fins.—Character states: (0) transparent or lightness yellow; (1) yellow, and orange or red at the margin (e.g. *N. sieboldii*, see Hosoya et al., 2003); (2) yellow (*N. temminckii*, see Hosoya et al., 2003).

Appendix 2: Plates

Plate 1 – 1. The cranium of *Zacco platypus*. A, dorsal view; B, lateral view.

Plate 1 – 2. The cranium of *Nipponocypris temminckii*. A, dorsal view; B, lateral view.

Plate 1 – 3. The cranium of *Nipponocypris sieboldii*. A, dorsal view; B, lateral view.

Plate 1 – 4. The cranium of *Nipponocypris koreanus*. A, dorsal view; B, lateral view.

Plate 1 – 5. The cranium of *Candidia barbatus*. A, dorsal view; B, lateral view.

Plate 1 – 6. The cranium of *Opsariichthys evolans*. A, dorsal view; B, lateral view.

Plate 1 – 7. The cranium of *Opsariichthys uncirostris*. A, dorsal view; B, lateral view.

Plate 1 – 8. The cranium of *Opsariichthys bidens*. A, dorsal view; B, lateral view.

Plate 1 – 9. The cranium of *Parazacco spilurus*. A, dorsal view; B, lateral view.

Plate 2 – 1. The cranium of *Zacco platypus*. A, ventral view; B, posterior view. fm = foramen magnum.

Plate 2 – 2. The cranium of *Nipponocypris temminckii*. A, ventral view; B, posterior view. fm = foramen magnum.

Plate 2 – 3. The cranium of *Nipponocypris sieboldii*. A, ventral view; B, posterior view. fm = foramen magnum.

Plate 2 – 4. The cranium of *Nipponocypris koreanus*. A, ventral view; B, posterior view. fm = foramen magnum.

Plate 2 – 5. The cranium of *Candidia barbatus*. A, ventral view; B, posterior view. fm = foramen magnum.

Plate 2 – 6. The cranium of *Opsariichthys evolans*. A, ventral view; B, posterior view. fm = foramen magnum.

Plate 2 – 7. The cranium of *Opsariichthys uncirostris*. A, ventral view; B, posterior view. fm = foramen magnum.

Plate 2 – 8. The cranium of *Opsariichthys bidens*. A, ventral view; B, posterior view. fm = foramen magnum.

Plate 2 – 9. The cranium of *Parazacco spilurus*. A, ventral view; B, posterior view. fm = foramen magnum.

Plate 3 – 1. The infraorbital bones of *Zacco platypus.* A, outside view; B, inside view.

Plate 3 – 2. The infraorbital bones of *Nipponocypris temminckii.* A, outside view; B, inside view.

Plate 3 – 3. The infraorbital bones of *Nipponocypris sieboldii.* A, outside view; B, inside view.

Plate 3 – 4. The infraorbital bones of *Nipponocypris koreanus.* A, outside view; B, inside view.

Plate 3 – 5. The infraorbital bones of *Candidia barbatus.* A, outside view; B, inside view.

Plate 3 – 6. The infraorbital bones of *Opsariichthys evolans.* A, outside view; B, inside view.

Plate 3 – 7. The infraorbital bones of *Opsariichthys uncirostris.* A, outside view; B, inside view.

Plate 3 – 8. The infraorbital bones of *Opsariichthys bidens.* A, outside view; B, inside view.

Plate 3 – 9. The infraorbital bones of *Parazacco spilurus.* A, outside view; B, inside view.

Plate 4 – 1. The upper jaws of *Zacco platypus*. A, outside view; B, inside view. nc = neurocranial condyle, plw = palatinal wing, pmw = premaxillary wing.

Plate 4 – 2. The upper jaws of *Nipponocypris temminckii*. A, outside view; B, inside view. nc = neurocranial condyle, plw = palatinal wing, pmw = premaxillary wing.

Plate 4 – 3. The upper jaws of *Nipponocypris sieboldii*. A, outside view; B, inside view. nc = neurocranial condyle, plw = palatinal wing, pmw = premaxillary wing.

Plate 4 – 4. The upper jaws of *Nipponocypris koreanus*. A, outside view; B, inside view. nc = neurocranial condyle, plw = palatinal wing, pmw = premaxillary wing.

Plate 4 – 5. The upper jaws of *Candidia barbatus*. A, outside view; B, inside view. nc = neurocranial condyle, plw = palatinal wing, pmw = premaxillary wing.

Plate 4 – 6. The upper jaws of *Opsariichthys evolans*. A, outside view; B, inside view. nc = neurocranial condyle, plw = palatinal wing, pmw = premaxillary wing.

Plate 4 – 7. The upper jaws of *Opsariichthys uncirostris*. A, outside view; B, inside view. nc = neurocranial condyle, plw = palatinal wing, pmw = premaxillary wing.

Plate 4 – 8. The upper jaws of *Opsariichthys bidens*. A, outside view; B, inside view. nc = neurocranial condyle, plw = palatinal wing, pmw = premaxillary wing.

Plate 4 – 9. The upper jaws of *Parazacco spilurus*. A, outside view; B, inside view. nc = neurocranial condyle, plw = palatinal wing, pmw = premaxillary wing.

Plate 5 – 1. The lower jaws of *Zacco platypus*. A, outside view; B, inside view. cp = coronoid process, Mr = Meckelian ridge, saf = suspensorial articulation facet.

Plate 5 – 2. The lower jaws of *Nipponocypris temminckii*. A, outside view; B, inside view. cp = coronoid process, Mr = Meckelian ridge, saf = suspensorial articulation facet.

Plate 5 – 3. The lower jaws of *Nipponocypris sieboldii*. A, outside view; B, inside view. cp = coronoid process, Mr = Meckelian ridge, saf = suspensorial articulation facet.

Plate 5 – 4. The lower jaws of *Nipponocypris koreanus*. A, outside view; B, inside view. cp = coronoid process, Mr = Meckelian ridge, saf = suspensorial articulation facet.

Plate 5 – 5. The lower jaws of *Candidia barbatus*. A, outside view; B, inside view. cp = coronoid process, Mr = Meckelian ridge, saf = suspensorial articulation facet.

Plate 5 – 6. The lower jaws of *Opsariichthys evolans*. A, outside view; B, inside view. cp = coronoid process, Mr = Meckelian ridge, saf = suspensorial articulation facet.

Plate 5 – 7. The lower jaws of *Opsariichthys uncirostris*. A, outside view; B, inside view. cp = coronoid process, Mr = Meckelian ridge, saf = suspensorial articulation facet.

Plate 5 – 8. The lower jaws of *Opsariichthys bidens*. A, outside view; B, inside view. cp = coronoid process, Mr = Meckelian ridge, saf = suspensorial articulation facet.

Plate 5 – 9. The lower jaws of *Parazacco spilurus*. A, outside view; B, inside view. cp = coronoid process, Mr = Meckelian ridge, saf = suspensorial articulation facet.

Plate 6 – 1. Outsider view the opercular bones and supensorium of *Zacco platypus*. acn = anterior condyle of the hyomandibular for the neurocranium, fmd = articulation facet for the mandibular, qpf = quadrate – pterygoid fenestra, pcn = posterior condyle of the hyomandibular for the neurocranium.

Plate 6 – 2. Outsider view the opercular bones and supensorium of *Nipponocypris temminckii*. acn = anterior condyle of the hyomandibular for the neurocranium, fmd = articulation facet for the mandibular, qpf = quadrate – pterygoid fenestra, pcn = posterior condyle of the hyomandibular for the neurocranium.

Plate 6 – 3. Outsider view the opercular bones and supensorium of *Nipponocypris sieboldii*. acn = anterior condyle of the hyomandibular for the neurocranium, fmd = articulation facet for the mandibular, qpf = quadrate – pterygoid fenestra, pcn = posterior condyle of the hyomandibular for the neurocranium.

Plate 6 – 4. Outsider view the opercular bones and supensorium of *Nipponocypris koreanus*. acn = anterior condyle of the hyomandibular for the neurocranium, fmd = articulation facet for the mandibular, qpf = quadrate – pterygoid fenestra, pcn = posterior condyle of the hyomandibular for the neurocranium.

Plate 6 – 5. Outsider view the opercular bones and supensorium of *Candidia barbatus*. acn = anterior condyle of the hyomandibular for the neurocranium, fmd = articulation facet for the mandibular, qpf = quadrate – pterygoid fenestra, pcn = posterior condyle of the hyomandibular for the neurocranium.

Plate 6 – 6. Outsider view the opercular bones and supensorium of *Opsariichthys evolans*. acn = anterior condyle of the hyomandibular for the neurocranium, fmd = articulation facet for the mandibular, qpf = quadrate – pterygoid fenestra, pcn = posterior condyle of the hyomandibular for the neurocranium.

Plate 6 – 7. Outsider view the opercular bones and supensorium of *Opsariichthys uncirostris*. acn = anterior condyle of the hyomandibular for the neurocranium, fmd = articulation facet for the mandibular, qpf = quadrate – pterygoid fenestra, pcn = posterior condyle of the hyomandibular for the neurocranium.

Plate 6 – 8. Outsider view the opercular bones and supensorium of *Opsariichthys bidens*. acn = anterior condyle of the hyomandibular for the neurocranium, fmd = articulation facet for the mandibular, qpf = quadrate – pterygoid fenestra, pcn = posterior condyle of the hyomandibular for the neurocranium.

Plate 6 – 9. Outsider view the opercular bones and supensorium of *Parazacco spilurus*. acn = anterior condyle of the hyomandibular for the neurocranium, fmd = articulation facet for the mandibular, qpf = quadrate – pterygoid fenestra, pcn = posterior condyle of the hyomandibular for the neurocranium.

Plate 7 – 1. Inside view the opercular bones and supensorium of *Zacco platypus*. acn = anterior condyle of the hyomandibular for the neurocranium, fmd = articulation facet for the mandibular, qpf = quadrate – pterygoid fenestra, pcn = posterior condyle of the hyomandibular for the neurocranium.

Plate 7 – 2. Inside view the opercular bones and supensorium of *Nipponocypris temminckii*. acn = anterior condyle of the hyomandibular for the neurocranium, fmd = articulation facet for the mandibular, qpf = quadrate – pterygoid fenestra, pcn = posterior condyle of the hyomandibular for the neurocranium.

Plate 7 – 3. Inside view the opercular bones and supensorium of *Nipponocypris sieboldii*. acn = anterior condyle of the hyomandibular for the neurocranium, fmd = articulation facet for the mandibular, qpf = quadrate – pterygoid fenestra, pcn = posterior condyle of the hyomandibular for the neurocranium.

Plate 7 – 4. Inside view the opercular bones and supensorium of *Nipponocypris koreanus*. acn = anterior condyle of the hyomandibular for the neurocranium, fmd = articulation facet for the mandibular, qpf = quadrate – pterygoid fenestra, pcn = posterior condyle of the hyomandibular for the neurocranium.

Plate 7 – 5. Inside view the opercular bones and supensorium of *Candidia barbatus*. acn = anterior condyle of the hyomandibular for the neurocranium, fmd = articulation facet for the mandibular, qpf = quadrate – pterygoid fenestra, pcn = posterior condyle of the hyomandibular for the neurocranium.

Plate 7 – 6. Inside view the opercular bones and supensorium of *Opsariichthys evolans*. acn = anterior condyle of the hyomandibular for the neurocranium, fmd = articulation facet for the mandibular, qpf = quadrate – pterygoid fenestra, pcn = posterior condyle of the hyomandibular for the neurocranium.

Plate 7 – 7. Inside view the opercular bones and supensorium of *Opsariichthys uncirostris*. acn = anterior condyle of the hyomandibular for the neurocranium, fmd = articulation facet for the mandibular, qpf = quadrate – pterygoid fenestra, pcn = posterior condyle of the hyomandibular for the neurocranium.

Plate 7 – 8. Inside view the opercular bones and supensorium of *Opsariichthys bidens*. acn = anterior condyle of the hyomandibular for the neurocranium, fmd = articulation facet for the mandibular, qpf = quadrate – pterygoid fenestra, pcn = posterior condyle of the hyomandibular for the neurocranium.

Plate 7 – 9. Inside view the opercular bones and supensorium of *Parazacco spilurus*. acn = anterior condyle of the hyomandibular for the neurocranium, fmd = articulation facet for the mandibular, qpf = quadrate – pterygoid fenestra, pcn = posterior condyle of the hyomandibular for the neurocranium.

Plate 8 – 1. The gill arches and pharyngeal bone of *Zacco platypus*. A, dorsal view of the gill arches; B and C, ceratobranchial 5 (pharyngeal bone).

Plate 8 – 2. The gill arches and pharyngeal bone of *Nipponocypris temminckii*. A, dorsal view of the gill arches; B and C, ceratobranchial 5 (pharyngeal bone).

Plate 8 – 3. The gill arches and pharyngeal bone of *Nipponocypris sieboldii*. A, dorsal view of the gill arches; B and C, ceratobranchial 5 (pharyngeal bone).

Plate 8 – 4. The gill arches and pharyngeal bone of *Nipponocypris koreanus*. A, dorsal view of the gill arches; B and C, ceratobranchial 5 (pharyngeal bone).

Plate 8 – 5. The gill arches and pharyngeal bone of *Candidia barbatus*. A, dorsal view of the gill arches; B and C, ceratobranchial 5 (pharyngeal bone).

Plate 8 – 6. The gill arches and pharyngeal bone of *Opsariichthys evolans*. A, dorsal view of the gill arches; B and C, ceratobranchial 5 (pharyngeal bone).

Plate 8 – 7. The gill arches and pharyngeal bone of *Opsariichthys uncirostris*. A, dorsal view of the gill arches; B and C, ceratobranchial 5 (pharyngeal bone).

Plate 8 – 8. The gill arches and pharyngeal bone of *Opsariichthys bidens*. A, dorsal view of the gill arches; B and C, ceratobranchial 5 (pharyngeal bone).

Plate 8 – 9. The gill arches and pharyngeal bone of *Parazacco spilurus*. A, dorsal view of the gill arches; B and C, ceratobranchial 5 (pharyngeal bone).

Plate 9 – 1. Outside view of the hyoid arches of *Zacco platypus*.

Plate 9 – 2. Outside view of the hyoid arches of *Nipponocypris temminckii*.

Plate 9 – 3. Outside view of the hyoid arches of *Nipponocypris sieboldii*.

Plate 9 – 4. Outside view of the hyoid arches of *Nipponocypris koreanus*.

Plate 9 – 5. Outside view of the hyoid arches of *Candidia barbatus*.

Plate 9 – 6. Outside view of the hyoid arches of *Opsariichthys evolans*.

Plate 9 – 7. Outside view of the hyoid arches of *Opsariichthys uncirostris*.

Plate 9 – 8. Outside view of the hyoid arches of *Opsariichthys bidens*.

Plate 9 – 9. Outside view of the hyoid arches of *Parazacco spilurus*.

Plate 10 – 1. Inside view of the hyoid arches of *Zacco platypus*. fch = fenstra on the ceratohyal.

Plate 10 – 2. Inside view of the hyoid arches of *Nipponocypris temminckii*. fch = fenstra on the ceratohyal.

Plate 10 – 3. Inside view of the hyoid arches of *Nipponocypris sieboldii*. fch = fenstra on the ceratohyal.

Plate 10 – 4. Inside view of the hyoid arches of *Nipponocypris koreanus*. fch = fenstra on the ceratohyal.

Plate 10 – 5. Inside view of the hyoid arches of *Candidia barbatus*. fch = fenstra on the ceratohyal.

Plate 10 – 6. Inside view of the hyoid arches of *Opsariichthys evolans*. fch = fenstra on the ceratohyal.

Plate 10 – 7. Inside view of the hyoid arches of *Opsariichthys uncirostris*. fch = fenstra on the ceratohyal.

Plate 10 – 8. Inside view of the hyoid arches of *Opsariichthys bidens*. fch = fenstra on the ceratohyal.

Plate 10 – 9. Inside view of the hyoid arches of *Parazacco spilurus*. fch = fenstra on the ceratohyal.

Plate 11 – 1. The urohyal of *Zacco platypus*. A, lateral view; B, dorsal view of urohyal; C, ventral view of urohyal.

Plate 11 – 2. The urohyal of *Nipponocypris temminckii*. A, lateral view; B, dorsal view of urohyal; C, ventral view of urohyal.

Plate 11 – 3. The urohyal of *Nipponocypris sieboldii*. A, lateral view; B, dorsal view of urohyal; C, ventral view of urohyal.

Plate 11 – 4. The urohyal of *Nipponocypris koreanus*. A, lateral view; B, dorsal view of urohyal; C, ventral view of urohyal.

Plate 11 – 5. The urohyal of *Candidia barbatus*. A, lateral view; B, dorsal view of urohyal; C, ventral view of urohyal.

Plate 11 – 6. The urohyal of *Opsariichthys evolans*. A, lateral view; B, dorsal view of urohyal; C, ventral view of urohyal.

Plate 11 – 7. The urohyal of *Opsariichthys uncirostris*. A, lateral view; B, dorsal view of urohyal; C, ventral view of urohyal.

Plate 11 – 8. The urohyal of *Opsariichthys bidens*. A, lateral view; B, dorsal view of urohyal; C, ventral view of urohyal.

Plate 11 – 9. The urohyal of *Parazacco spilurus*. A, lateral view; B, dorsal view of urohyal; C, ventral view of urohyal.

Plate 12 – 1. The posterior region of head and the Weberian ossicles of *Zacco platypus*. na3 = neural arch 3, sn3 = supraneural 3 bone.

Plate 12 – 2. The Weberian ossicles of *Nipponocypris temminckii*. na3 = neural arch 3, sn3 = supraneural 3 bone.

Plate 12 – 3. The Weberian ossicles of *Nipponocypris sieboldii*. na3 = neural arch 3, sn3 = supraneural 3 bone.

Plate 12 – 4. The Weberian ossicles of *Nipponocypris koreanus*. na3 = neural arch 3, sn3 = supraneural 3 bone.

Plate 12 – 5. The Weberian ossicles of *Candidia barbatus*. na3 = neural arch 3, sn3 = supraneural 3 bone.

Plate 12 – 6. The Weberian ossicles of *Opsariichthys evolans*. na3 = neural arch 3, sn3 = supraneural 3 bone.

Plate 12 – 7. The Weberian ossicles of *Opsariichthys uncirostris*. na3 = neural arch 3, sn3 = supraneural 3 bone.

Plate 12 – 8. The the Weberian ossicles of *Opsariichthys bidens*. na3 = neural arch 3, sn3 = supraneural 3 bone.

Plate 12 – 9. The Weberian ossicles of *Parazacco spilurus*. na3 = neural arch 3, sn3 = supraneural 3 bone.

Plate 13 – 1. The caudal skeleton of *Zacco platypus*. hpu = haemal spine of preural centrum, npu = neural spine of preural centrum, pp = hypurapophysis, pu1 + u1 = first preural centrum + first ural vertebra.

Plate 13 – 2. The caudal skeleton of *Nipponocypris temminckii*. hpu = haemal spine of preural centrum, npu = neural spine of preural centrum, pp = hypurapophysis, pu1 + u1 = first preural centrum + first ural vertebra.

Plate 13 – 3. The caudal skeleton of *Nipponocypris sieboldii*. hpu = haemal spine of preural centrum, npu = neural spine of preural centrum, pp = hypurapophysis, pu1 + u1 = first preural centrum + first ural vertebra.

Plate 13 – 4. The caudal skeleton of *Nipponocypris koreanus*. hpu = haemal spine of preural centrum, npu = neural spine of preural centrum, pp = hypurapophysis, pu1 + u1 = first preural centrum + first ural vertebra.

Plate 13 – 5. The caudal skeleton of *Candidia barbatus*. hpu = haemal spine of preural centrum, npu = neural spine of preural centrum, pp = hypurapophysis, pu1 + u1 = first preural centrum + first ural vertebra.

Plate 13 – 6. The caudal skeleton of *Opsariichthys evolans*. hpu = haemal spine of preural centrum, npu = neural spine of preural centrum, pp = hypurapophysis, pu1 + u1 = first preural centrum + first ural vertebra.

Plate 13 – 7. The caudal skeleton of *Opsariichthys uncirostris*. hpu = haemal spine of preural centrum, npu = neural spine of preural centrum, pp = hypurapophysis, pu1 + u1 = first preural centrum + first ural vertebra.

Plate 13 – 8. The caudal skeleton of *Opsariichthys bidens*. hpu = haemal spine of preural centrum, npu = neural spine of preural centrum, pp = hypurapophysis, pu1 + u1 = first preural centrum + first ural vertebra.

Plate 13 – 9. The caudal skeleton of *Parazacco spilurus*. hpu = haemal spine of preural centrum, npu = neural spine of preural centrum, pp = hypurapophysis, pu1 + u1 = first preural centrum + first ural vertebra.

Plate 14 – 1. The supraneurals of *Zacco platypus*.

Plate 14 – 2. The supraneurals of *Nipponocypris temminckii*.

Plate 14 – 3. The supraneurals of *Nipponocypris sieboldii*.

Plate 14 – 4. The supraneurals of *Nipponocypris koreanus*.

Plate 14 – 5. The supraneurals of *Candidia barbatus*.

Plate 14 – 6. The supraneurals of *Opsariichthys evolans*.

Plate 14 – 7. The supraneurals of *Opsariichthys uncirostris*.

Plate 14 – 8. The supraneurals of *Opsariichthys bidens*.

Plate 14 – 9. The supraneurals of *Parazacco spilurus*.

Plate 15 – 1. The dorsal and anal fins of *Zacco platypus*. A, doral fin; B, anal fin.

Plate 15 – 2. The dorsal and anal fins of *Nipponocypris temminckii*. A, doral fin; B, anal fin.

Plate 15 – 3. The dorsal and anal fins of *Nipponocypris sieboldii*. A, doral fin; B, anal fin.

Plate 15 – 4. The dorsal and anal fins of *Nipponocypris koreanus*. A, doral fin; B, anal fin.

Plate 15 – 5. The dorsal and anal fins of *Candidia barbatus*. A, doral fin; B, anal fin.

Plate 15 – 6. The dorsal and anal fins of *Opsariichthys evolans*. A, doral fin; B, anal fin.

Plate 15 – 7. The dorsal and anal fins of *Opsariichthys uncirostris*. A, doral fin; B, anal fin.

Plate 15 – 8. The dorsal and anal fins of *Opsariichthys bidens*. A, doral fin; B, anal fin.

Plate 15 – 9. The dorsal and anal fins of *Parazacco spilurus*. A, doral fin; B, anal fin.

Plate 16 – 1. The shoulder girdle of *Zacco platypus*. A, inside view; B, outside view. sf = scapula foramen.

Plate 16 – 2. The shoulder girdle of *Nipponocypris temminckii*. A, inside view; B, outside view. sf = scapula foramen.

Plate 16 – 3. The shoulder girdle of *Nipponocypris sieboldii*. A, inside view; B, outside view. sf = scapula foramen.

Plate 16 – 4. The shoulder girdle of *Nipponocypris koreanus*. A, inside view; B, outside view. sf = scapula foramen.

Plate 16 – 5. The shoulder girdle of *Candidia barbatus*. A, inside view; B, outside view. sf = scapula foramen.

Plate 16 – 6. The shoulder girdle of *Opsariichthys evolans*. A, inside view; B, outside view. sf = scapula foramen.

Plate 16 – 7. The shoulder girdle of *Opsariichthys uncirostris*. A, inside view; B, outside view. sf = scapula foramen.

Plate 16 – 8. The shoulder girdle of *Opsariichthys bidens*. A, inside view; B, outside view. sf = scapula foramen.

Plate 16 – 9. The shoulder girdle of *Parazacco spilurus*. A, inside view; B, outside view. sf = scapula foramen.

Plate 17 – 1. The pelvic girdle of *Zacco platypus*. A, dorsal view; B, lateral view; C, ventral view; D, ventral view without finrays.

Plate 17 – 2. The pelvic girdle of *Nipponocypris temminckii*. A, dorsal view; B, lateral view; C, ventral view; D, ventral view without finrays.

Plate 17 – 3. The pelvic girdle of *Nipponocypris sieboldii*. A, dorsal view; B, lateral

view; C, ventral view; D, ventral view without finrays.

Plate 17 – 4. The pelvic girdle of *Nipponocypris koreanus*. A, dorsal view; B, lateral view; C, ventral view; D, ventral view without finrays.

Plate 17 – 5. The pelvic girdle of *Candidia barbatus*. A, dorsal view; B, lateral view; C, ventral view; D, ventral view without finrays.

Plate 17 – 6. The pelvic girdle of *Opsariichthys evolans*. A, dorsal view; B, lateral view; C, ventral view; D, ventral view without finrays.

Plate 17 – 7. The pelvic girdle of *Opsariichthys uncirostris*. A, dorsal view; B, lateral view; C, ventral view; D, ventral view without finrays.

Plate 17 – 8. The pelvic girdle of *Opsariichthys bidens*. A, dorsal view; B, lateral view; C, ventral view; D, ventral view without finrays.

Plate 17 – 9. The pelvic girdle of *Parazacco spilurus*. A, dorsal view; B, lateral view; C, ventral view; D, ventral view without finrays.

Plate 1-1

A


5 mm

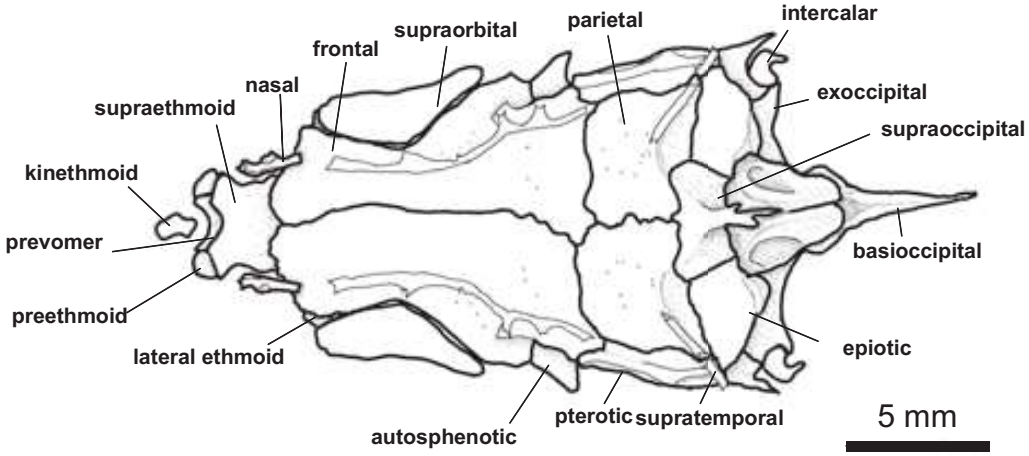
supraorbital
parietal
intercalar
frontal
nasal
exoccipital
supraethmoid
supraoccipital
kinethmoid
basioccipital
prevomer
preethmoid
epiotic
lateral ethmoid
autosphenotic
pterotic
supratemporal
5 mm

B


5 mm

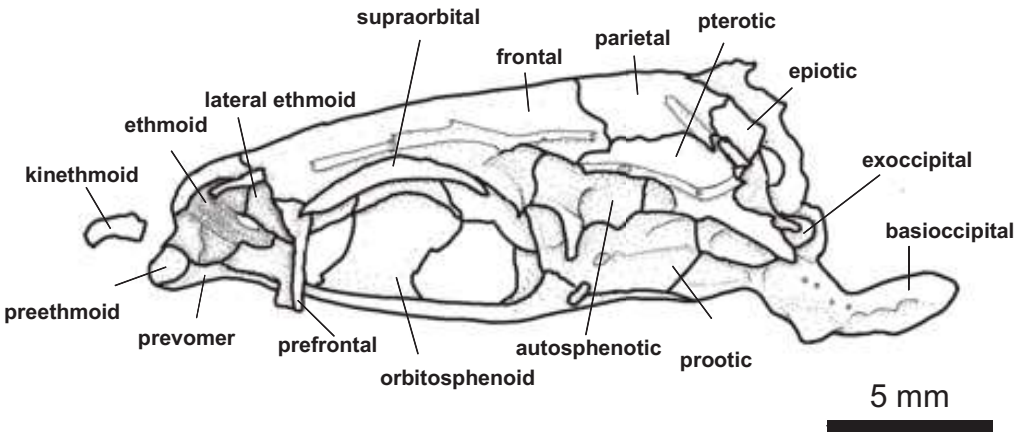
supraorbital
pterotic
parietal
frontal
epiotic
lateral ethmoid
ethmoid
exoccipital
kinethmoid
basioccipital
preethmoid
prevomer
prefrontal
autosphenotic
prootic
orbitosphenoid
5 mm

Plate 1-2

A

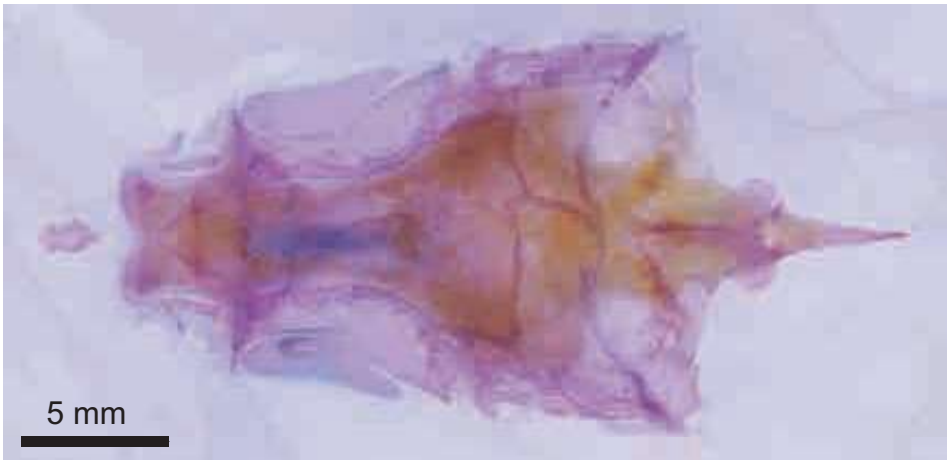
5 mm

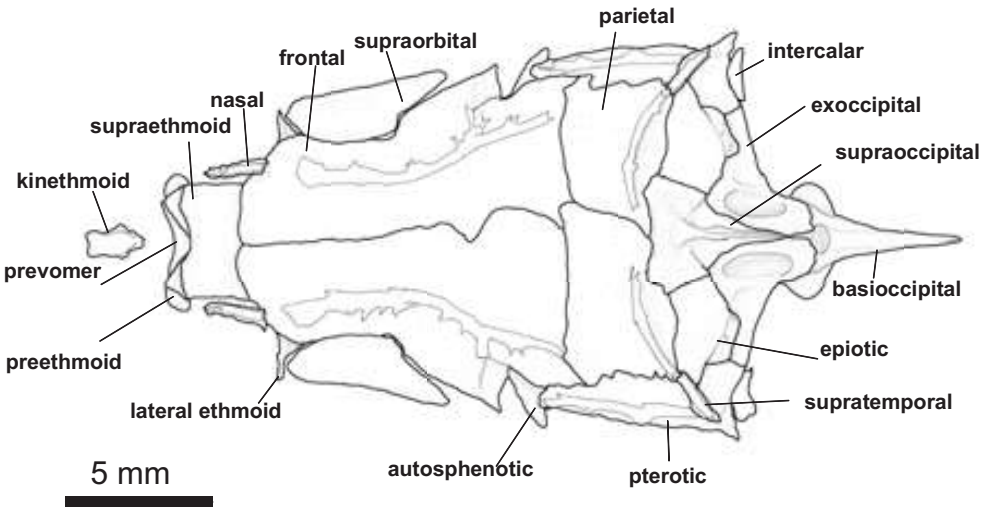
parietal
supraorbital
frontal
intercalar
nasal
exoccipital
supraethmoid
supraoccipital
kinethmoid
prevomer
basioccipital
epiotic
preethmoid
supratemporal
lateral ethmoid
autosphenotic
pterotic
5 mm

B


5 mm

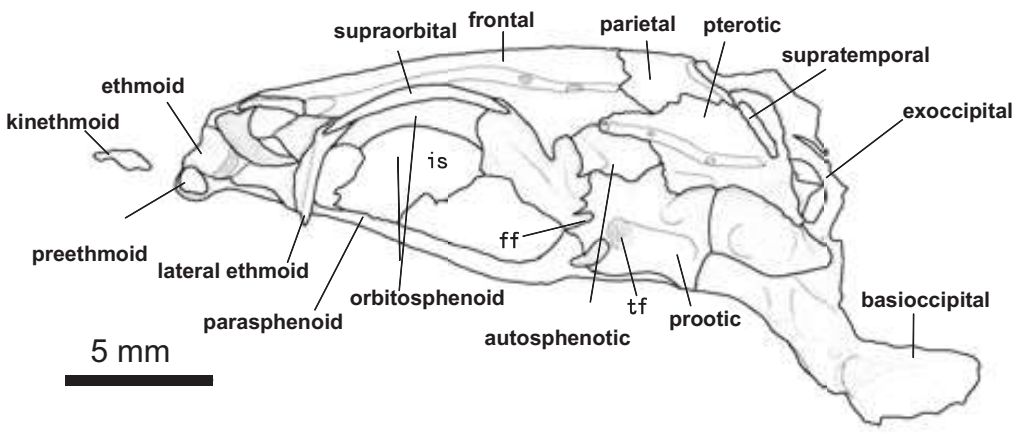
supraorbital
frontal
parietal
pterotic
supratemporal
ethmoid
kinethmoid
exoccipital
is
ff
preethmoid
lateral ethmoid
orbitosphenoid
tf
prootic
basioccipital
parasphenoid
autosphenotic
5 mm

Plate 1-3

A


5 mm

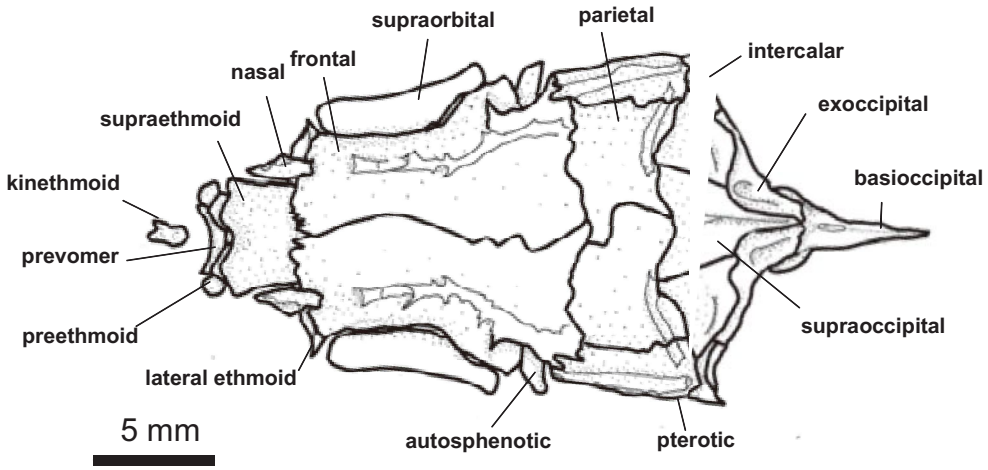
supraorbital
parietal
intercalar
nasal
frontal
exoccipital
supraethmoid
basioccipital
kinethmoid
prevomer
supraoccipital
preethmoid
lateral ethmoid
5 mm
autosphenotic
pterotic

B

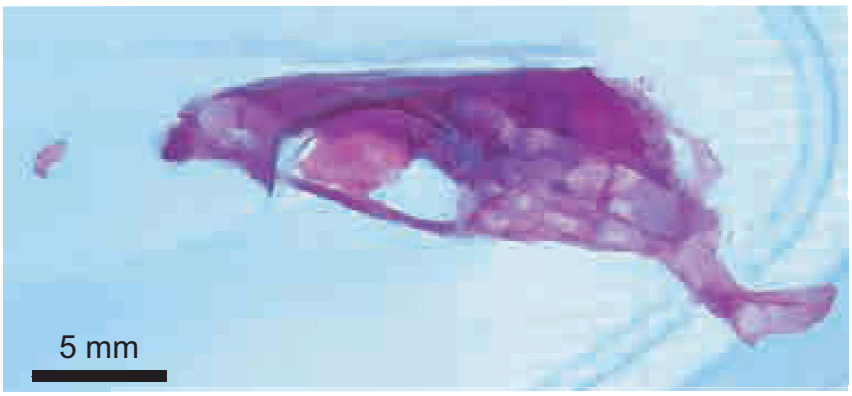
5 mm

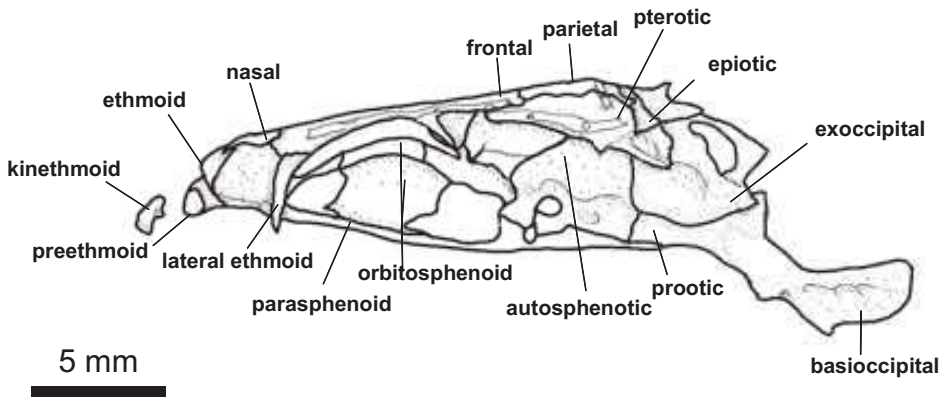
pterotic
parietal
frontal
epiotic
nasal
ethmoid
exoccipital
kinethmoid
preethmoid
lateral ethmoid
orbitosphenoid
prootic
parasphenoid
autosphenotic
5 mm
basioccipital

Plate 1-4

A

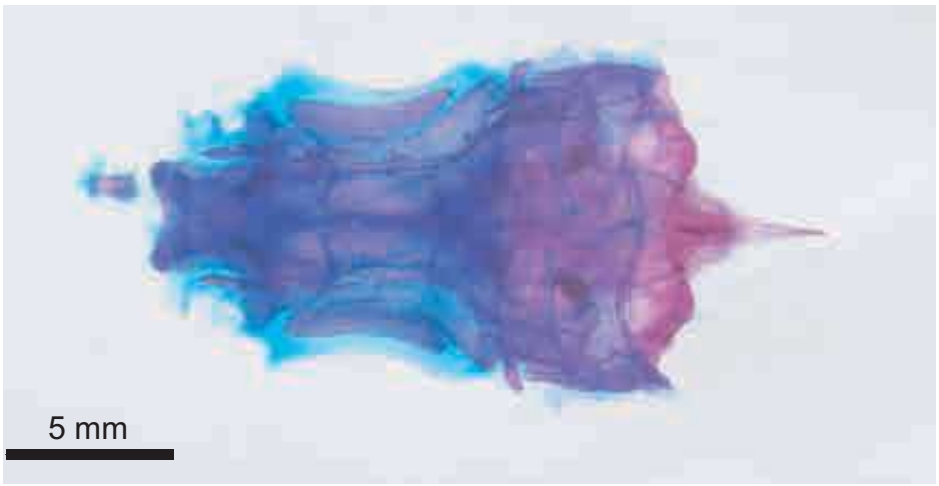
5 mm

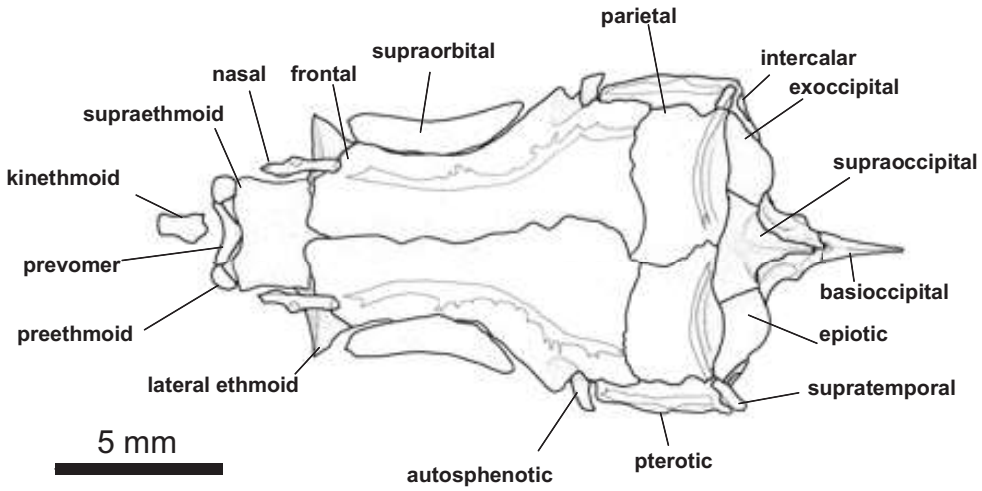
parietal
supraorbital
intercalar
nasal
frontal
exoccipital
supraethmoid
supraoccipital
kinethmoid
prevomer
basioccipital
preethmoid
epiotic
lateral ethmoid
supratemporal
5 mm
autosphenotic
pterotic

B


5 mm

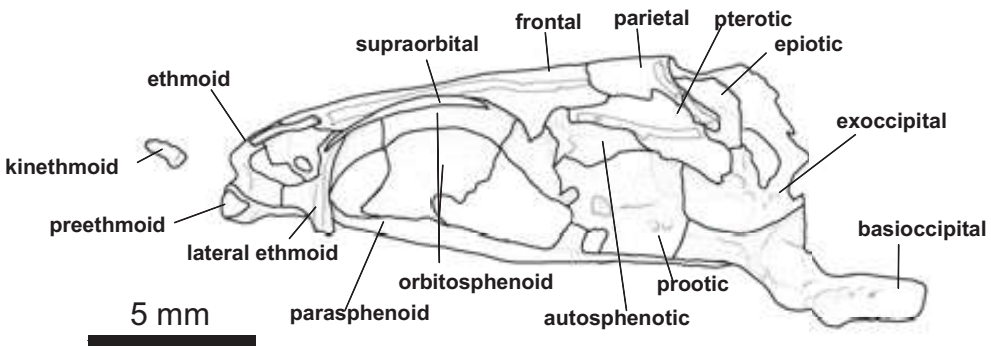
frontal
parietal
pterotic
supraorbital
epiotic
ethmoid
exoccipital
kinethmoid
basioccipital
preethmoid
lateral ethmoid
orbitosphenoid
prootic
5 mm
parasphenoid
autosphenotic

Plate 1-5

A

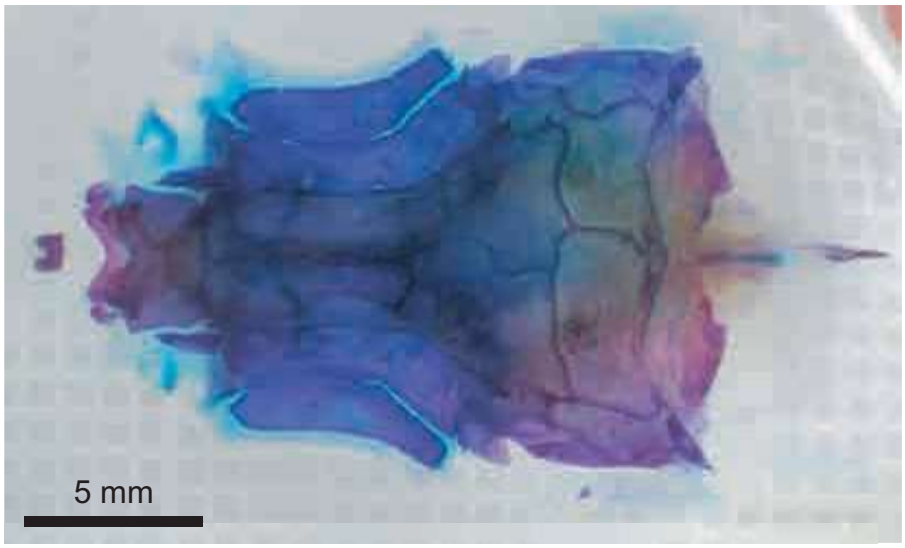
5 mm

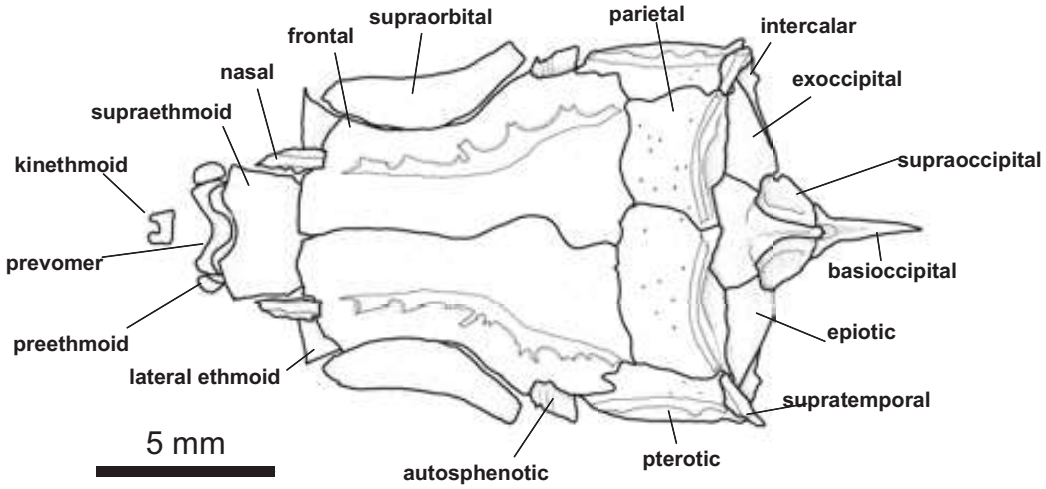
supraorbital
parietal
frontal
intercalar
nasal
exoccipital
supraethmoid
supraoccipital
kinethmoid
prevomer
basioccipital
epiotic
preethmoid
lateral ethmoid
supratemporal
5 mm
autosphenotic
pterotic

B


5 mm

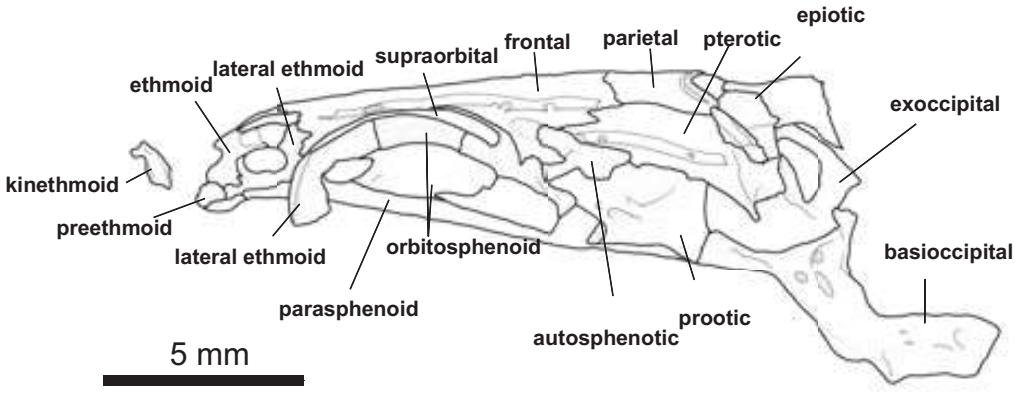
epiotic
frontal
parietal
pterotic
supraorbital
lateral ethmoid
ethmoid
exoccipital
kinethmoid
preethmoid
orbitosphenoid
lateral ethmoid
basioccipital
parasphenoid
prootic
autosphenotic
5 mm

Plate 1-6

A

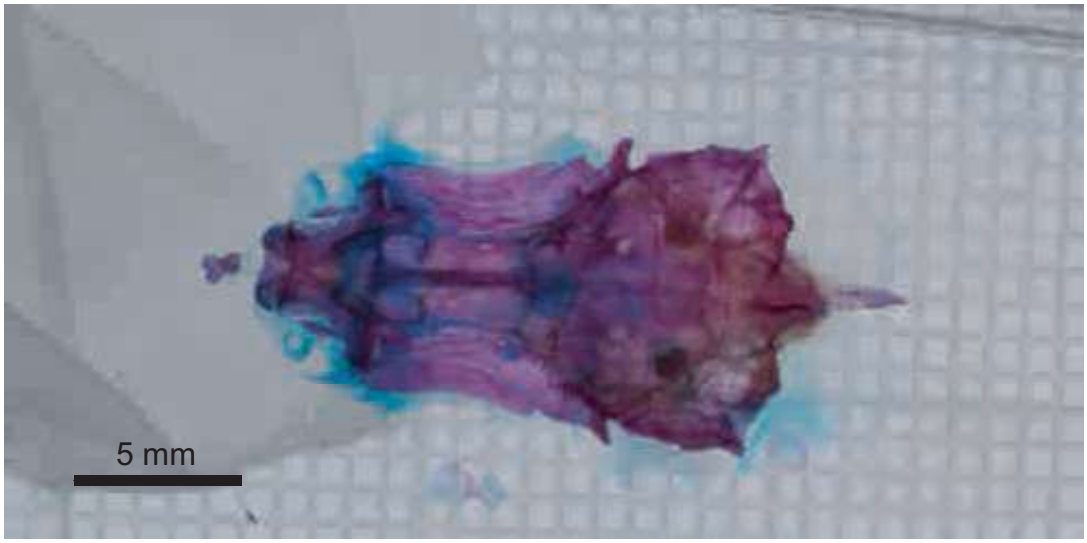
5 mm

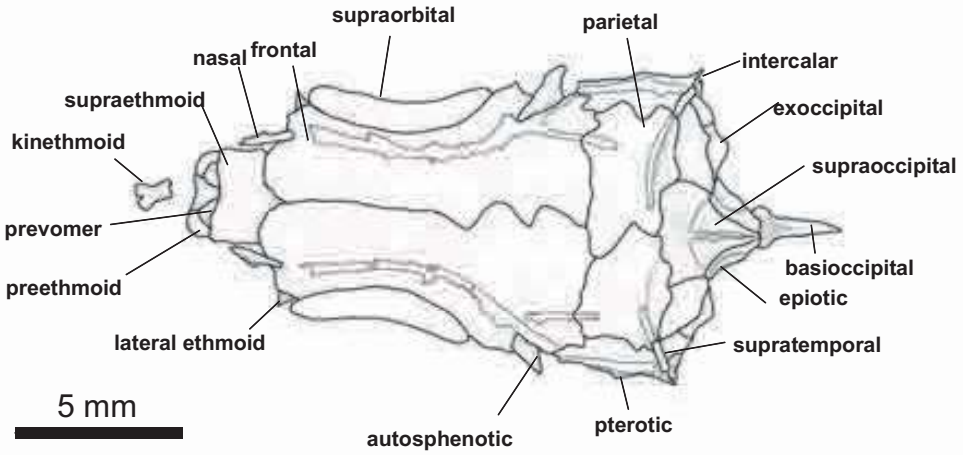
supraorbital
parietal
nasal
frontal
intercalar
supraethmoid
exoccipital
kinethmoid
supraoccipital
prevomer
basioccipital
preethmoid
epiotic
lateral ethmoid
supratemporal
5 mm
autosphenotic
pterotic

B


5 mm

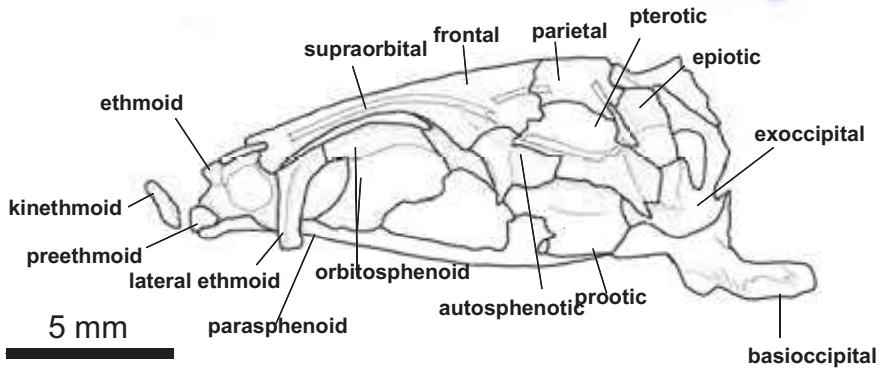
pterotic
supraorbital
frontal
parietal
epiotic
ethmoid
exoccipital
kinethmoid
preethmoid
orbitosphenoid
lateral ethmoid
prootic
autosphenotic
5 mm
parasphenoid
basioccipital

Plate 1-7

A

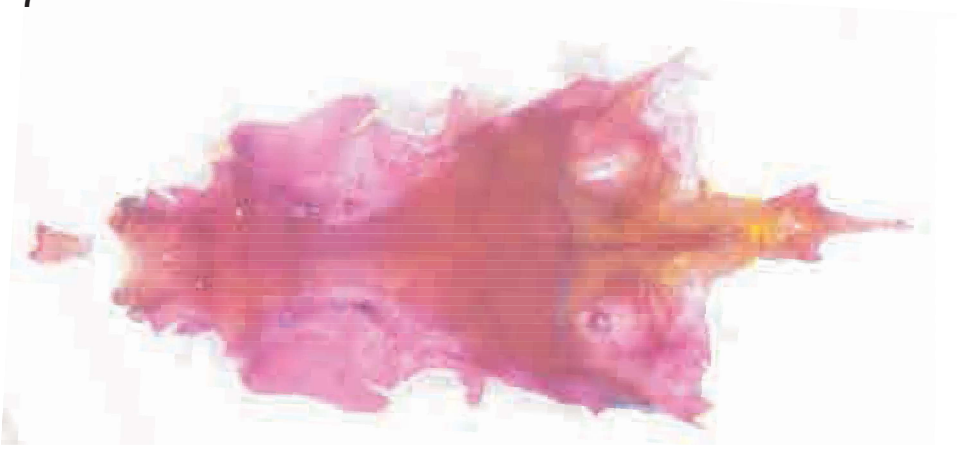

1cm

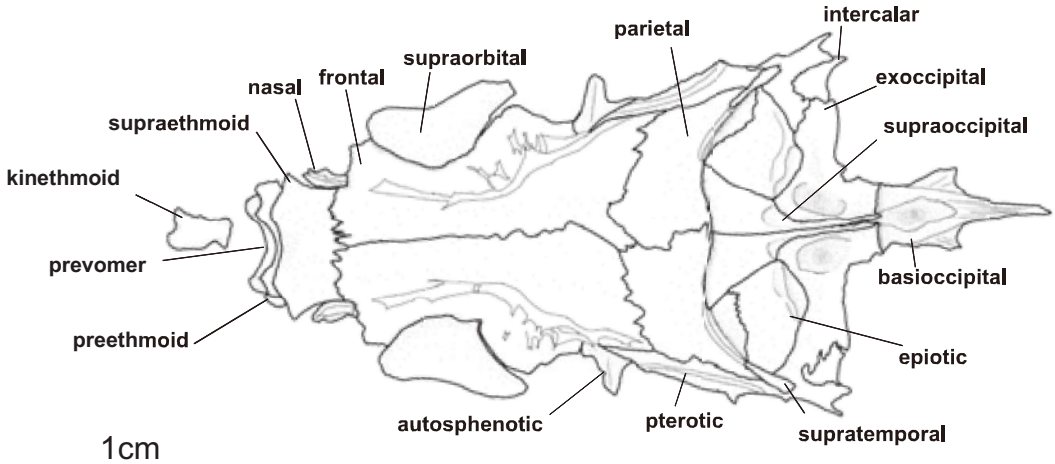

1cm

B

1cm

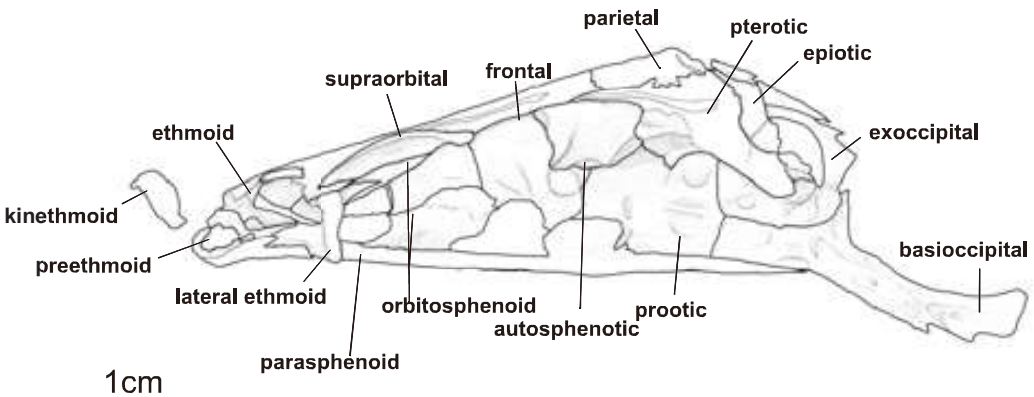

1cm

Plate 1-8

A

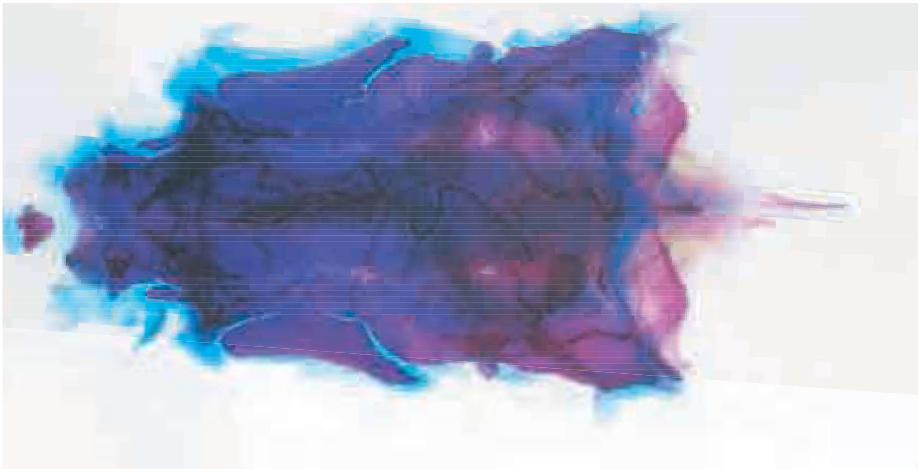

5 mm

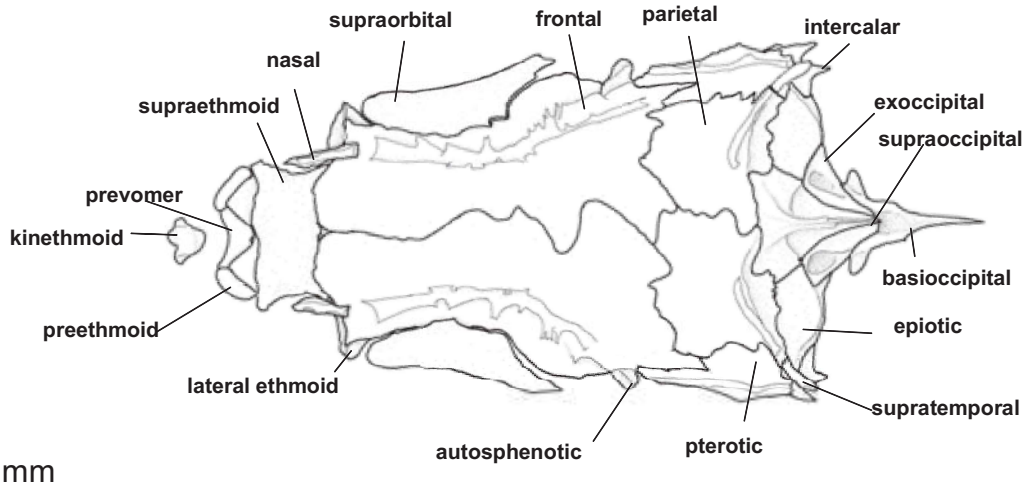

5 mm

B

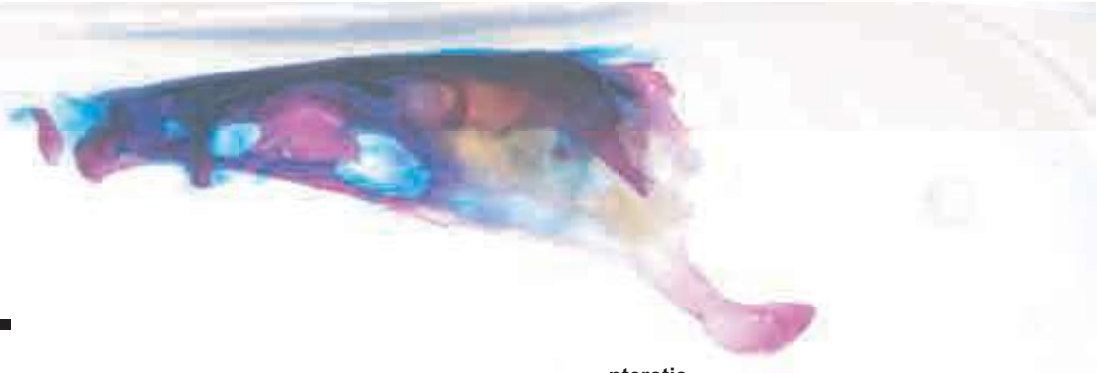

5 mm

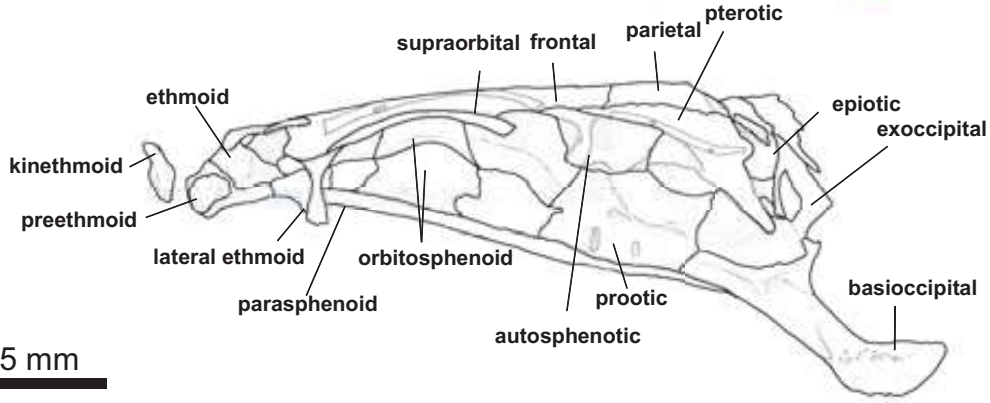

5 mm

Plate 1-9

A

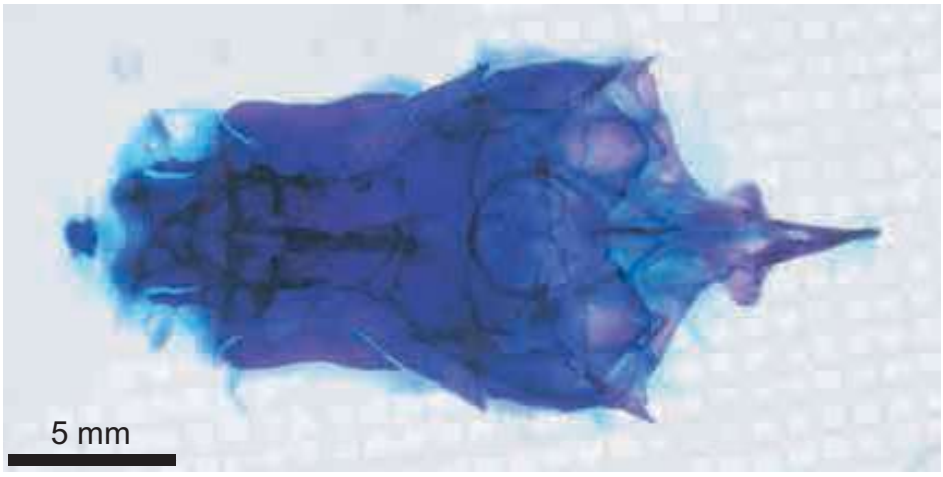
5 mm

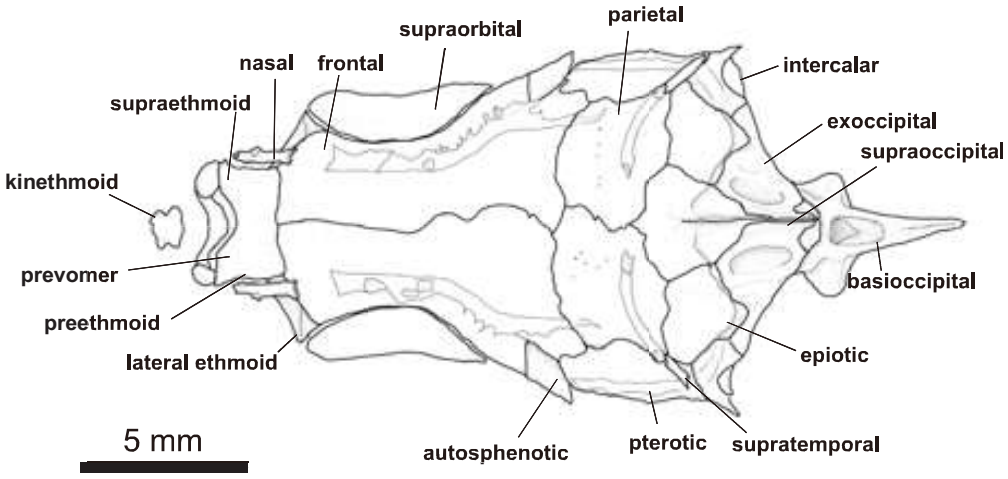
supraorbital
parietal
nasal
frontal
intercalar
supraethmoid
exoccipital
supraoccipital
kinethmoid
prevomer
basioccipital
preethmoid
epiotic
lateral ethmoid
5 mm
autosphenotic
pterotic
supratemporal


5 mm

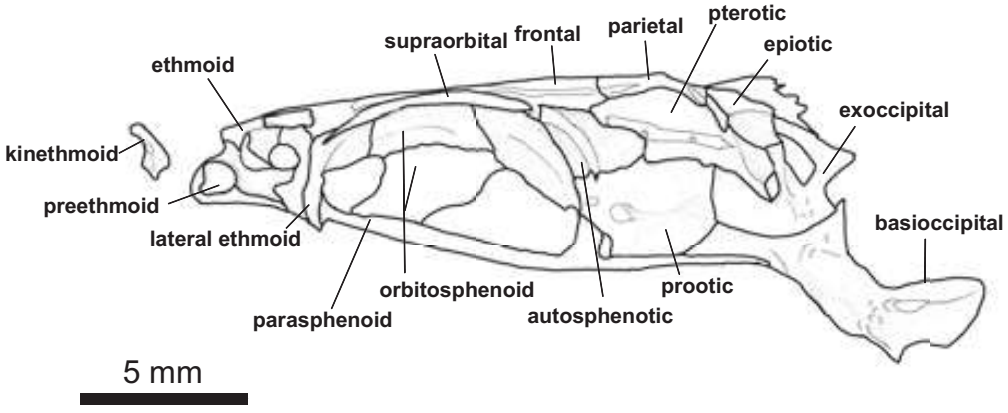
supraorbital
frontal
parietal
pterotic
epiotic
ethmoid
exoccipital
kinethmoid
preethmoid
basioccipital
lateral ethmoid
orbitosphenoid
prootic
parasphenoid
autosphenotic
5 mm

Plate 2-1

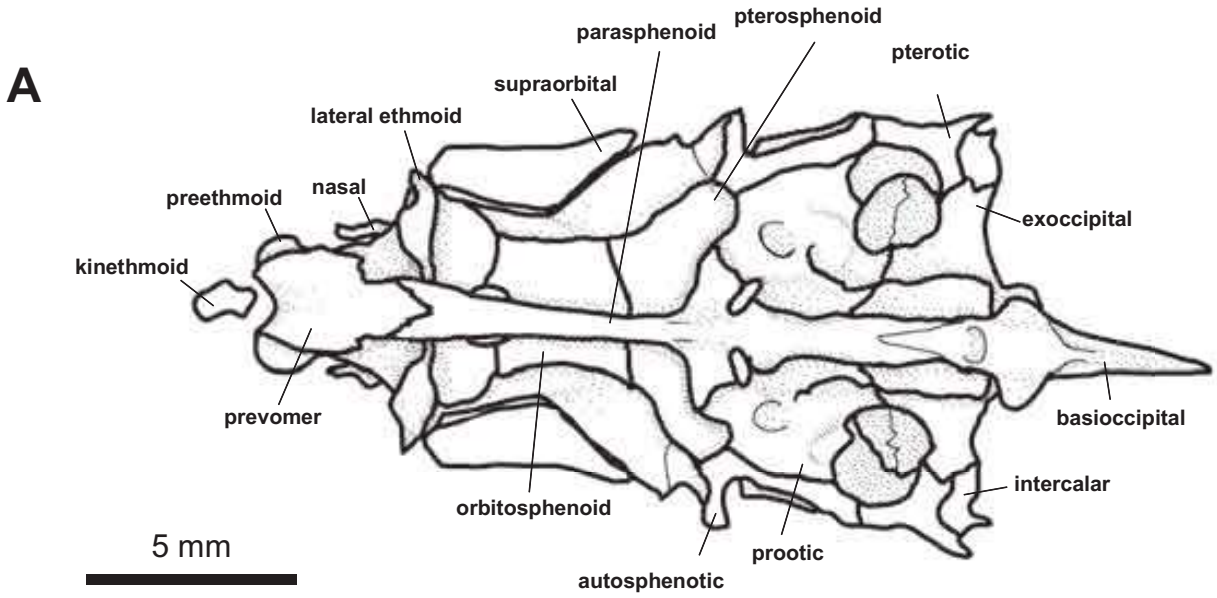
A
parasphenoid
pterosphenoid
pterotic
supraorbital
lateral ethmoid
preethmoid
nasal
exoccipital
kinethmoid
prevomer
basioccipital
intercalar
orbitosphenoid
prootic
autosphenotic
5 mm


5 mm

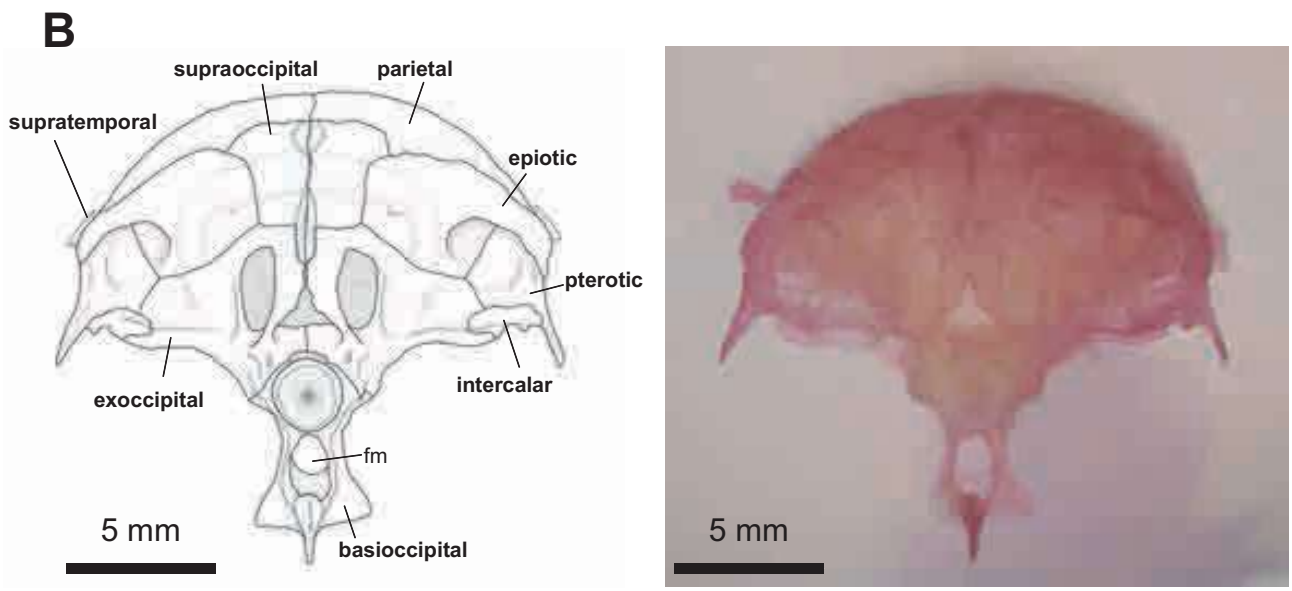
B
supraoccipital
parietal
supratemporal
epiotic
pterotic
exoccipital
intercalar
fm
5 mm
basioccipital
5 mm

Plate 2-2

A

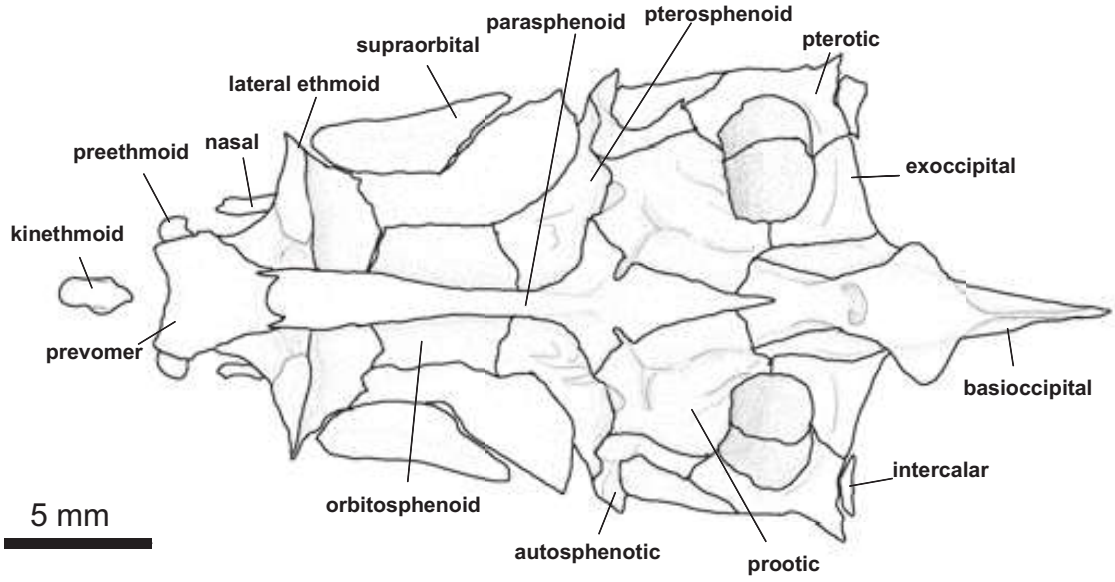
parasphenoid
pterosphenoid
supraorbital
pterotic
lateral ethmoid
preethmoid
nasal
exoccipital
kinethmoid
prevomer
basioccipital
intercalar
orbitosphenoid
autosphenotic
prootic
5 mm

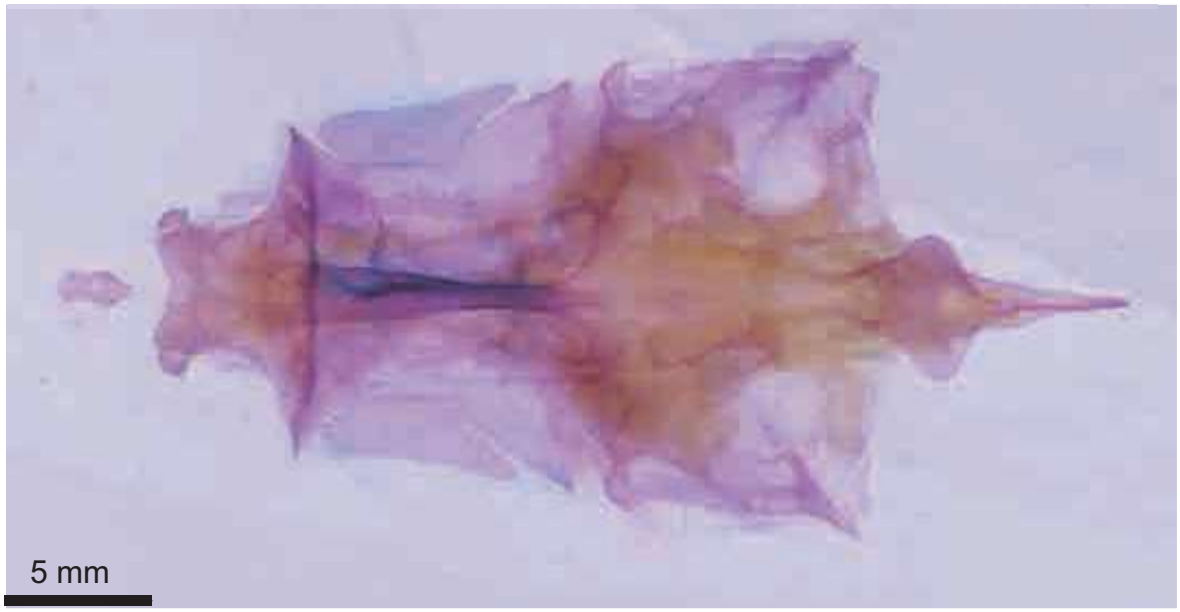
5 mm

B

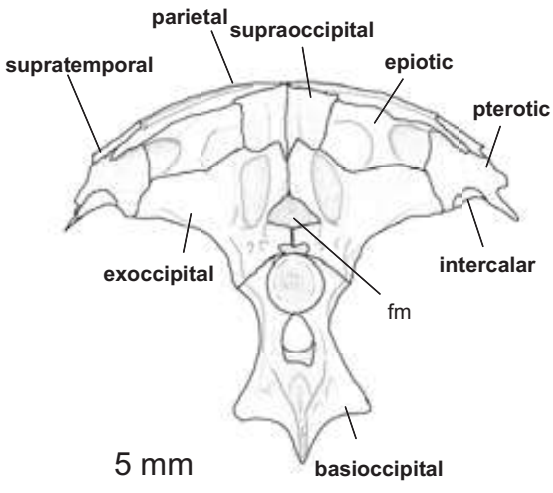
parietal
supraoccipital
supratemporal
epiotic
pterotic
exoccipital
intercalar
fm
5 mm
basioccipital


5 mm

Plate 2-3

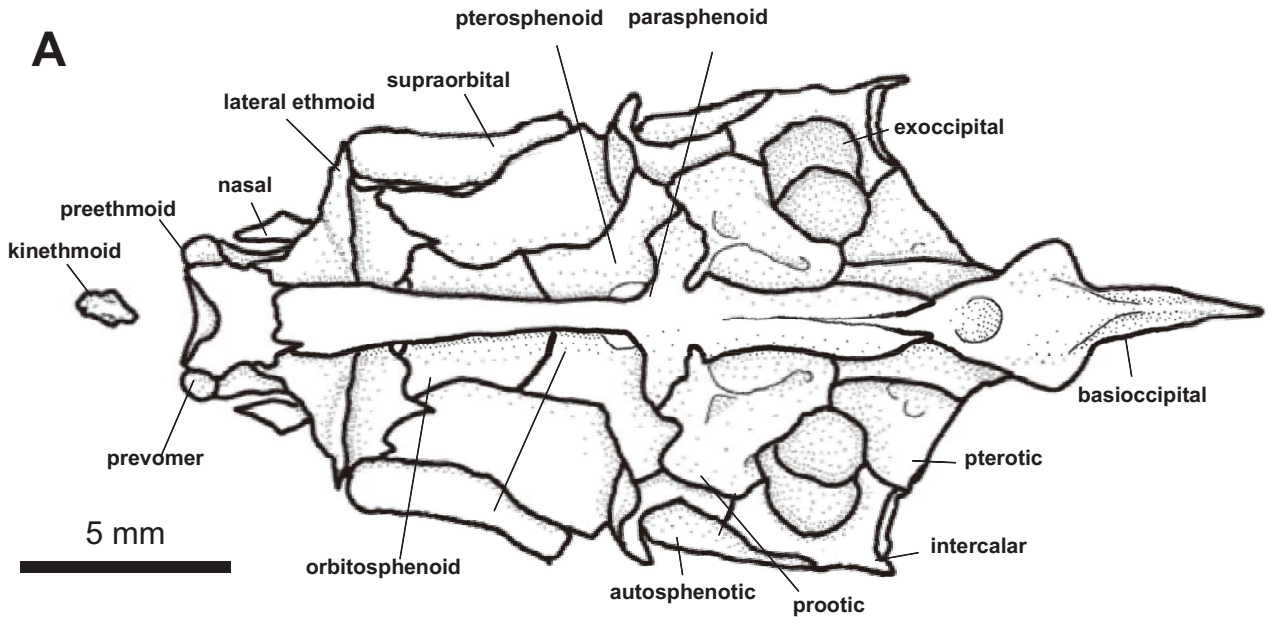
A
pterosphenoid
parasphenoid
supraorbital
lateral ethmoid
exoccipital
nasal
preethmoid
kinethmoid
basioccipital
prevomer
pterotic
5 mm
intercalar
orbitosphenoid
autosphenotic
prootic

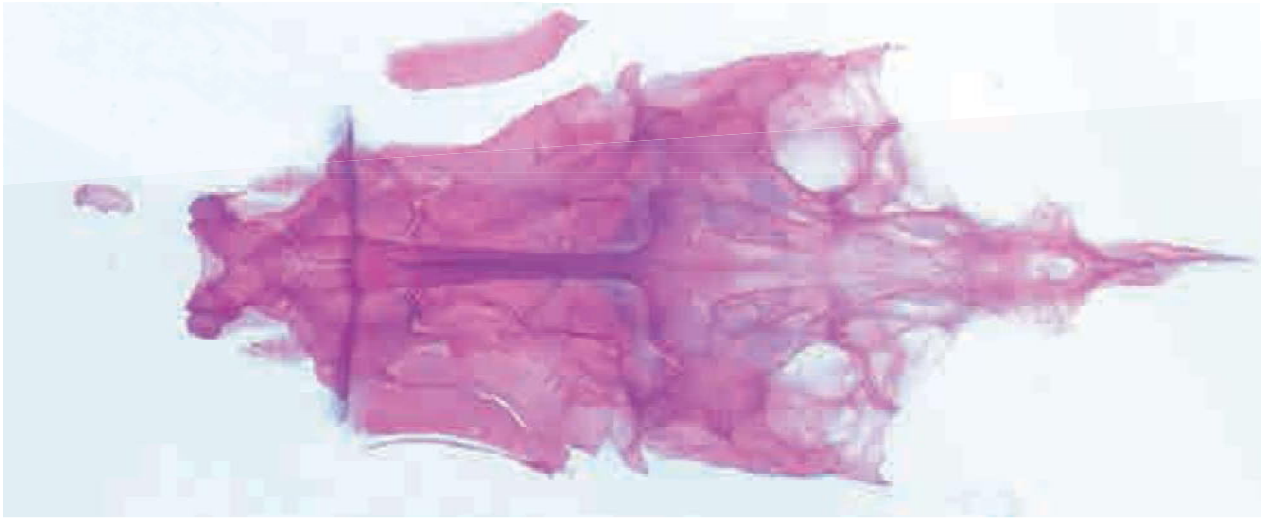

5 mm

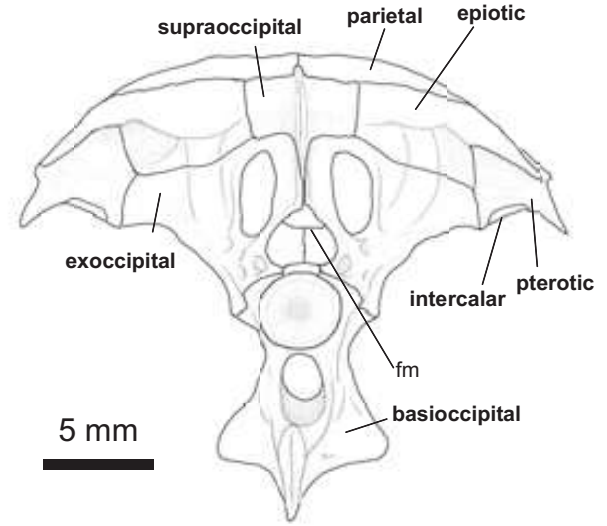
B
supraoccipital
parietal
epiotic
exoccipital
intercalar
pterotic
fm
basioccipital
5 mm

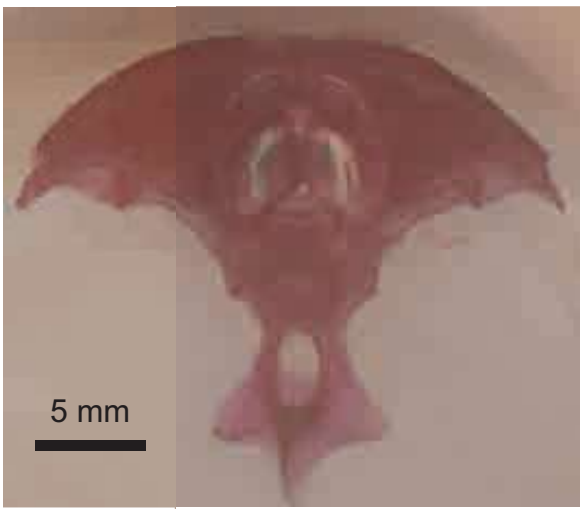
5 mm

Plate 2-4

A

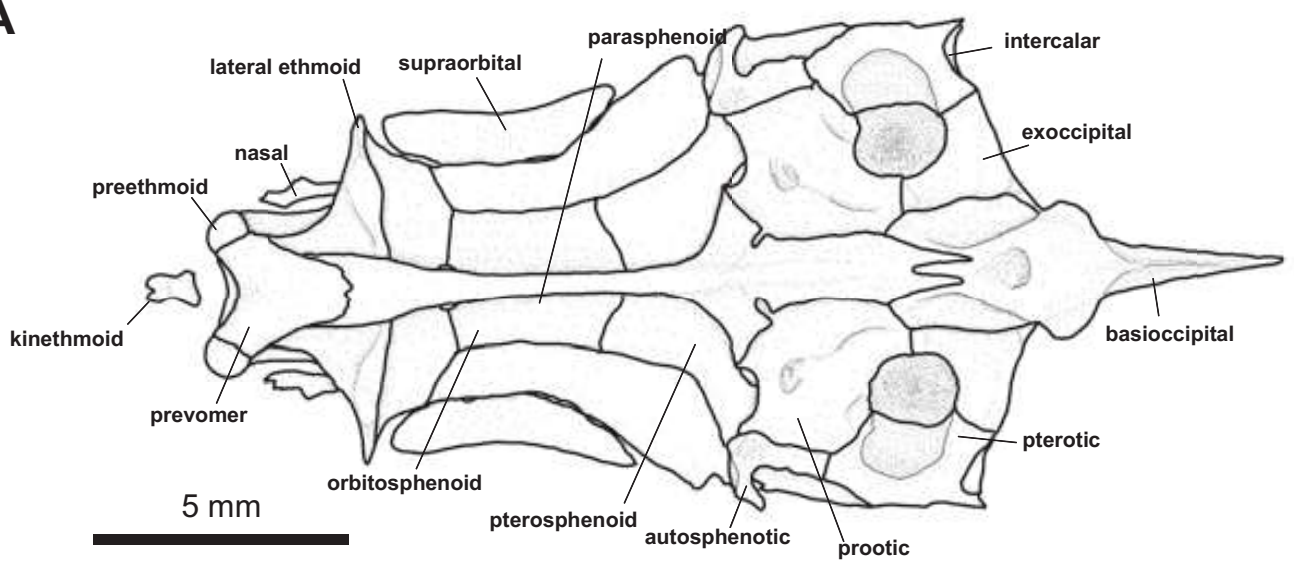
parasphenoid
intercalar
lateral ethmoid
supraorbital
exoccipital
nasal
preethmoid
kinethmoid
basioccipital
prevomer
pterotic
orbitosphenoid
5 mm
pterosphenoid
autosphenotic
prootic

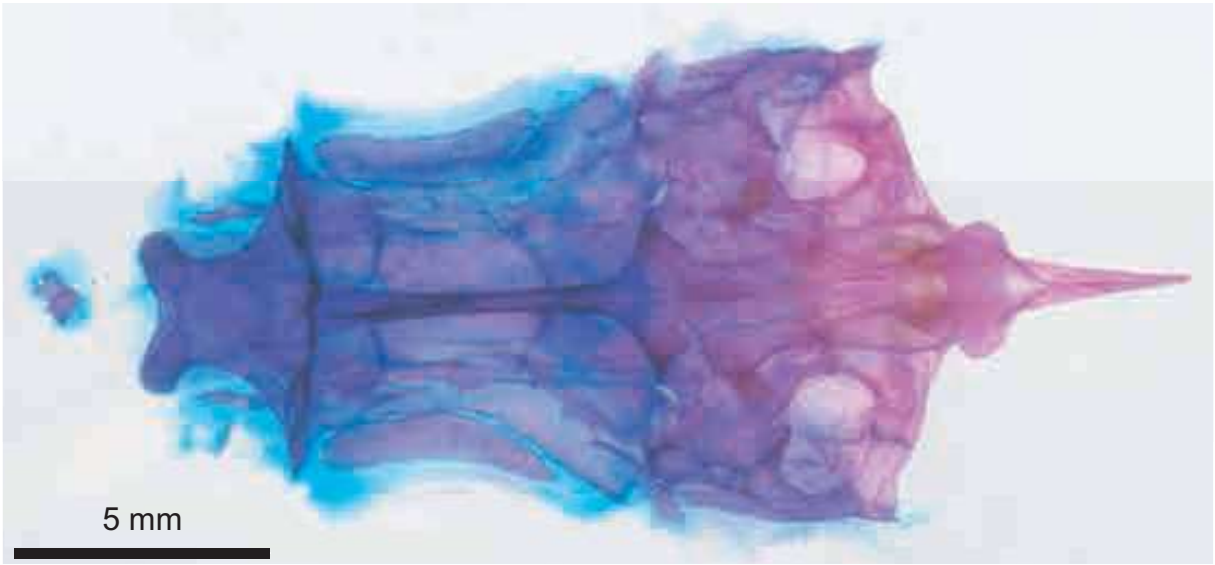
5 mm

B

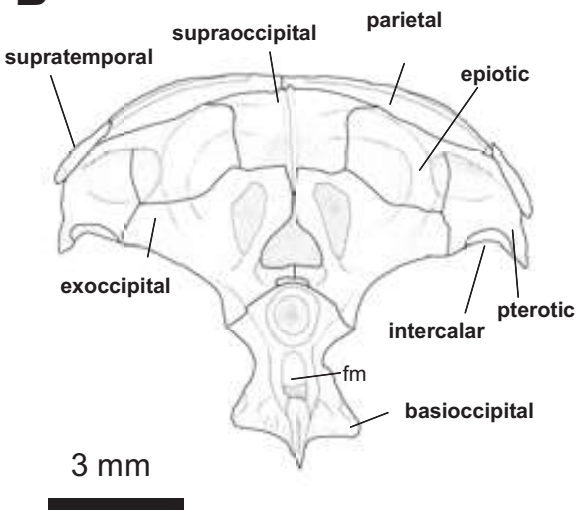
supraoccipital
parietal
supratemporal
epiotic
exoccipital
pterotic
intercalar
fm
basioccipital
3 mm

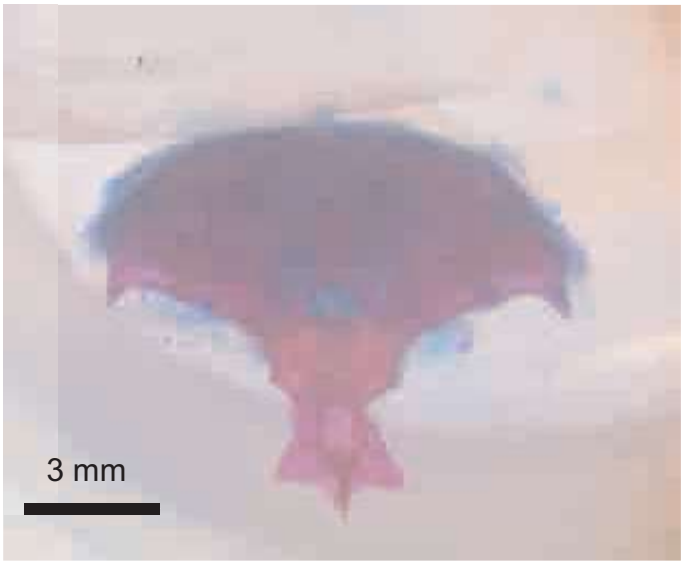
3 mm

Plate 2-5

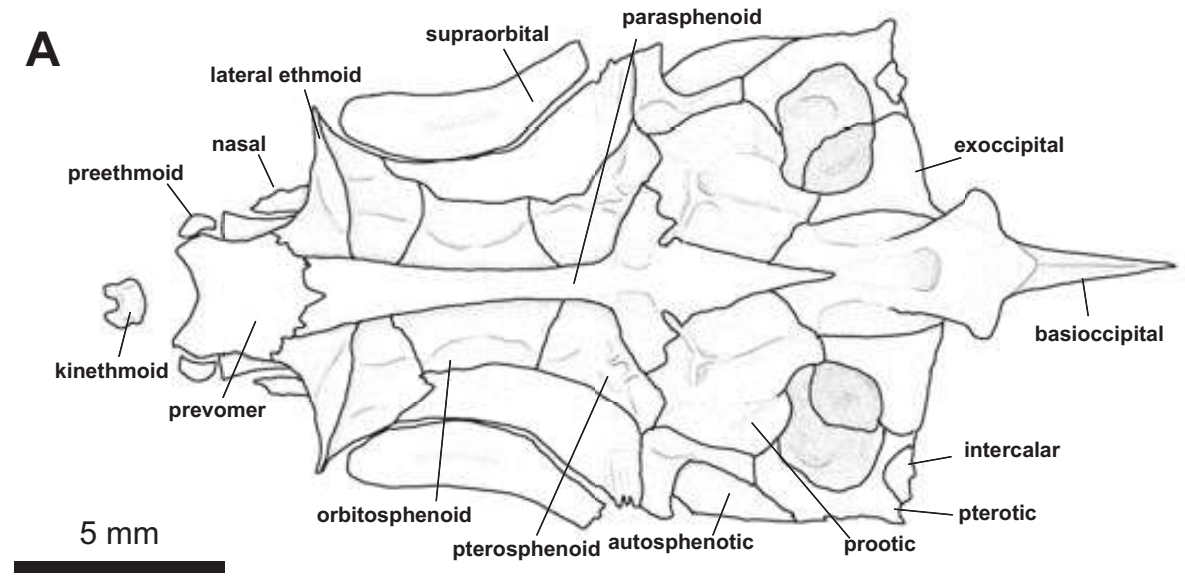
A
supraorbital
parasphenoid
lateral ethmoid
nasal
preethmoid
exoccipital
basioccipital
kinethmoid
prevomer
intercalar
orbitosphenoid
pterotic
pterosphenoid
autosphenotic
prootic
5 mm

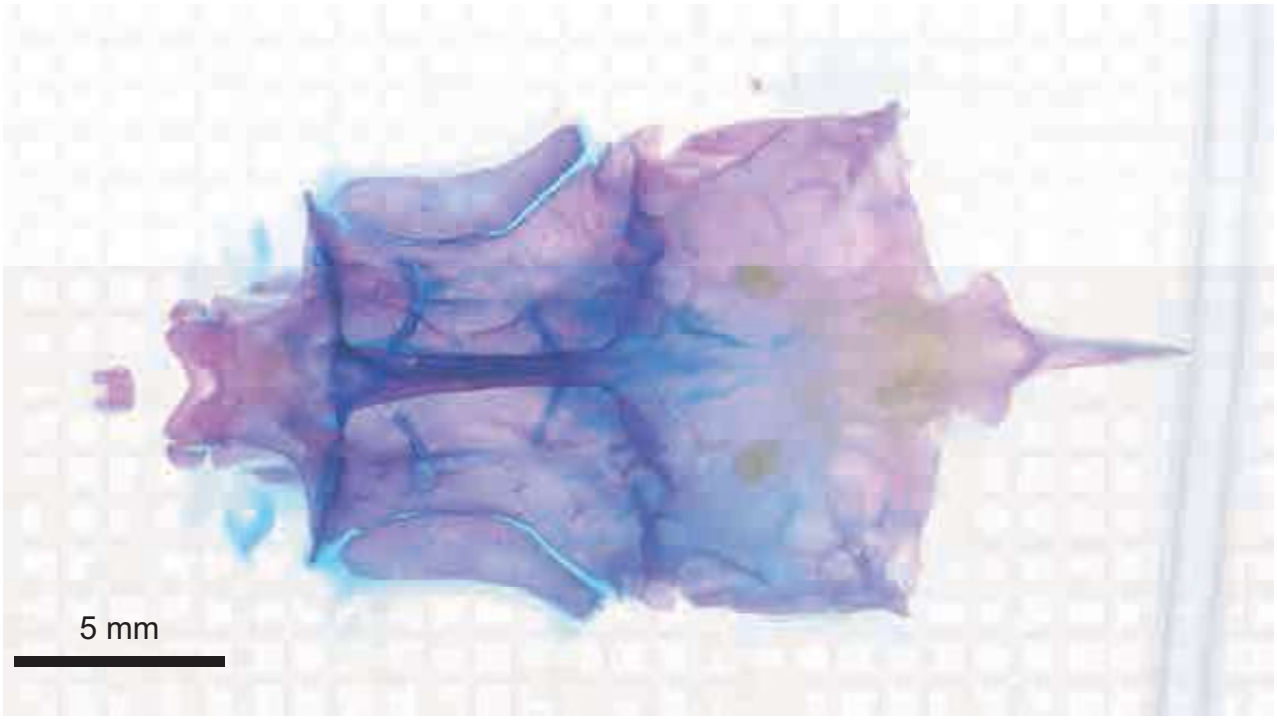
5 mm

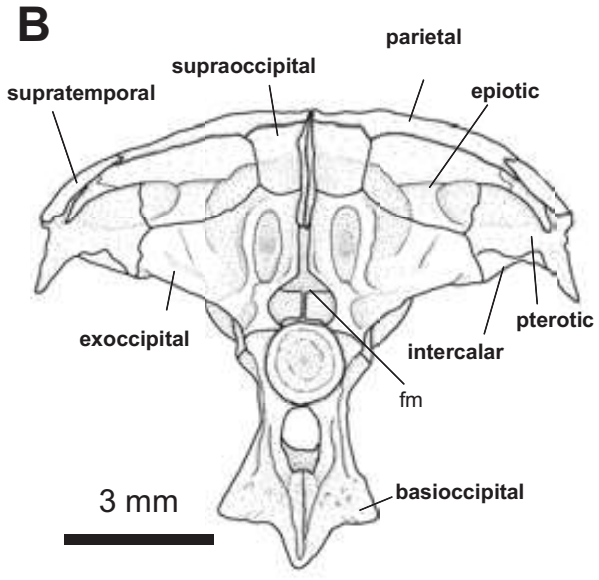
B
parietal
supraoccipital
supratemporal
epiotic
exoccipital
pterotic
intercalar
fm
basioccipital
3 mm

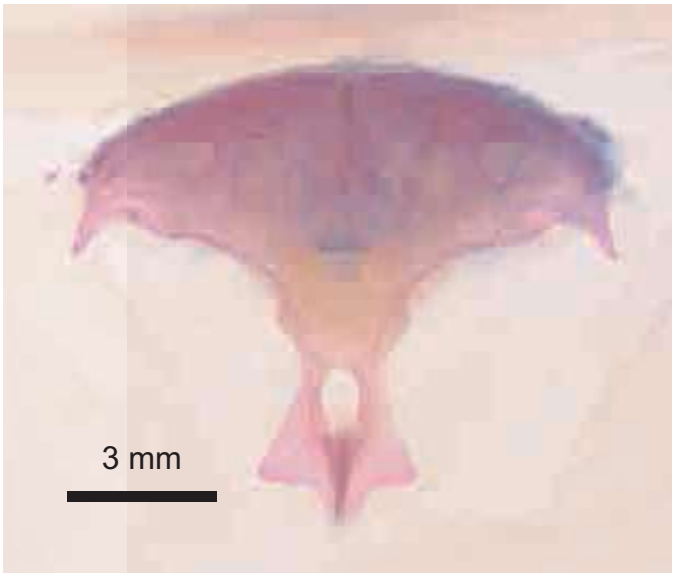
3 mm

Plate 2-6

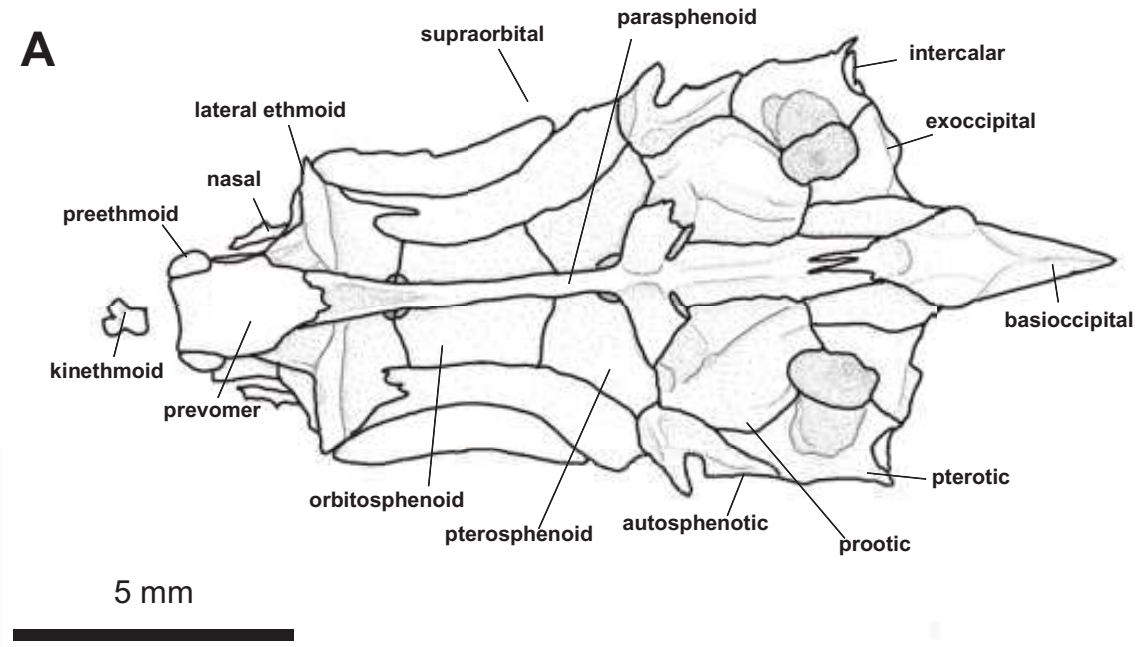
A
supraorbital
parasphenoid
intercalar
lateral ethmoid
exoccipital
nasal
preethmoid
basioccipital
kinethmoid
prevomer
orbitosphenoid
pterosphenoid
autosphenotic
prootic
pterotic
5 mm


5 mm

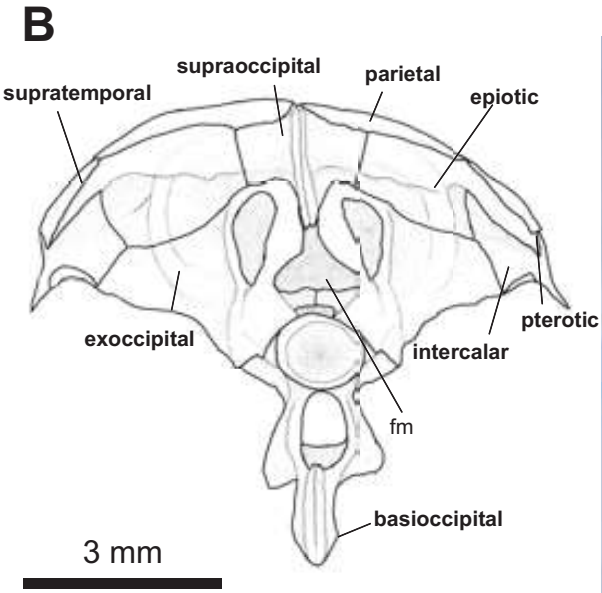
B
supraoccipital
parietal
supratemporal
epiotic
exoccipital
pterotic
intercalar
fm
basioccipital
3 mm

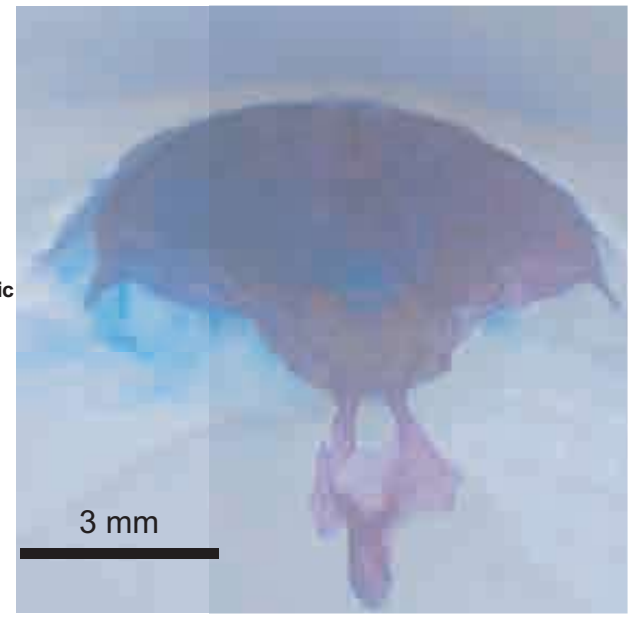
3 mm

Plate 2-7

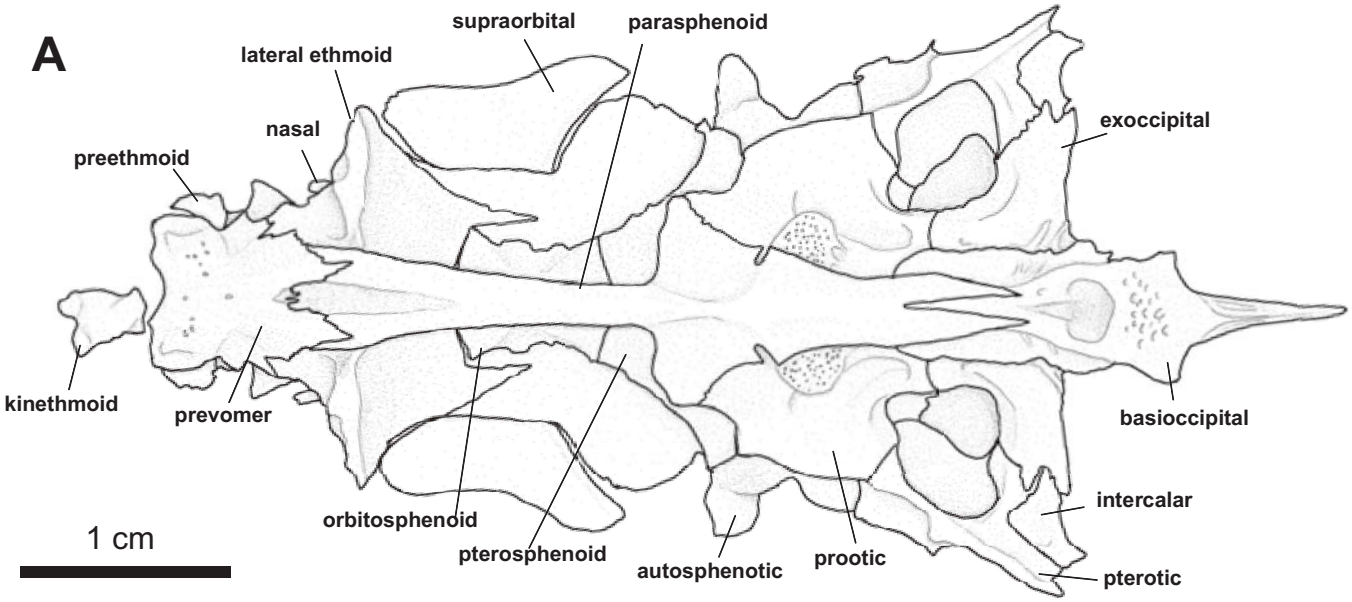
A
supraorbital
parasphenoid
lateral ethmoid
nasal
preethmoid
exoccipital
kinethmoid
prevomer
basioccipital
intercalar
orbitosphenoid
pterosphenoid
autosphenotic
prootic
pterotic
1 cm


1cm

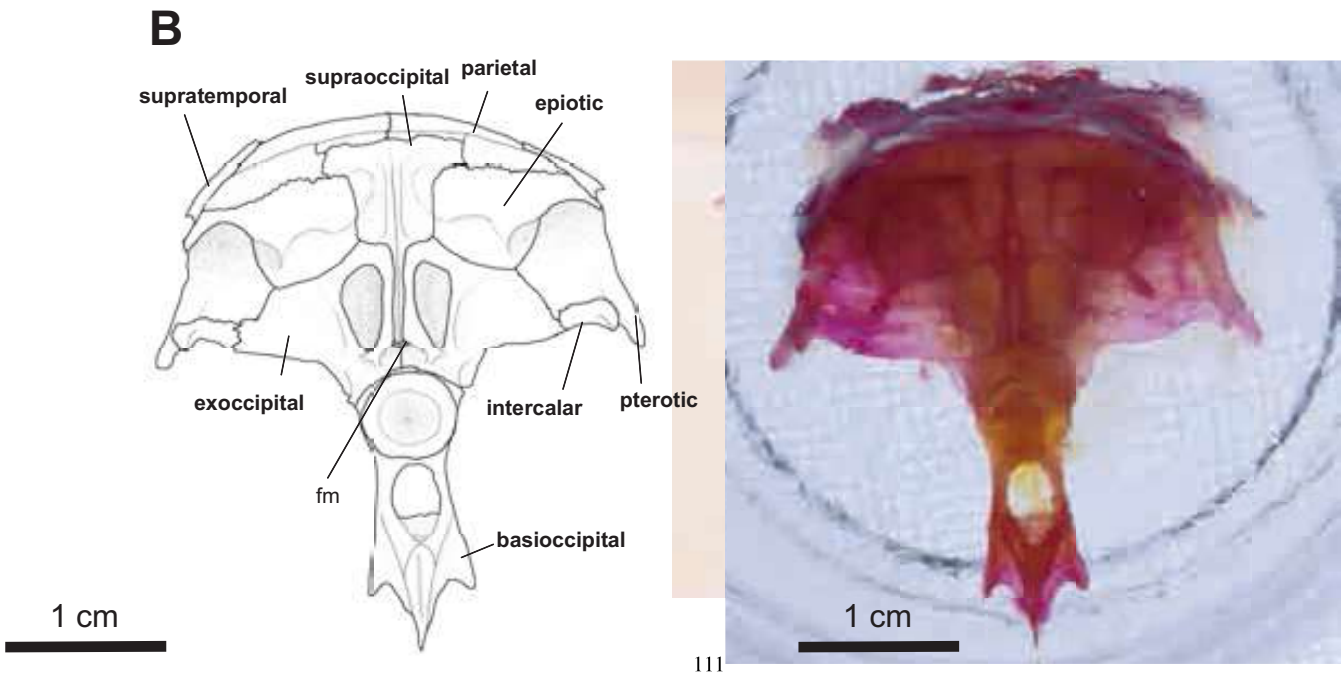
B
supratemporal
supraoccipital
parietal
epiotic
exoccipital
intercalar
pterotic
fm
basioccipital
1 cm
1 cm

Plate 2-8

A

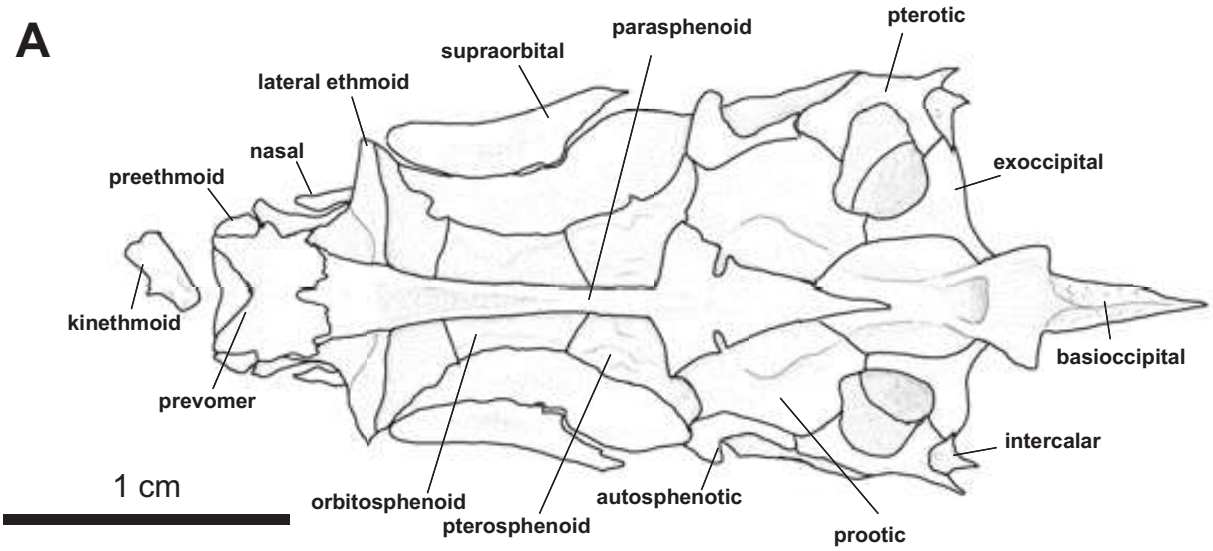

1 cm

B

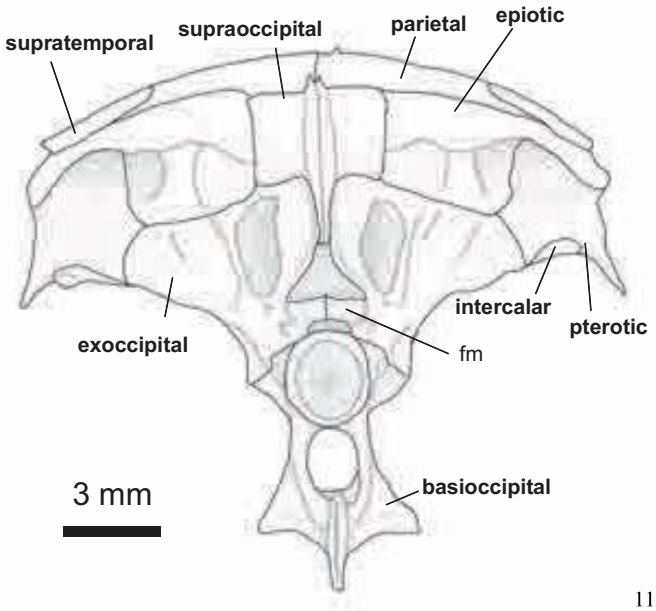

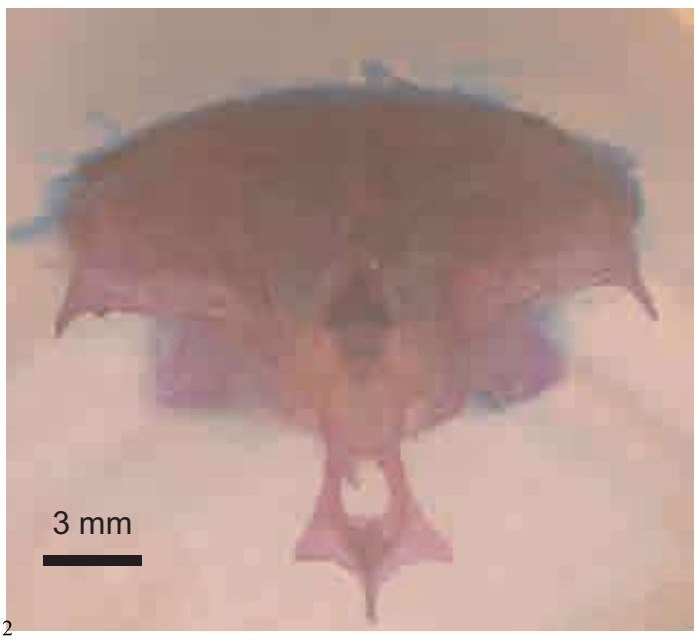

Plate 2-9

A

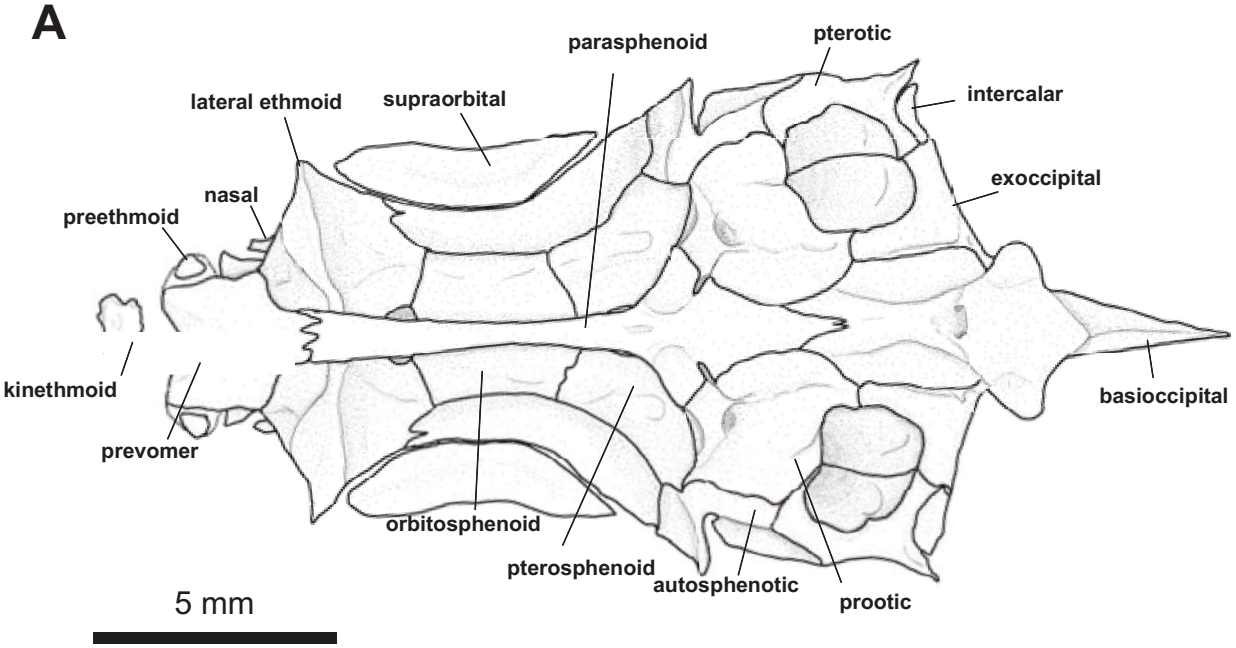
parasphenoid
pterotic
lateral ethmoid
supraorbital
intercalar
exoccipital
nasal
preethmoid
kinethmoid
basioccipital
prevomer
orbitosphenoid
pterosphenoid
autosphenotic
prootic
5 mm

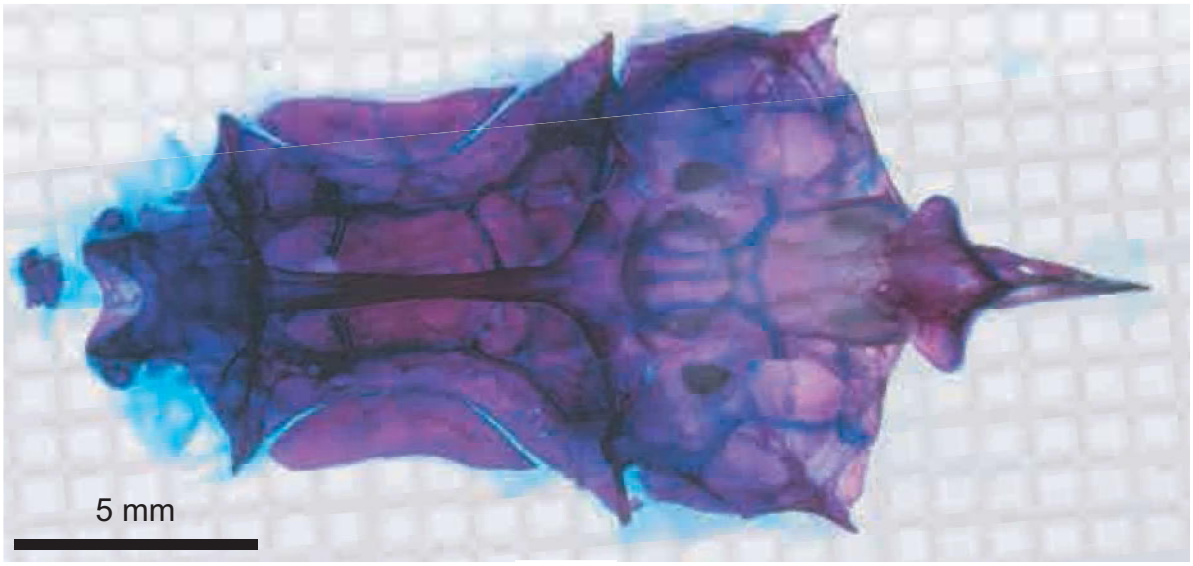
5 mm

B

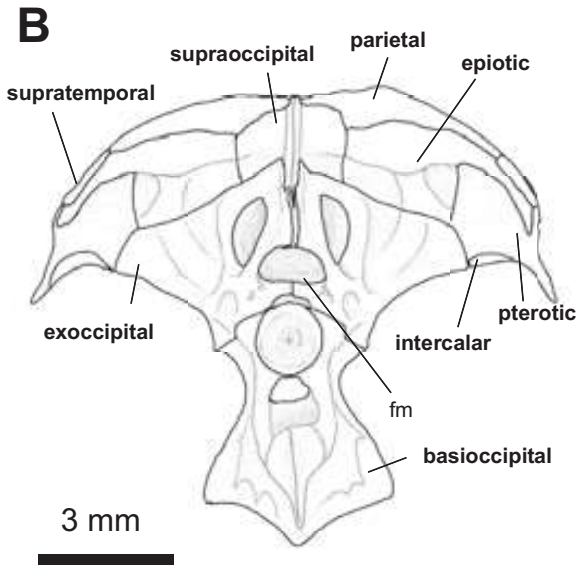
supraoccipital
parietal
epiotic
supratemporal
exoccipital
intercalar
pterotic
fm
basioccipital
3 mm

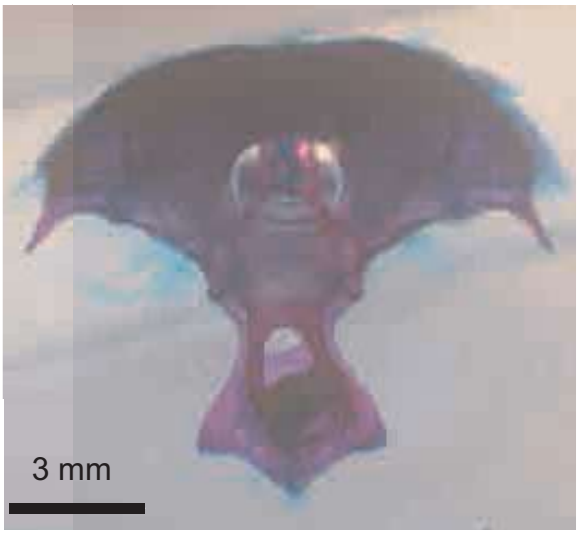
3 mm

Plate 3-1

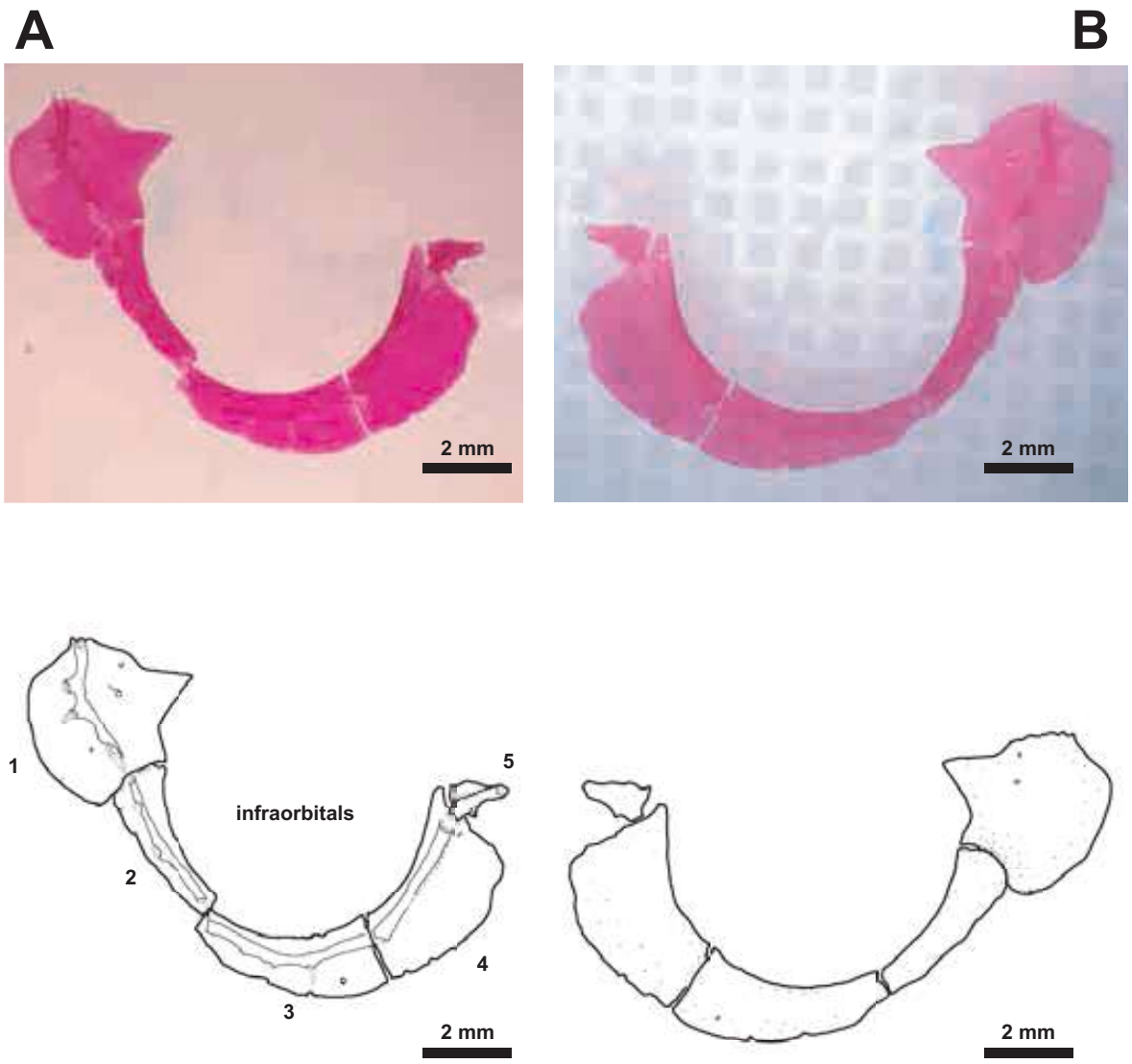

Plate 3-2

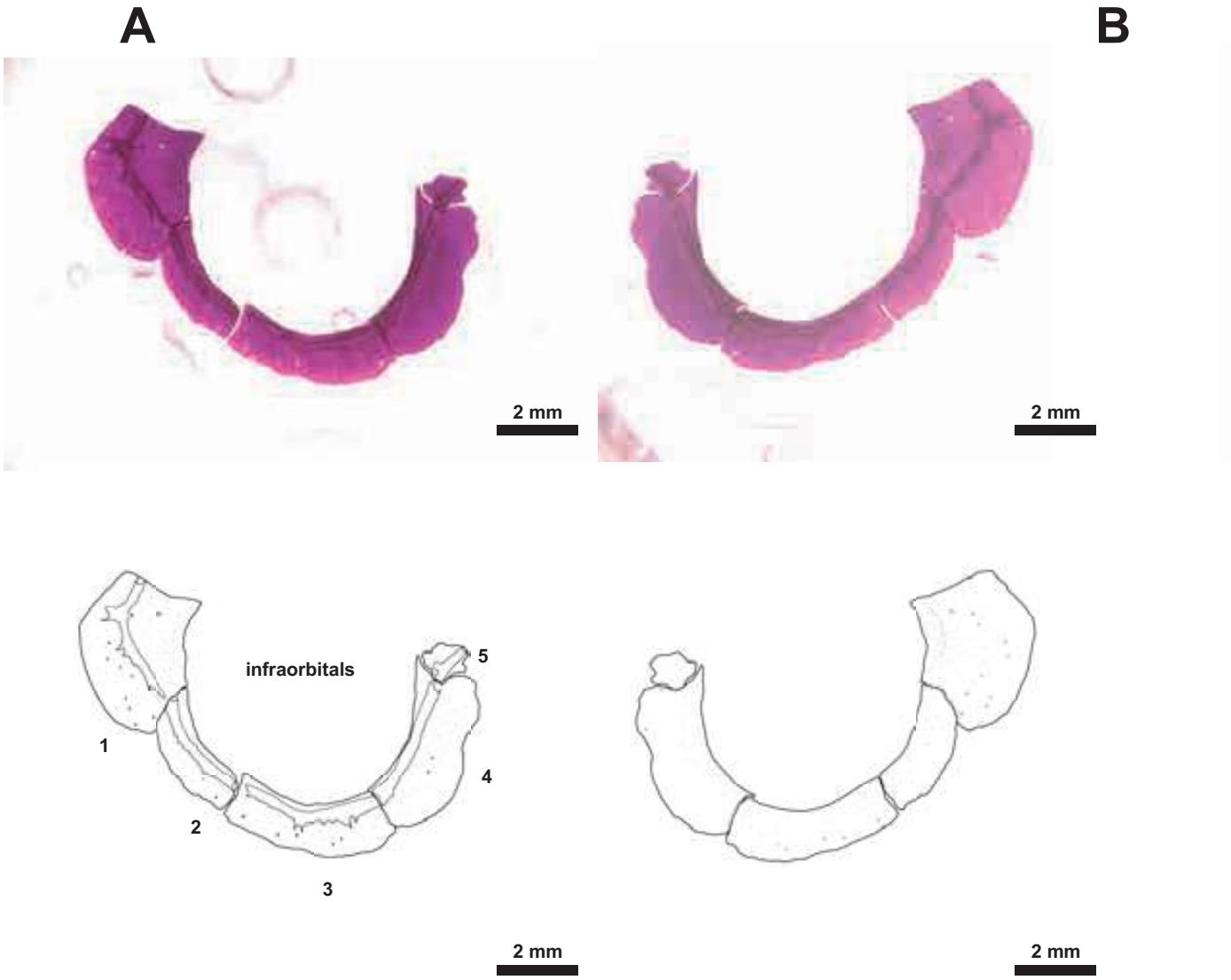

Plate 3-3

A

B

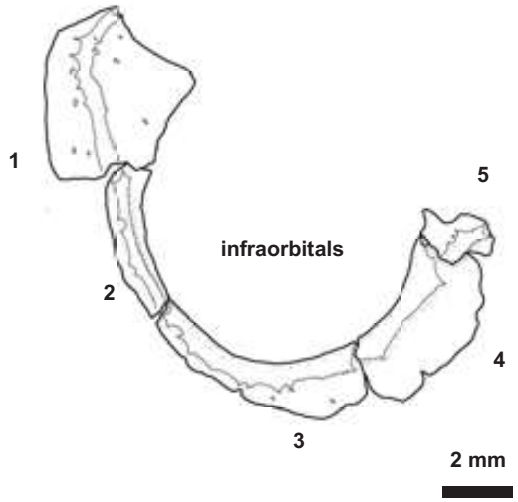

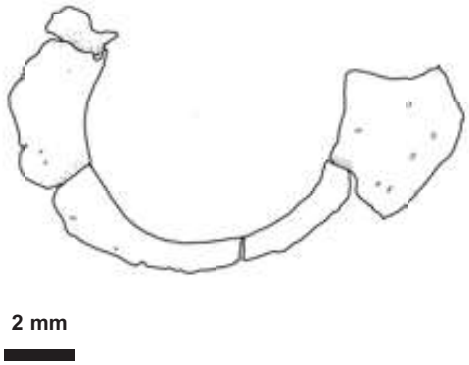

Plate 3-4

A

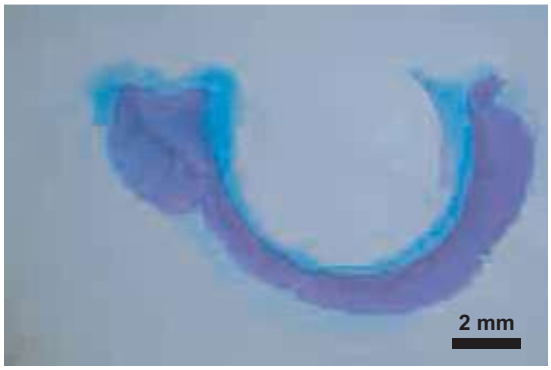

B

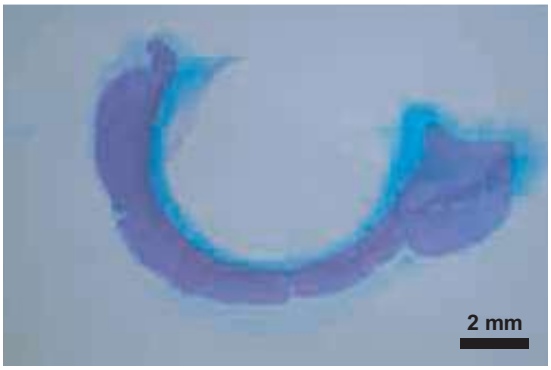

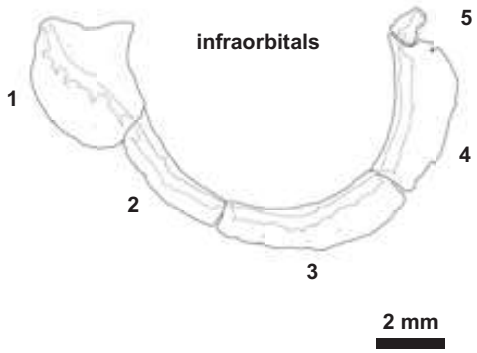

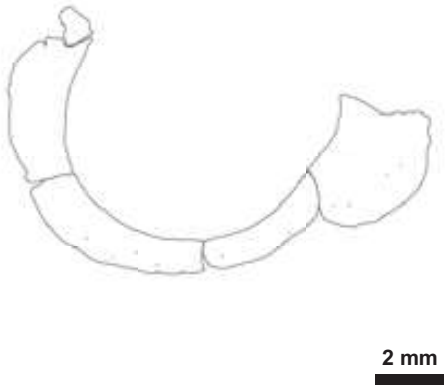

Plate 3-5

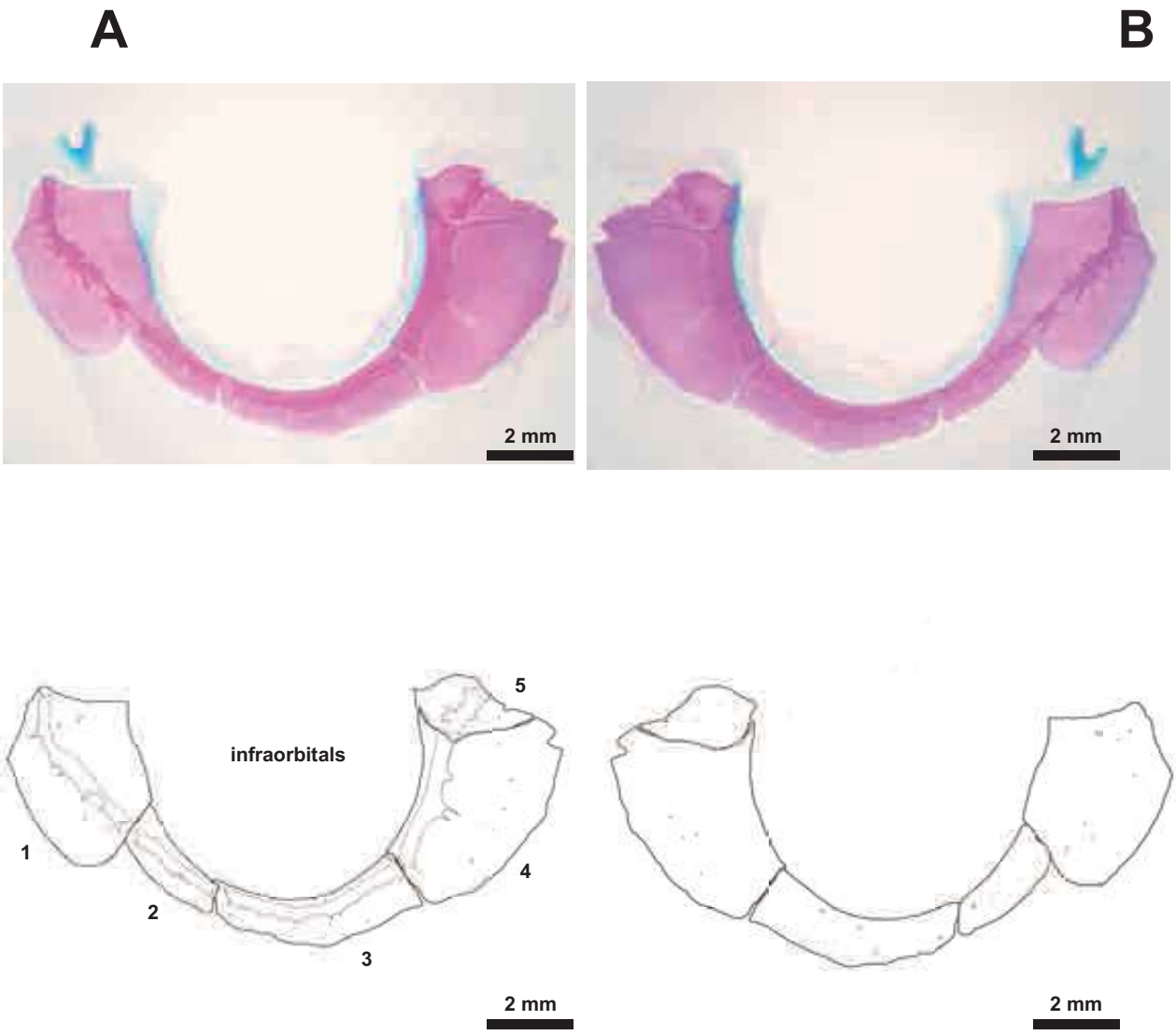

Plate 3-6

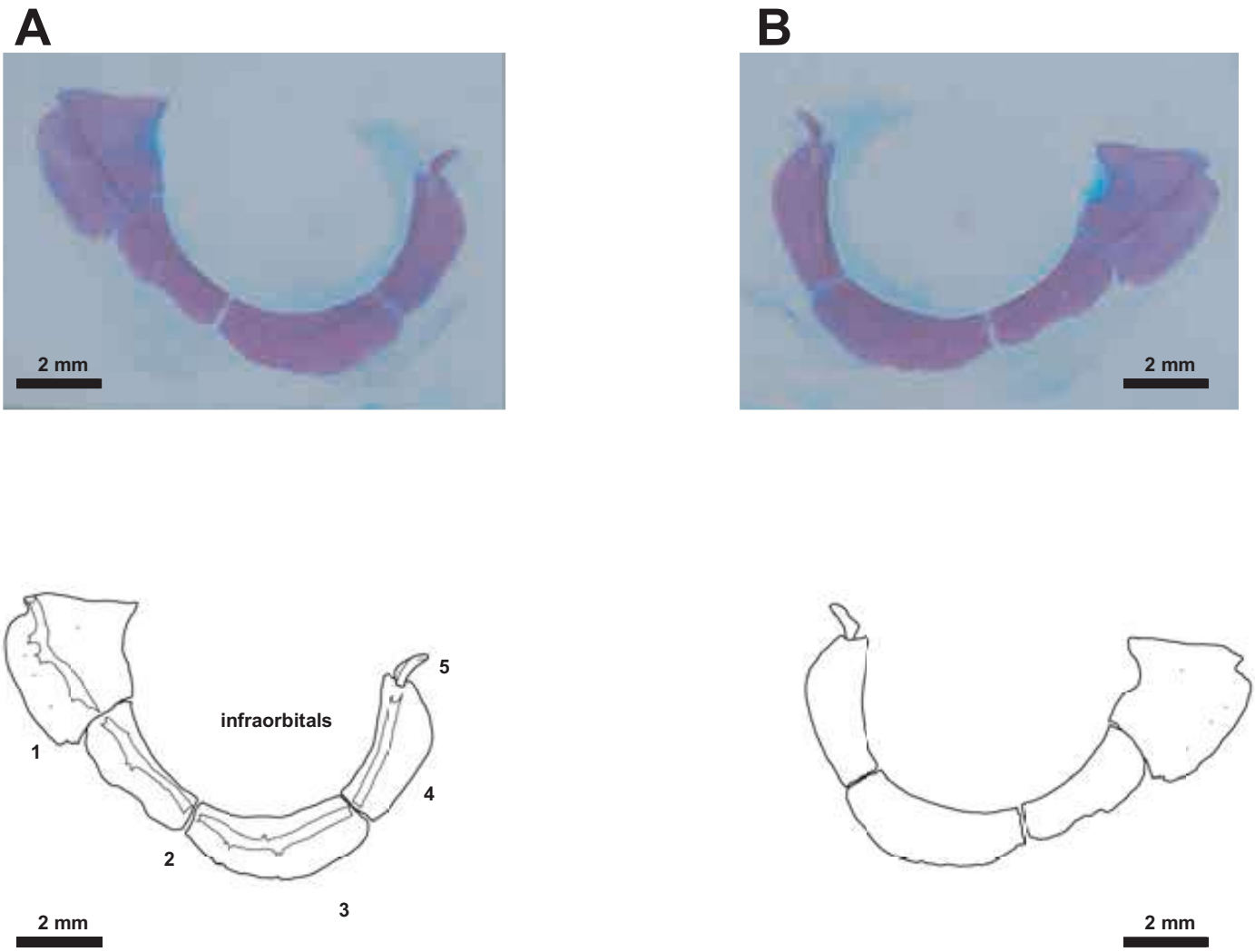

Plate 3-7

A

1 cm

B

1 cm

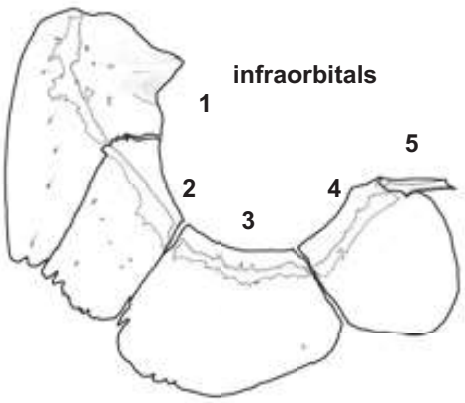

1 cm

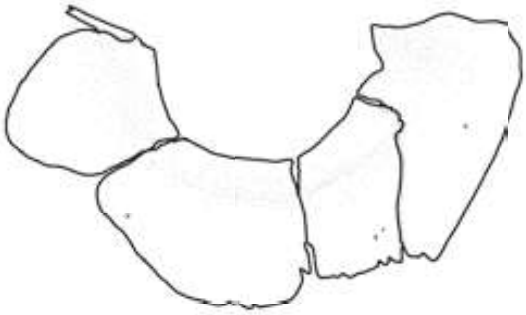

1 cm

Plate 3-8

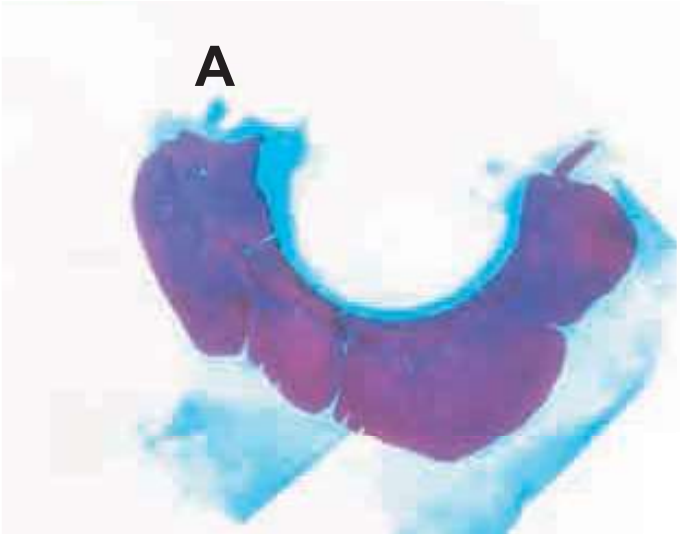

2 mm

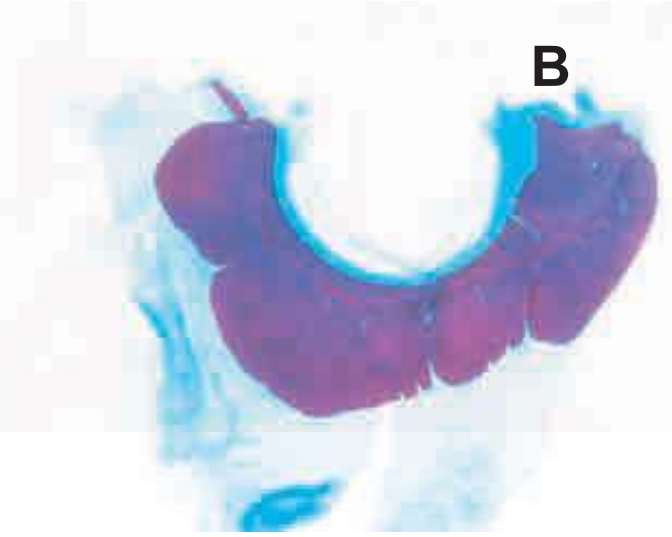

2 mm

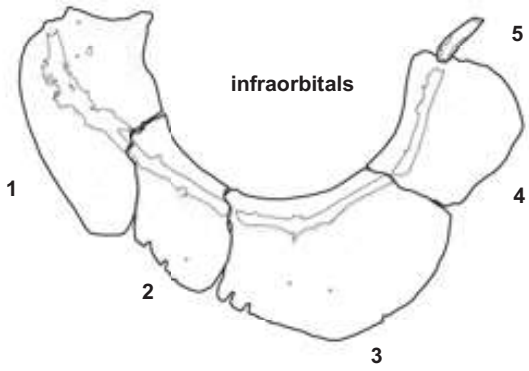

2 mm

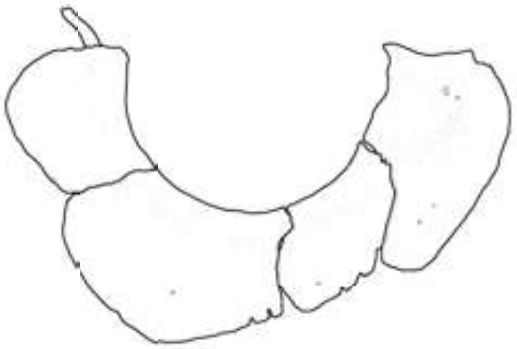

2 mm

Plate 3-9

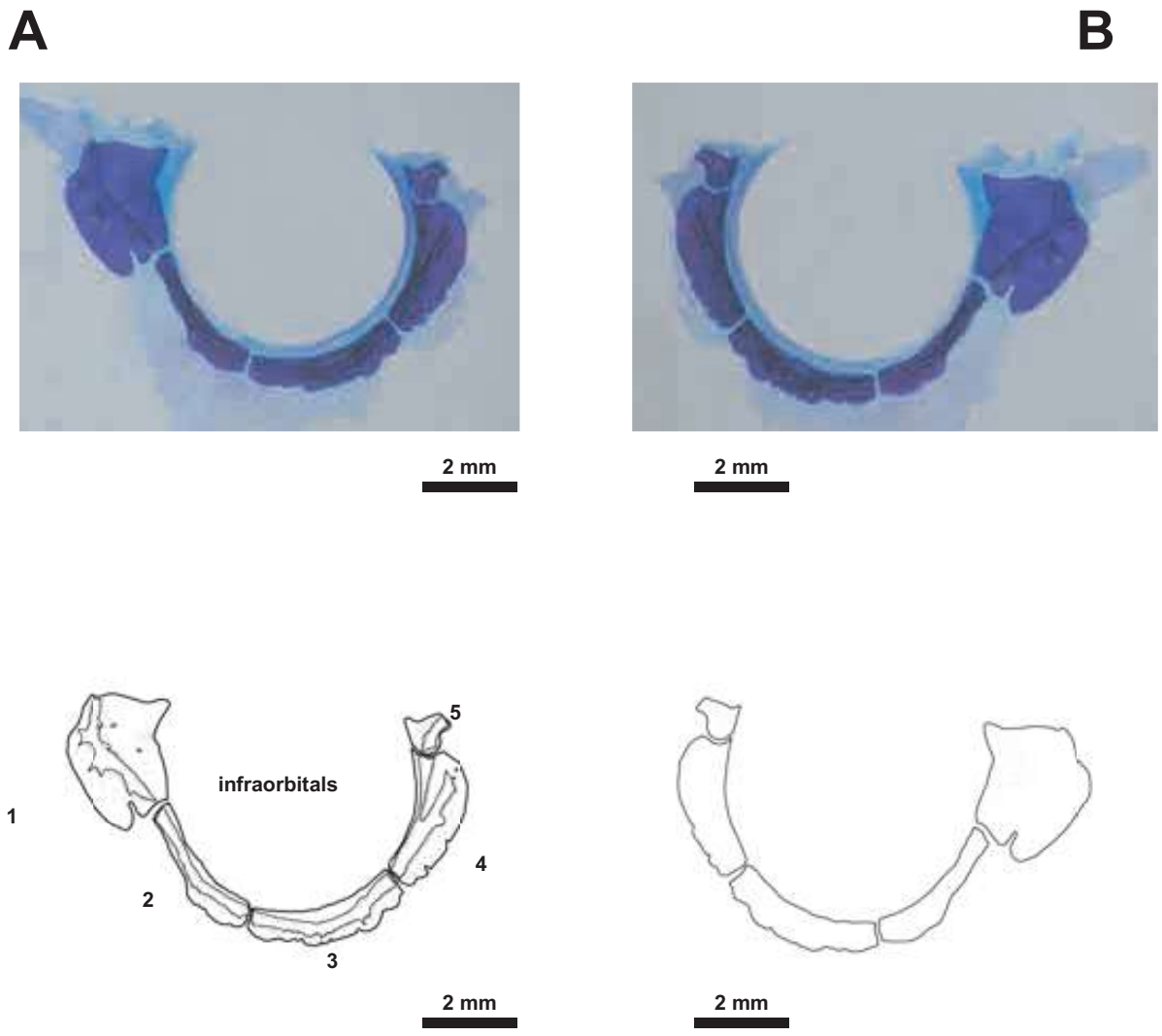

Plate 4-1

A

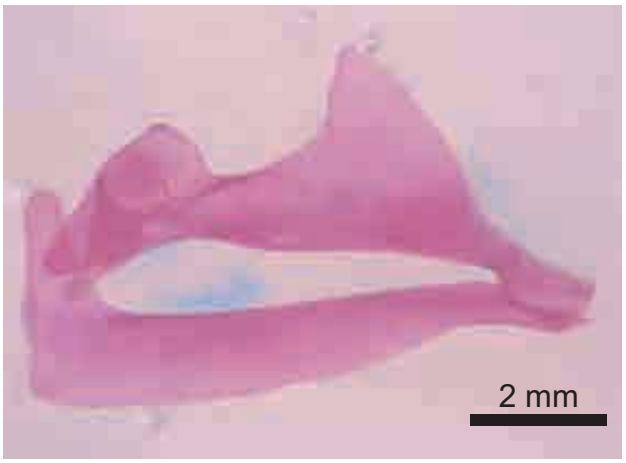
2 mm

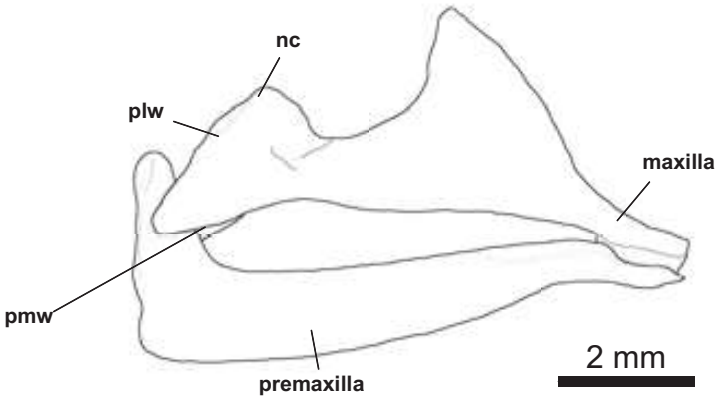
nc
plw
maxilla
pmw
premaxilla
2 mm

B

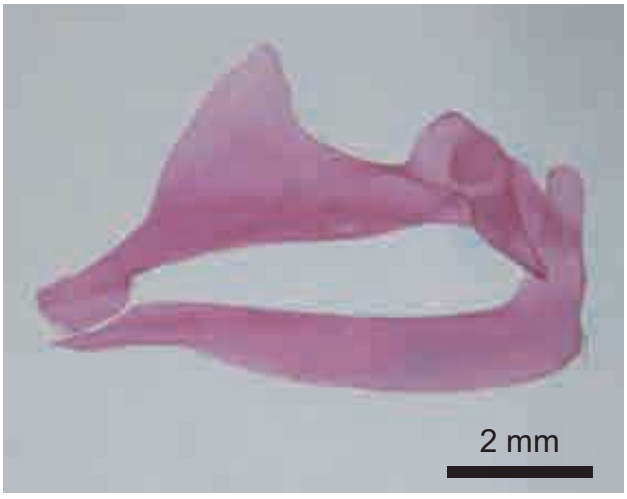
2 mm

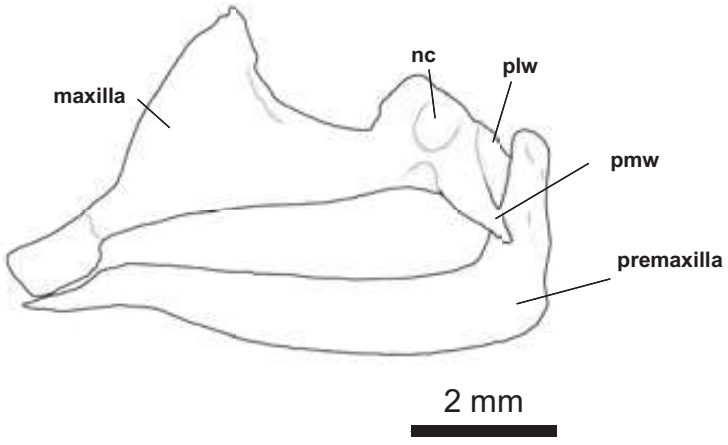
maxilla
nc
plw
pmw
premaxilla
2 mm

Plate 4-2

A


2 mm

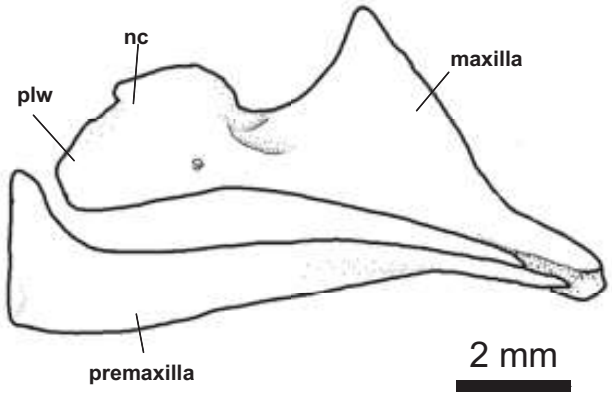
nc
maxilla
plw
premaxilla
2 mm

B

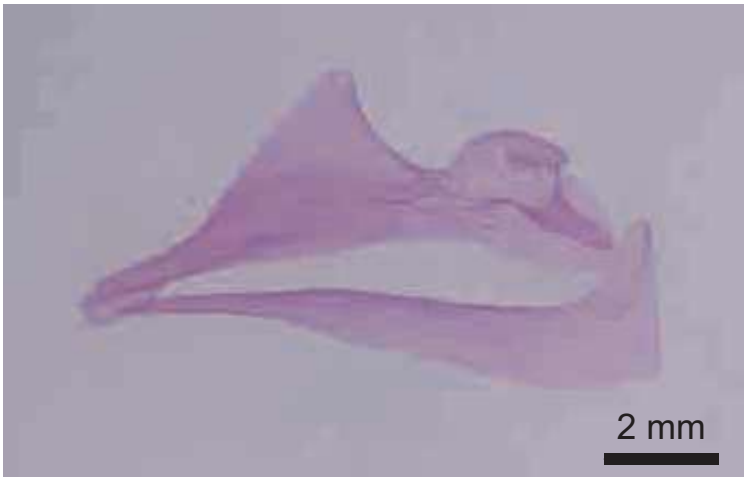
2 mm

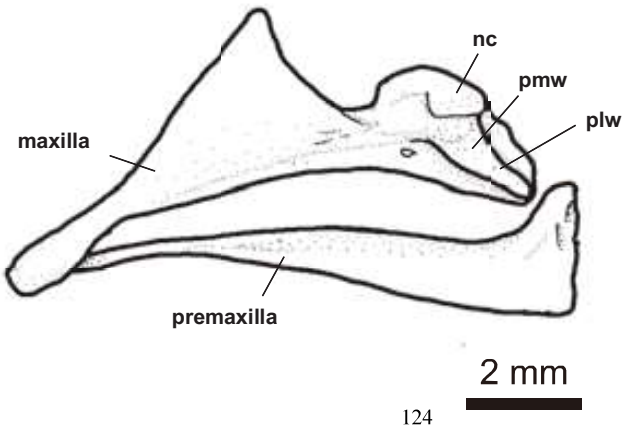
nc
pmw
plw
maxilla
premaxilla
2 mm

Plate 4-3

A

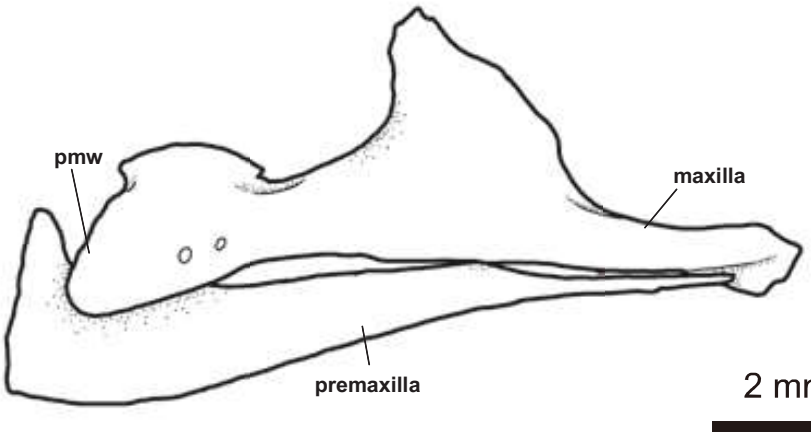
pmw
maxilla
premaxilla
2 mm


2 mm

B

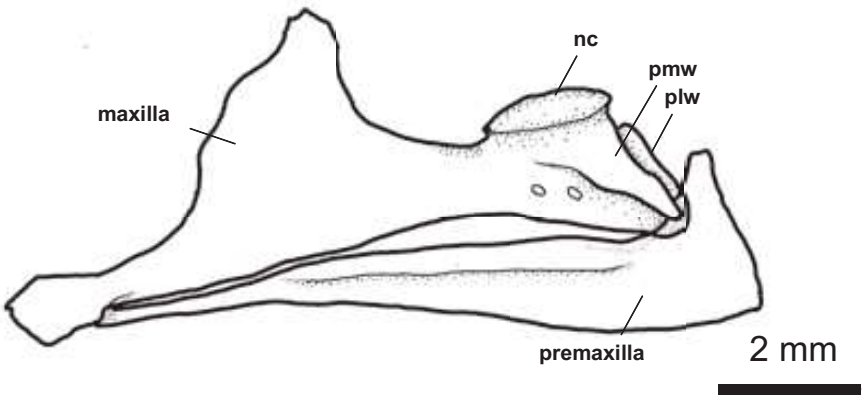
nc
pmw
plw
maxilla
premaxilla
2 mm

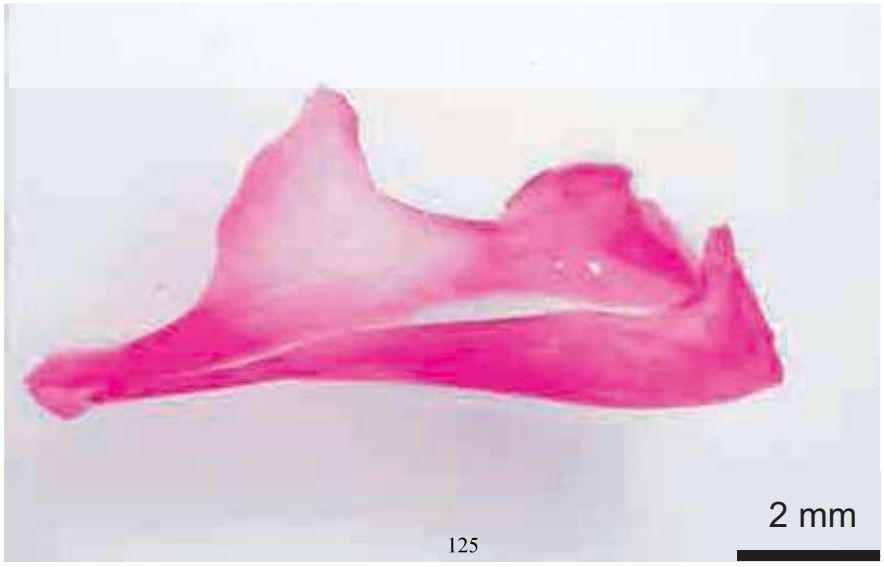
2 mm

Plate 4-4

A

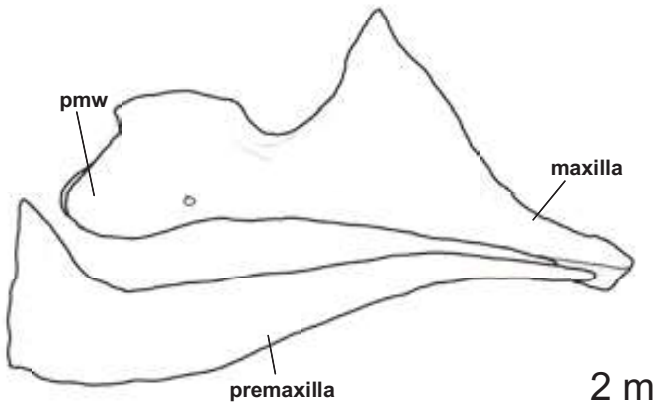
pmw
maxilla
premaxilla
2 mm

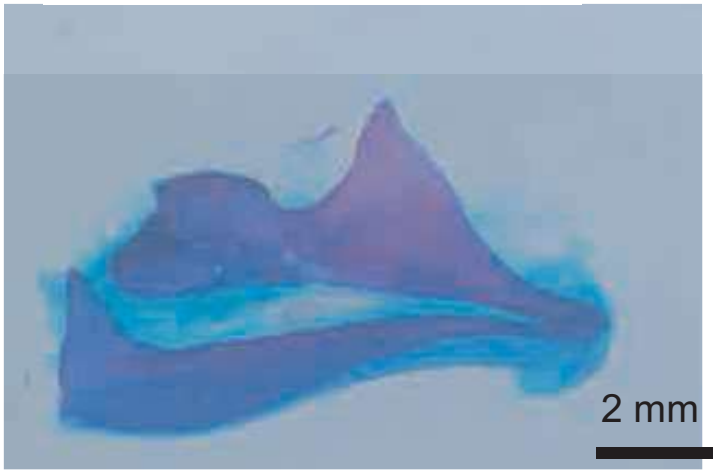
2 mm

B

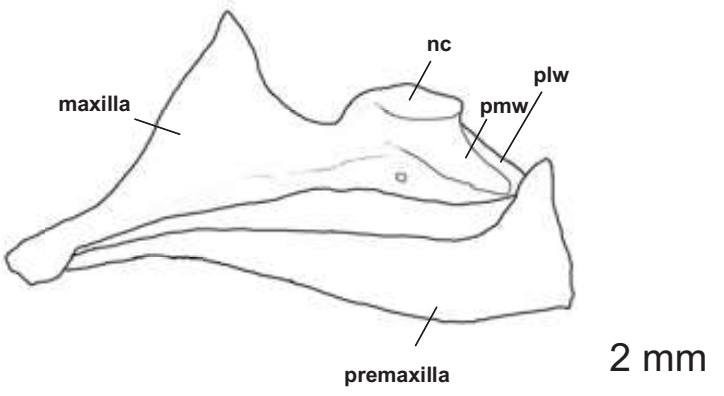
nc
plw
maxilla
pmw
premaxilla
2 mm

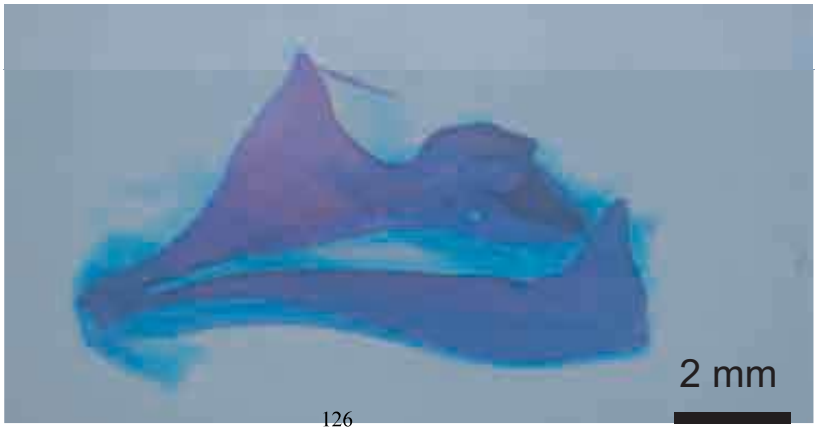
2 mm

Plate 4-5

A

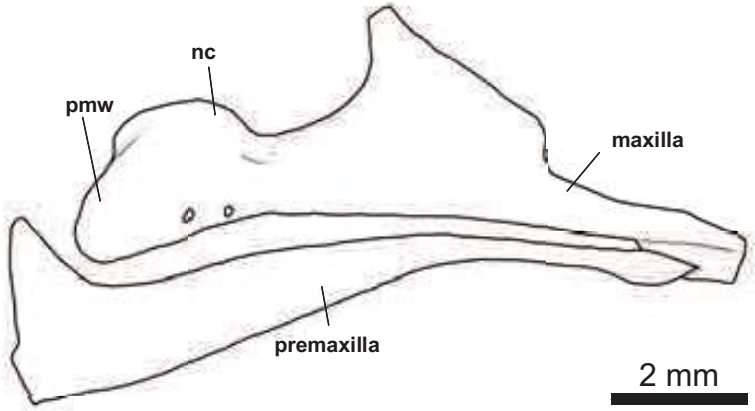
nc
pmw
maxilla
premaxilla
2 mm


2 mm

B

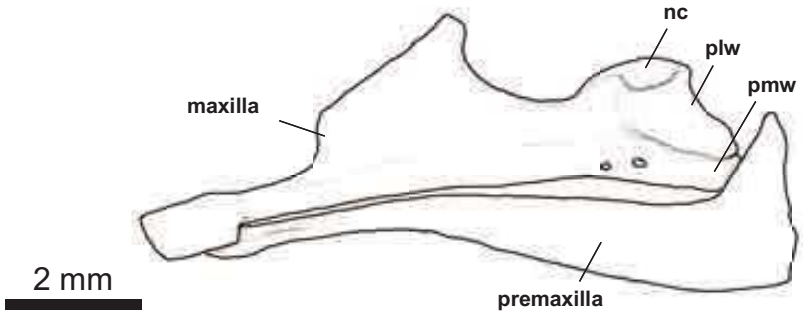
nc
plw
pmw
maxilla
2 mm
premaxilla


2 mm

Plate 4-6

A

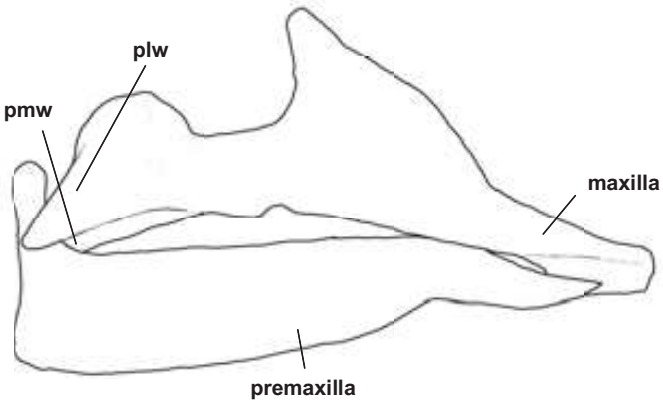

2 mm

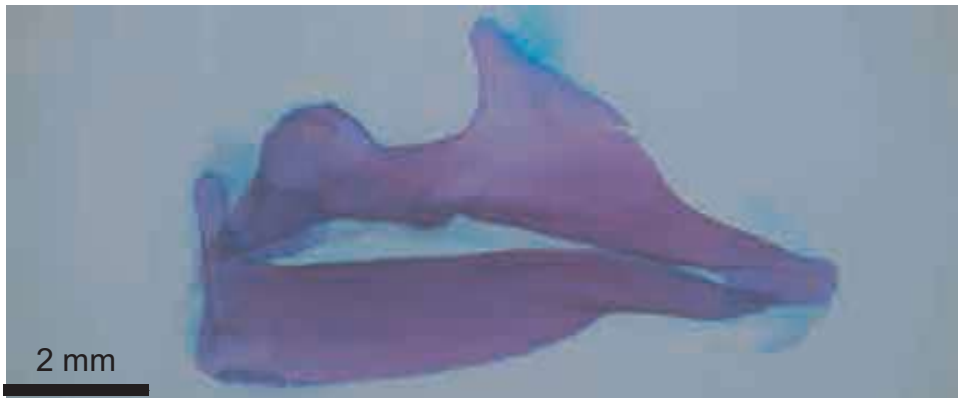

B

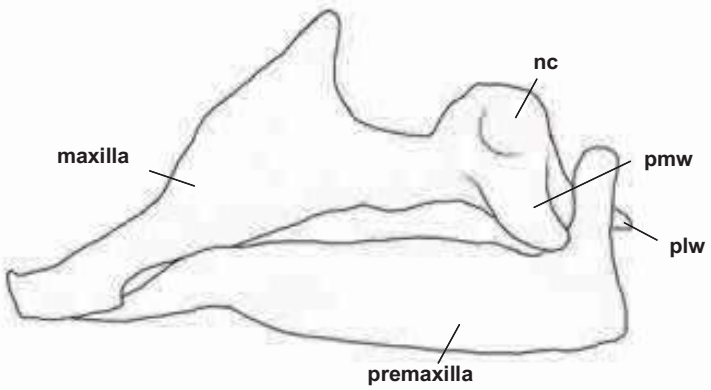

2 mm

2 mm

Plate 4-7

A

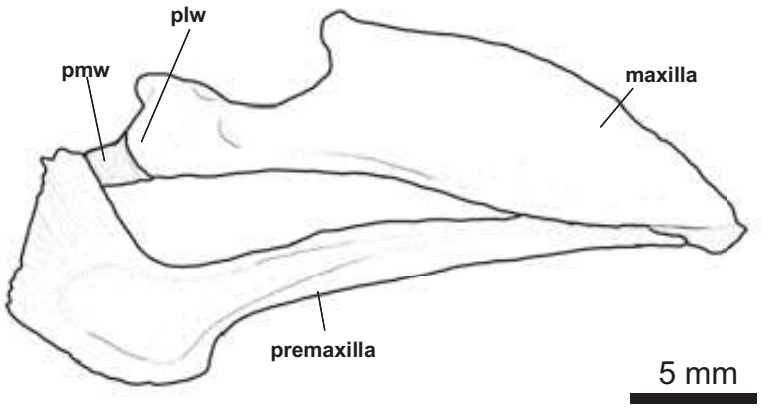
plw
pmw
maxilla
premaxilla
5 mm

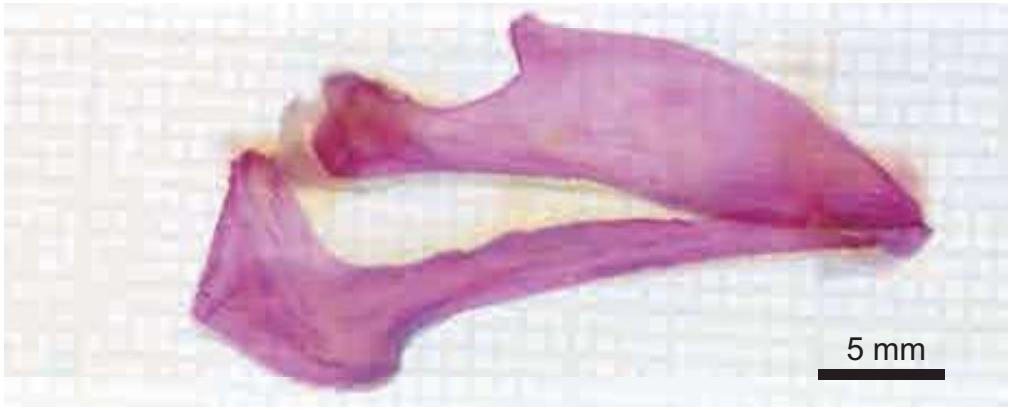
5 mm

B

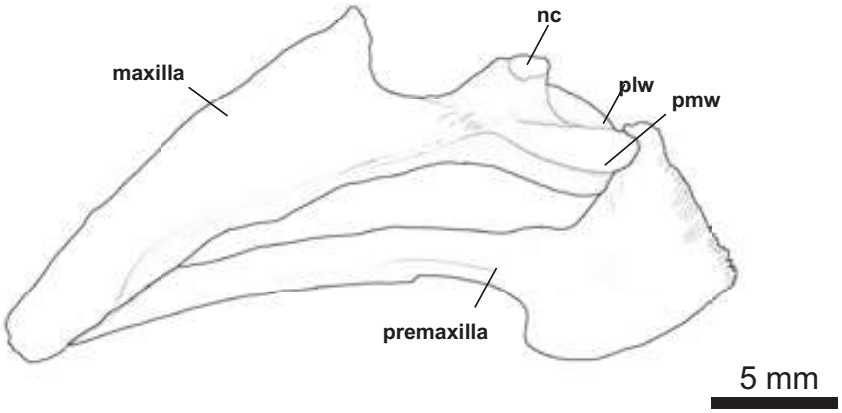
nc
maxilla
plw
pmw
premaxilla
5 mm


5 mm

Plate 4-8

A

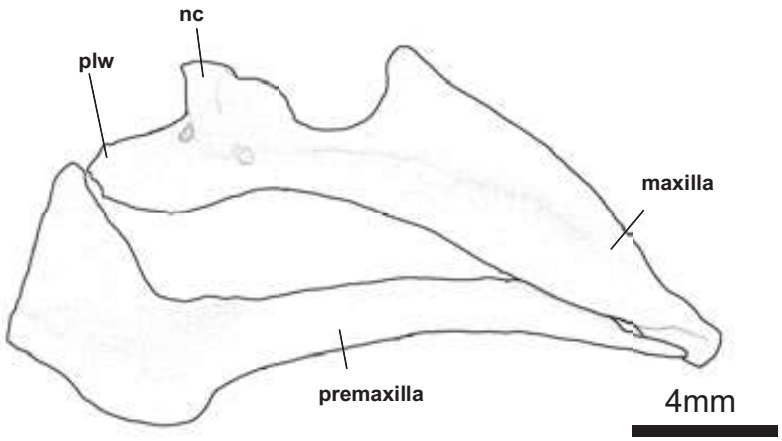

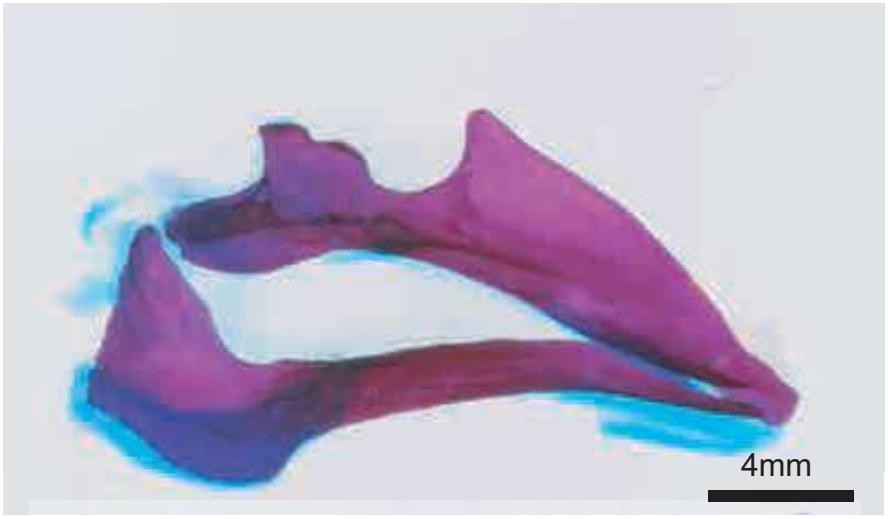

B

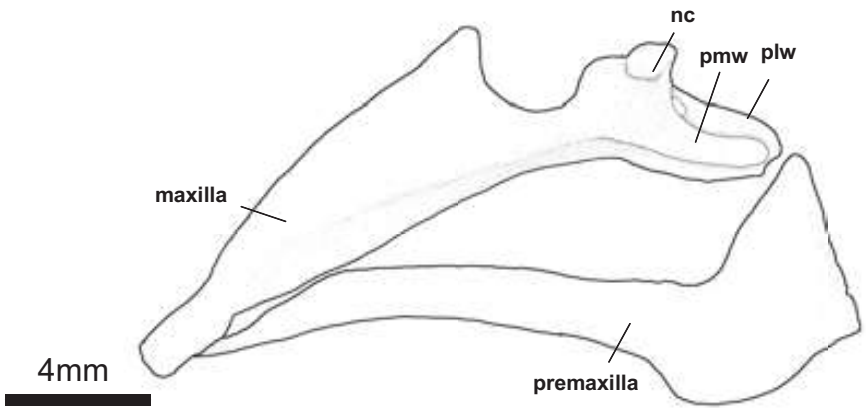

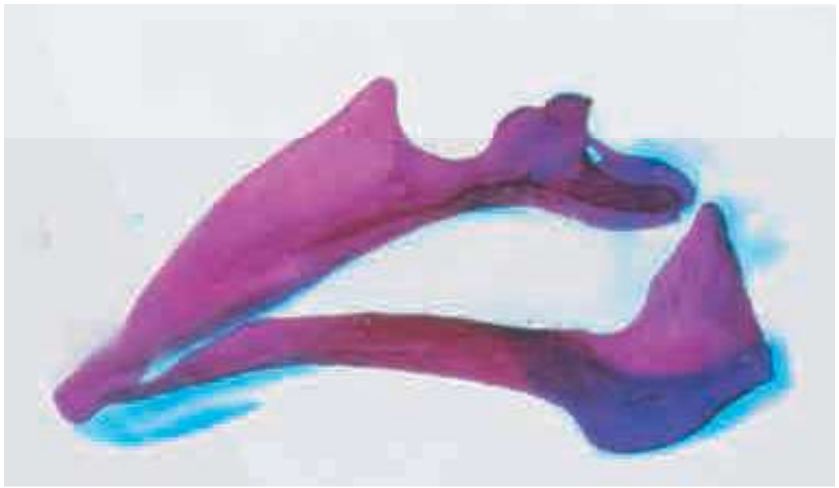

4mm

Plate 4-9

A

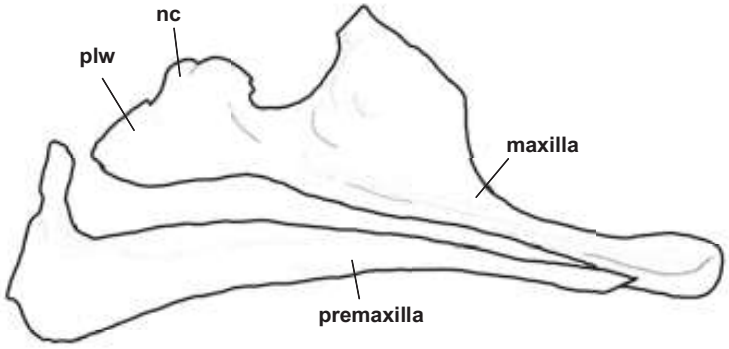

2 mm

B

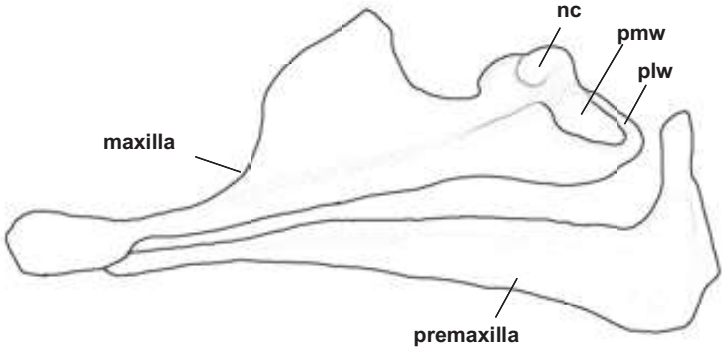

2 mm

Plate 5-1

A

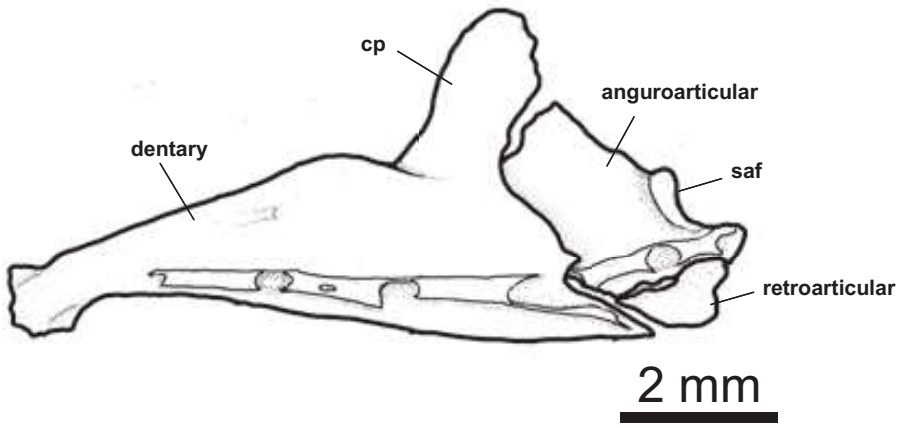
cp
anguroarticular
dentary
saf
retroarticular
2 mm


2 mm

B

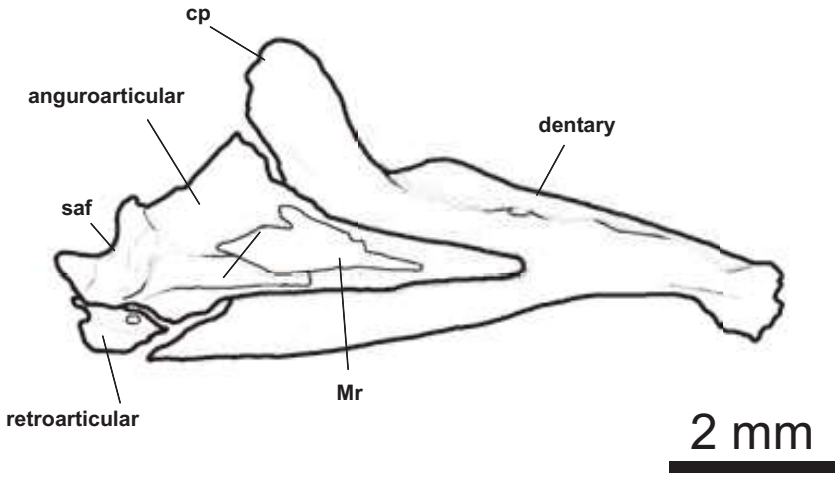
cp
anguroarticular
dentary
saf
Mr
retroarticular
2 mm


2 mm

Plate 5-2

A


2 mm

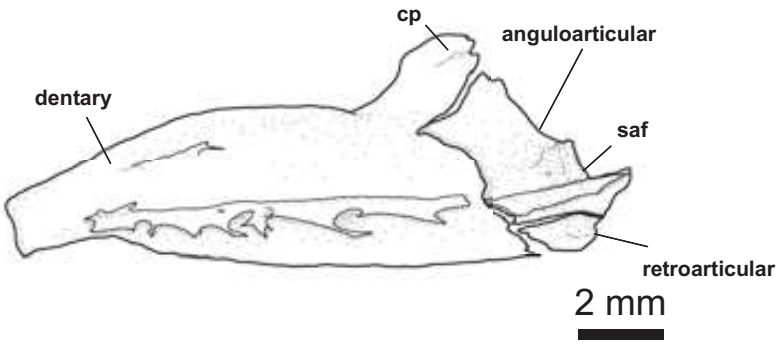
cp
anguloarticular
dentary
saf
retroarticular
2 mm

B


2 mm

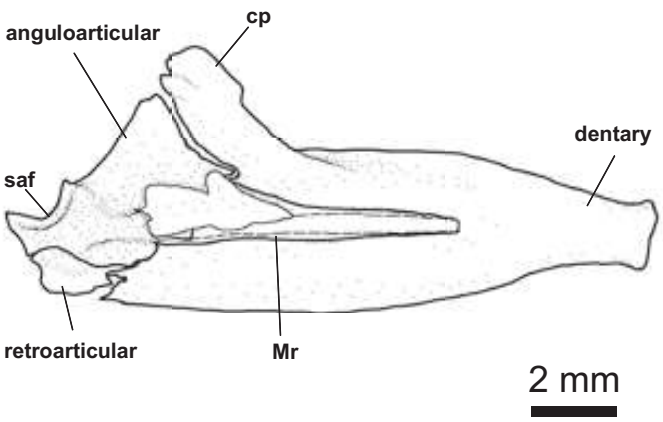
anguloarticular
cp
dentary
saf
retroarticular
Mr
2 mm

Plate 5-3

A

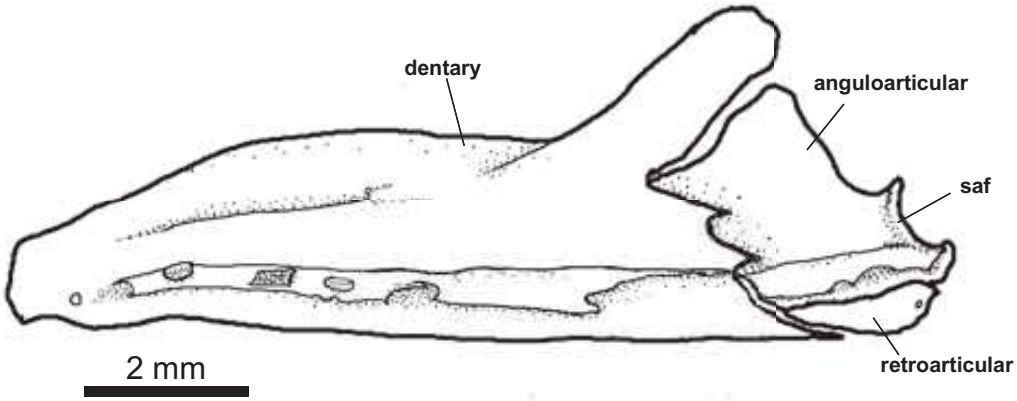
dentary
anguloarticular
saf
retroarticular
2 mm

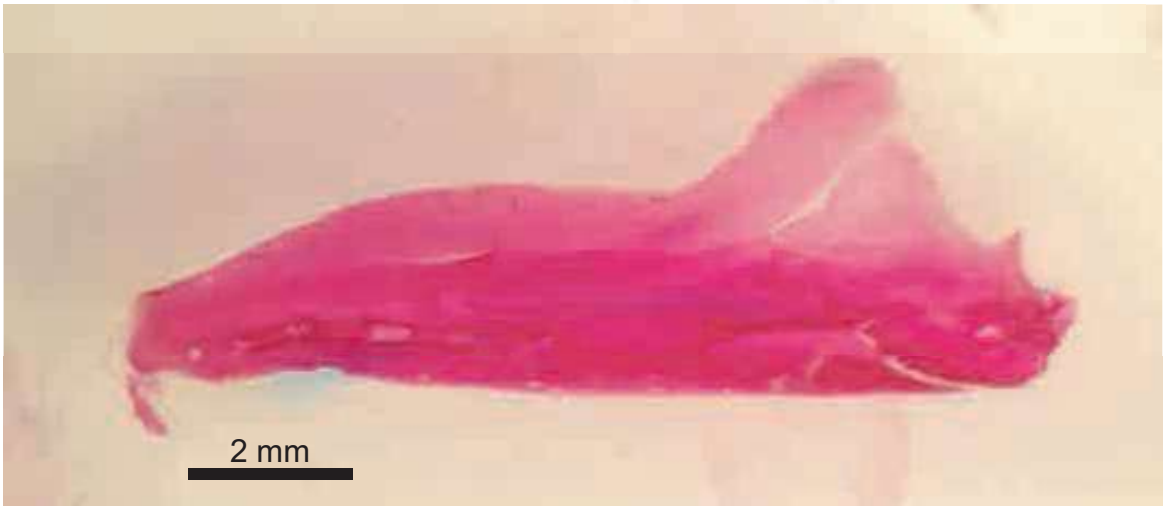
2 mm

B

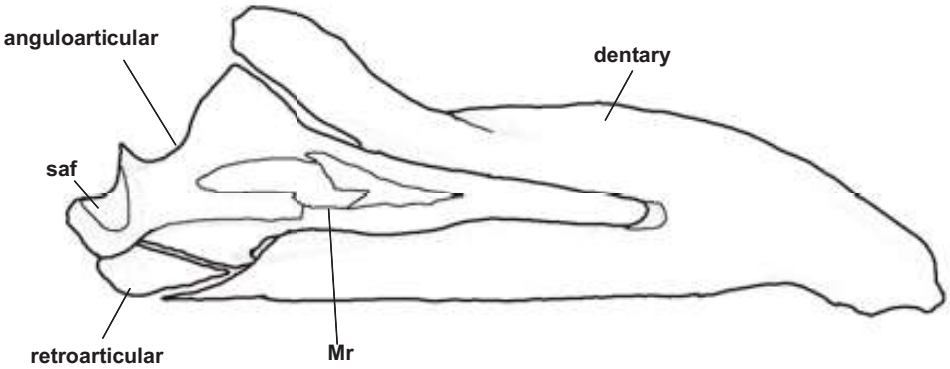
anguloarticular
dentary
saf
retroarticular
Mr
2 mm

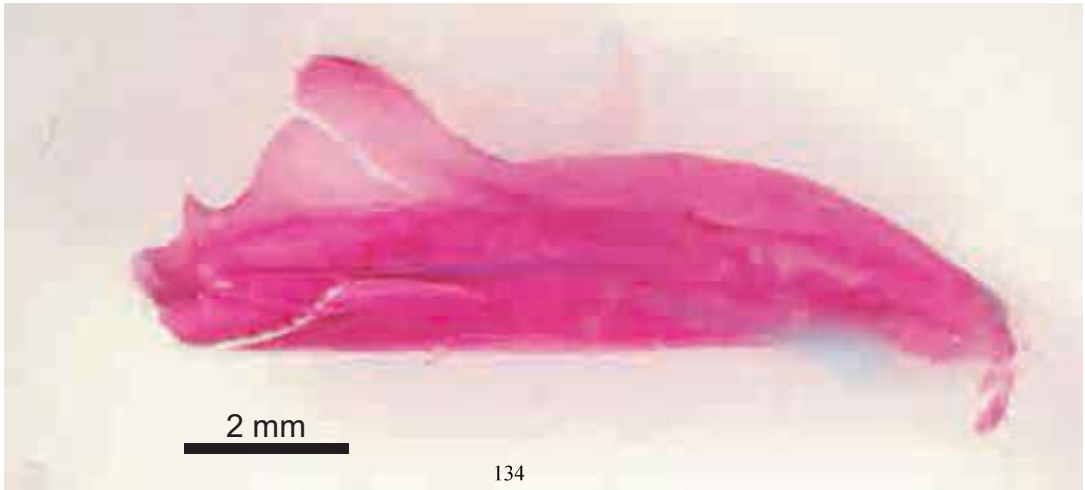
2 mm

Plate 5-4

A

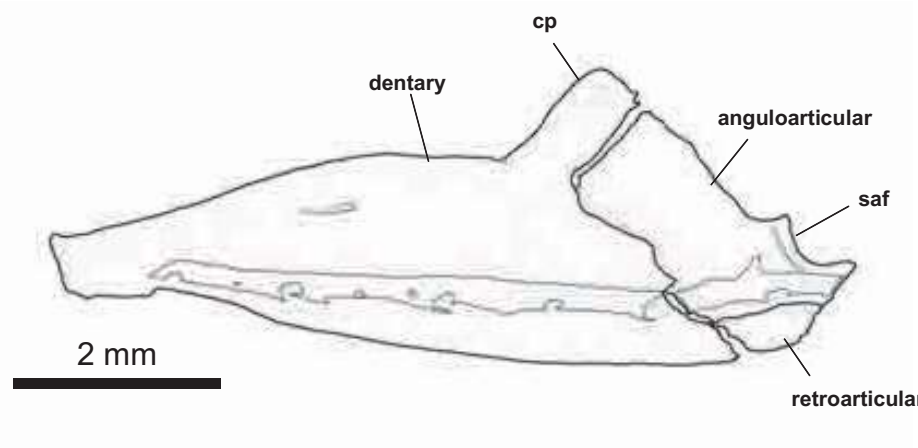
cp
dentary
anguloarticular
saf
2 mm
retroarticular

B


2 mm

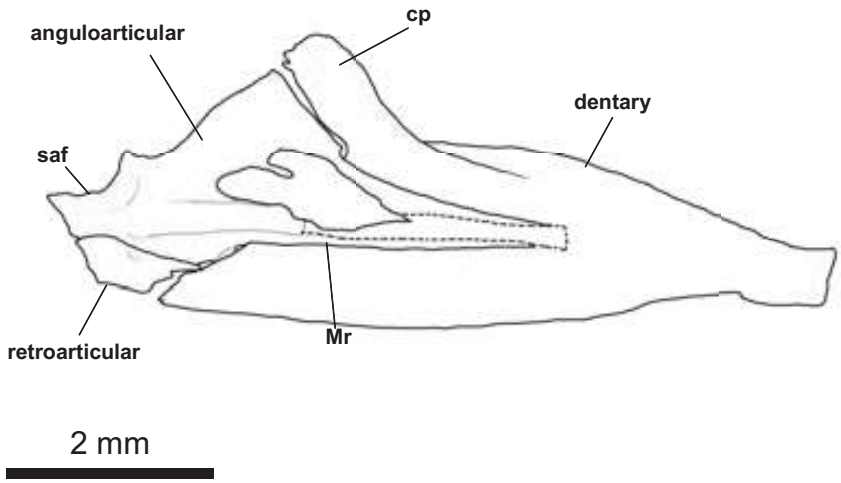
anguloarticular
cp
dentary
saf
Mr
retroarticular
2 mm


2 mm

Plate 5-5

A

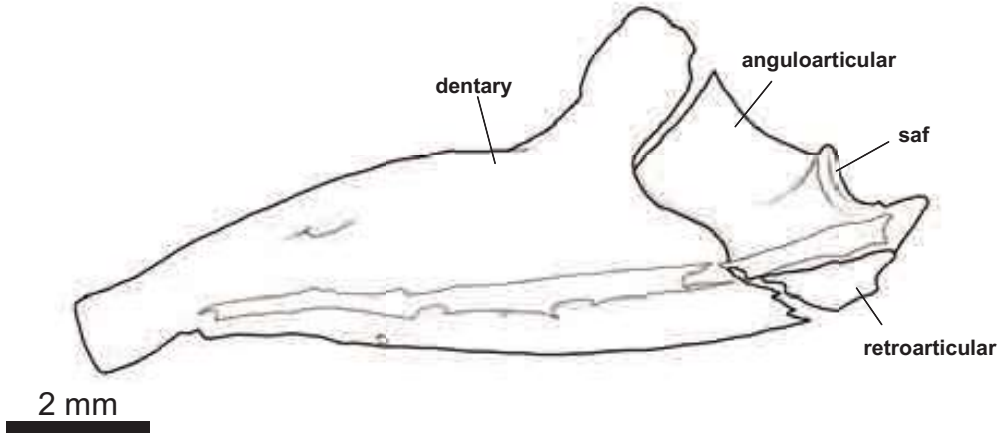
dentary
anguloarticular
saf
retroarticular
2 mm


2 mm

B

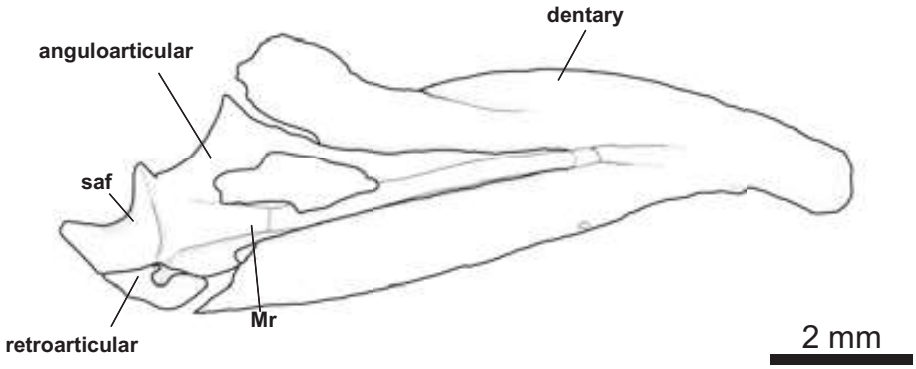
dentary
anguloarticular
saf
Mr
retroarticular
2 mm

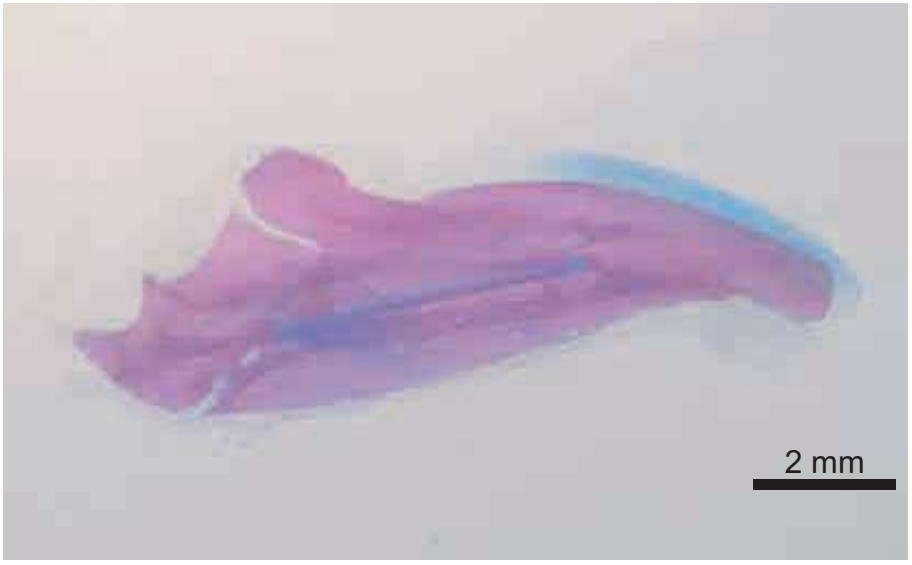
2 mm

Plate 5-6

A

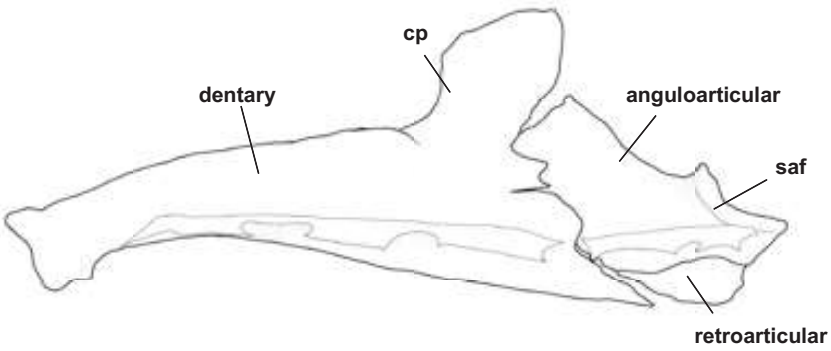

2 mm

B

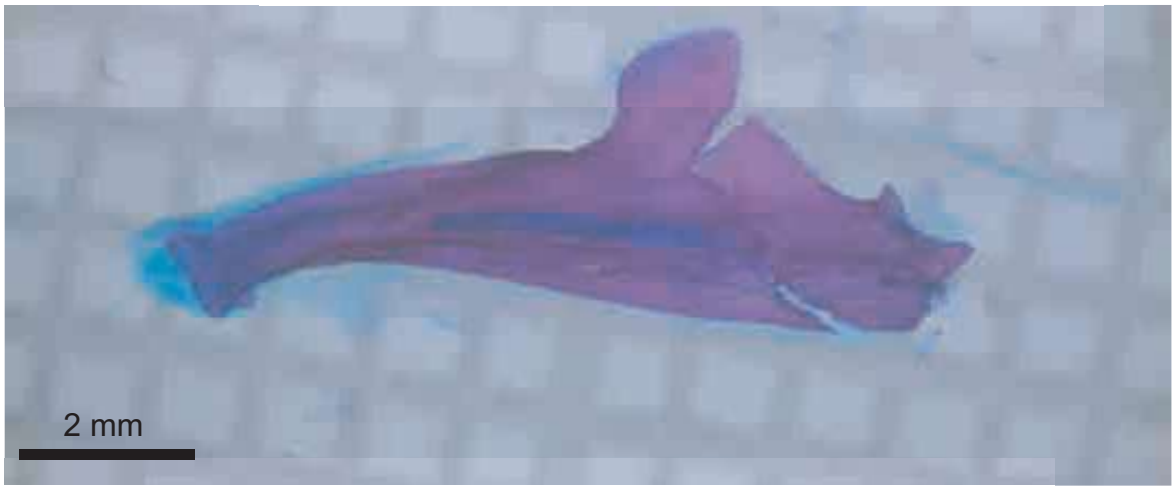

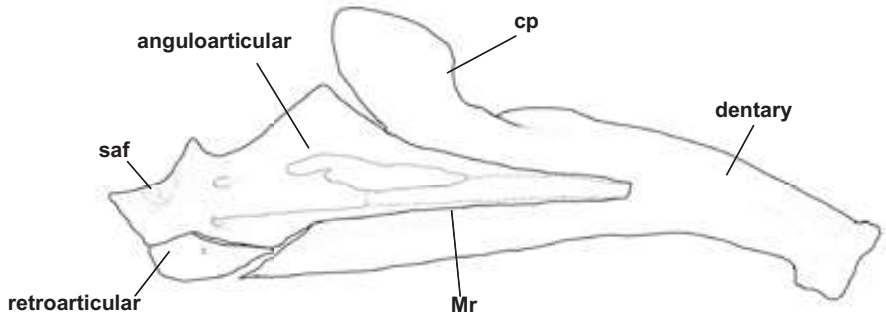

2 mm

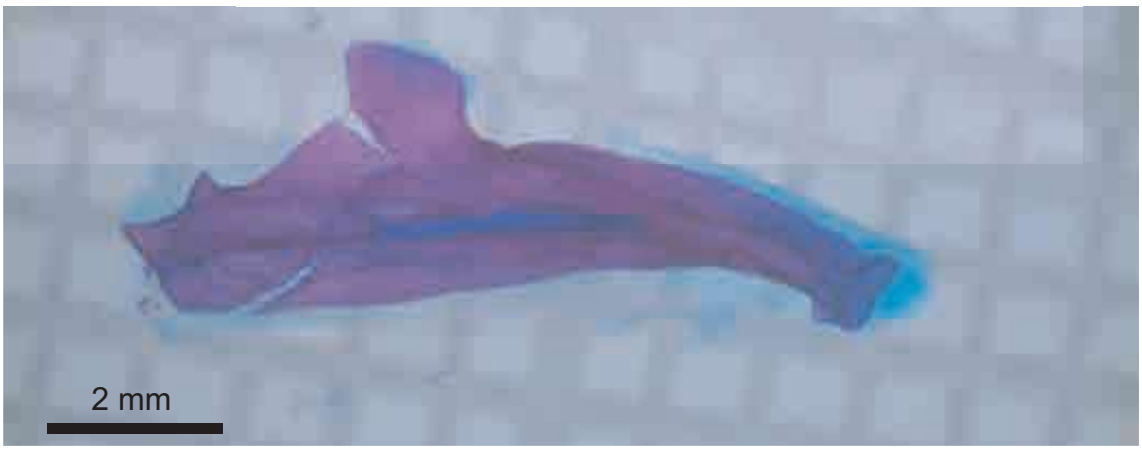

Plate 5-7

A

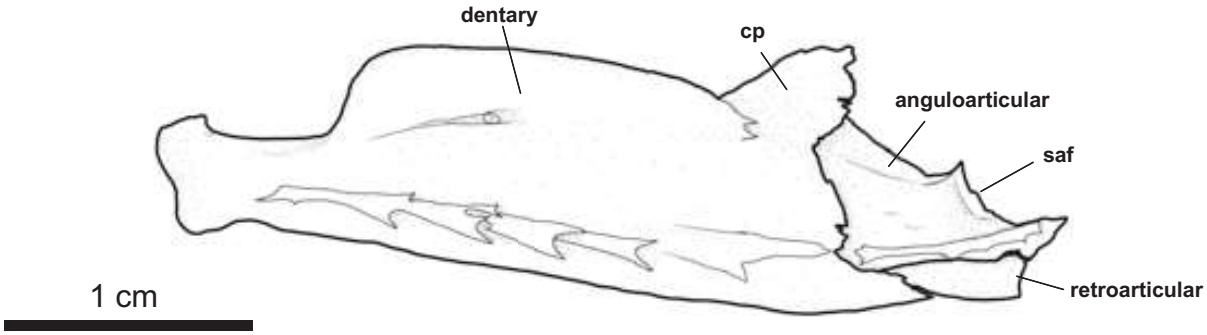
dentary
cp
anguloarticular
saf
retroarticular
1 cm

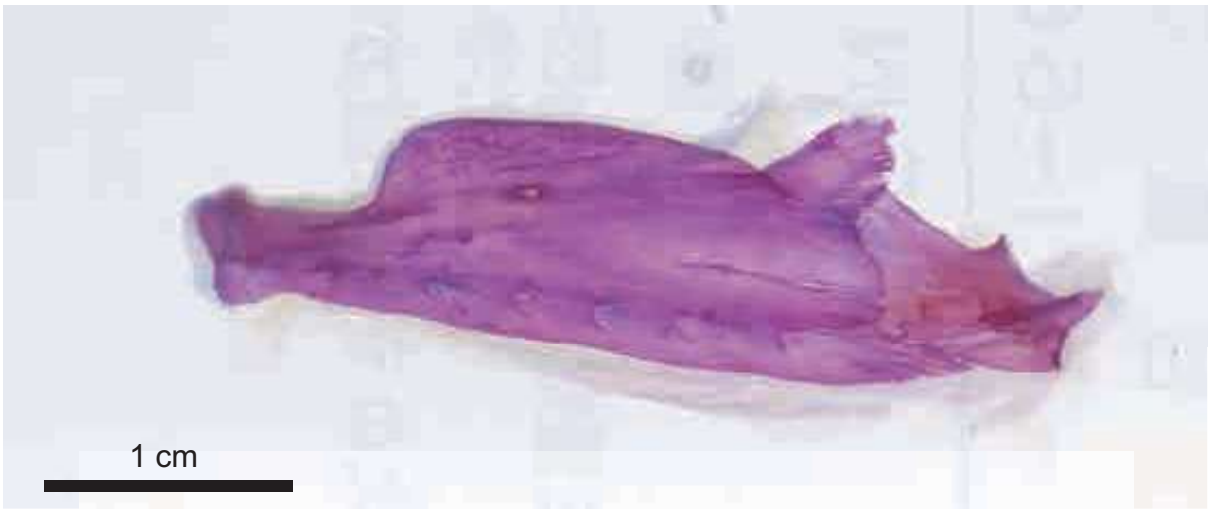
1 cm

B

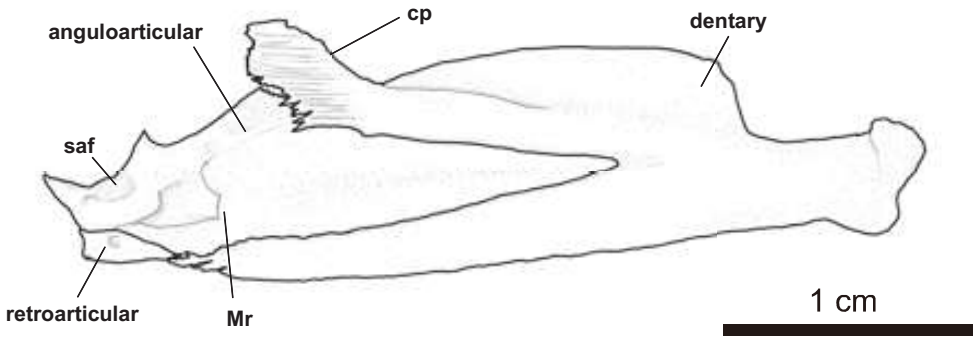
anguloarticular
cp
dentary
saf
retroarticular
Mr
1 cm


1 cm

Plate 5-8

A

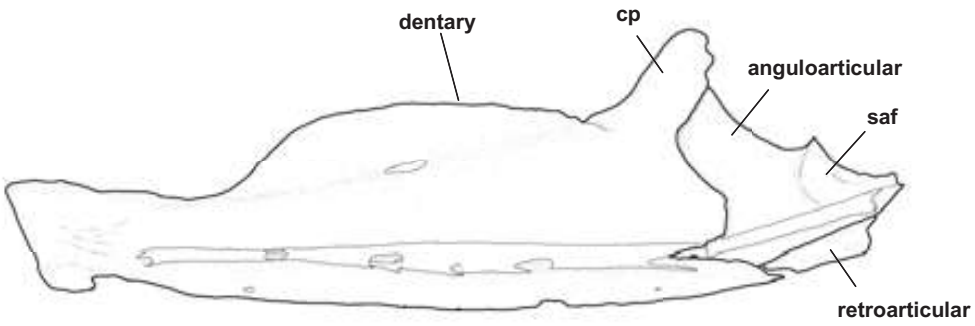

2 mm

B

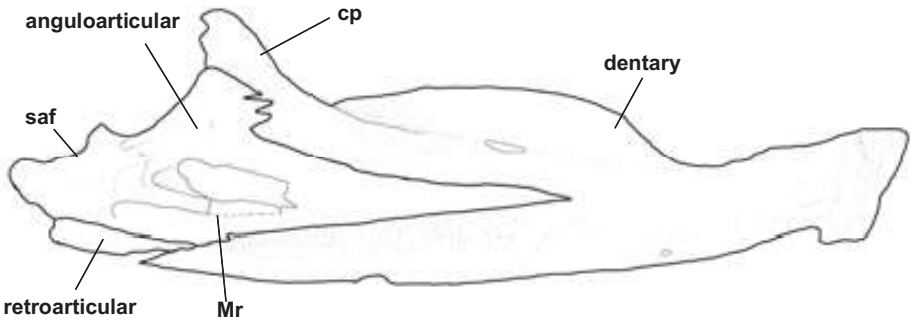

2 mm

Plate 5-9

A

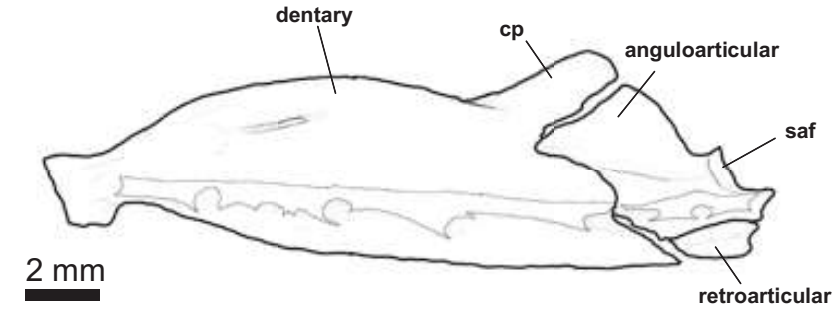
dentary
cp
anguloarticular
saf
2 mm
retroarticular

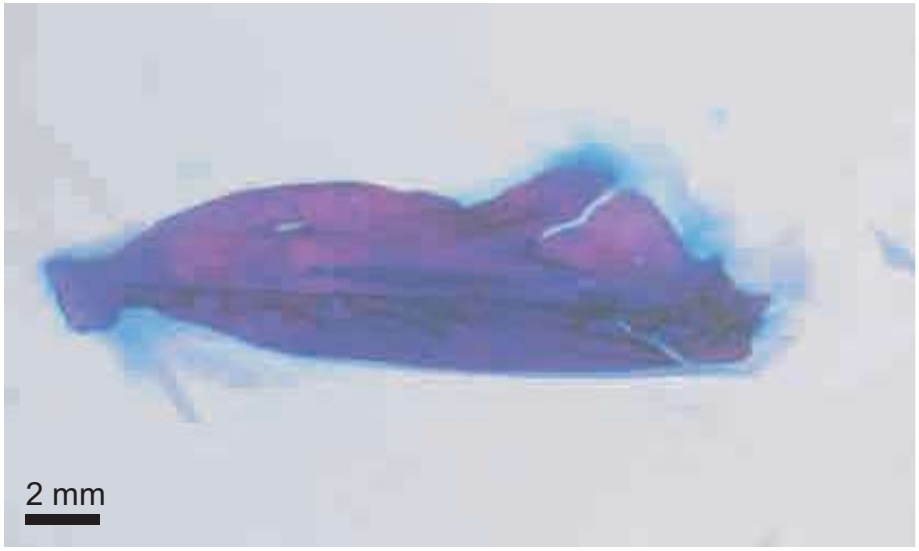
2 mm

B

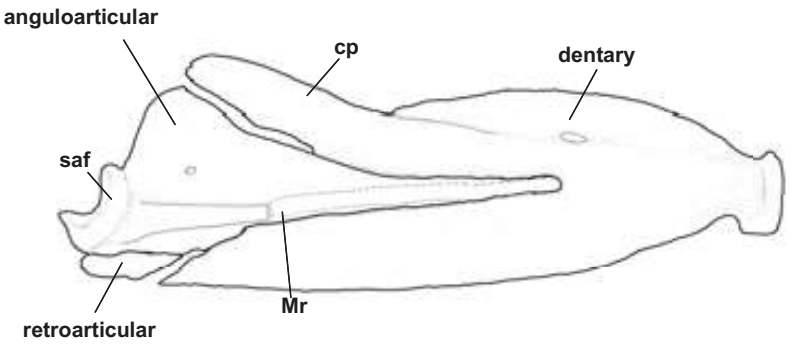
anguloarticular
cp
dentary
saf
Mr
retroarticular
2 mm

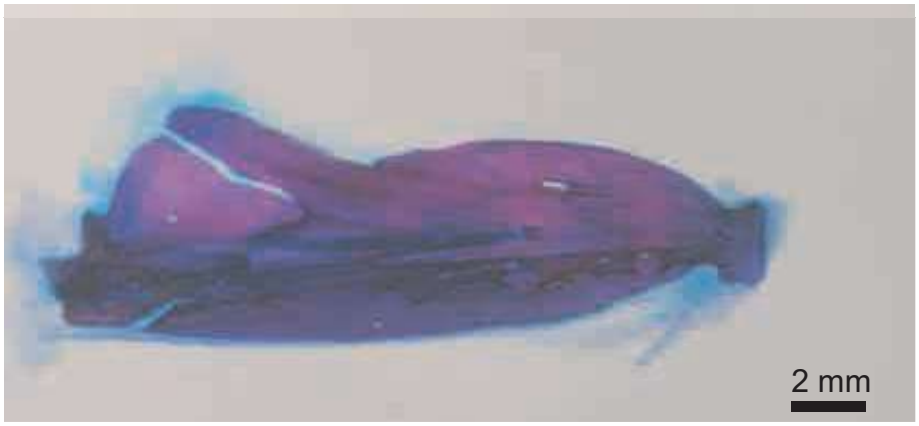
2 mm

Plate 6-1

A

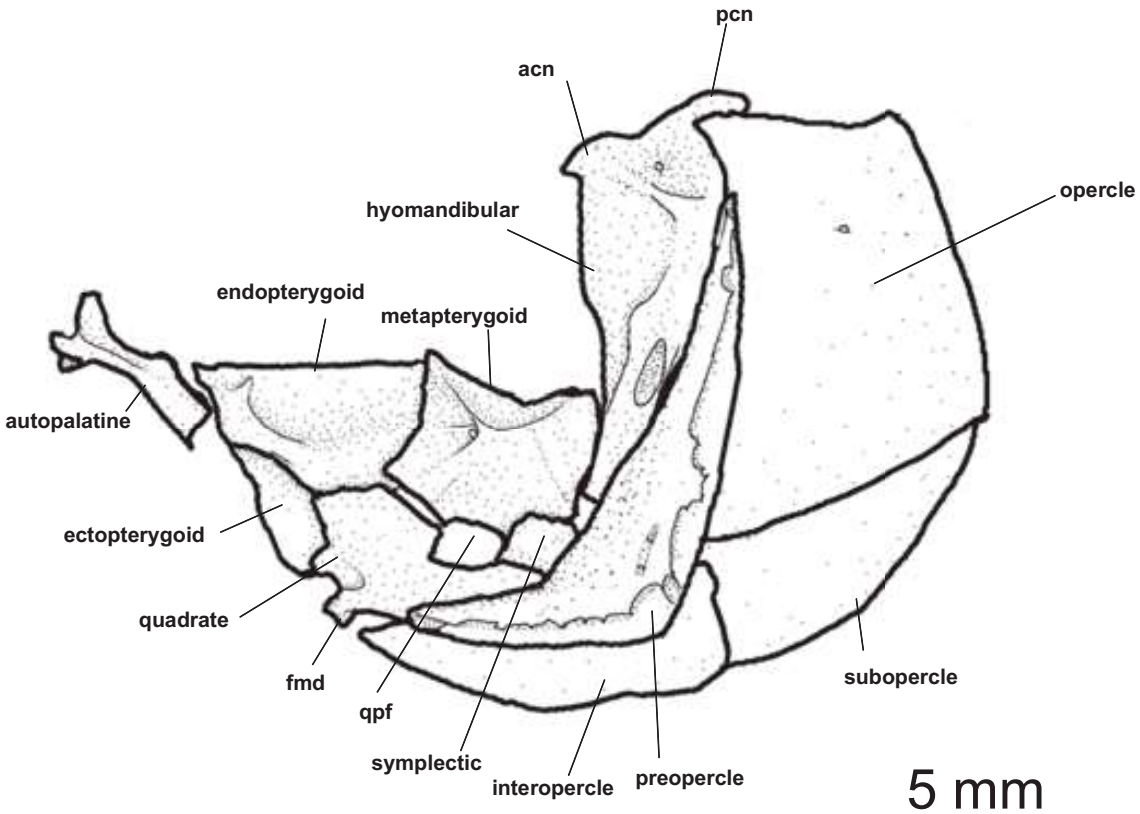
pcn
acn
opercle
hyomandibular
endopterygoid
metapterygoid
autopalatine
ectopterygoid
quadrate
fmd
qpf
symplectic
interopercle
preopercle
subopercle
5 mm

B


5 mm

Plate 6-2

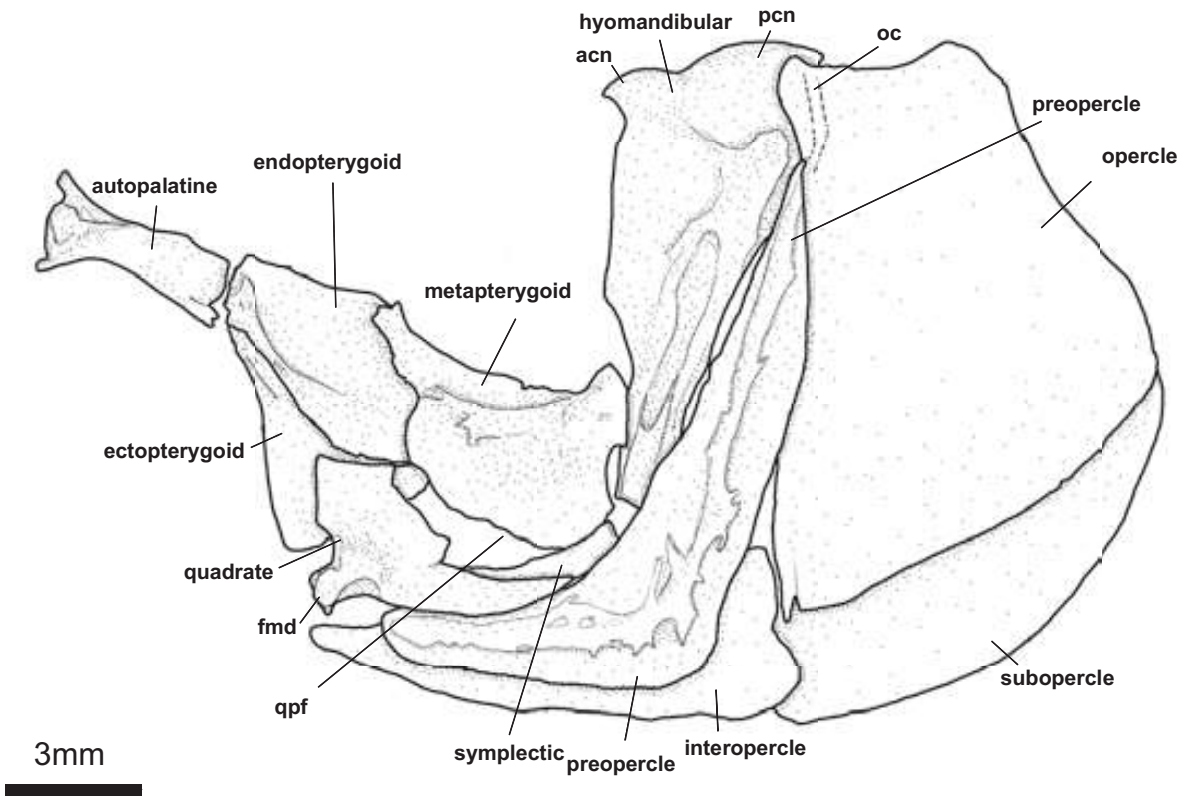
hyomandibular
pcn
oc
acn
preopercle
opercle
endopterygoid
autopalatine
metapterygoid
ectopterygoid
quadrate
fmd
qpf
symplectic
preopercle
interopercle
subopercle
3mm


3mm

Plate 6-3

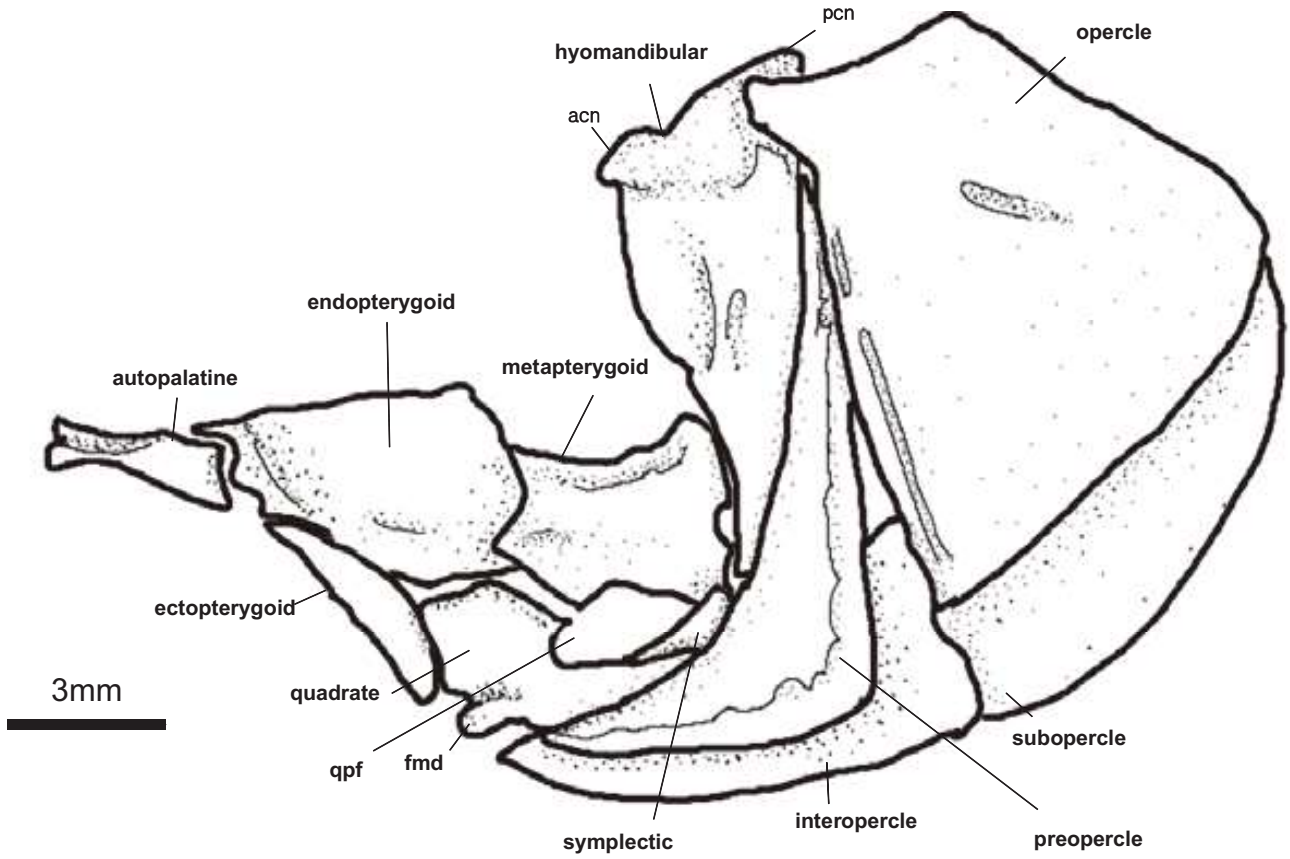
pcn
hyomandibular
opercle
acn
endopterygoid
autopalatine
metapterygoid
ectopterygoid
3mm
quadrate
qpf
fmd
symplectic
interopercle
subopercle
preopercle


3mm

Plate 6-4

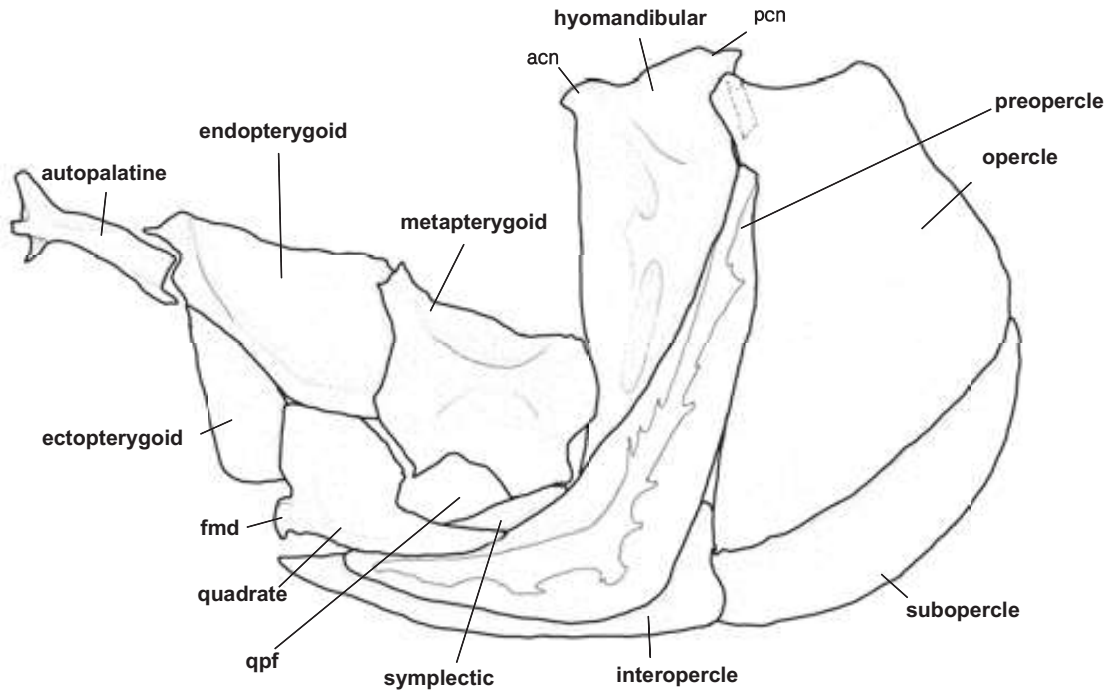
hyomandibular
pcn
acn
preopercle
opercle
endopterygoid
autopalatine
metapterygoid
ectopterygoid
fmd
quadrate
qpf
symplectic
interopercle
subopercle
3mm

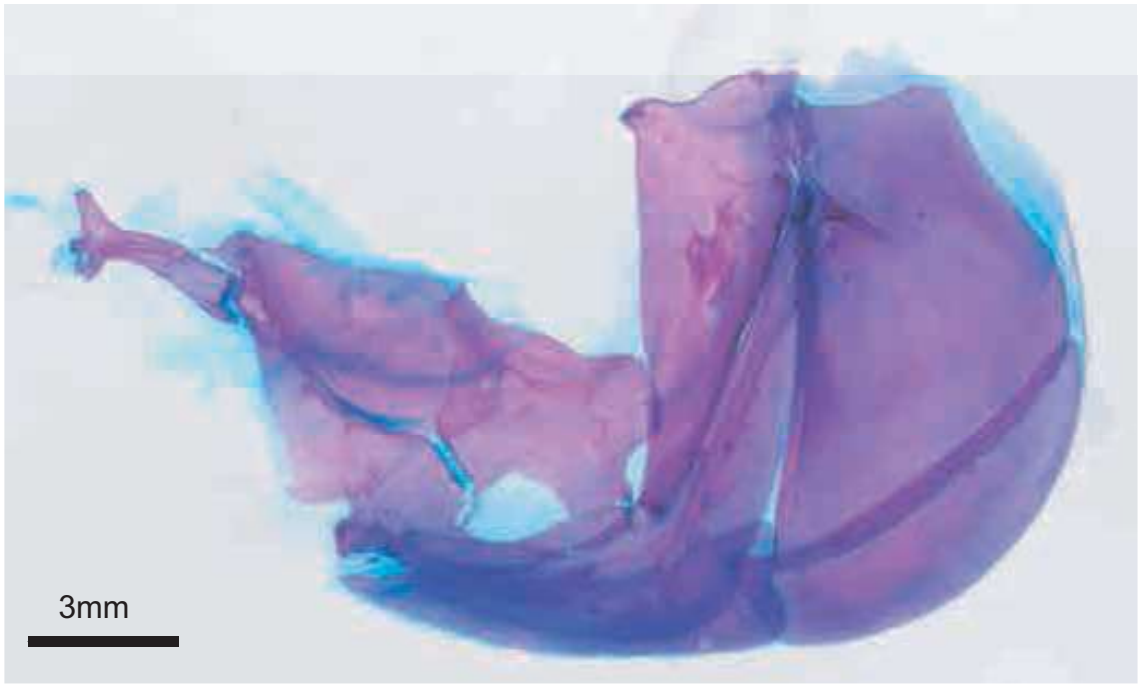
3mm

Plate 6-5

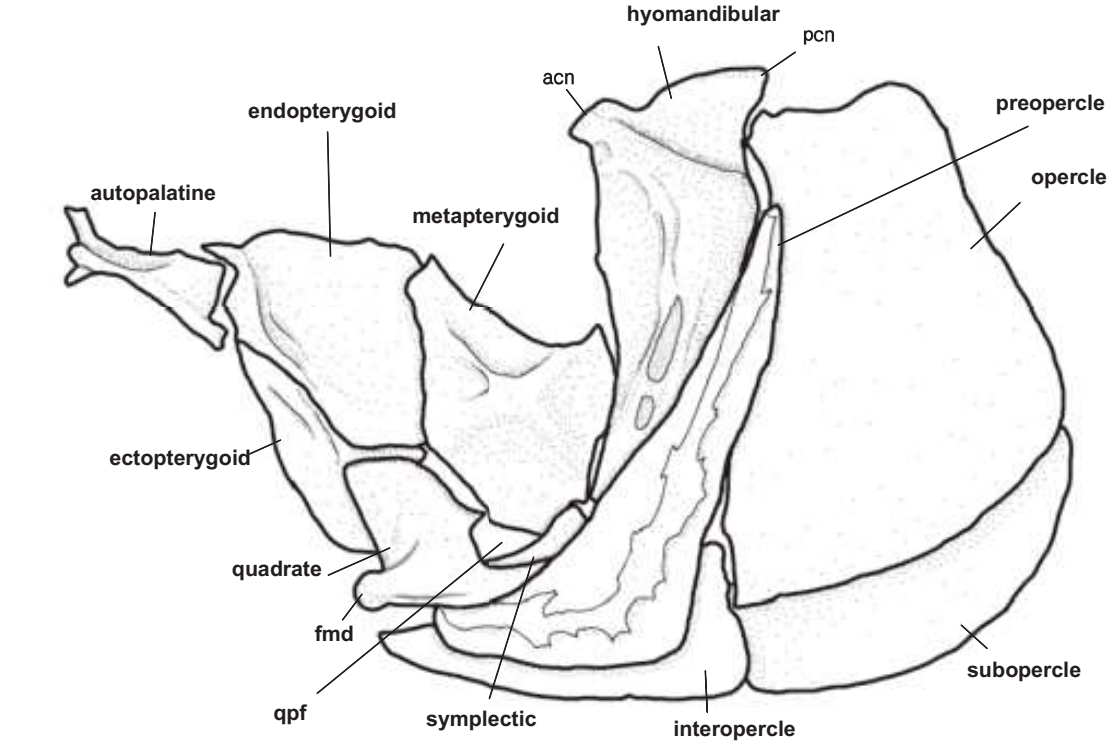
hyomandibular
pcn
acn
endopterygoid
preopercle
opercle
autopalatine
metapterygoid
ectopterygoid
quadrate
fmd
qpf
symplectic
interopercle
subopercle
3mm

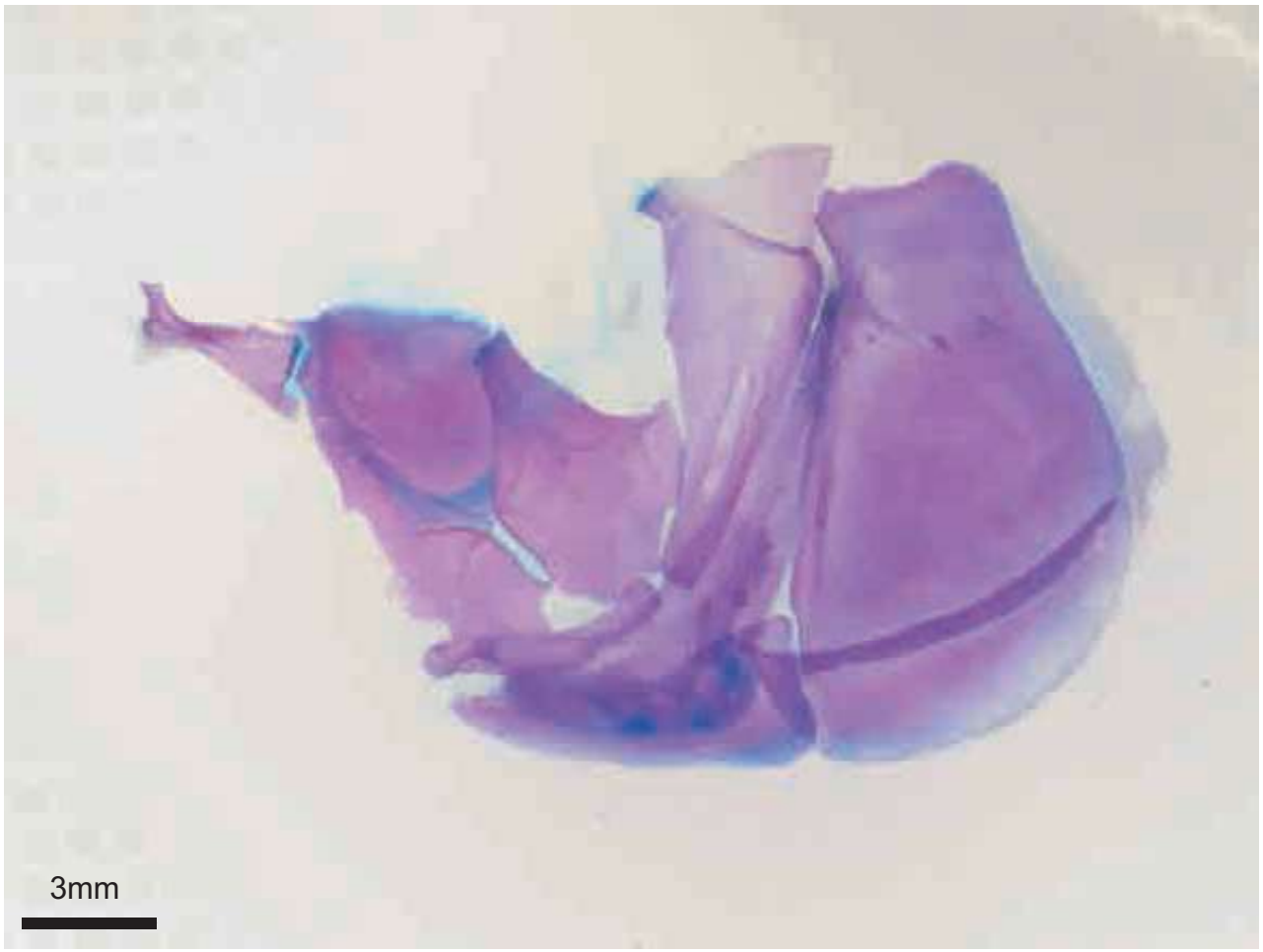
3mm

Plate 6-6

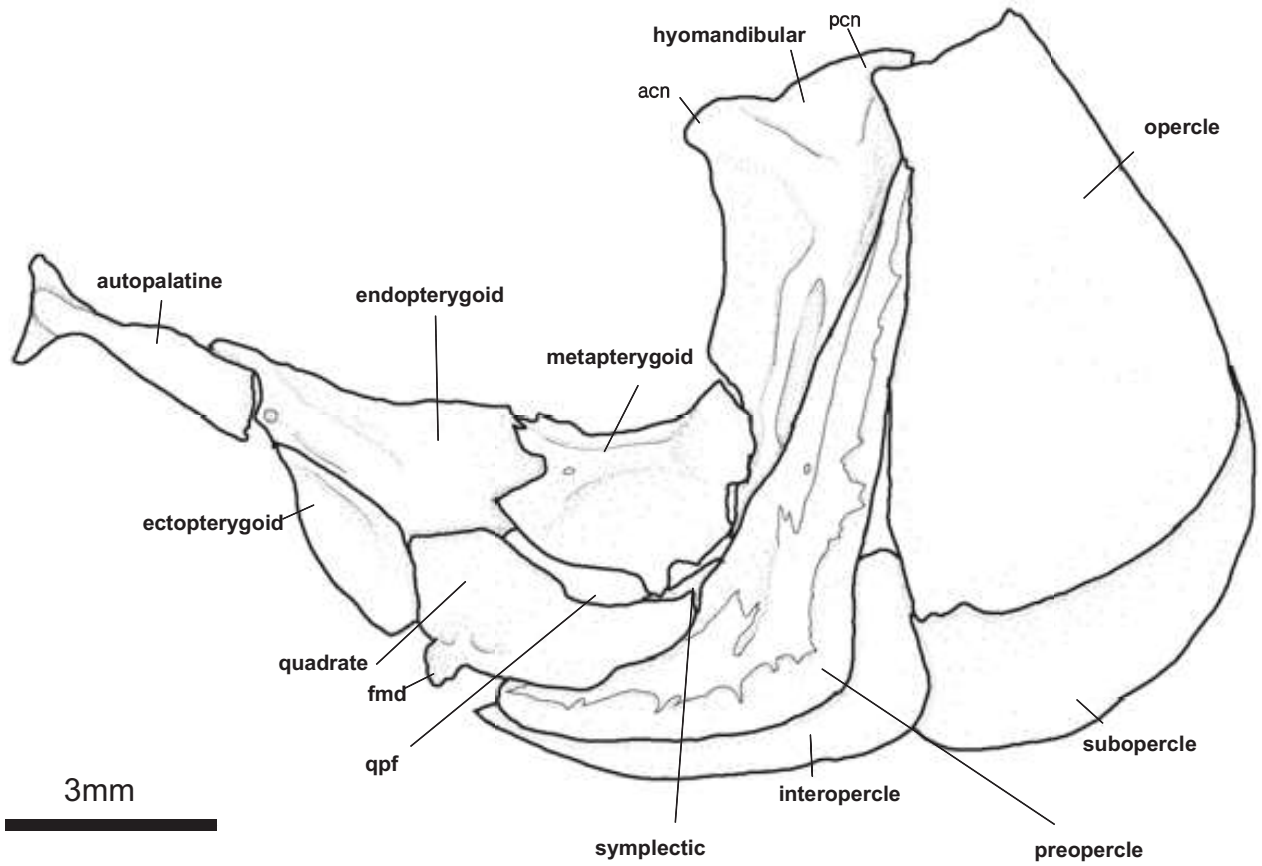
hyomandibular
pcn
acn
opercle
autopalatine
endopterygoid
metapterygoid
ectopterygoid
quadrate
fmd
qpf
3mm
symplectic
interopercle
subopercle
preopercle

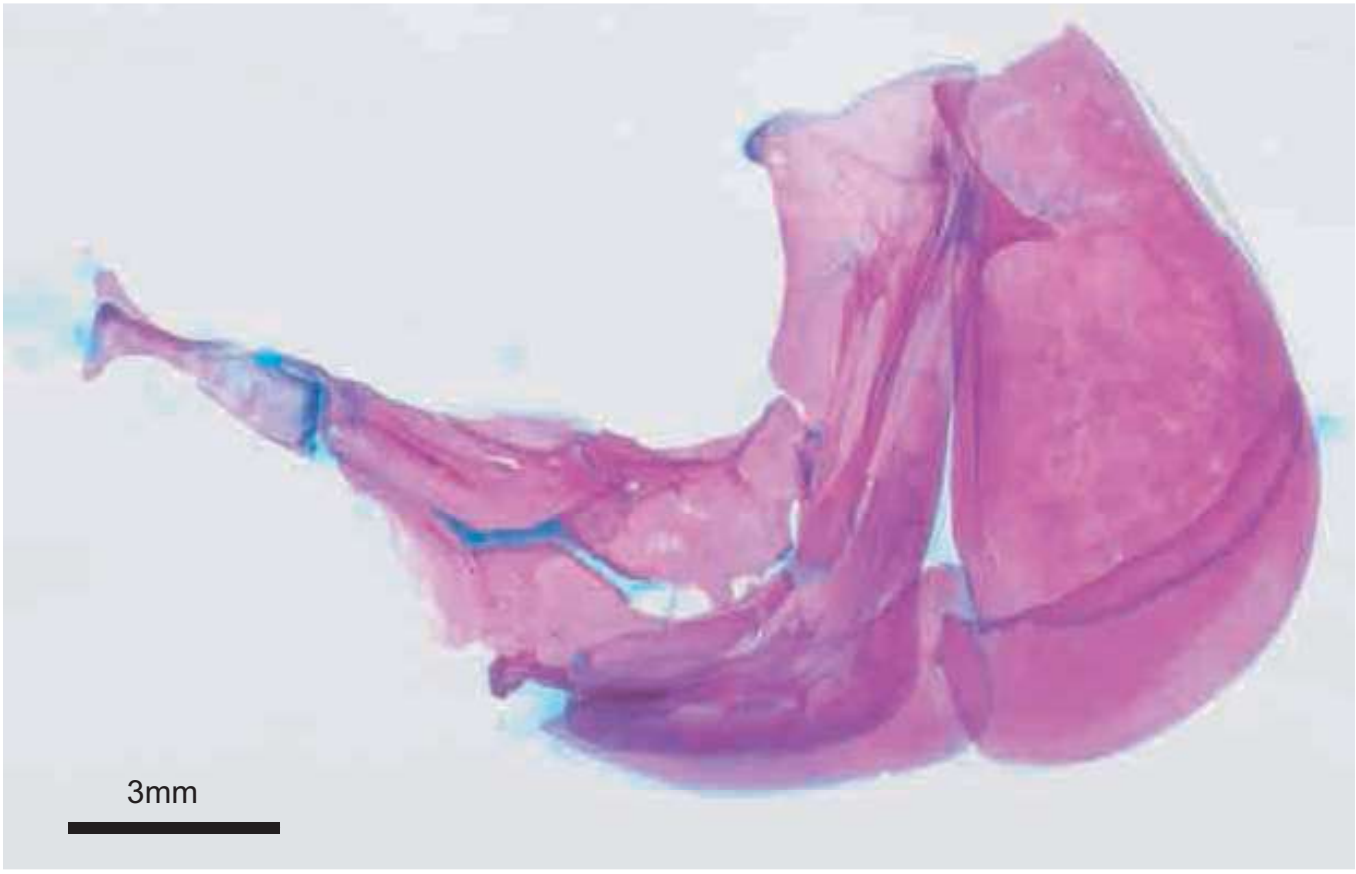
3mm

Plate 6-7

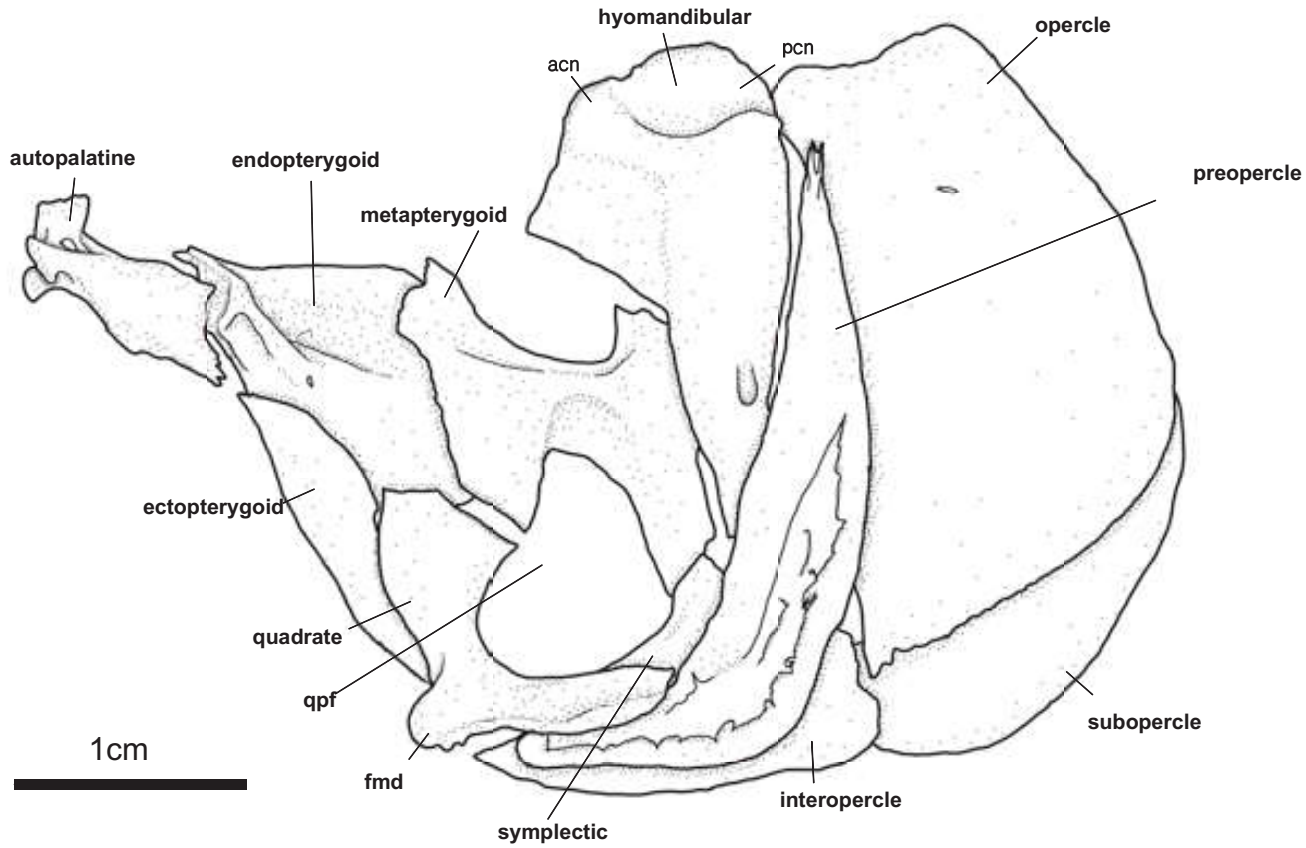
hyomandibular
opercle
acn
pcn
autopalatine
endopterygoid
preopercle
metapterygoid
ectopterygoid
quadrate
qpf
suboperclе
1cm
fmd
interopercle
symplectic

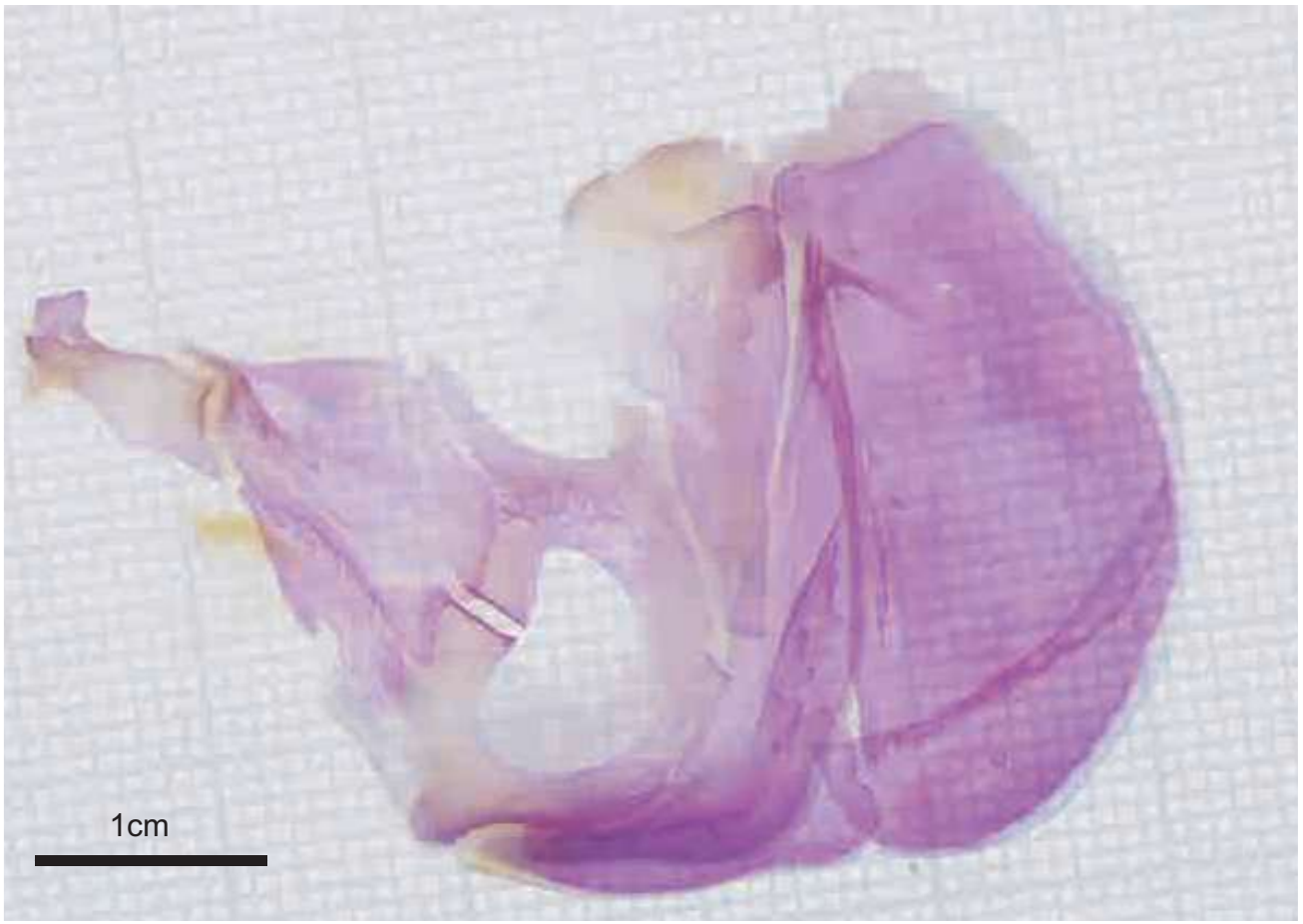
1cm

Plate 6-8

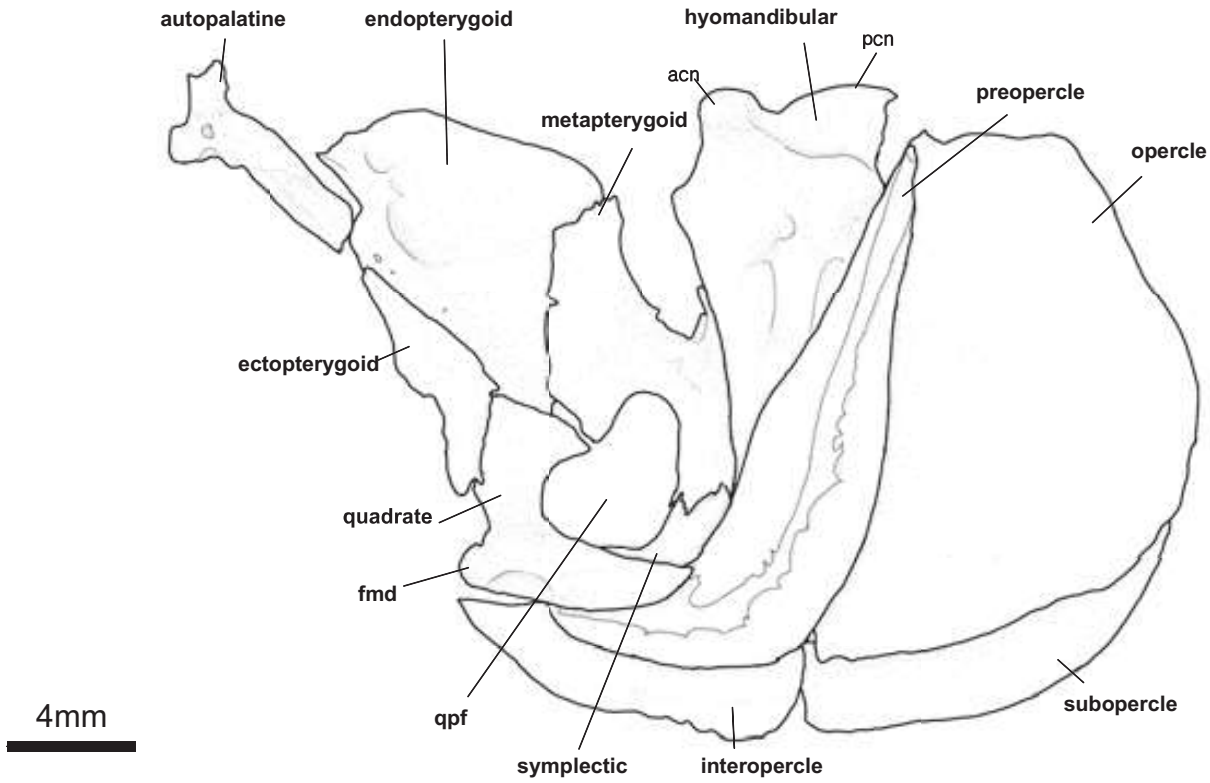
autopalatine
endopterygoid
hyomandibular
pcn
acn
preopercle
metapterygoid
opercle
ectopterygoid
quadrate
fmd
qpf
symplectic
interopercle
subopercle
4mm


4mm

Plate 6-9

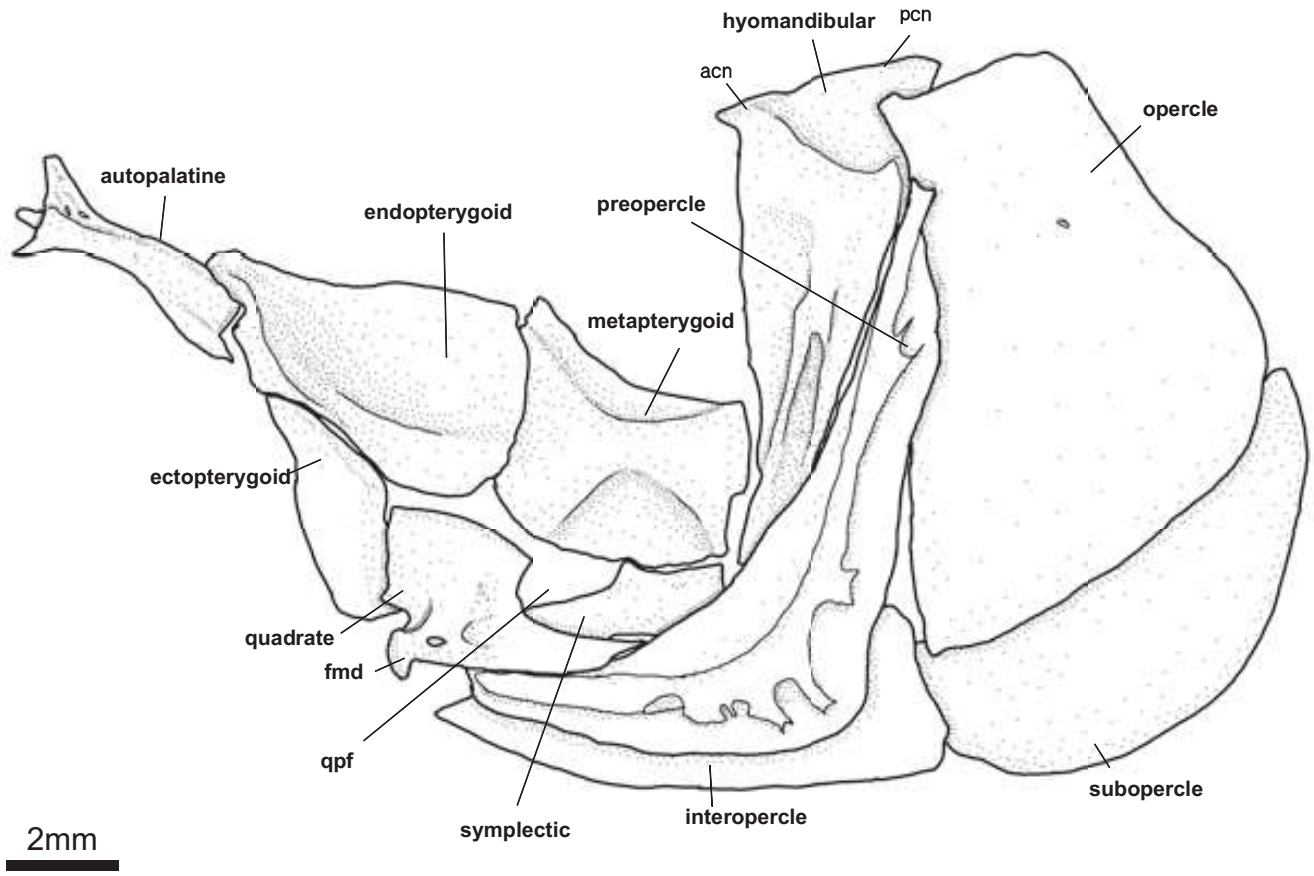
hyomandibular
pcn
acn
opercle
autopalatine
endopterygoid
preopercle
metapterygoid
ectopterygoid
quadrate
fmd
qpf
symplectic
interopercle
subopercle
2mm


2mm

Plate 7-1

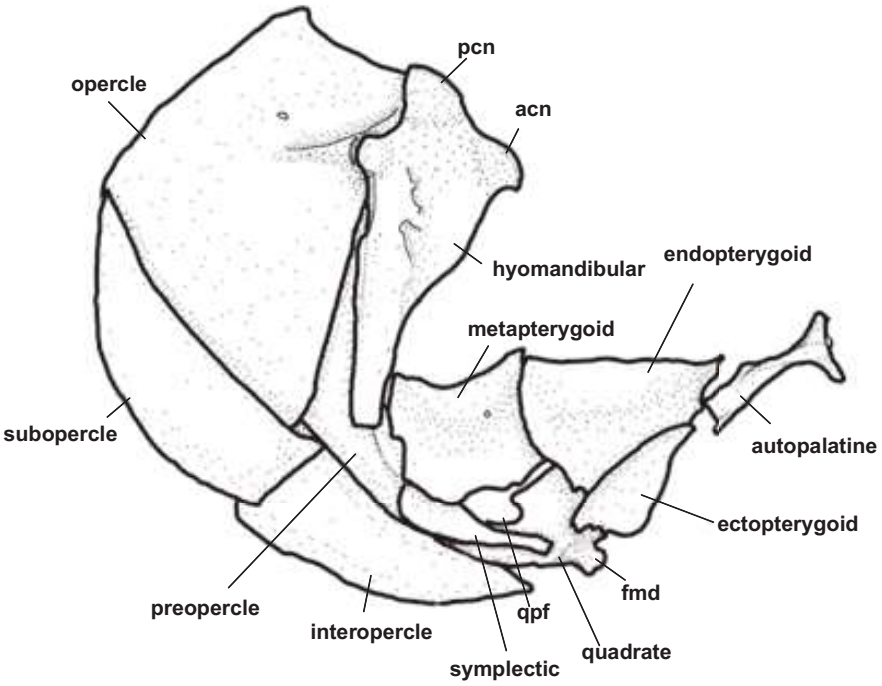
pcn
opercle
acn
hyomandibular
endopterygoid
metapterygoid
subopercle
autopalatine
ectopterygoid
fmd
preopercle
qpf
interopercle
quadrate
symplectic
5 mm


5 mm

Plate 7-2

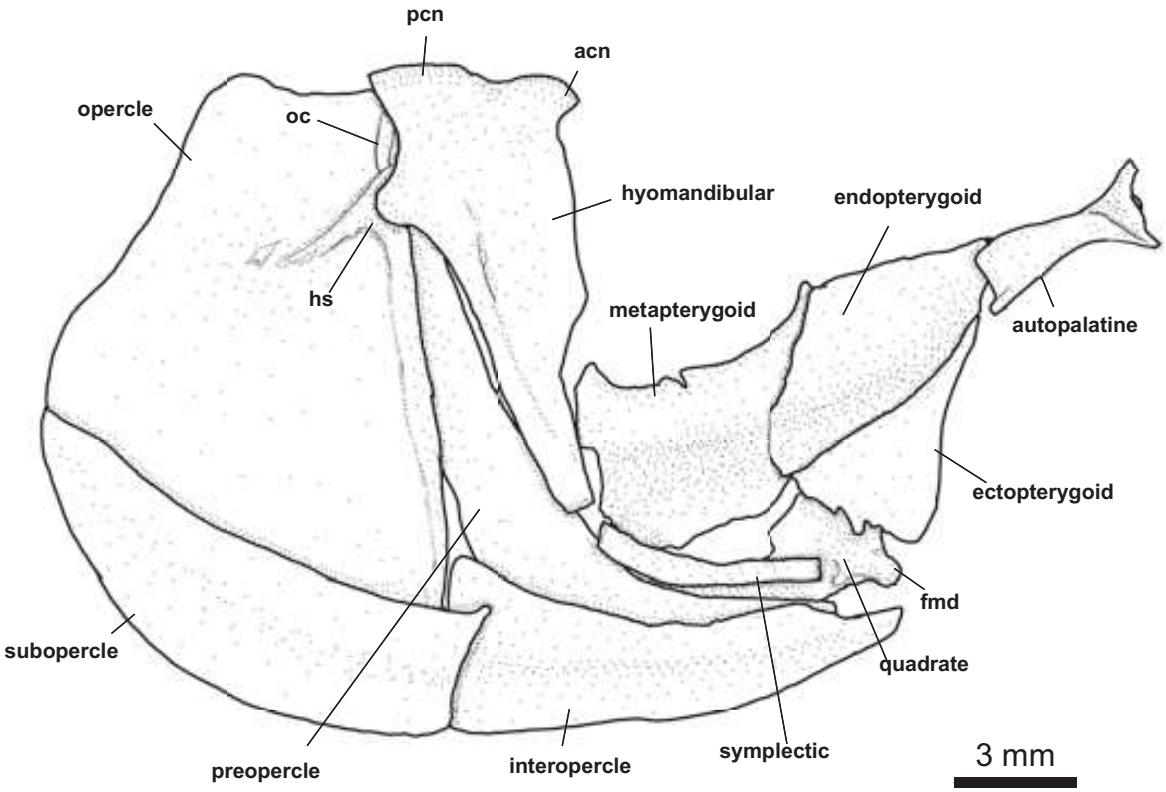
pcn
acn
opercle
oc
hyomandibular
endopterygoid
hs
metapterygoid
autopalatine
ectopterygoid
fmd
subopercle
quadrate
preopercle
interopercle
symplectic
3 mm


3 mm

Plate 7-3

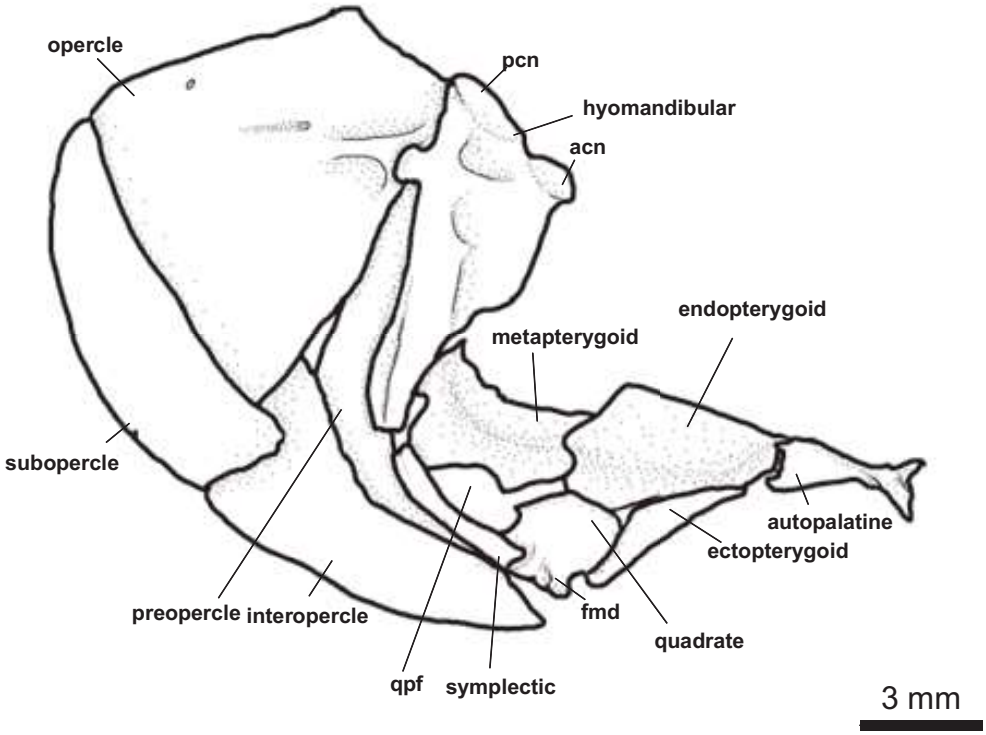
opercle
pcn
hyomandibular
acn
endopterygoid
metapterygoid
subopercle
autopalatine
ectopterygoid
preopercle
interopercle
fmd
quadrate
qpf
symplectic
3 mm


3 mm

Plate 7-4

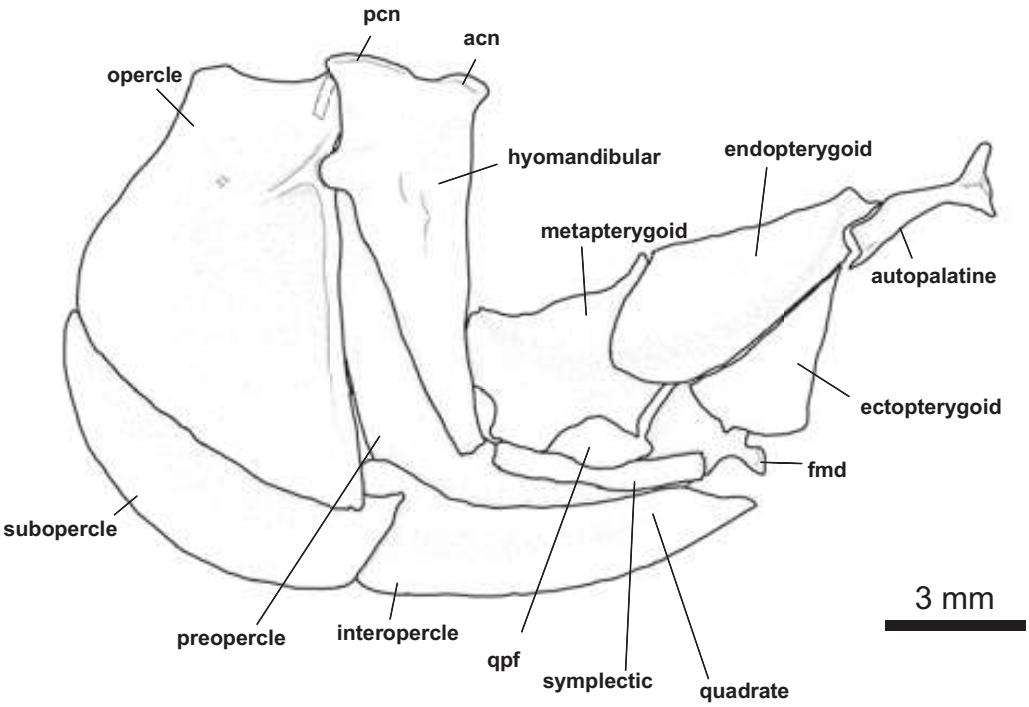
pcn
acn
opercle
hyomandibular
endopterygoid
metapterygoid
autopalatine
ectopterygoid
fmd
subopercle
preopercle
interopercle
qpf
symplectic
quadrate
3 mm

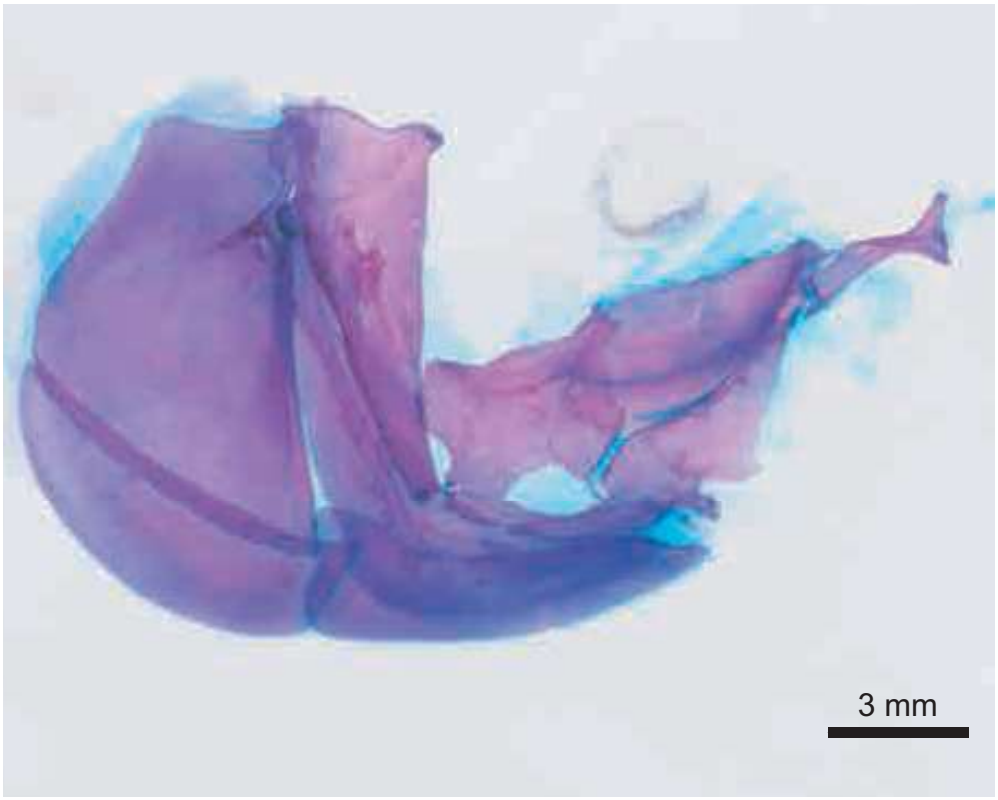
3 mm

Plate 7-5

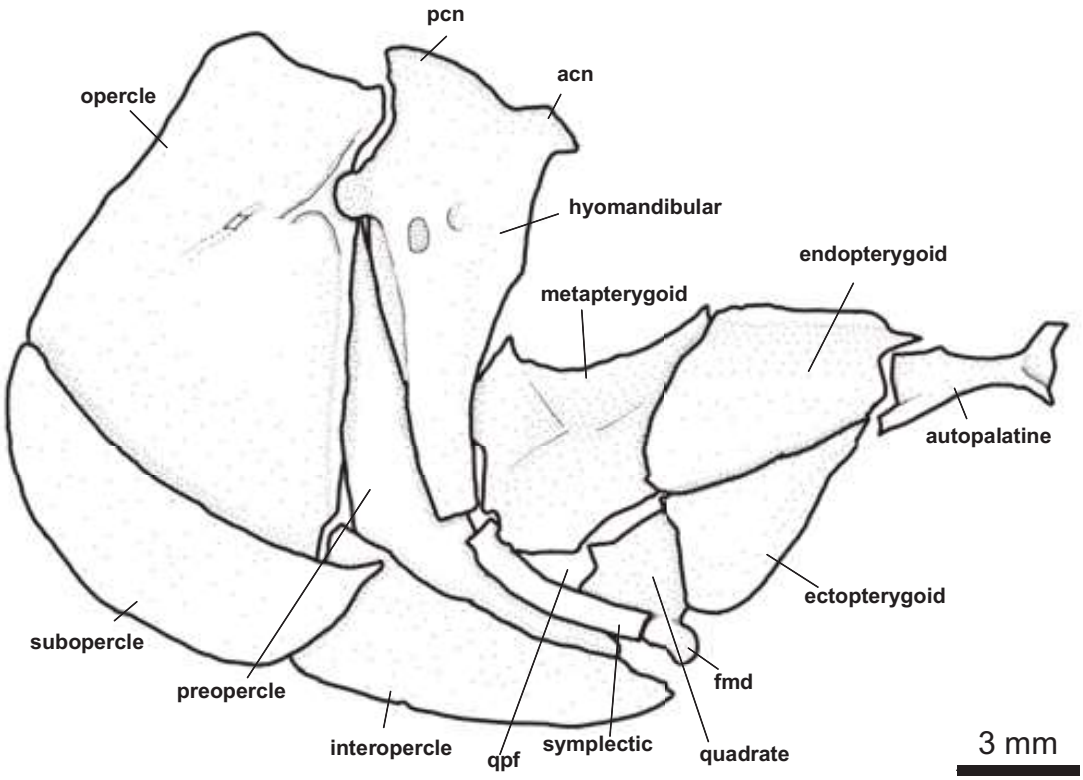
pcn
acn
opercle
hyomandibular
endopterygoid
metapterygoid
autopalatine
ectopterygoid
subopercle
preopercle
fmd
interopercle
qpf
symplectic
quadrate
3 mm

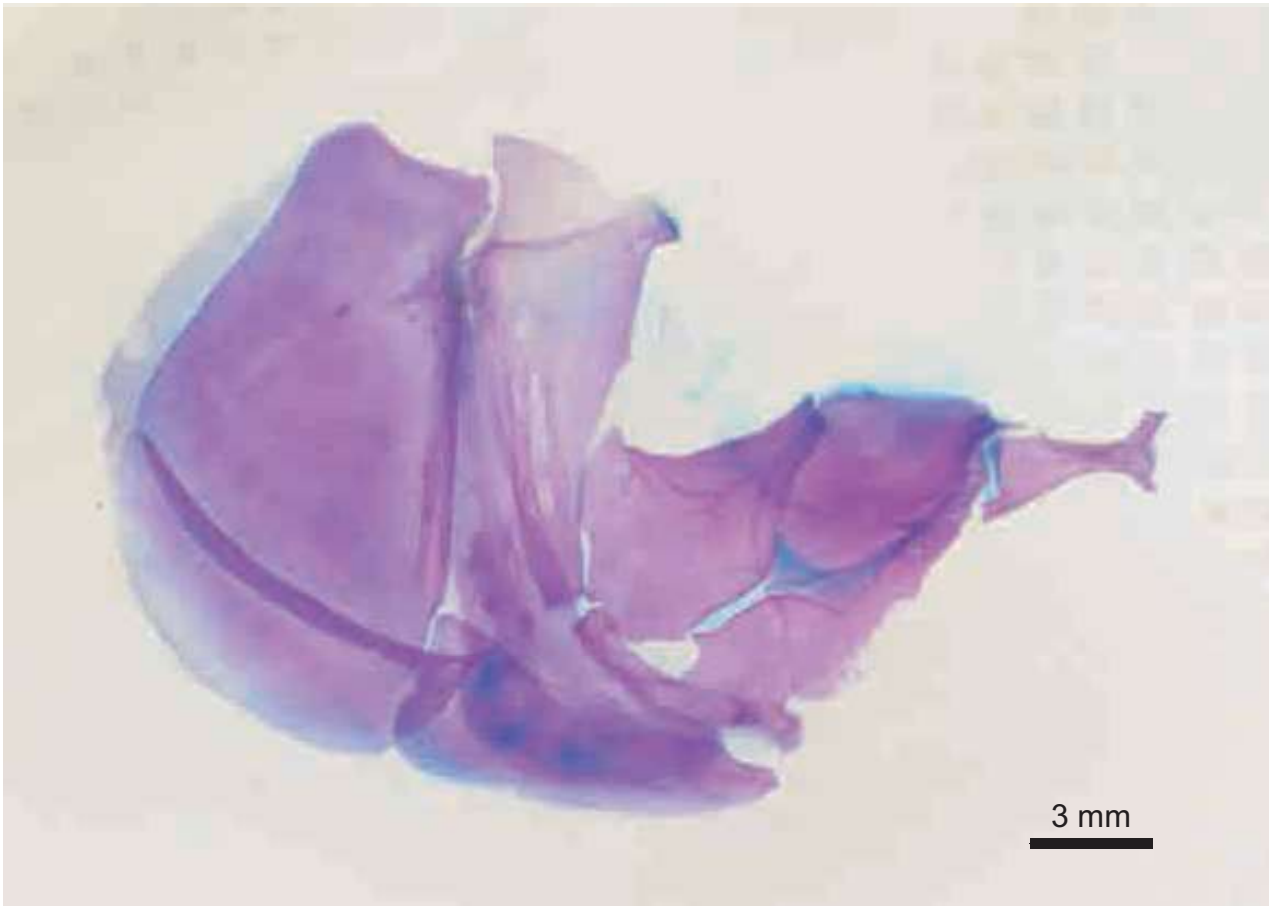
3 mm

Plate 7-6

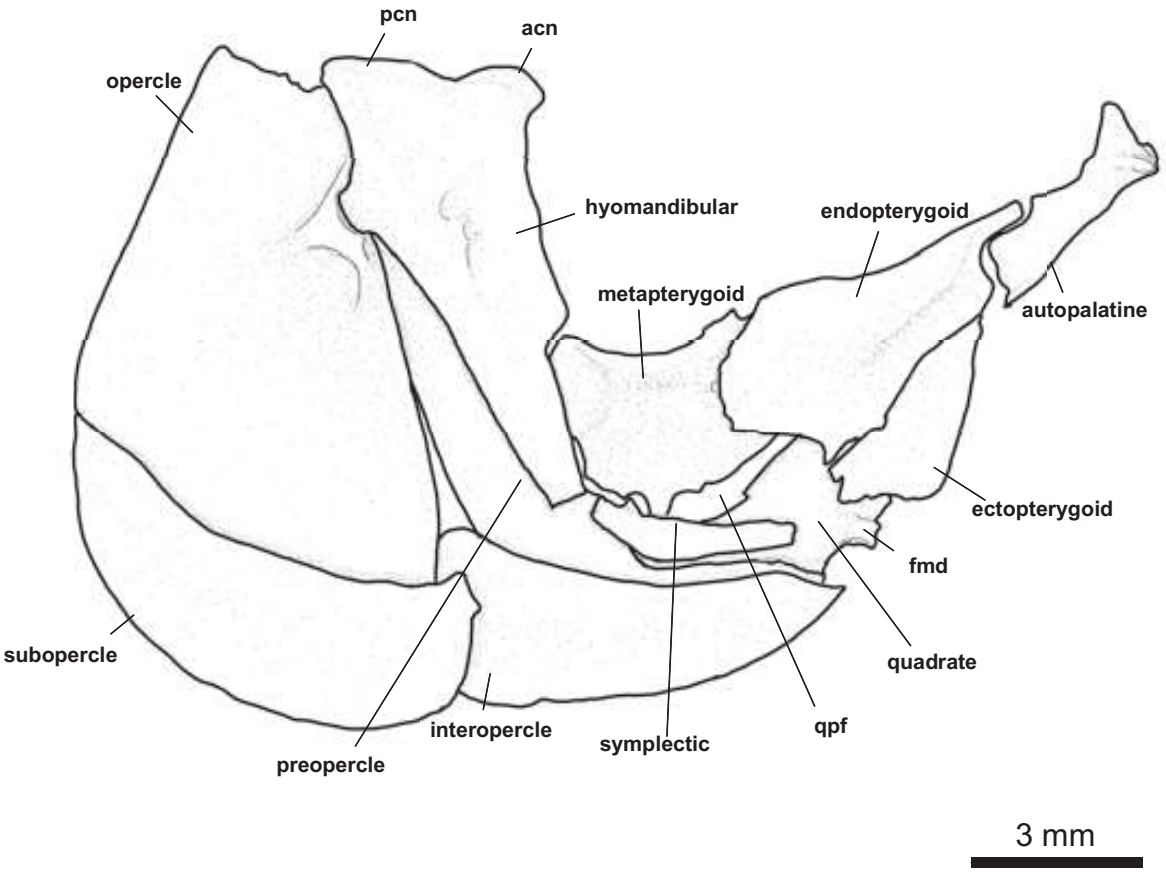
pcn
acn
opercle
hyomandibular
endopterygoid
metapterygoid
autopalatine
ectopterygoid
fmd
quadrate
qpf
symplectic
interopercle
preopercle
subopercle
3 mm

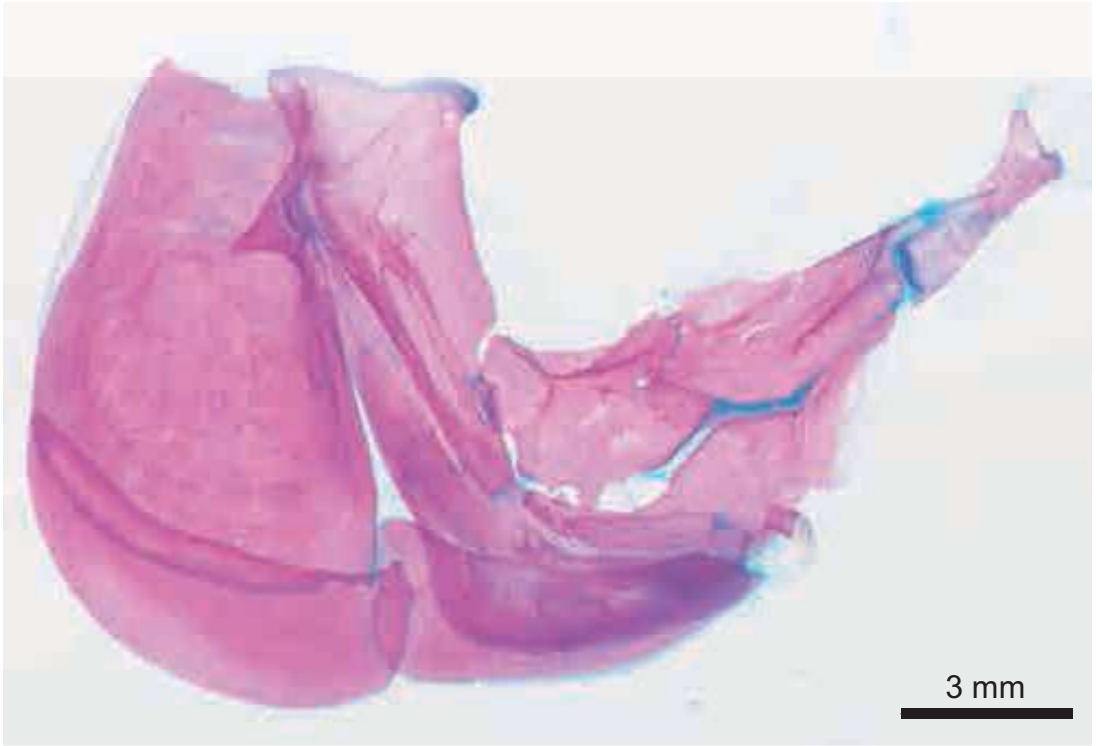
3 mm

Plate 7-7

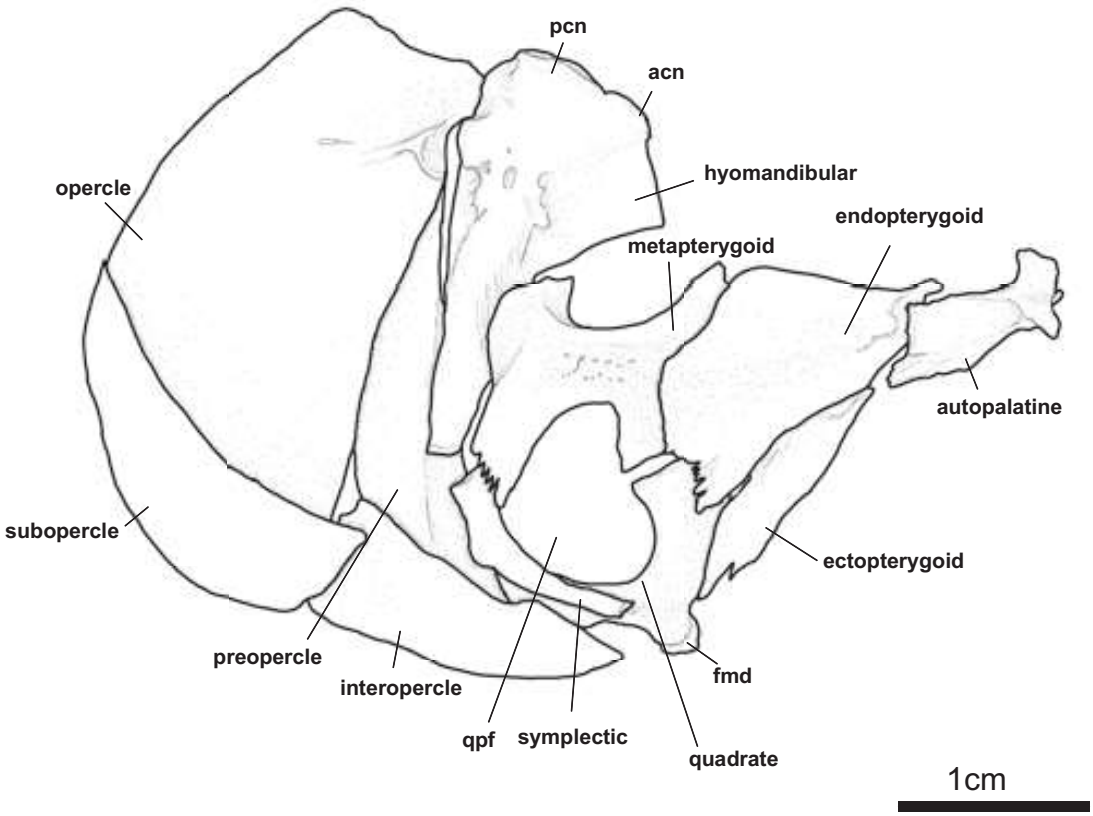
pcn
acn
hyomandibular
opercle
endopterygoid
metapterygoid
autopalatine
subopercle
ectopterygoid
preopercle
interopercle
fmd
qpf
symplectic
quadrate
1cm

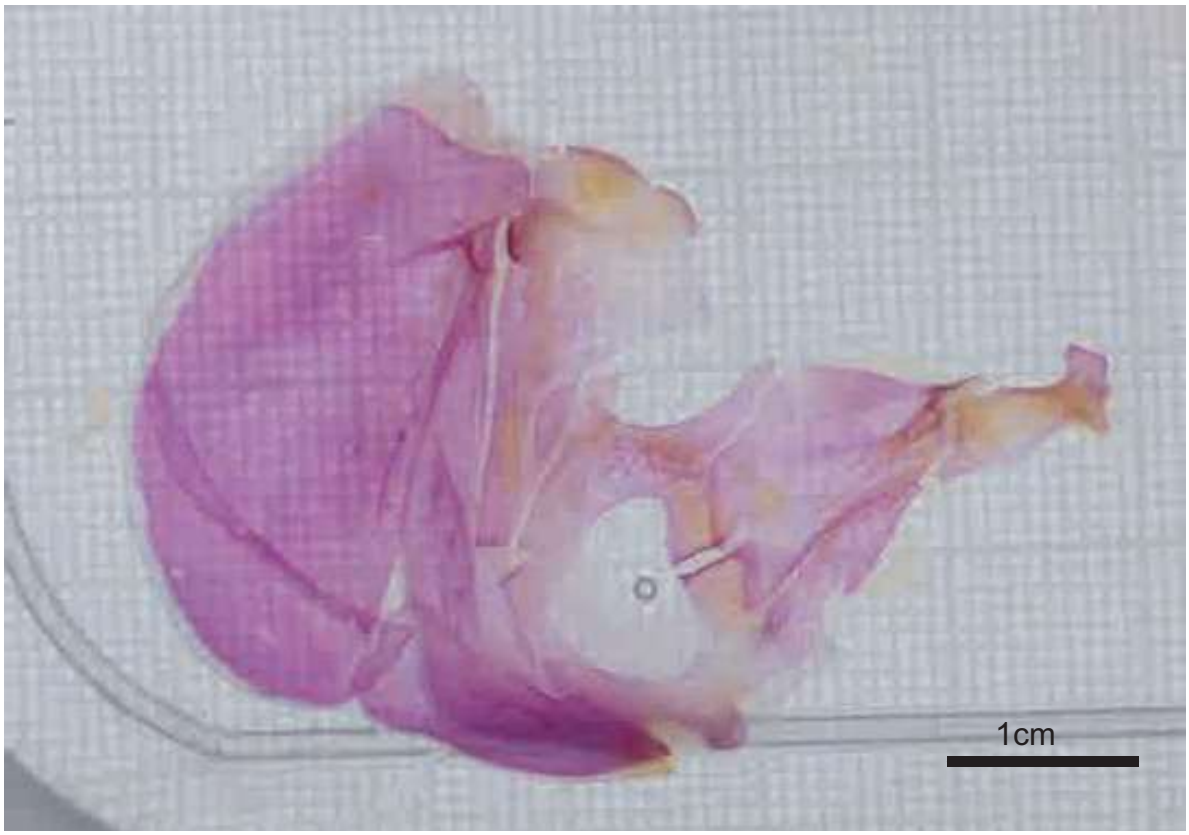
1cm

Plate 7-8

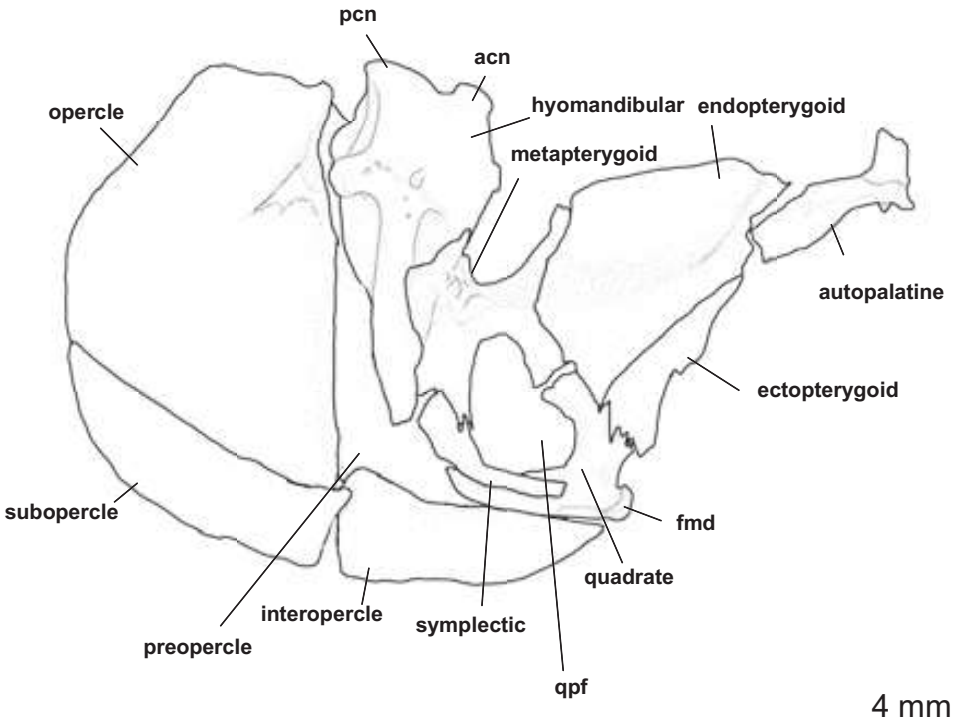
pcn
acn
opercle
hyomandibular
endopterygoid
metapterygoid
autopalatine
ectopterygoid
subopercle
fmd
quadrate
interopercle
symplectic
preopercle
qpf
4 mm


4 mm

3 mm

Plate 7-9

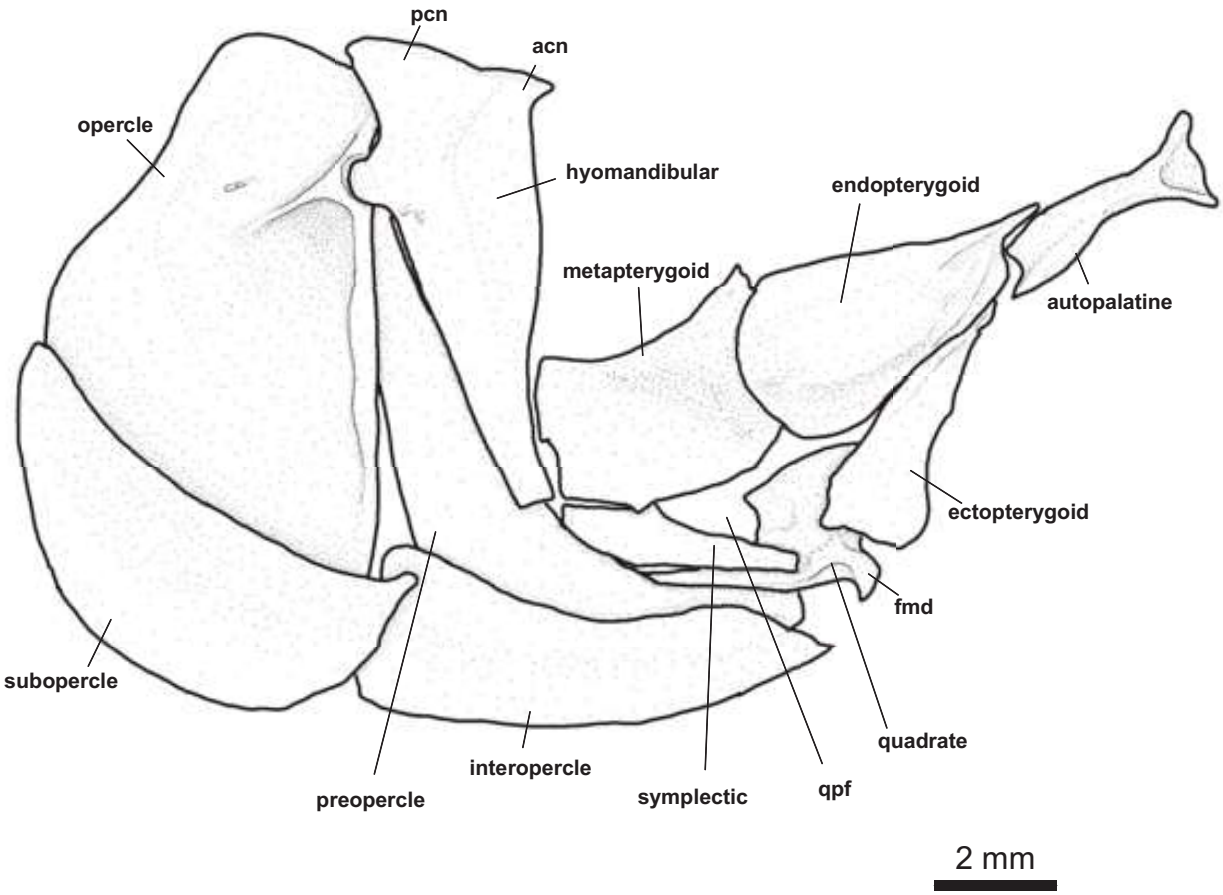
pcn
acn
opercle
hyomandibular
endopterygoid
metapterygoid
autopalatine
ectopterygoid
fmd
subopercle
quadrate
interopercle
preopercle
symplectic
qpf
2 mm

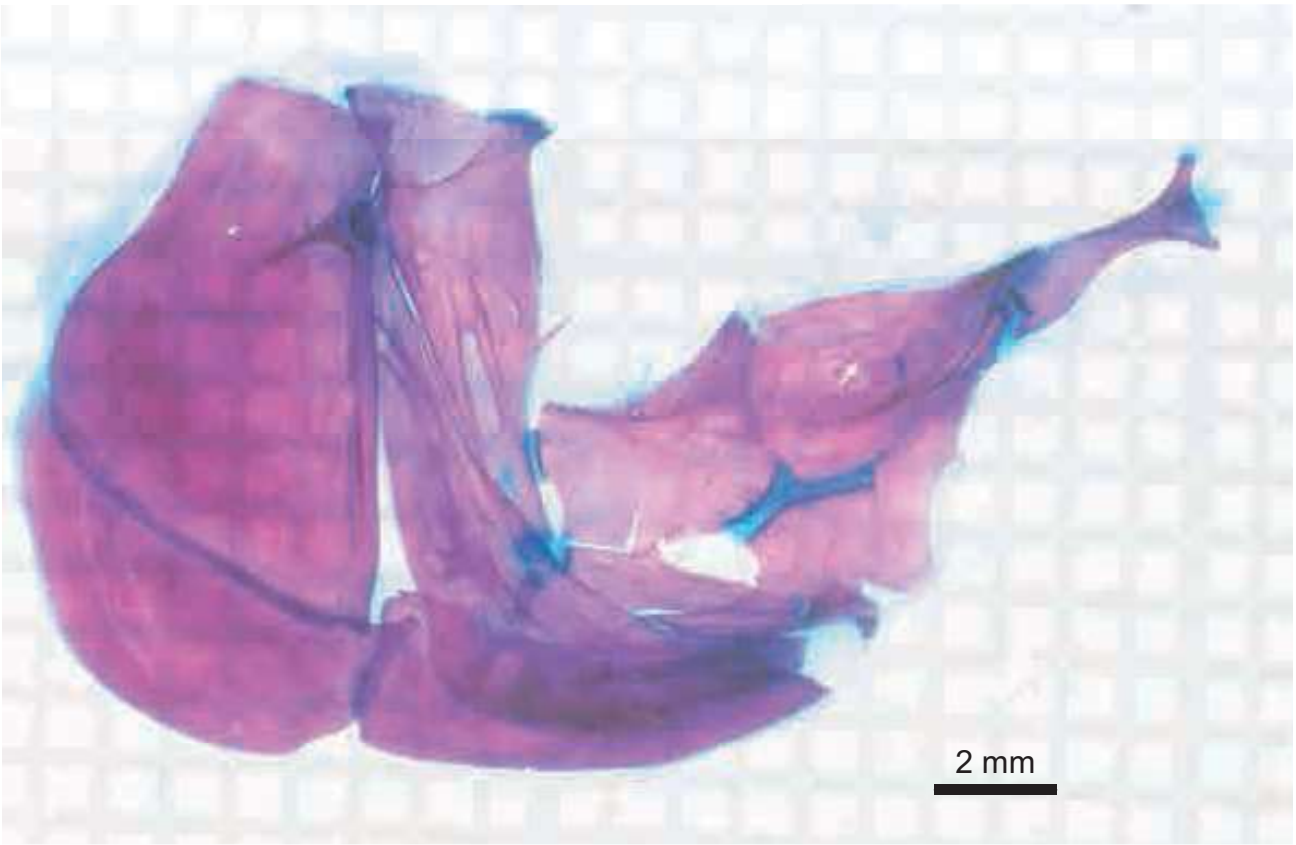
2 mm

Plate 8-1

A

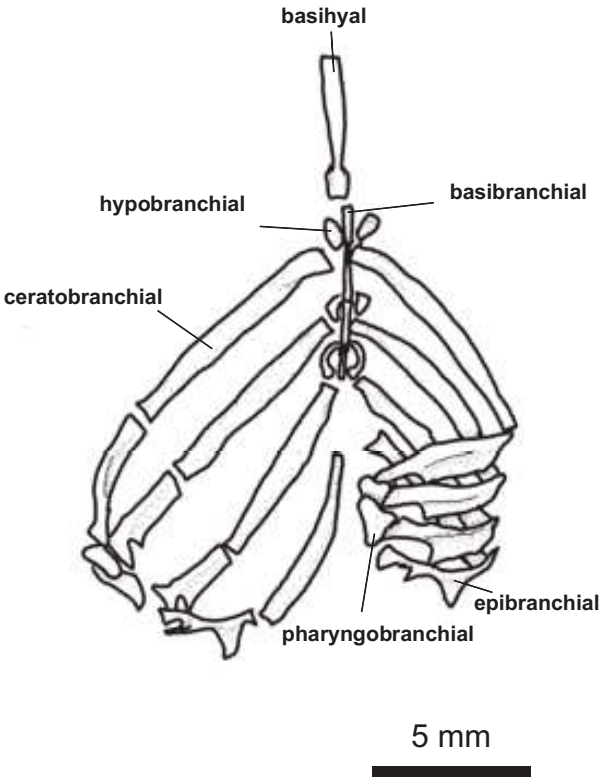
basihyal
hypobranchial
basibranchial
ceratobranchial
epibranchial
pharyngobranchial
5 mm


5 mm

B

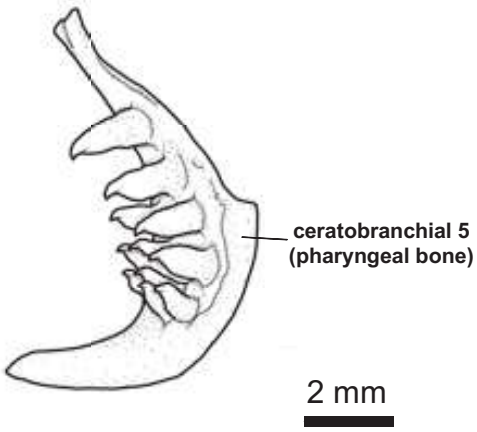
ceratobranchial 5
(pharyngeal bone)
2 mm


2 mm

C

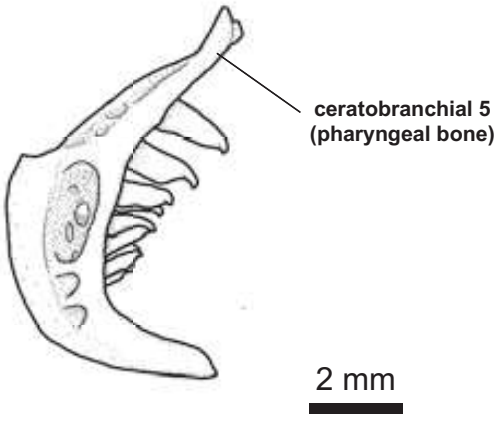
ceratobranchial 5
(pharyngeal bone)
2 mm


2 mm

Plate 8-2

A

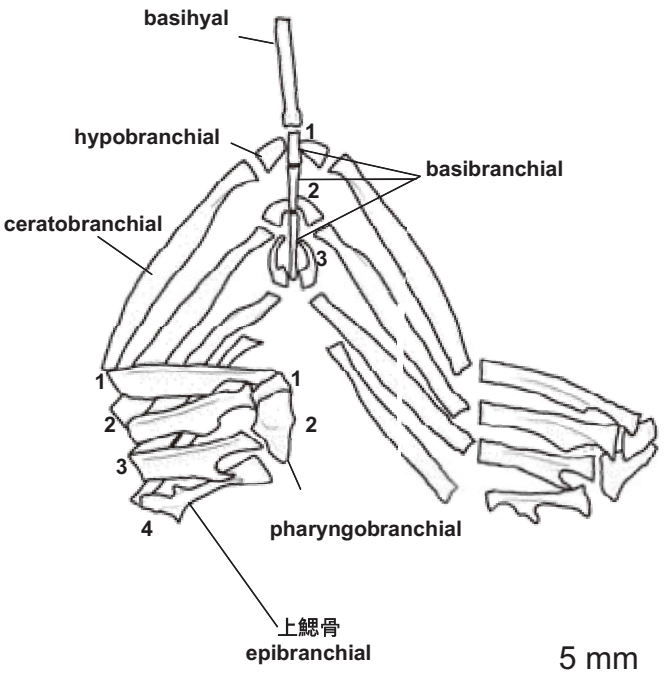
basihyal
hypobranchial
basibranchial
ceratobranchial
1
2
3
1
2
3
4
1
2
pharyngobranchial
上鰓骨
epibranchial
5 mm


5 mm

B

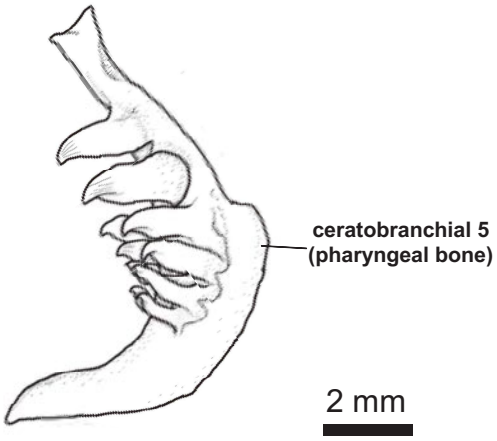
ceratobranchial 5
(pharyngeal bone)
2 mm

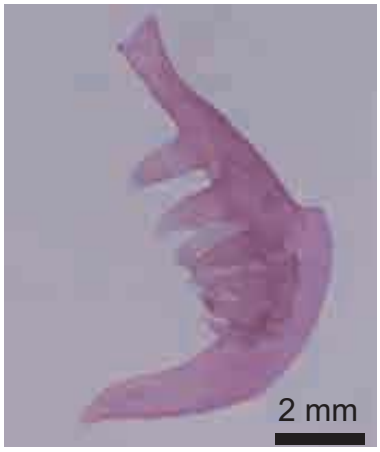
2 mm

C

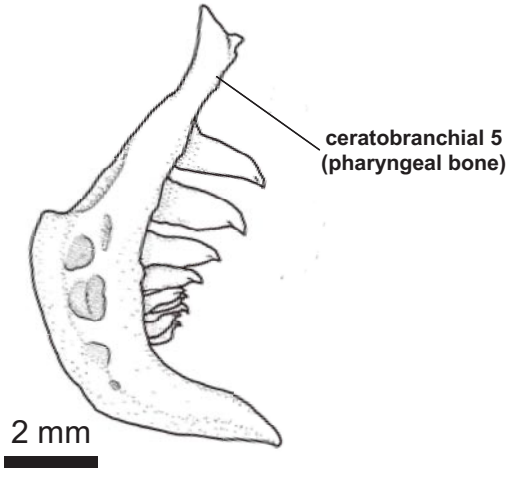
ceratobranchial 5
(pharyngeal bone)
2 mm


2 mm

Plate 8-3

A

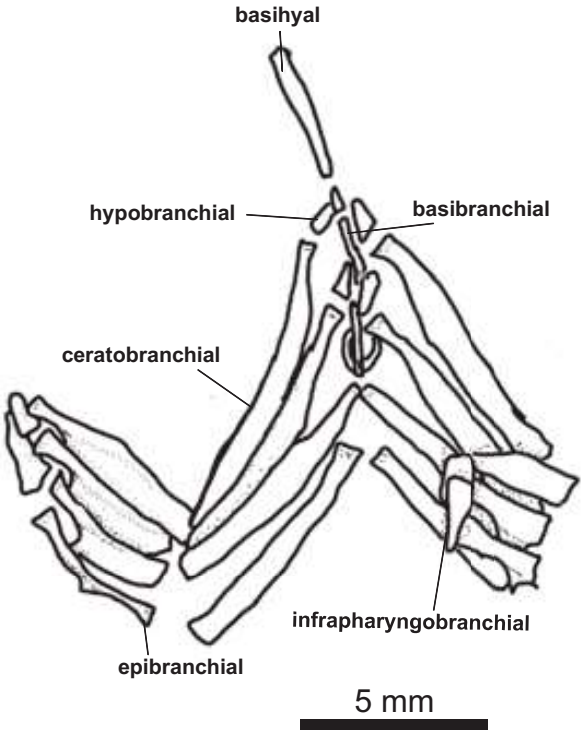
basihyal
hypobranchial
basibranchial
ceratobranchial
infrapharyngobranchial
epibranchial
5 mm


5 mm

B

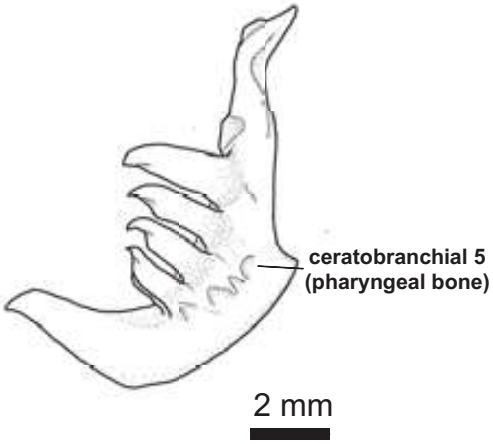
ceratobranchial 5
(pharyngeal bone)
2 mm

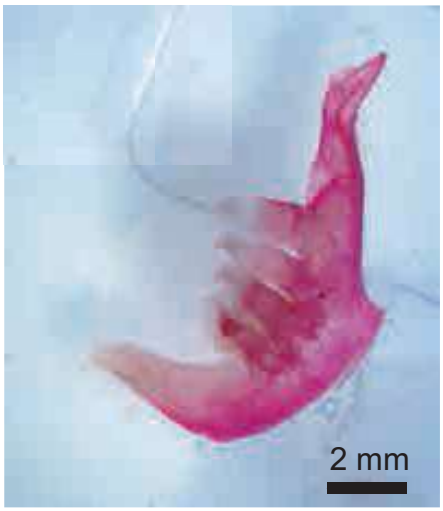
2 mm

C

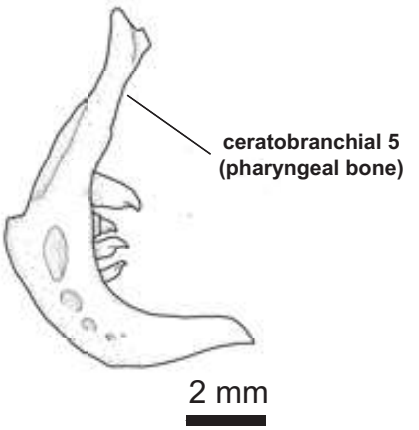
ceratobranchial 5
(pharyngeal bone)
2 mm

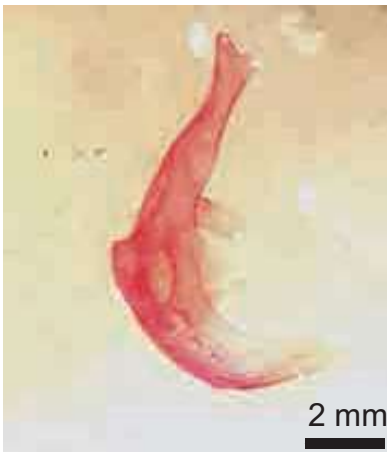
2 mm

Plate 8-4

A

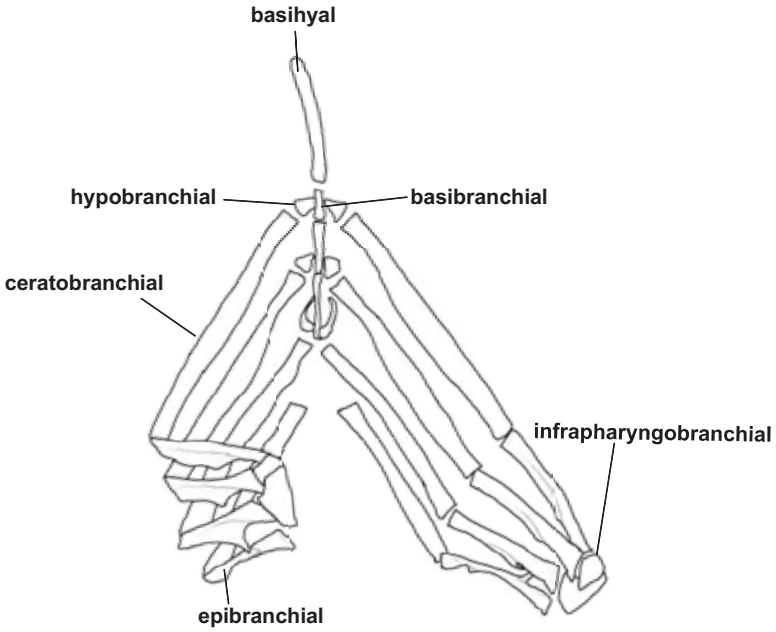

5 mm

5 mm

B

2 mm

2 mm

C

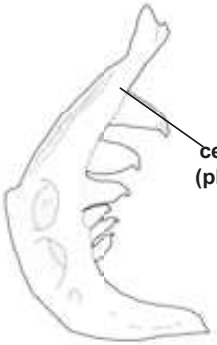

2 mm

2 mm

Plate 8-5

A

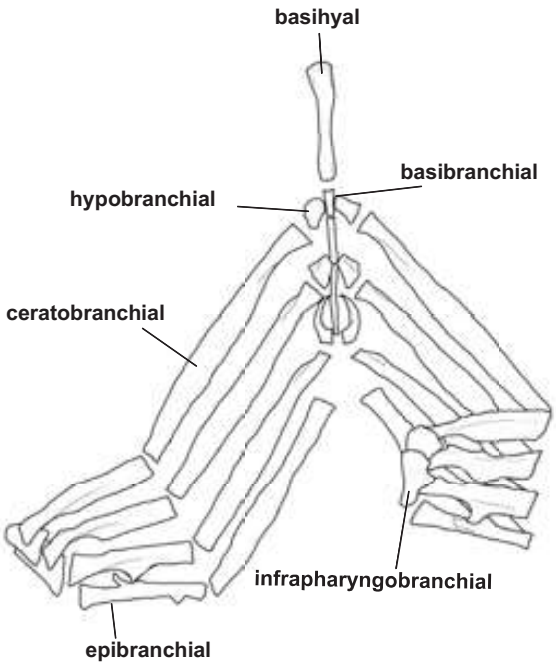
basihyal
basibranchial
hypobranchial
ceratobranchial
infrapharyngobranchial
epibranchial
5 mm


5 mm

B

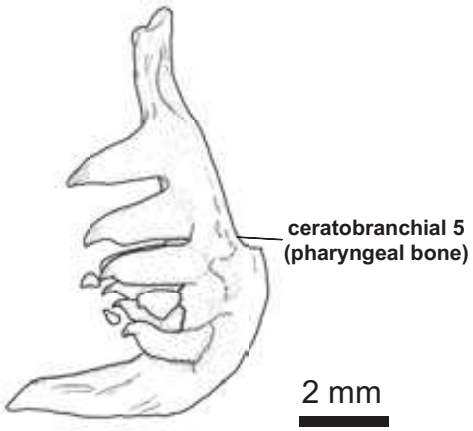
ceratobranchial 5
(pharyngeal bone)
2 mm


2 mm

C

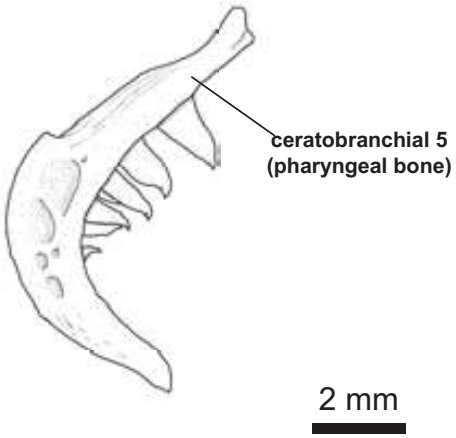
ceratobranchial 5
(pharyngeal bone)
2 mm


2 mm

Plate 8-6

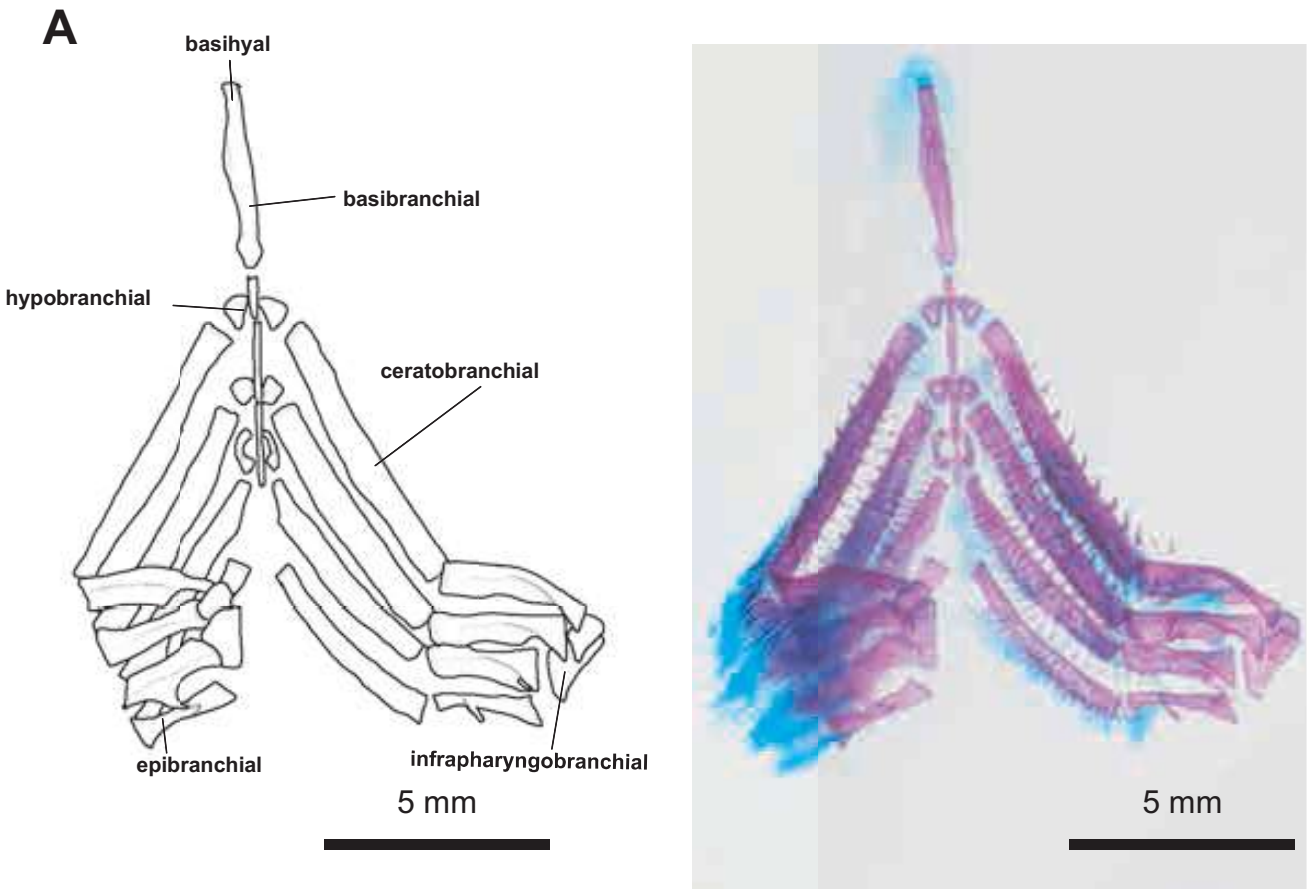
A
basihyal
basibranchial
hypobranchial
ceratobranchial
epibranchial
infrapharyngobranchial
5 mm
5 mm
B
ceratobranchial 5
(pharyngeal bone)
2 mm
2 mm
C
ceratobranchial 5
(pharyngeal bone)
2 mm
2 mm

Plate 8-7

A

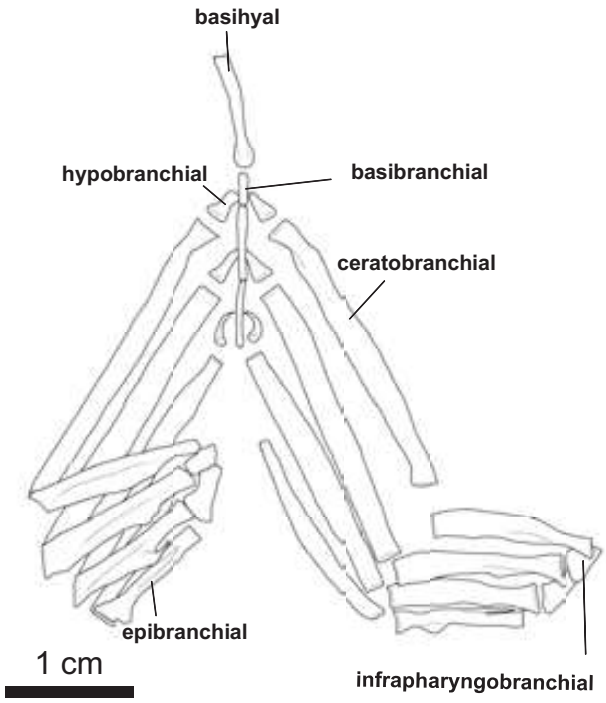
basihyal
hypobranchial
basibranchial
ceratobranchial
epibranchial
1 cm
infrapharyngobranchial


1 cm

B

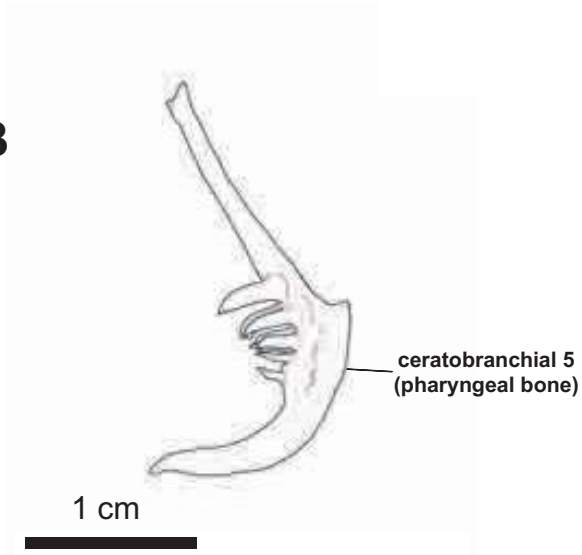
ceratobranchial 5
(pharyngeal bone)
1 cm


1 cm

C

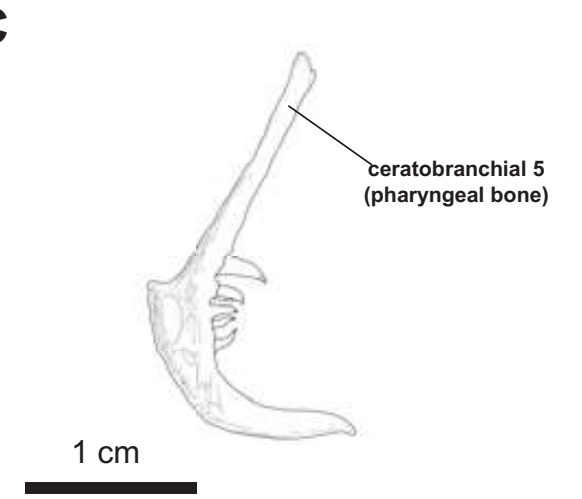
ceratobranchial 5
(pharyngeal bone)
1 cm


1 cm

Plate 8-8

A

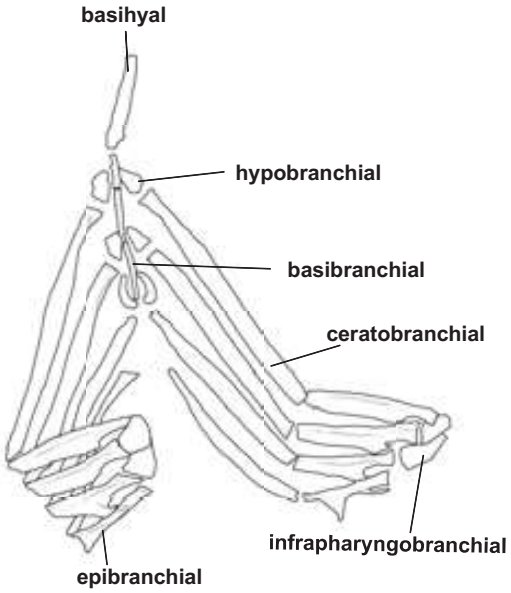

5 mm

5 mm

B

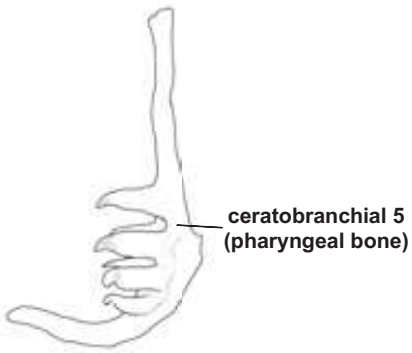

4 mm

4 mm

C

4 mm

4 mm

Plate 8-9

A

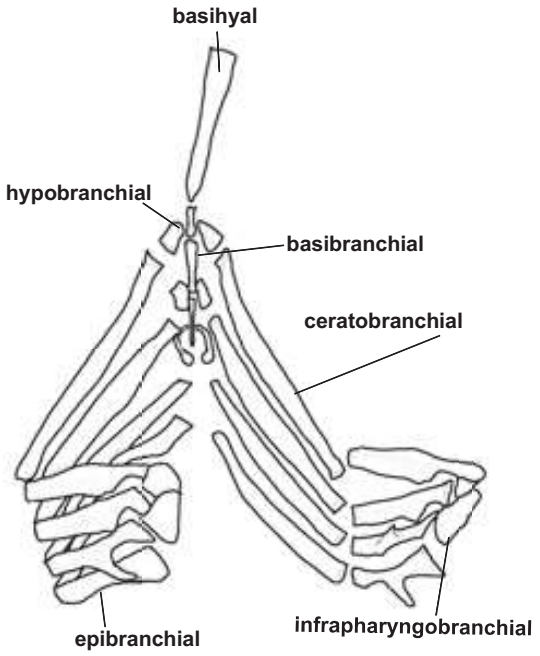
basihyal
hypobranchial
basibranchial
ceratobranchial
epibranchial
infrapharyngobranchial
5 mm


5 mm

B

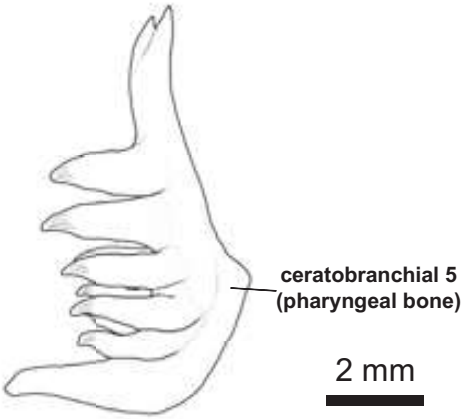
ceratobranchial 5
(pharyngeal bone)
2 mm

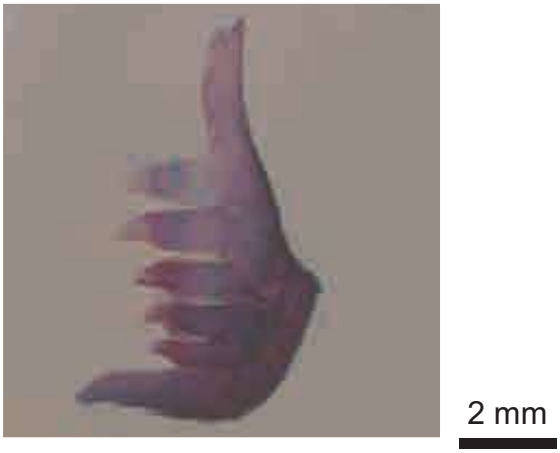
2 mm

C

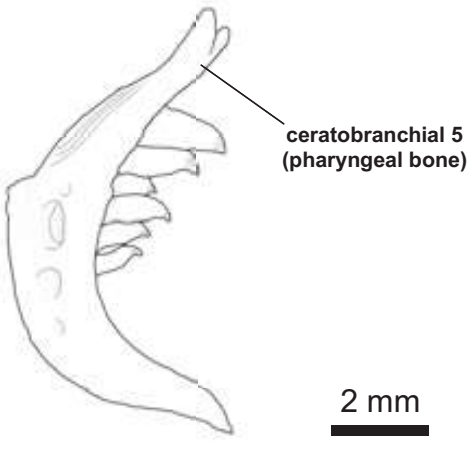
ceratobranchial 5
(pharyngeal bone)
2 mm

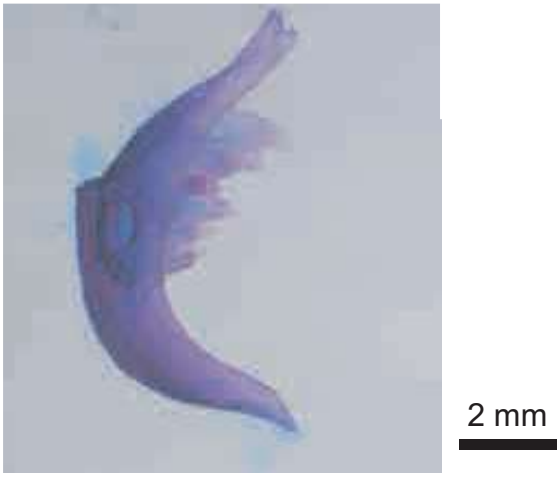
2 mm

Plate 9-1

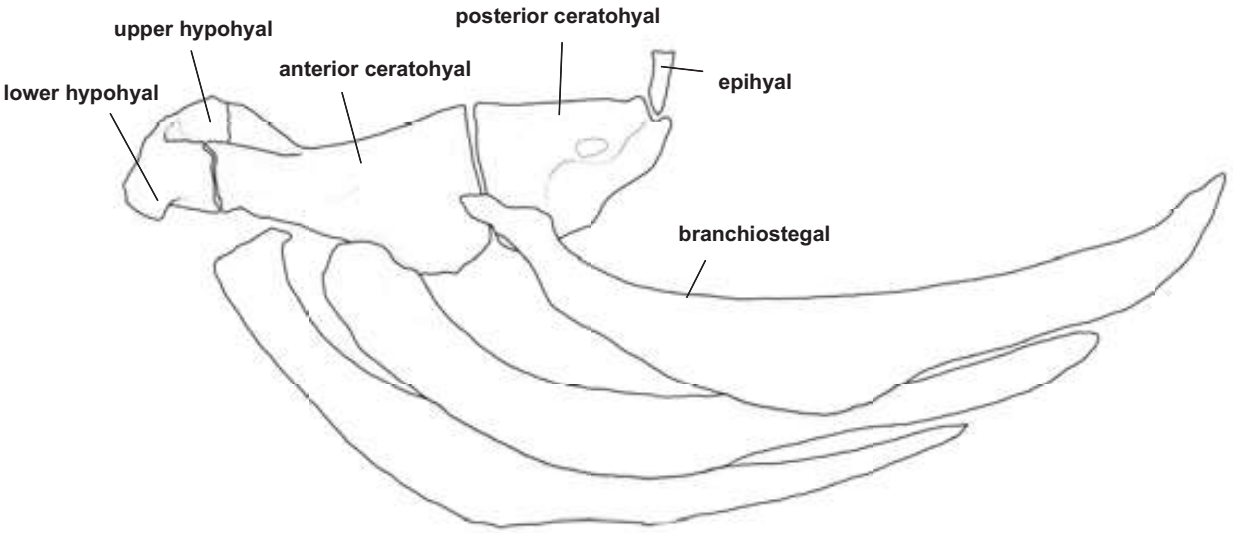
upper hypohyal
posterior ceratohyal
anterior ceratohyal
epihyal
lower hypohyal
branchiostegal
2 mm

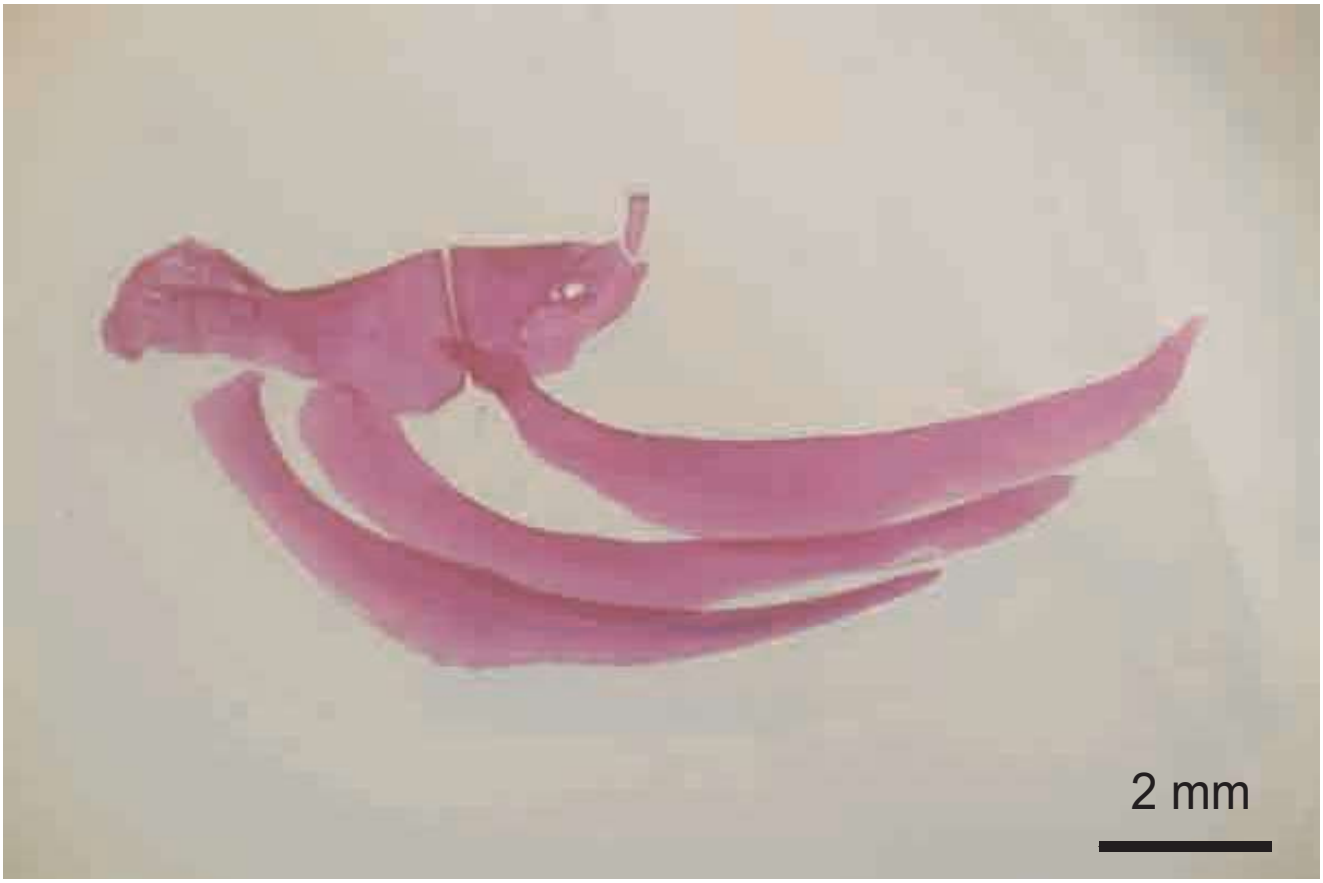
2 mm

Plate 9-2

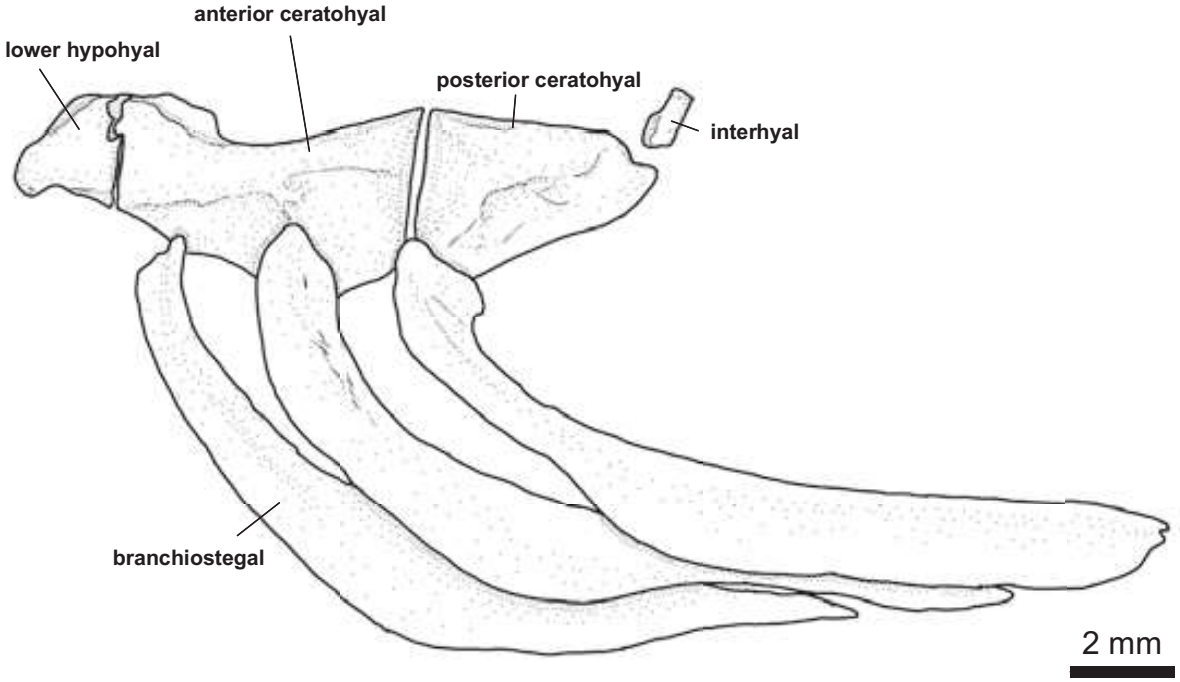
anterior ceratohyal
lower hypohyal
posterior ceratohyal
interhyal
branchiostegal
2 mm


2 mm

Plate 9-3

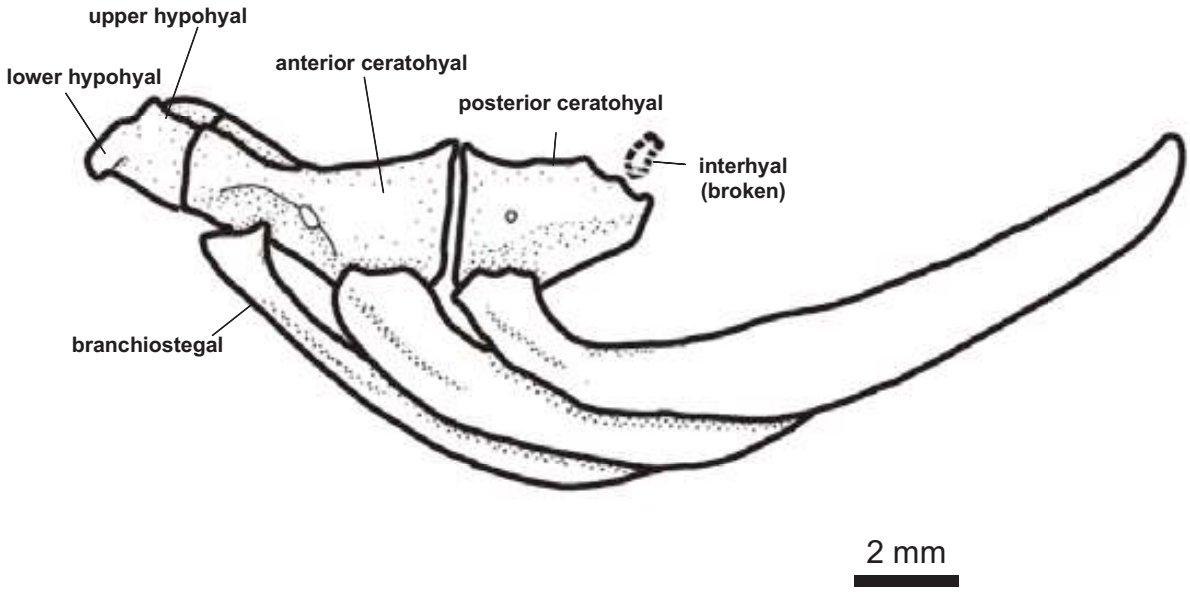
upper hypohyal
lower hypohyal
anterior ceratohyal
posterior ceratohyal
interhyal
(broken)
branchiostegal
2 mm


2 mm

Plate 9-4

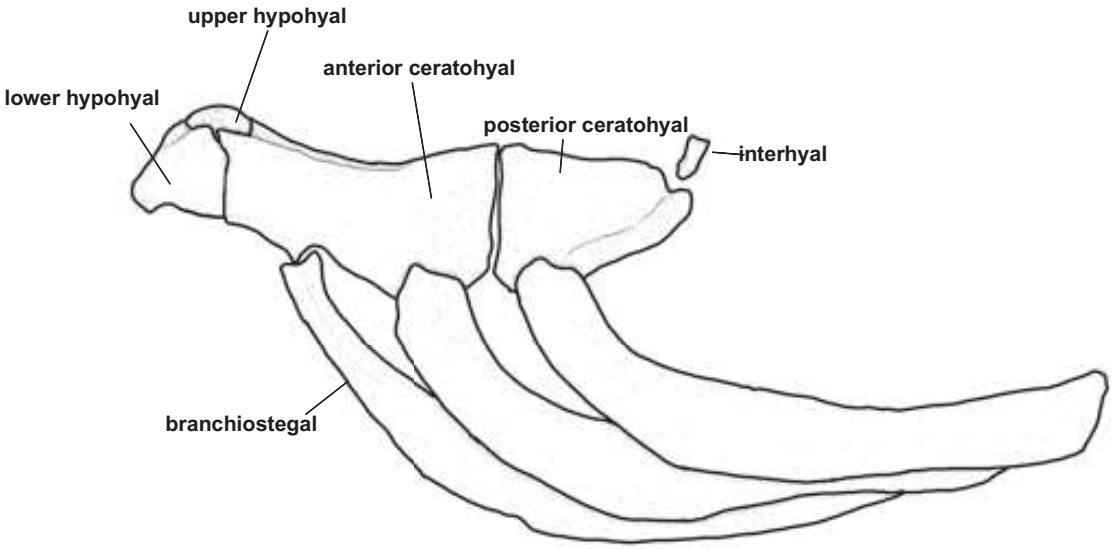
upper hypohyal
anterior ceratohyal
lower hypohyal
posterior ceratohyal
interhyal
branchiostegal

2 mm


2 mm

Plate 9-5

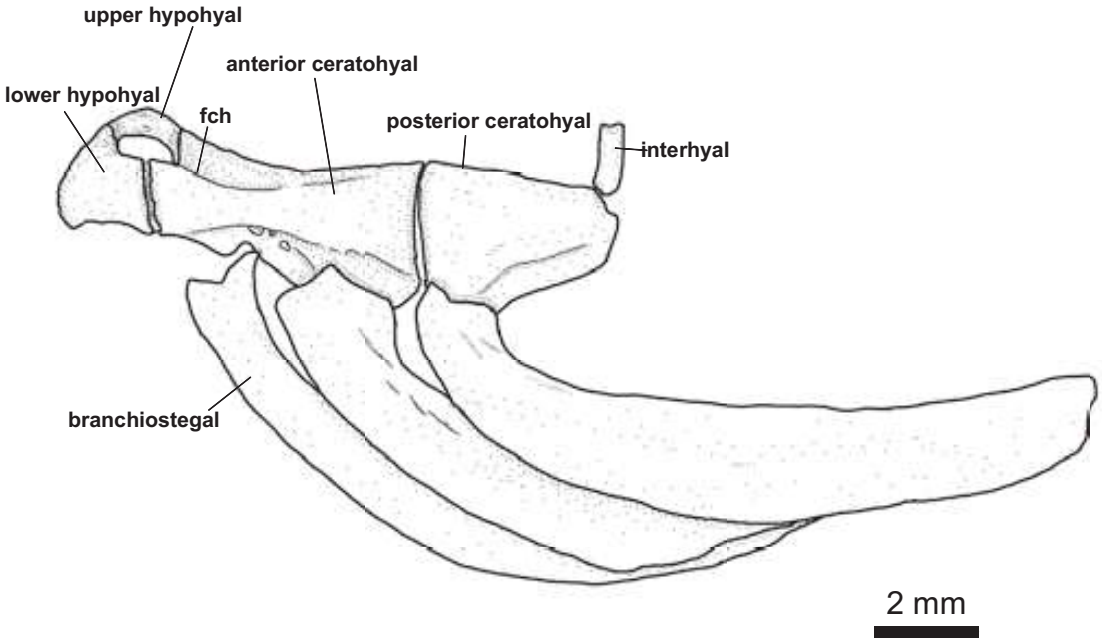
upper hypohyal
anterior ceratohyal
lower hypohyal
fch
posterior ceratohyal
interhyal
branchiostegal
2 mm

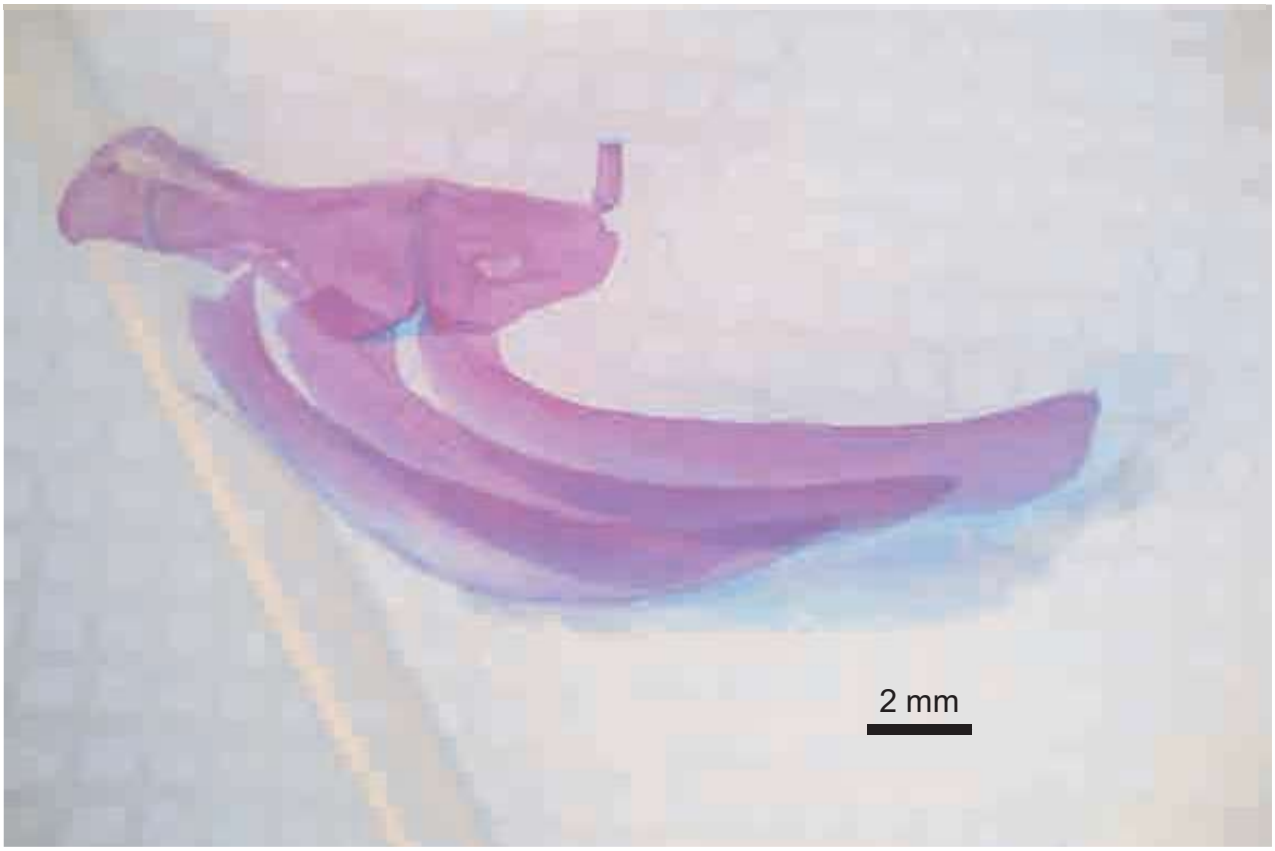
2 mm

Plate 9-6

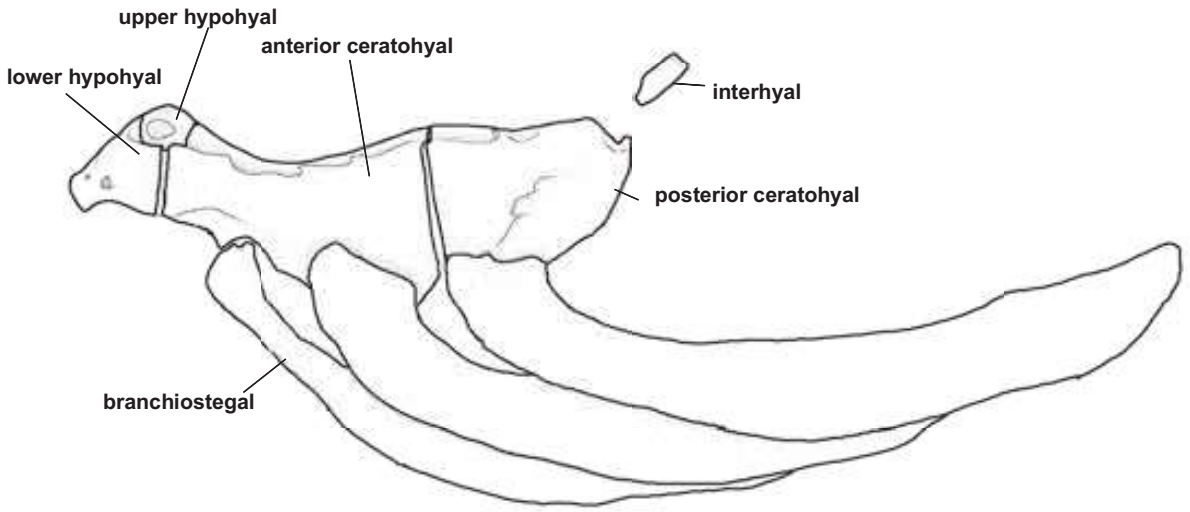

2 mm

2 mm

Plate 9-7

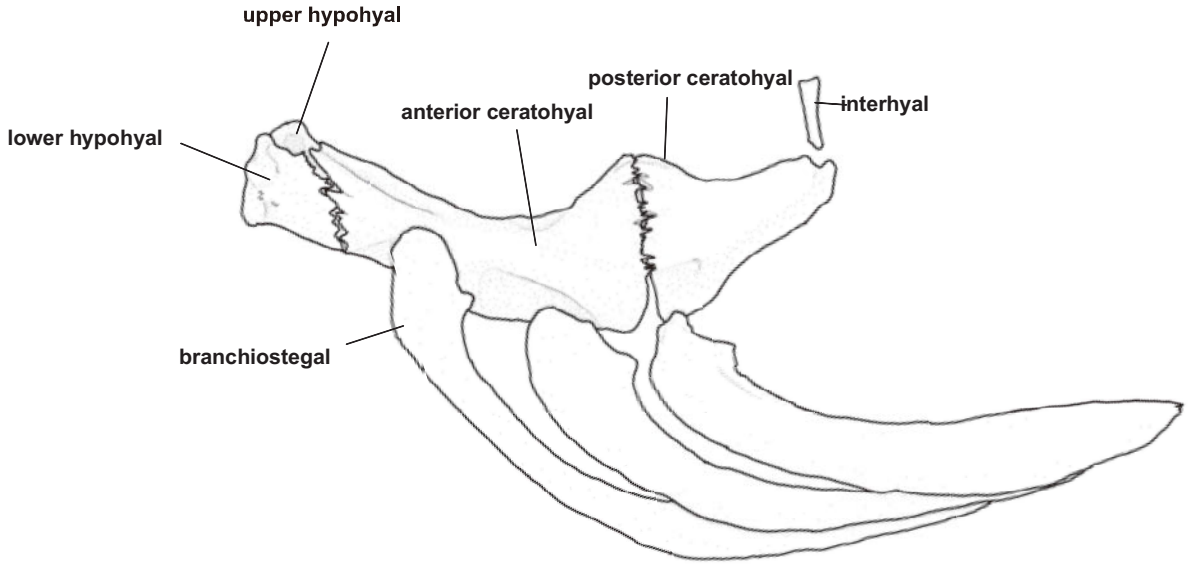
upper hypohyal
posterior ceratohyal
interhyal
anterior ceratohyal
lower hypohyal
branchiostegal
1cm


1cm

Plate 9-8

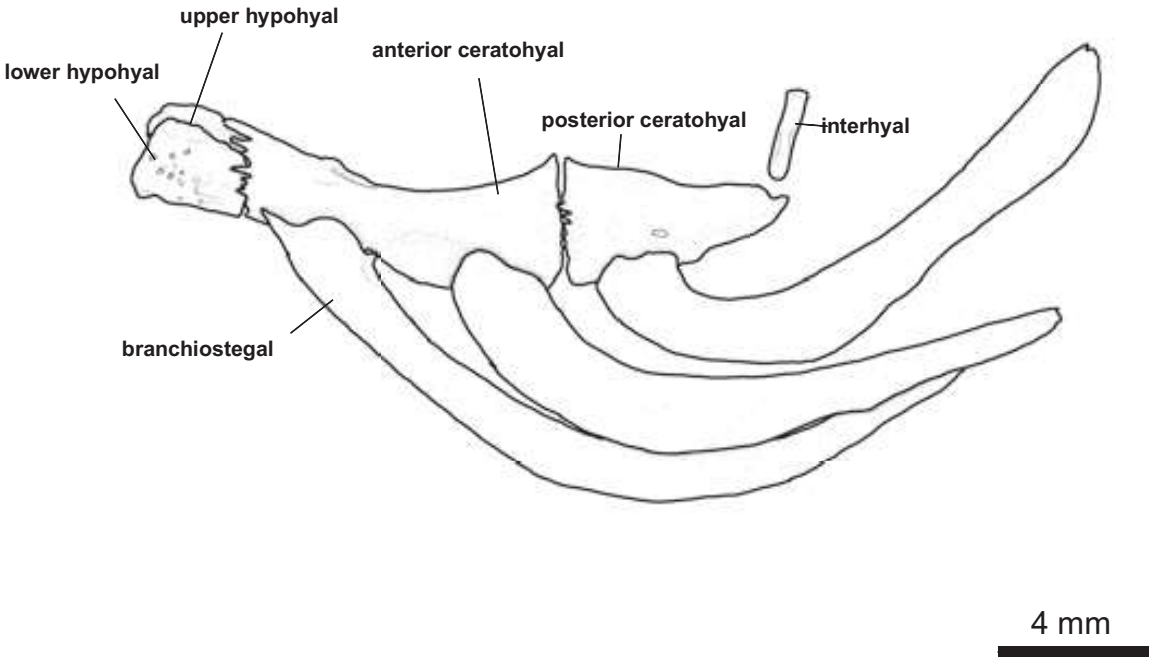
upper hypohyal
lower hypohyal
anterior ceratohyal
posterior ceratohyal
interhyal
branchiostegal
4 mm


4 mm

Plate 9-9

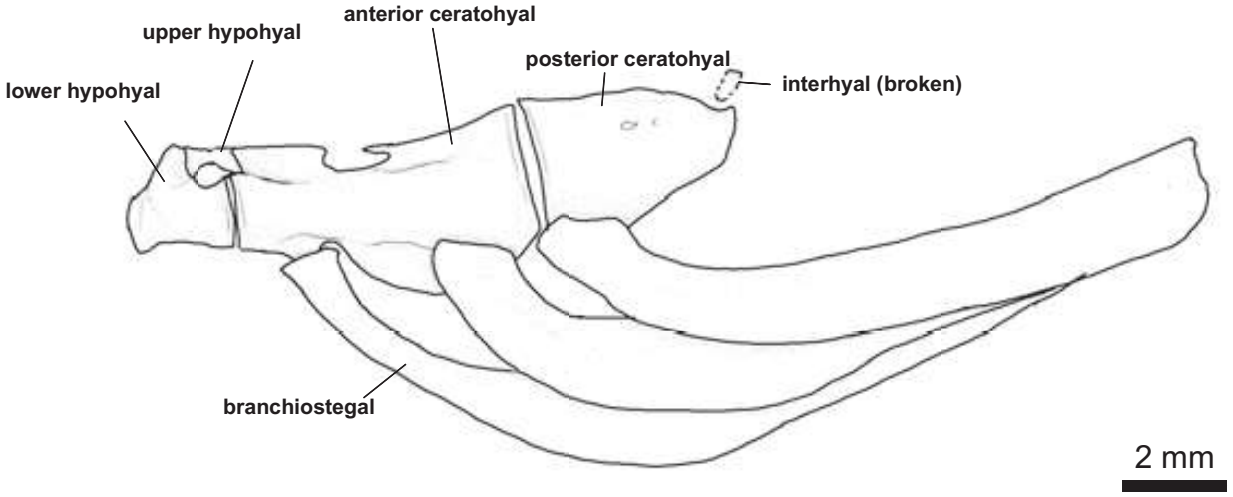
anterior ceratohyal
upper hypohyal
posterior ceratohyal
interhyal (broken)
lower hypohyal
branchiostegal
2 mm


2 mm

Plate 10-1

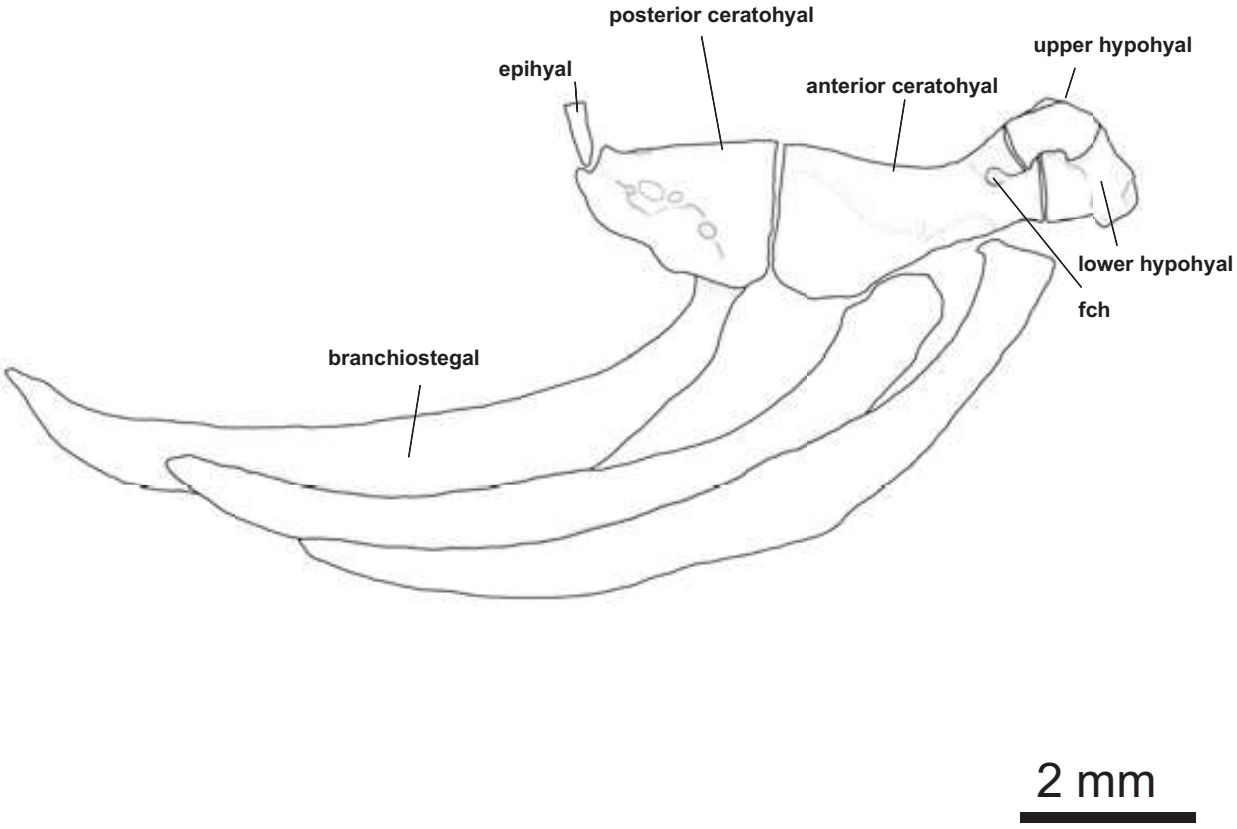
posterior ceratohyal
epihyal
upper hypohyal
anterior ceratohyal
lower hypohyal
fch
branchiostegal
2 mm

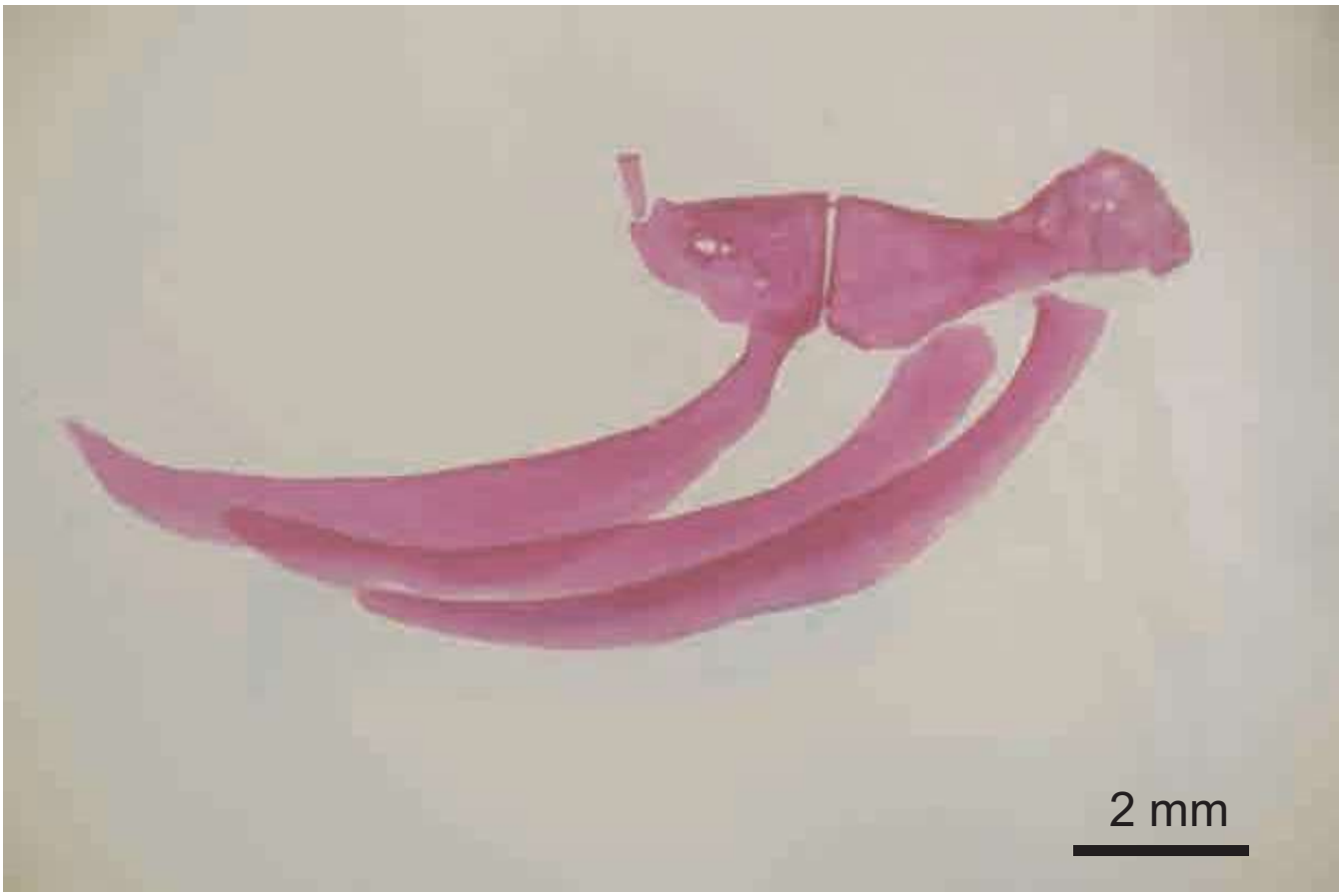
2 mm

Plate 10-2

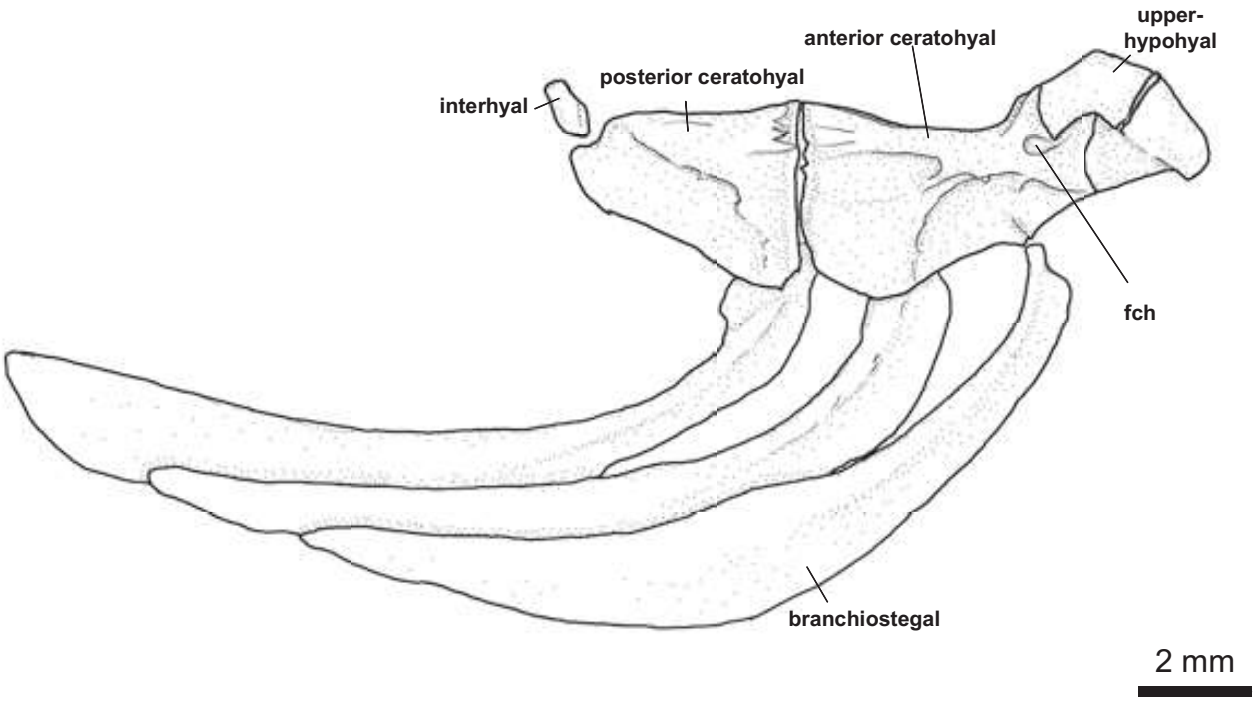
upper-
hypohyal
anterior ceratohyal
posterior ceratohyal
interhyal
fch
branchiostegal
2 mm


2 mm

Plate 10-3

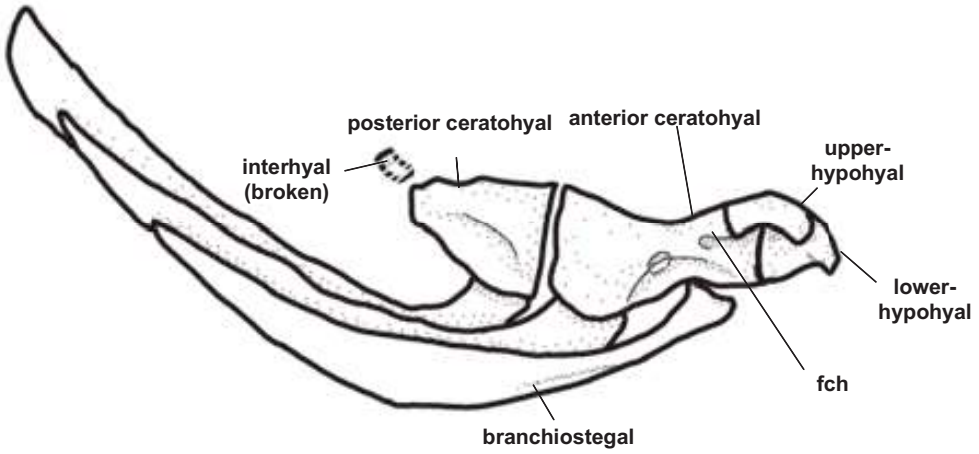
posterior ceratohyal
anterior ceratohyal
interhyal
(broken)
upper-
hypohyal
lower-
hypohyal
fch
branchiostegal
2 mm


2 mm

Plate 10-4

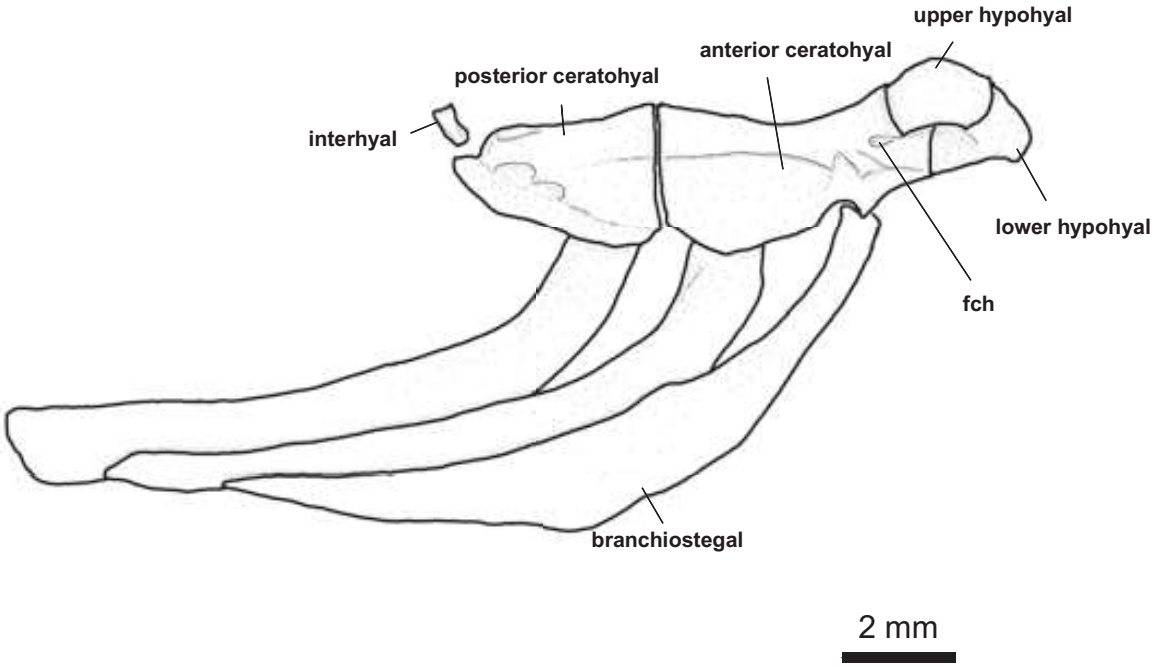
upper hypohyal
anterior ceratohyal
posterior ceratohyal
interhyal
lower hypohyal
fch
branchiostegal
2 mm

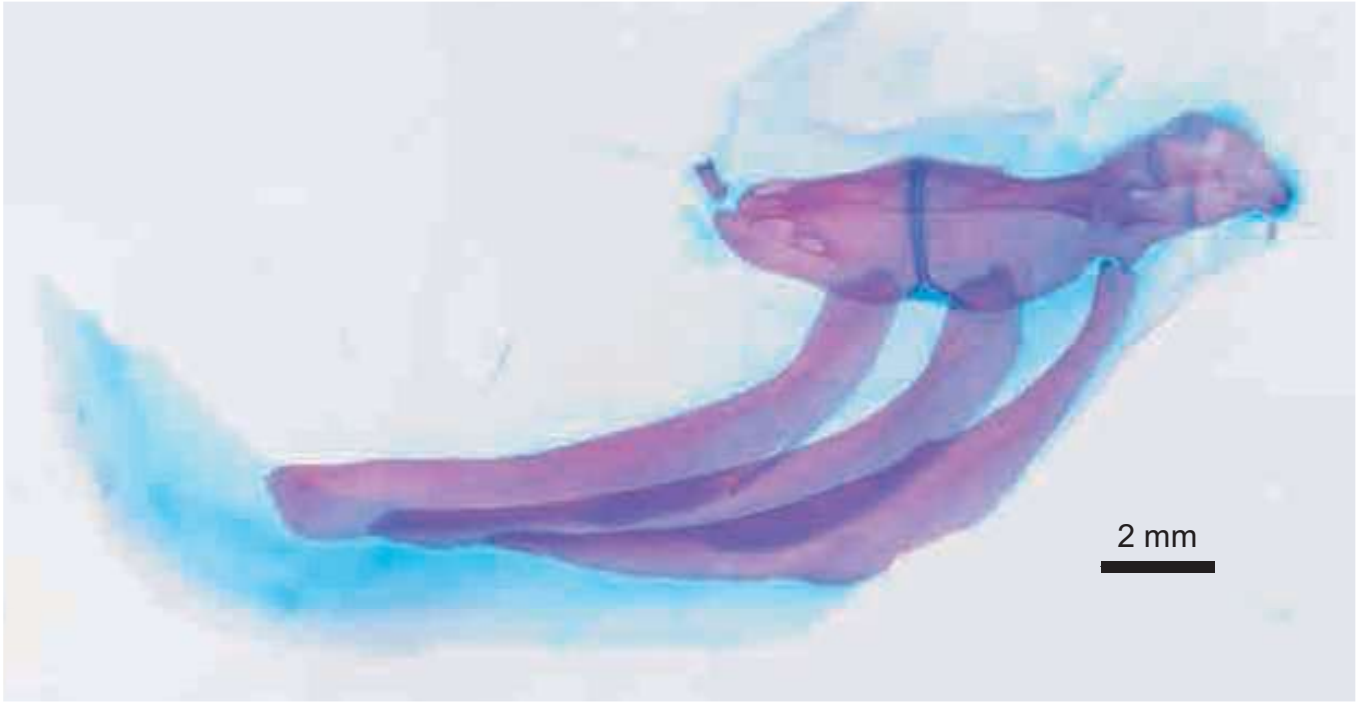
2 mm

Plate 10-5

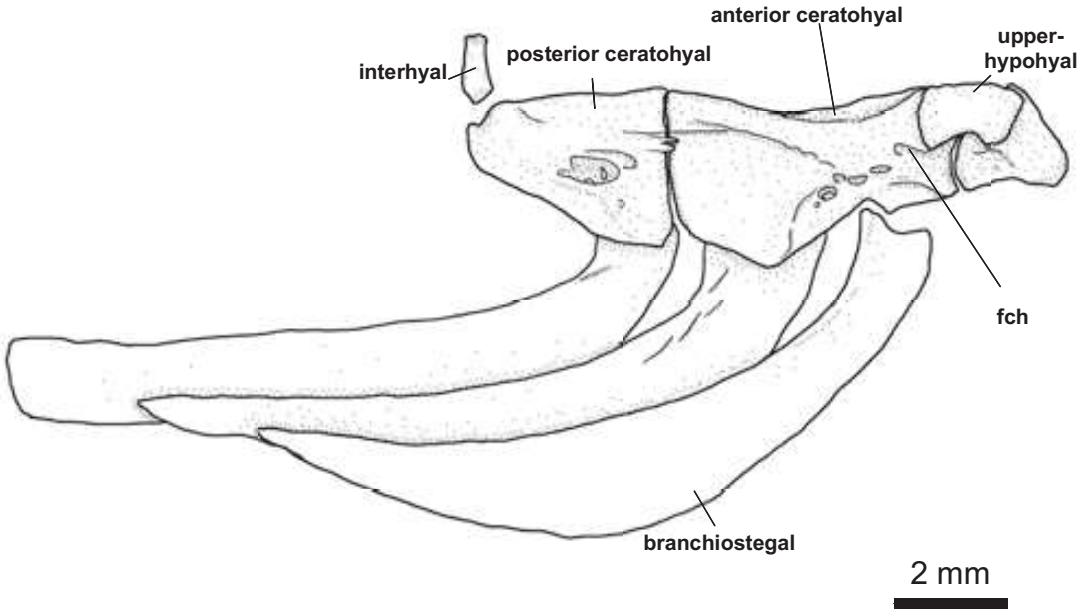
anterior ceratohyal
upper-
hypohyal
interhyal
posterior ceratohyal
fch
branchiostegal
2 mm

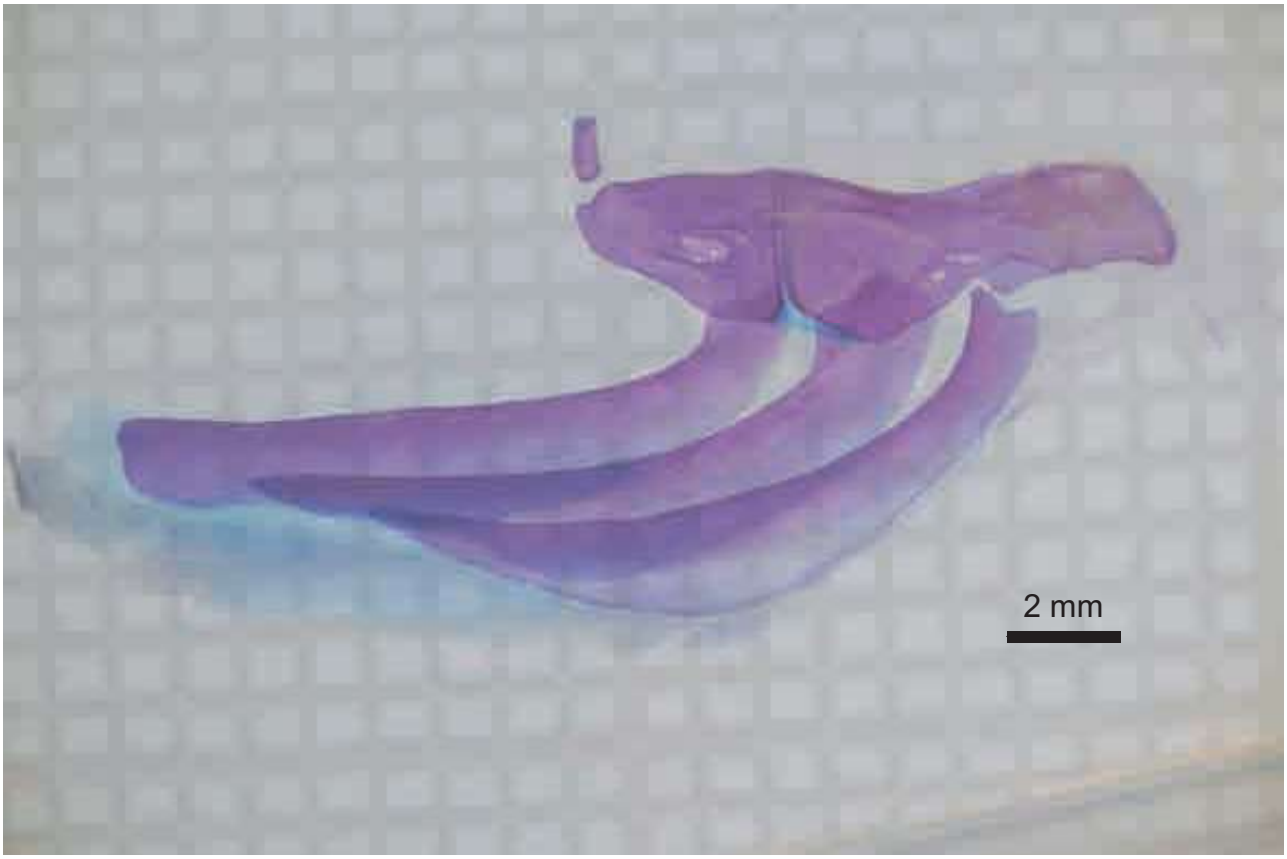
2 mm

Plate 10-6

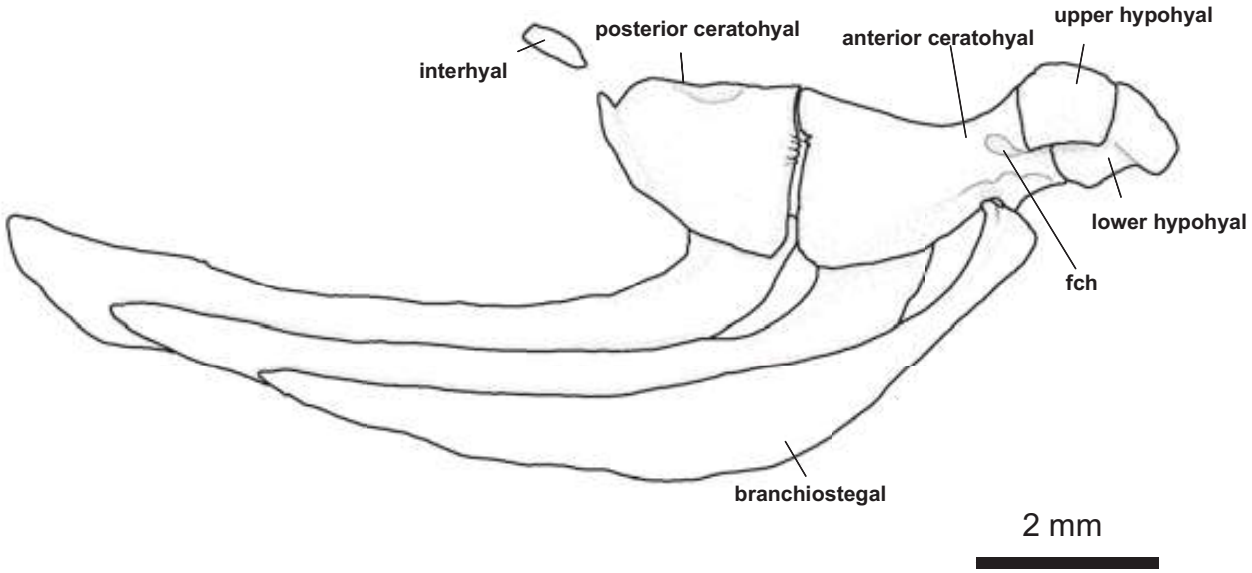
interhyal
posterior ceratohyal
anterior ceratohyal
upper hypohyal
lower hypohyal
fch
branchiostegal
2 mm


2 mm

Plate 10-7

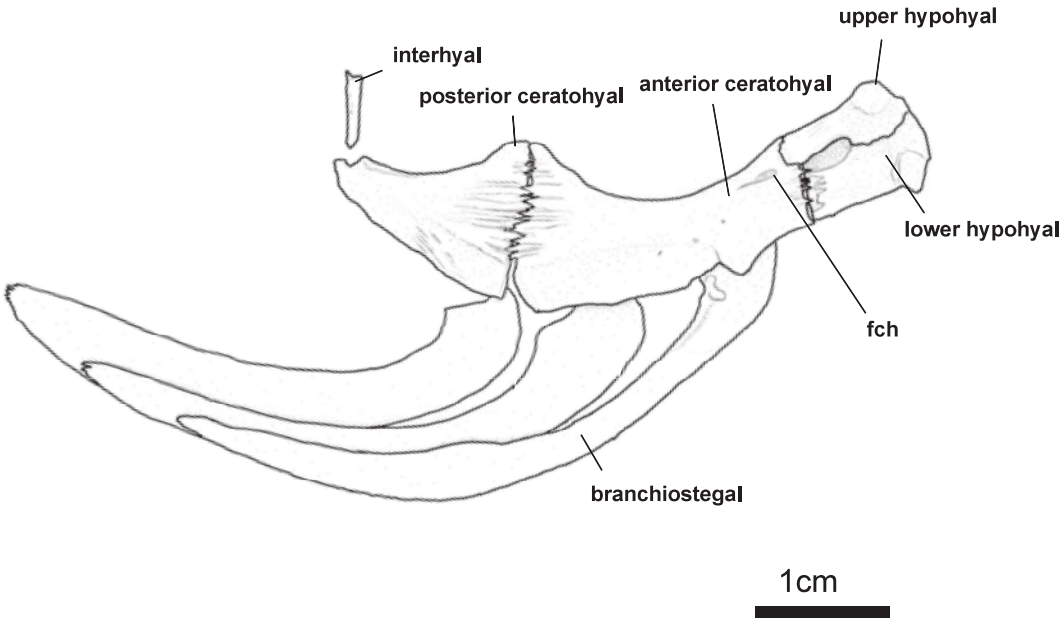
upper hypohyal
interhyal
posterior ceratohyal
anterior ceratohyal
lower hypohyal
fch
branchiostegal
1cm


1cm

Plate 10-8

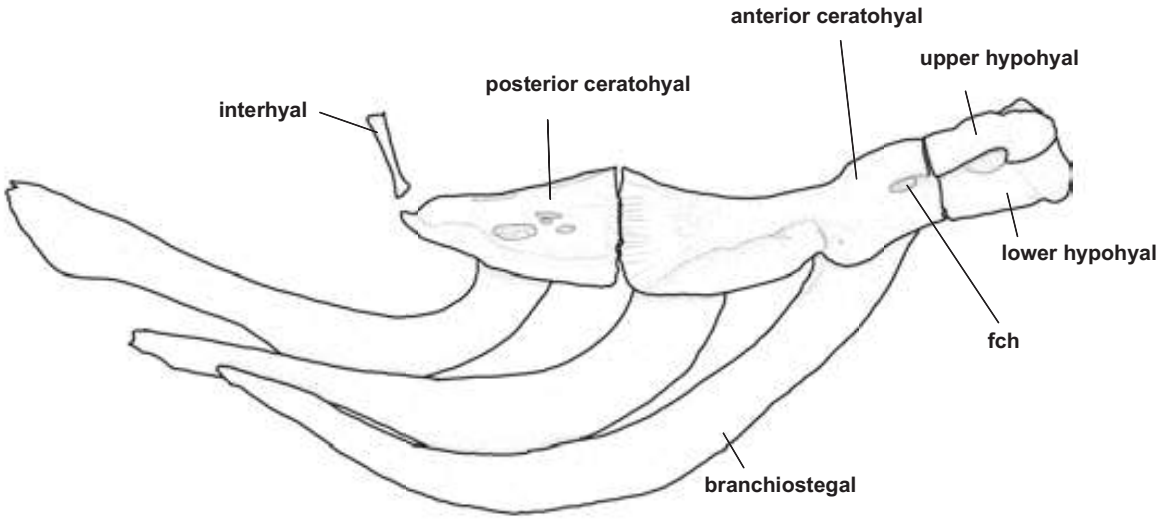
anterior ceratohyal
upper hypohyal
posterior ceratohyal
interhyal
lower hypohyal
fch
branchiostegal
4 mm


4 mm

Plate 10-9

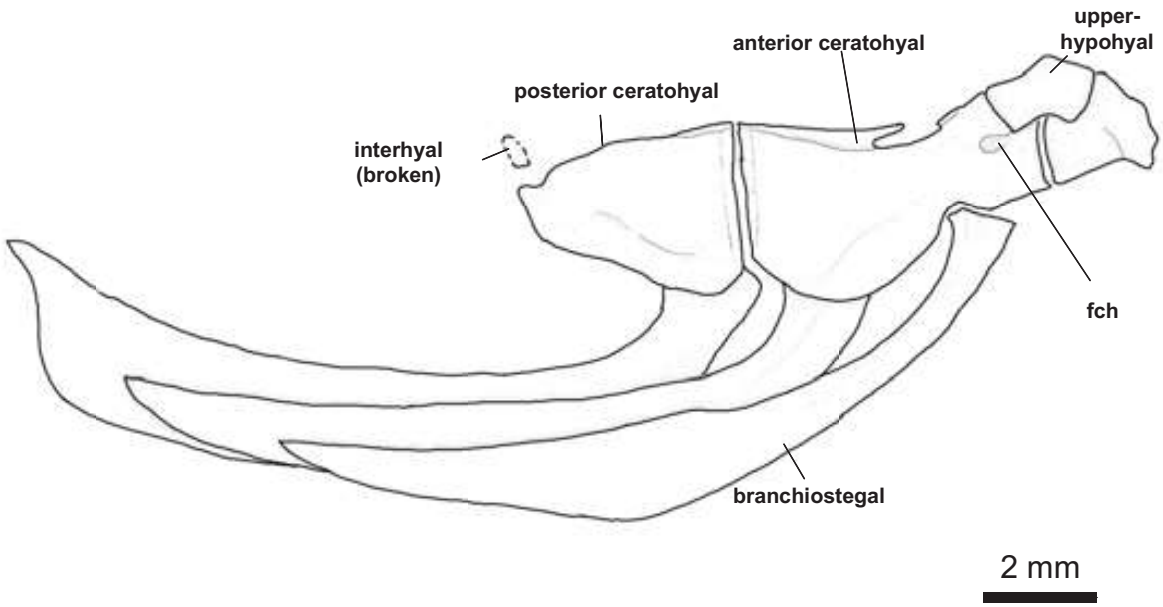
upper-
hypohyal
anterior ceratohyal
posterior ceratohyal
interhyal
(broken)
fch
branchiostegal
2 mm


2 mm

Plate 11-1

A

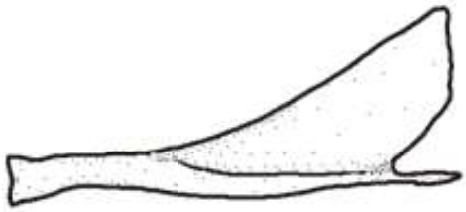

2 mm

2 mm

B

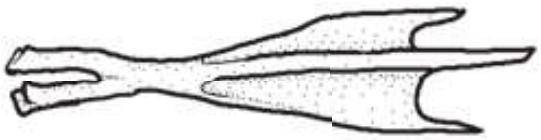

2 mm

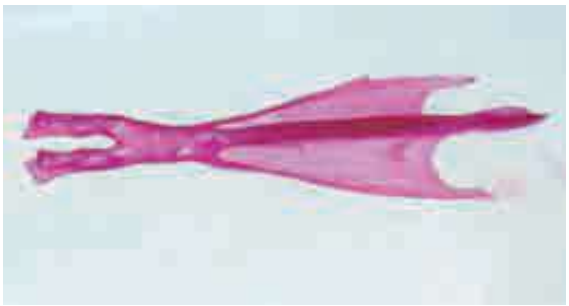

2 mm

C

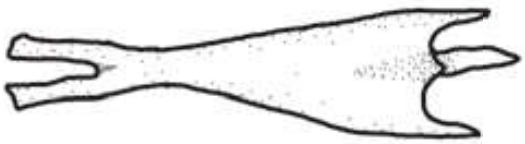

2 mm

2 mm

Plate 11-2

A

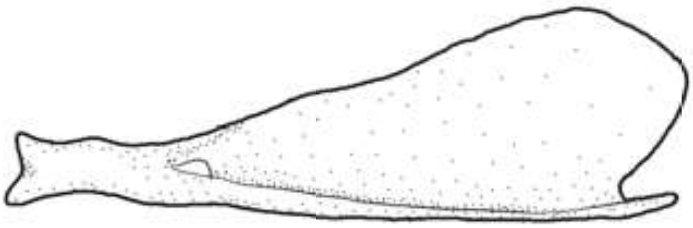

2 mm

2 mm

B

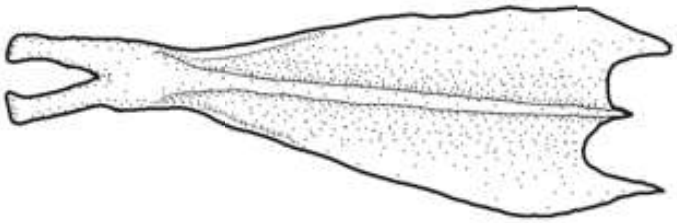

2 mm

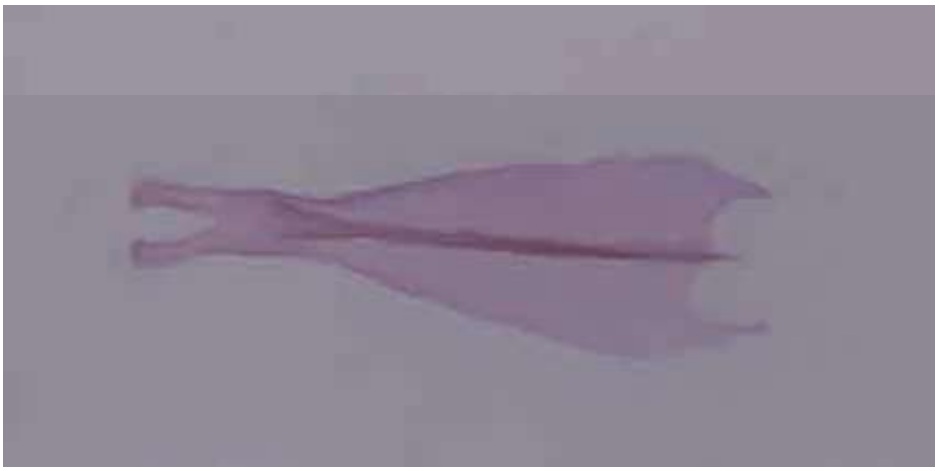

2 mm

C

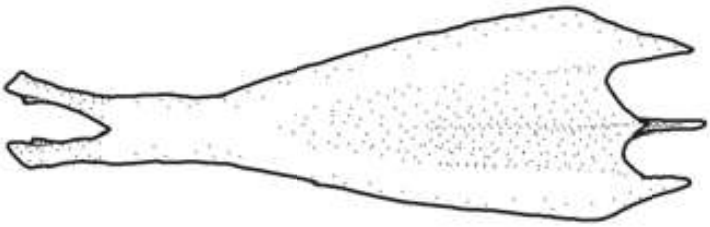

2 mm

2 mm

Plate 11-3

A

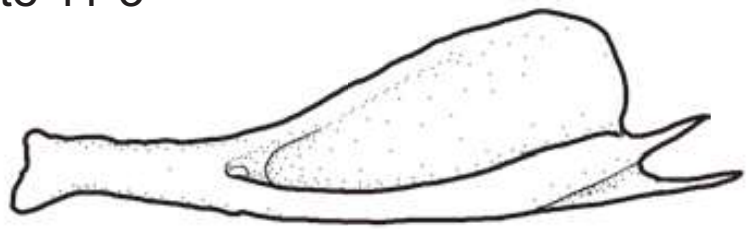

2 mm

2 mm

B

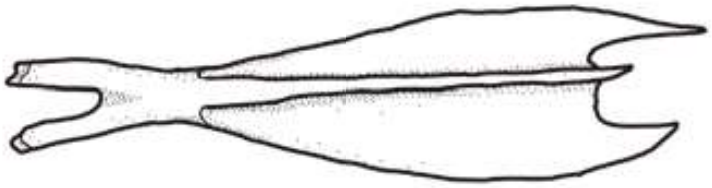

2 mm

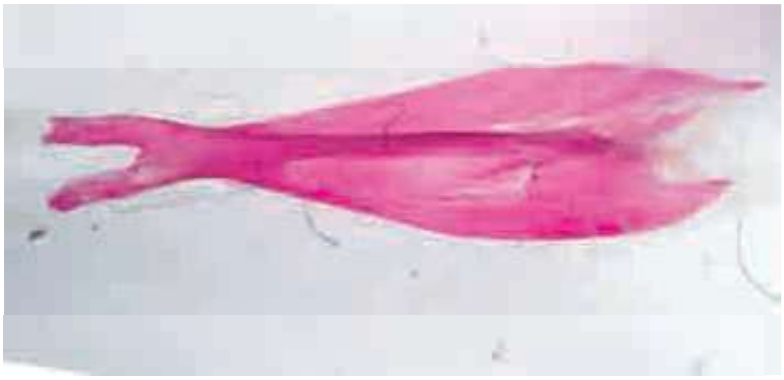

2 mm

C

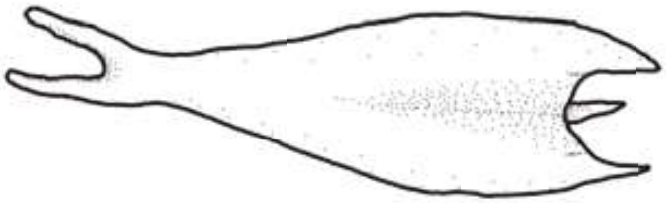

2 mm

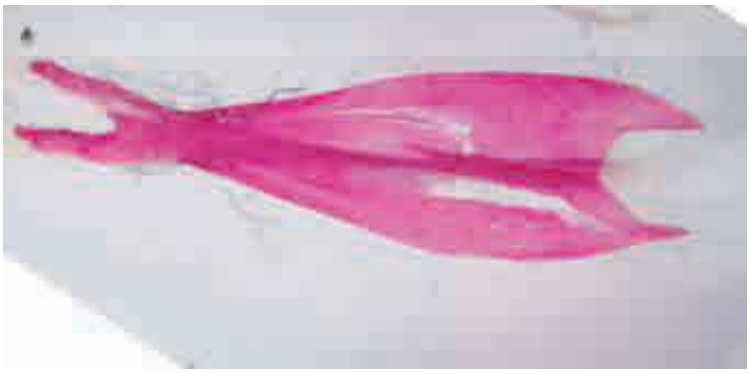

2 mm

Plate 11-4

A

2 mm

2 mm

B

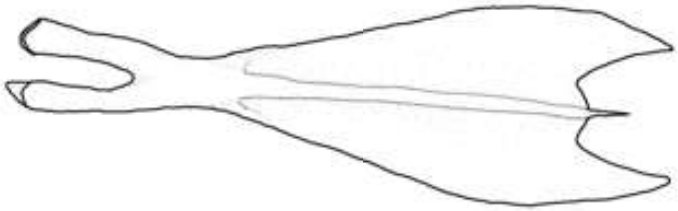

2 mm

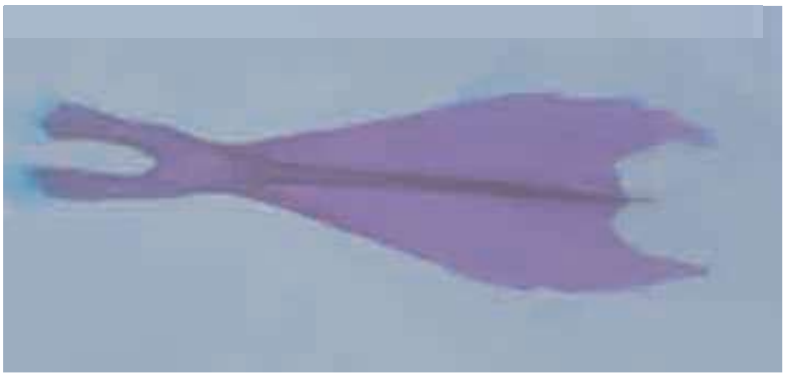

2 mm

C

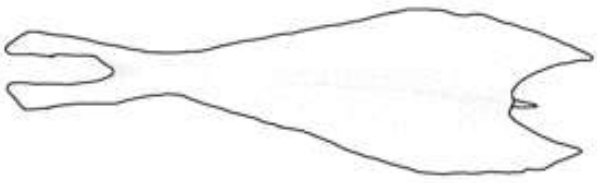

2 mm

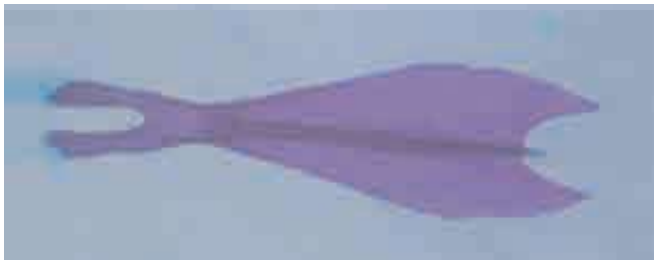

2 mm

Plate 11-5

A

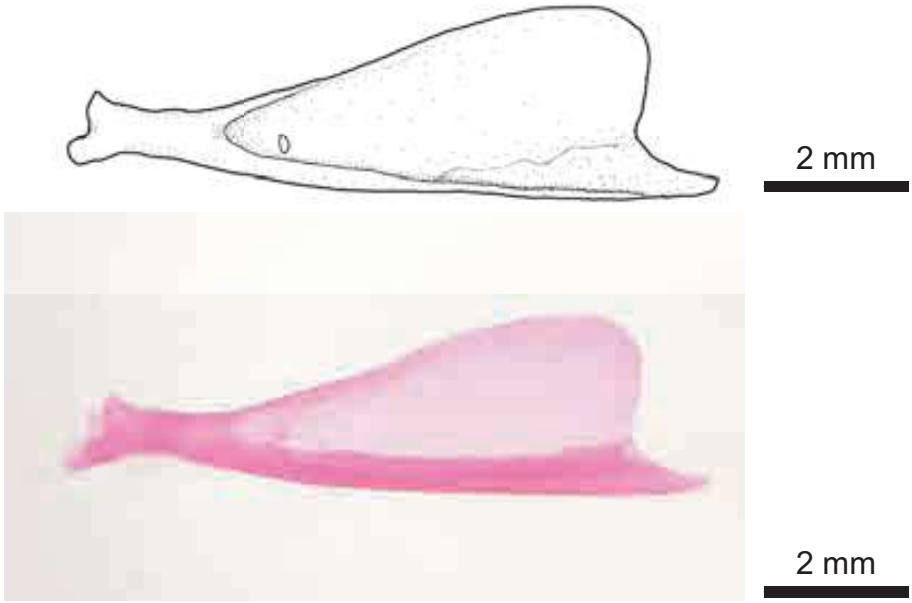

B

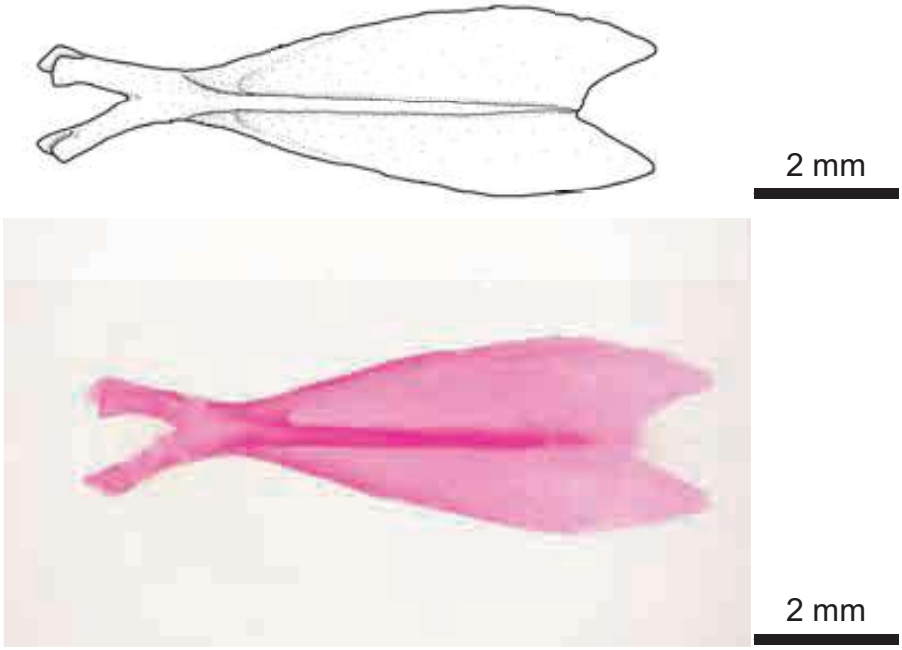

C

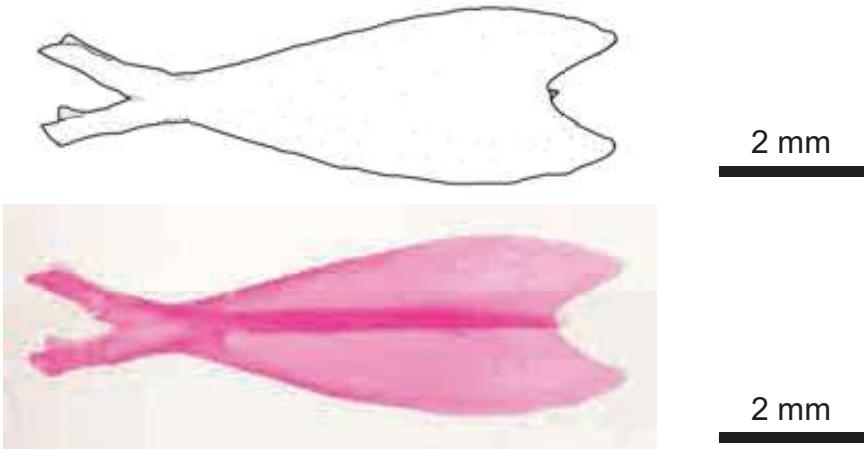

Plate 11-6

A

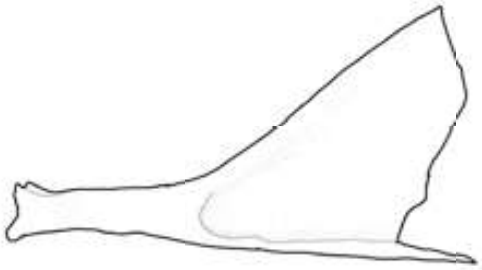

2 mm

2 mm

B

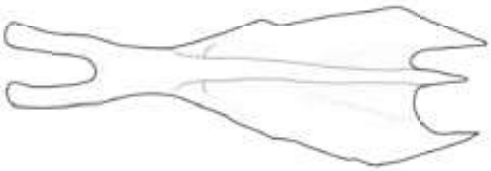

2 mm

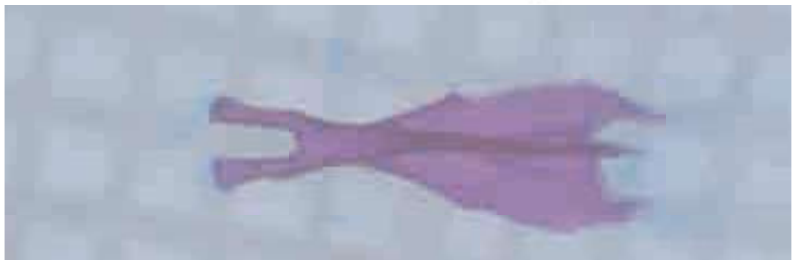

2 mm

C

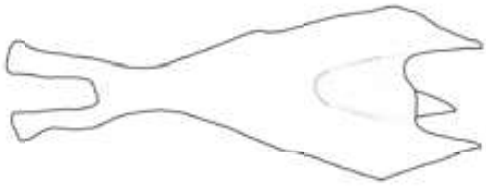

2 mm

2 mm

Plate 11-7

A

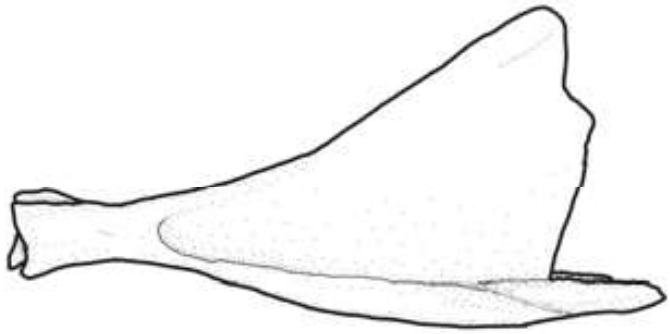

5 mm

5 mm

B

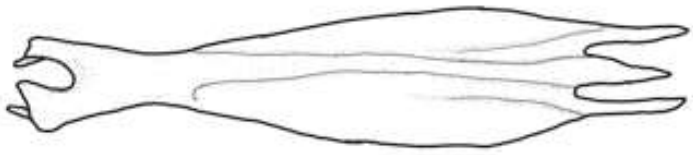

5 mm

5 mm

C

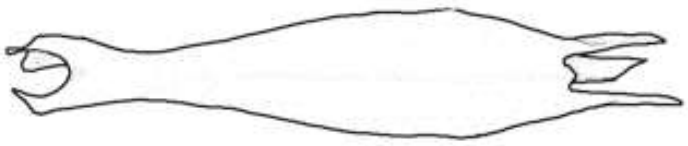

5 mm

5 mm

Plate 11-8

A

4 mm

4 mm

B

4 mm

4 mm

C

4 mm

4 mm

Plate 11-9

A

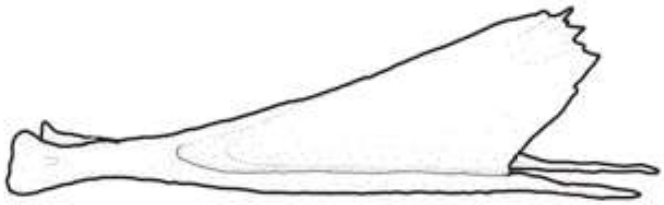

2 mm

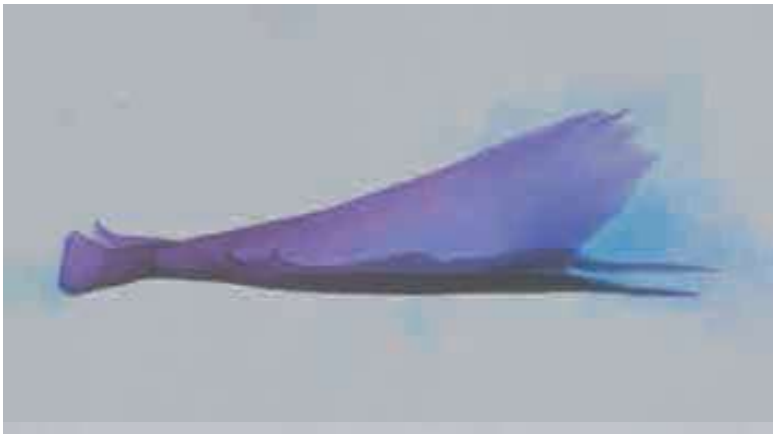

2 mm

B

2 mm

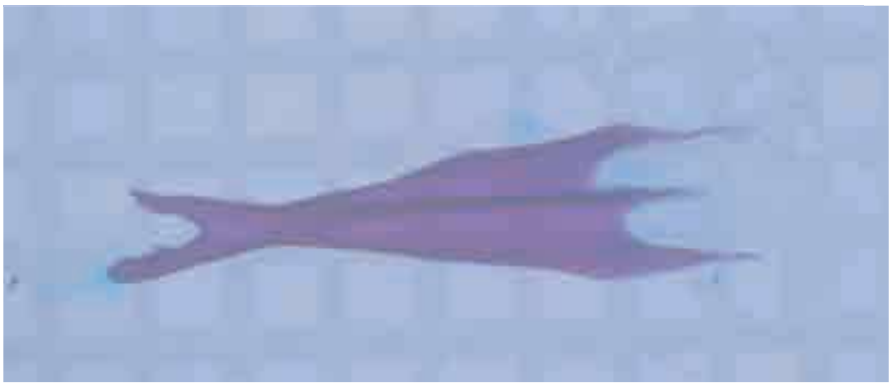

2 mm

C

2 mm

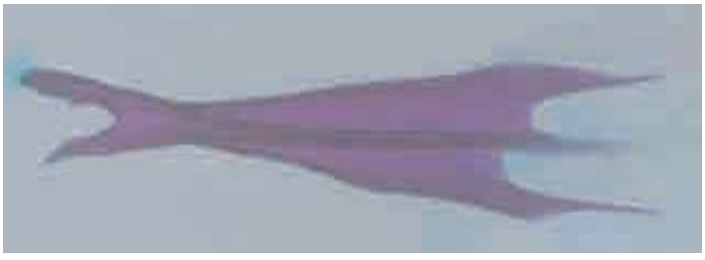

2 mm

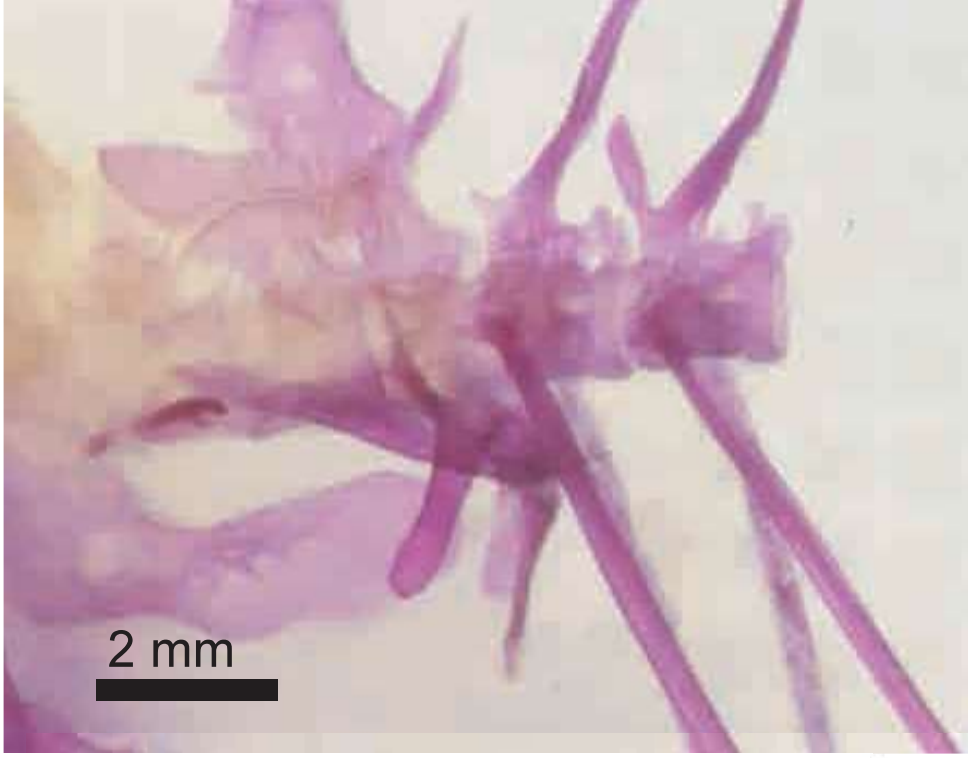
2 mm

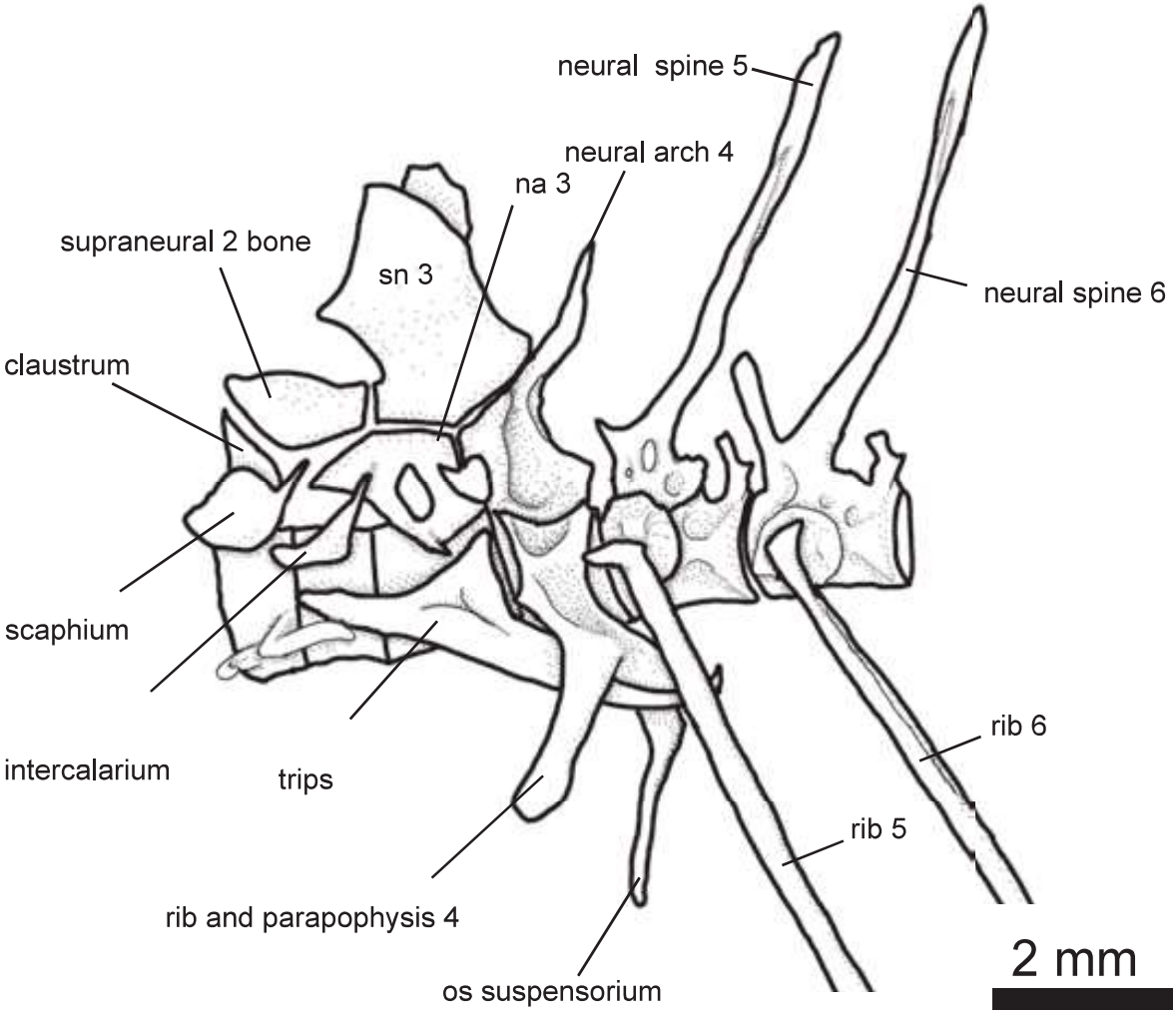
neural spine 5
neural arch 4
na 3
supraneural 2 bone
sn 3
neural spine 6
claustrum
scaphium
rib 6
intercalarium
trips
rib 5
rib and parapophysis 4
os suspensorium
2 mm

Plate 12-2


2 mm

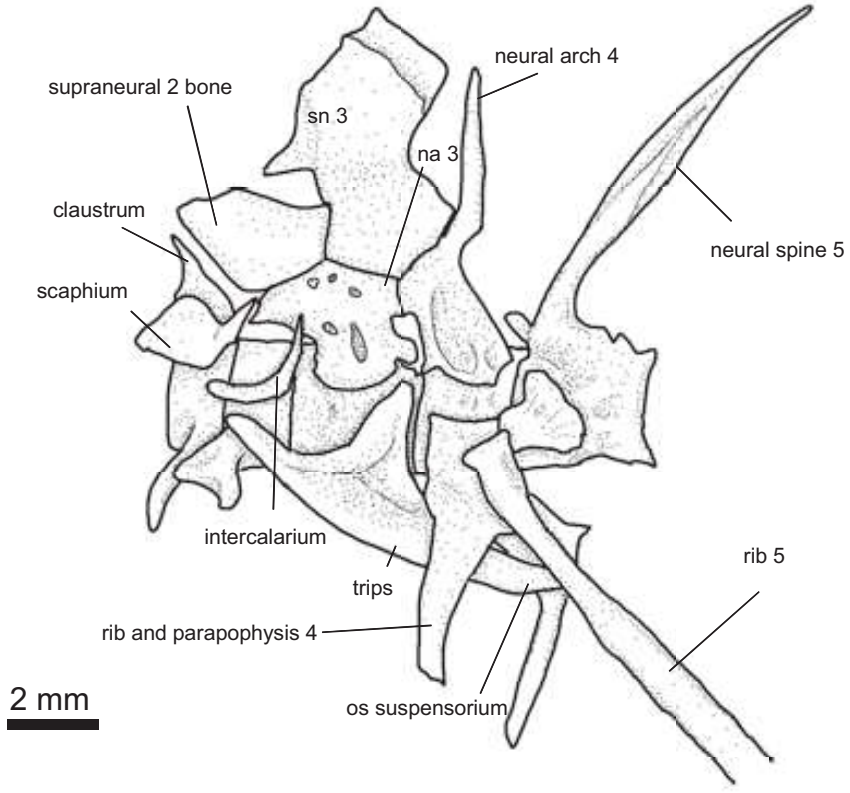
supraneural 2 bone
sn 3
neural arch 4
na 3
claustrum
neural spine 5
scaphium
intercalarium
rib 5
trips
rib and parapophysis 4
os suspensorium
2 mm

Plate 12-3

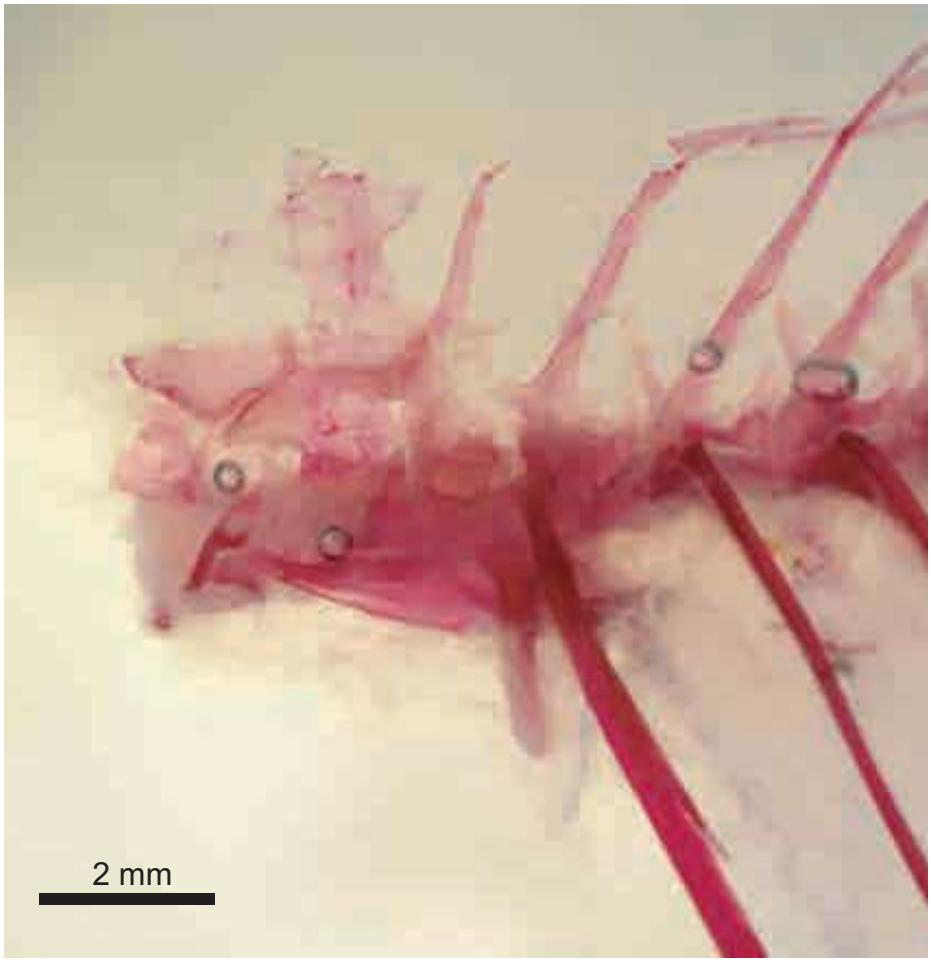
2 mm

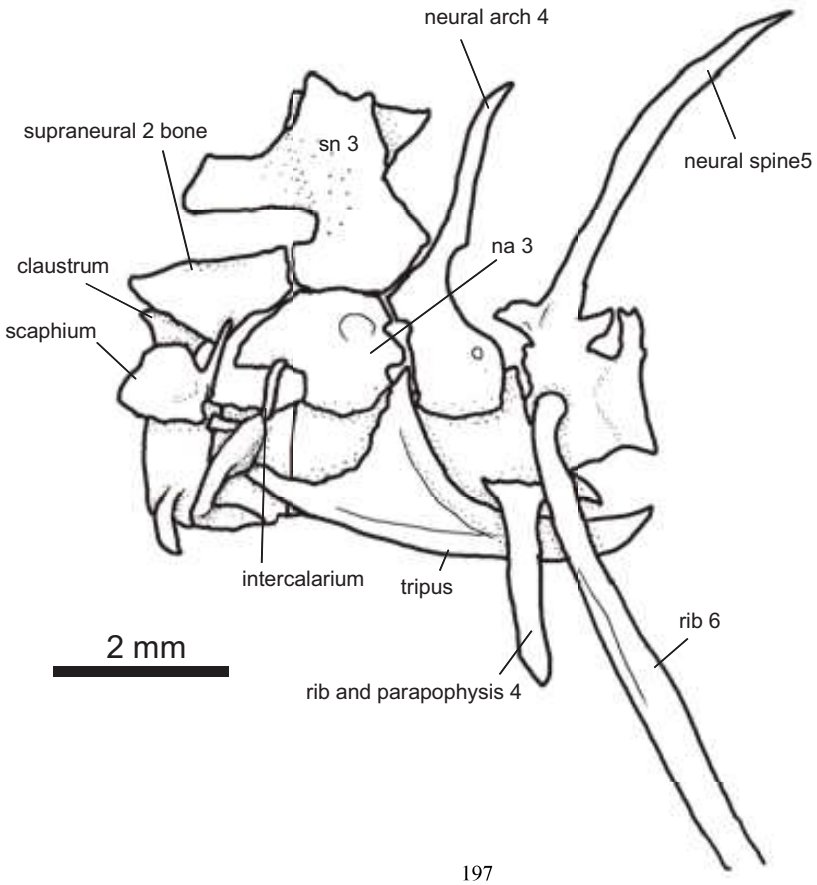
neural arch 4
supraneural 2 bone
sn 3
neural spine5
na 3
claustrum
scaphium
intercalarium
tripus
rib 6
2 mm
rib and parapophysis 4

Plate 12-4

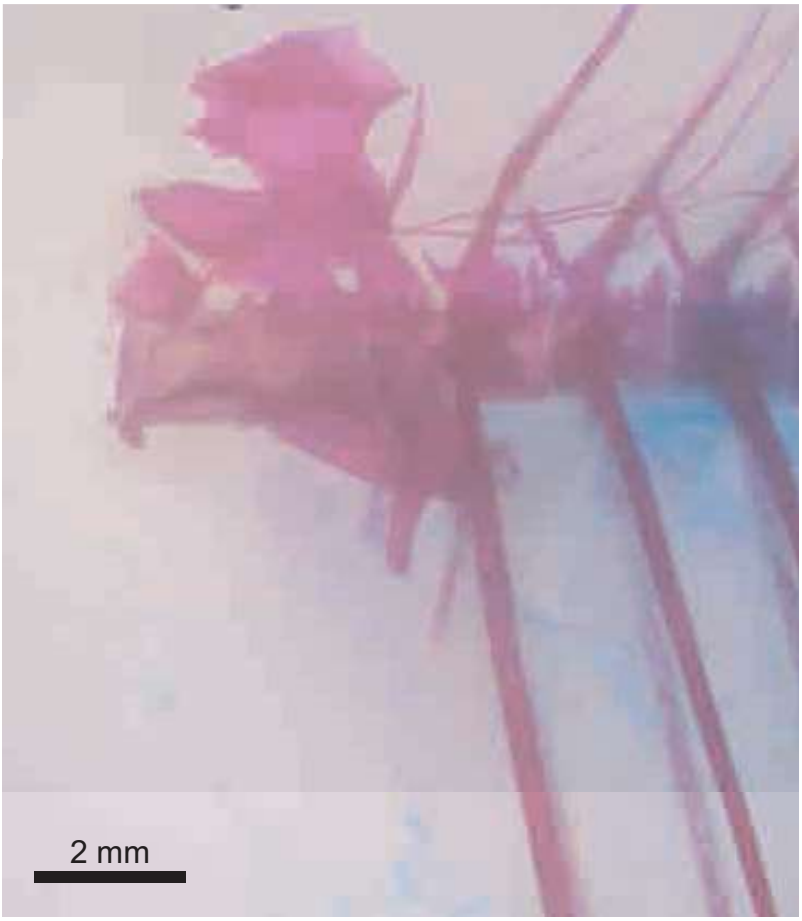
2 mm

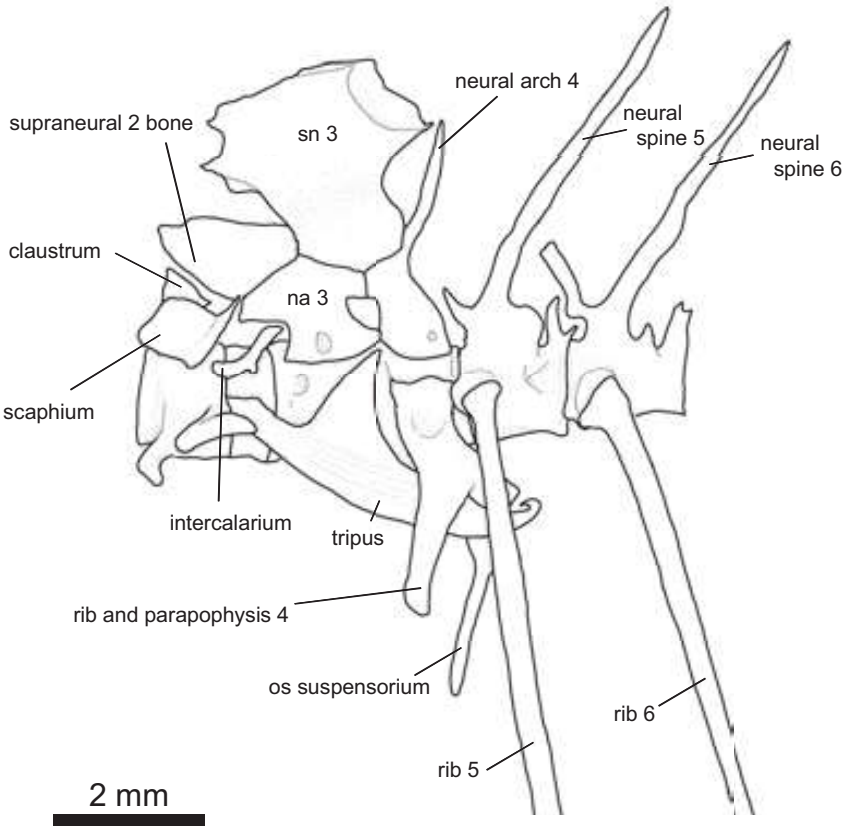
neural arch 4
supraneural 2 bone
sn 3
neural
spine 5
neural
spine 6
claustrum
na 3
scaphium
intercalarium
tripus
rib and parapophysis 4
os suspensorium
rib 6
rib 5
2 mm

Plate 12-5


2 mm

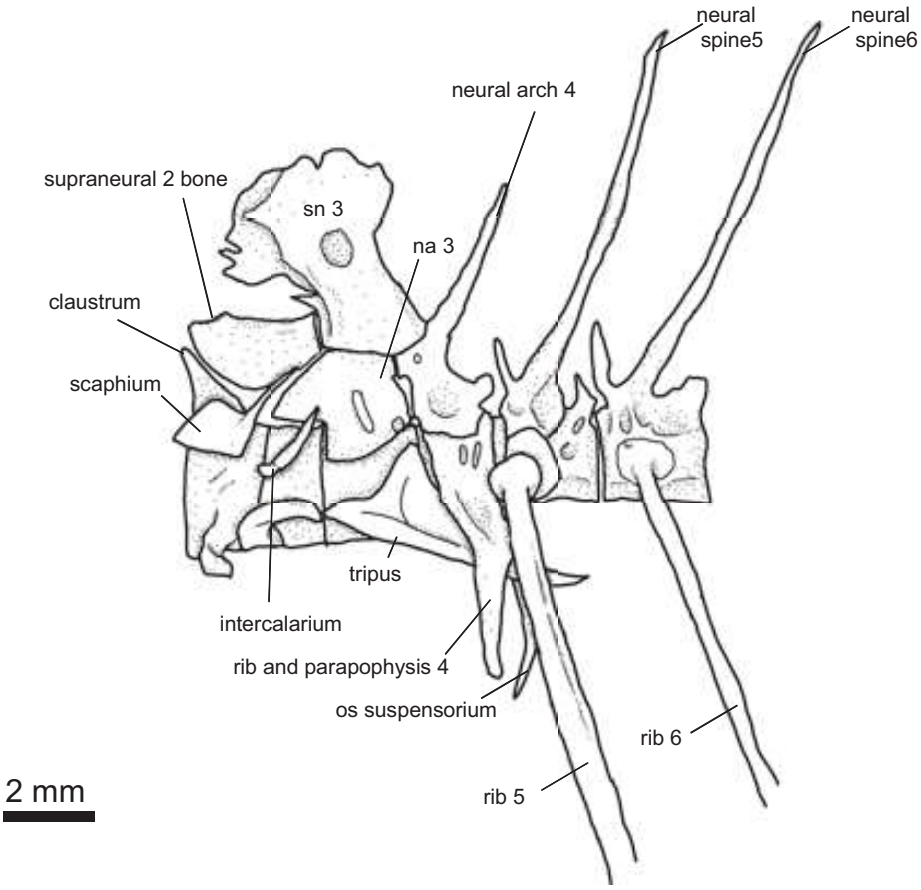
neural spine5
neural spine6
neural arch 4
supraneural 2 bone
sn 3
na 3
claustrum
scaphium
tripus
intercalarium
rib and parapophysis 4
os suspensorium
rib 6
rib 5
2 mm

Plate 12-6

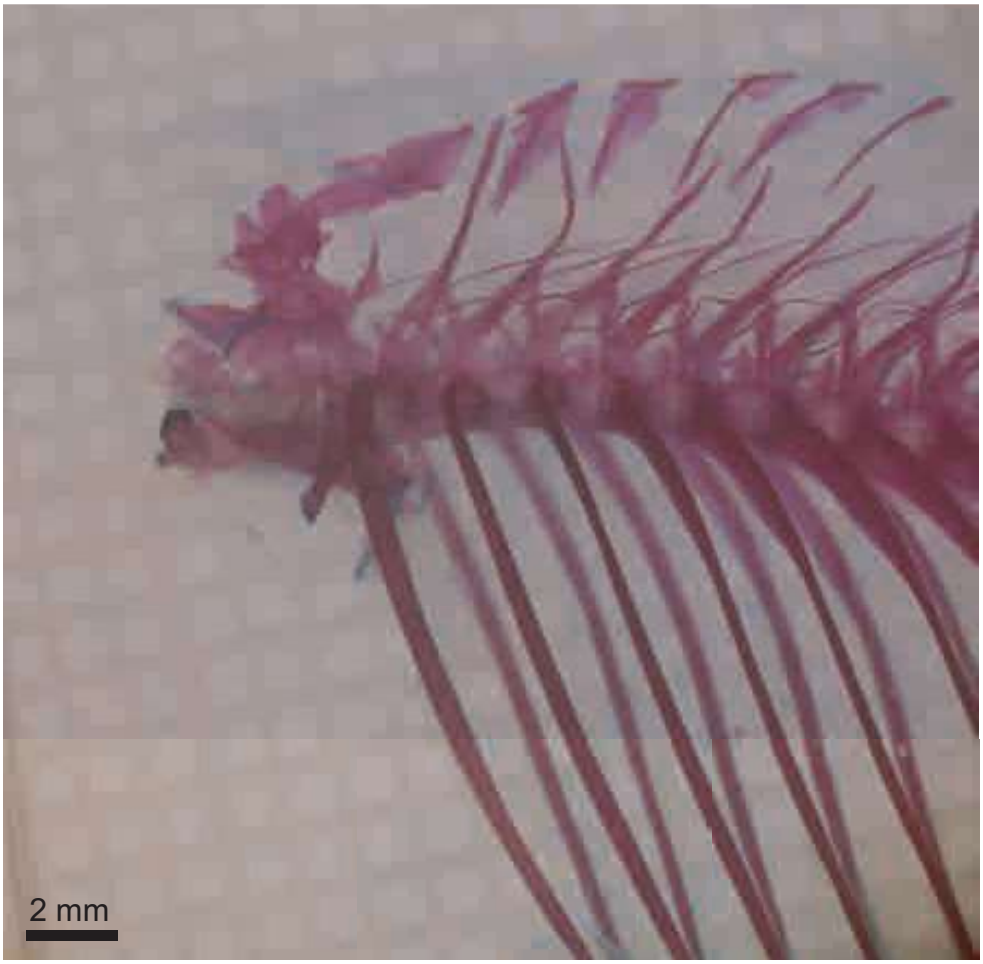
2 mm

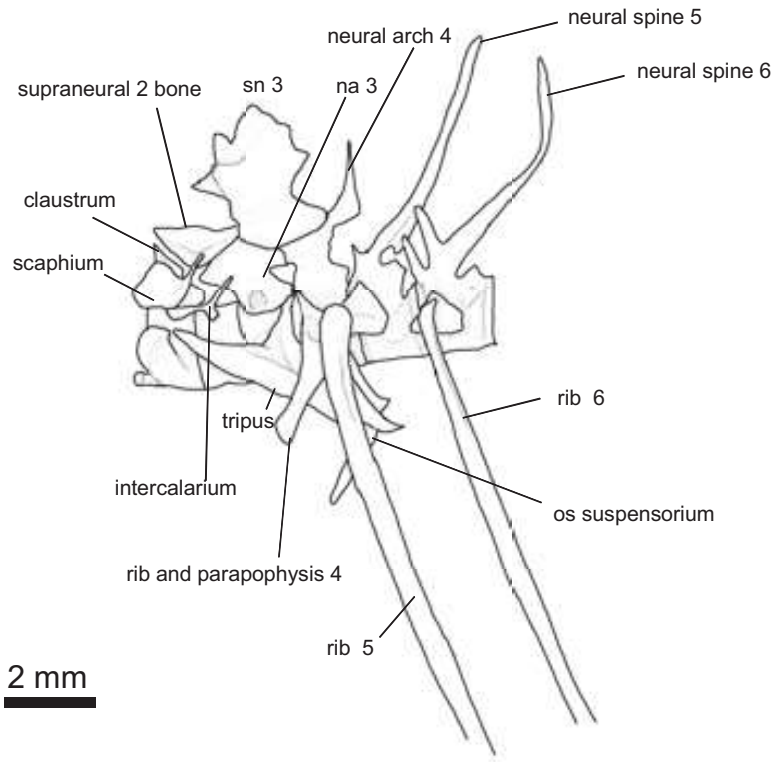
neural spine 5
neural arch 4
neural spine 6
supraneural 2 bone
sn 3
na 3
claustrum
scaphium
rib 6
tripus
intercalarium
os suspensorium
rib and parapophysis 4
rib 5
2 mm

Plate 12-7

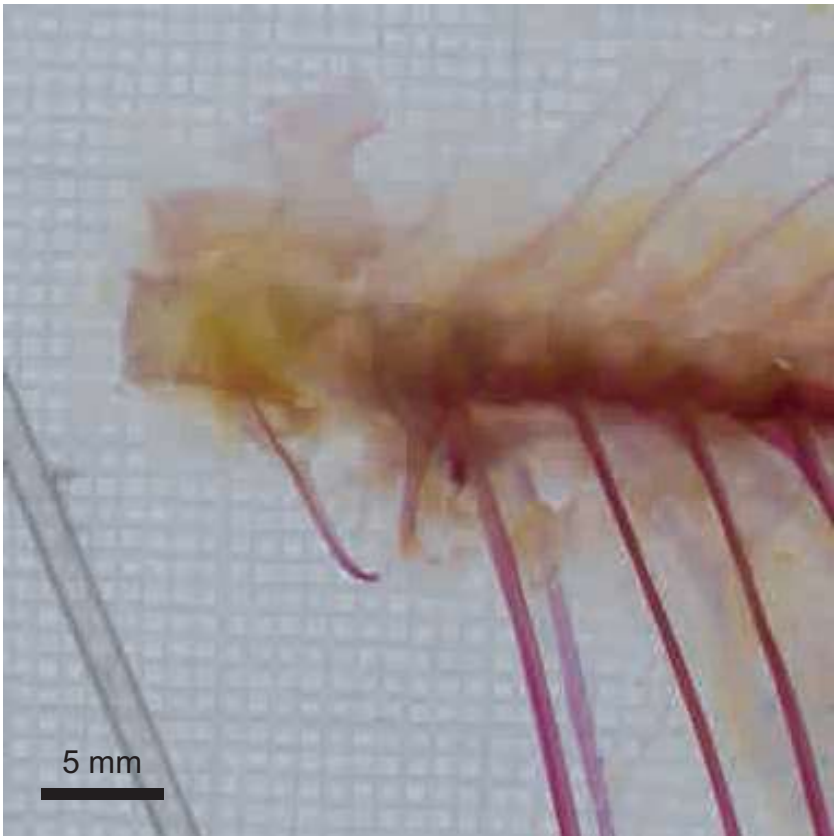
5 mm

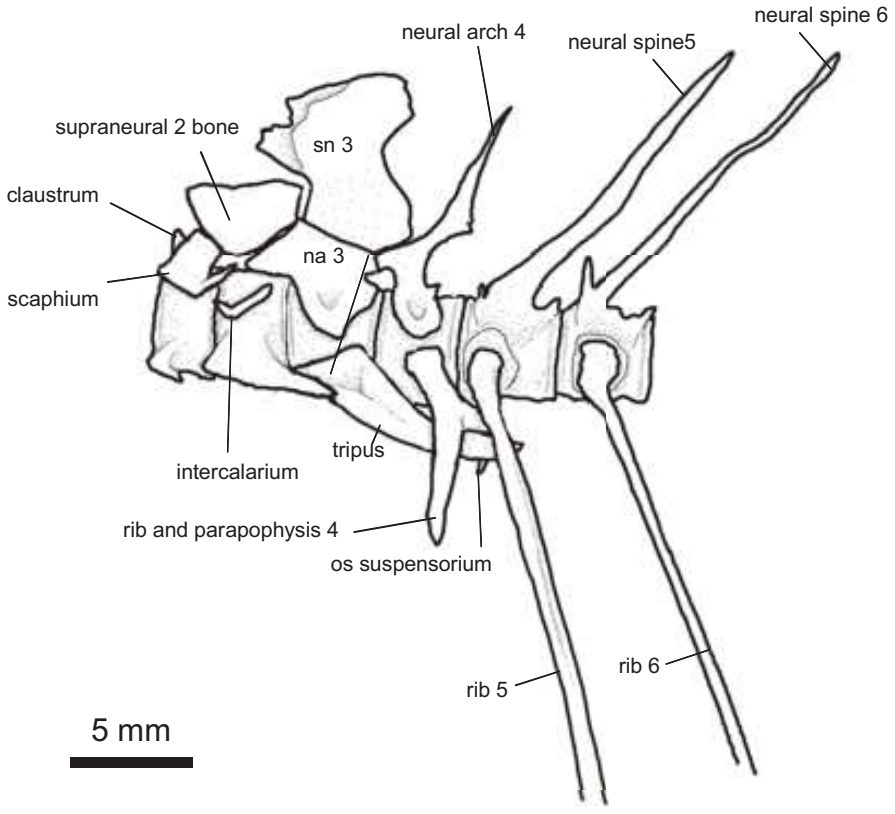
neural arch 4
neural spine5
neural spine 6
supraneural 2 bone
sn 3
claustrum
na 3
scaphium
tripus
intercalarium
rib and parapophysis 4
os suspensorium
rib 5
rib 6
5 mm

Plate 12-8

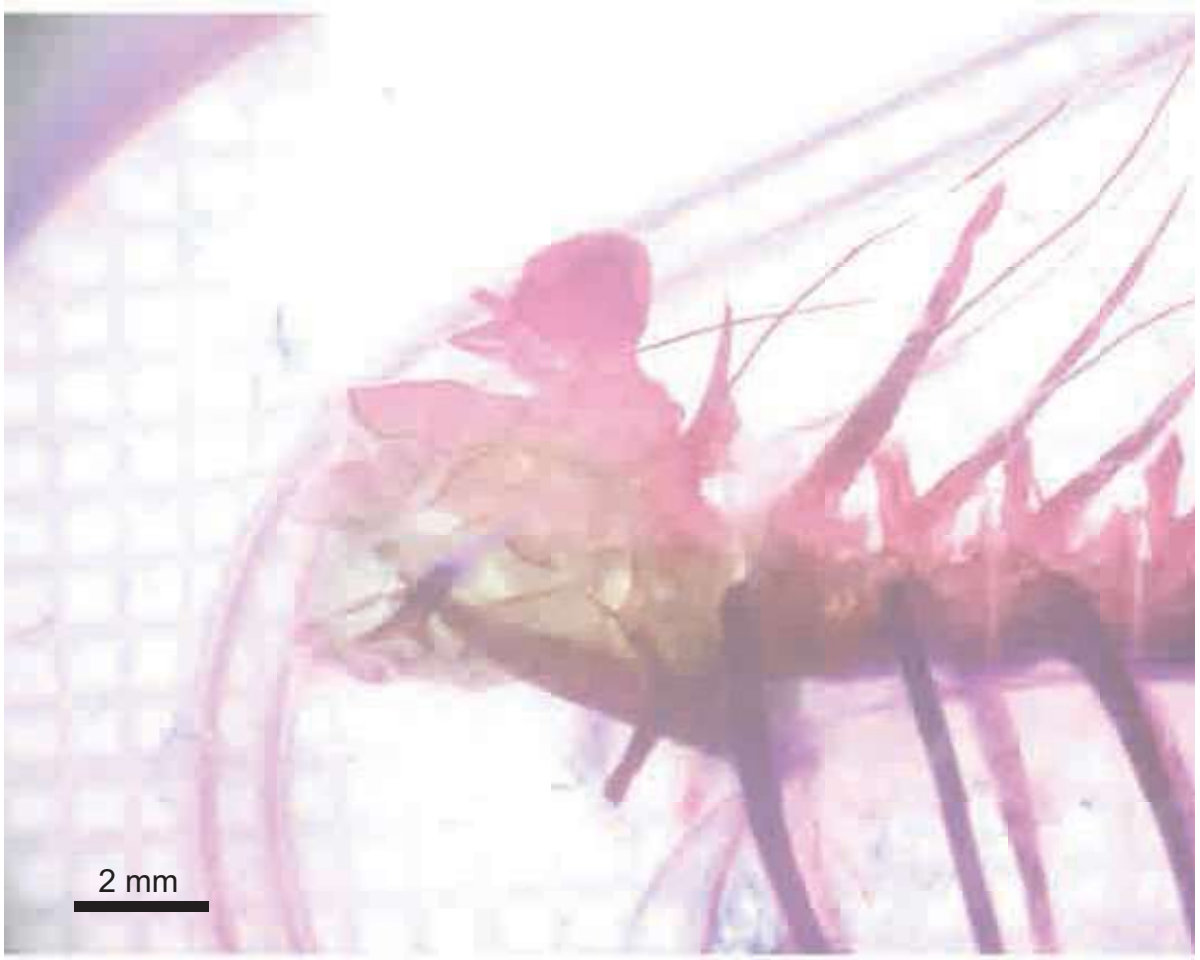
2 mm

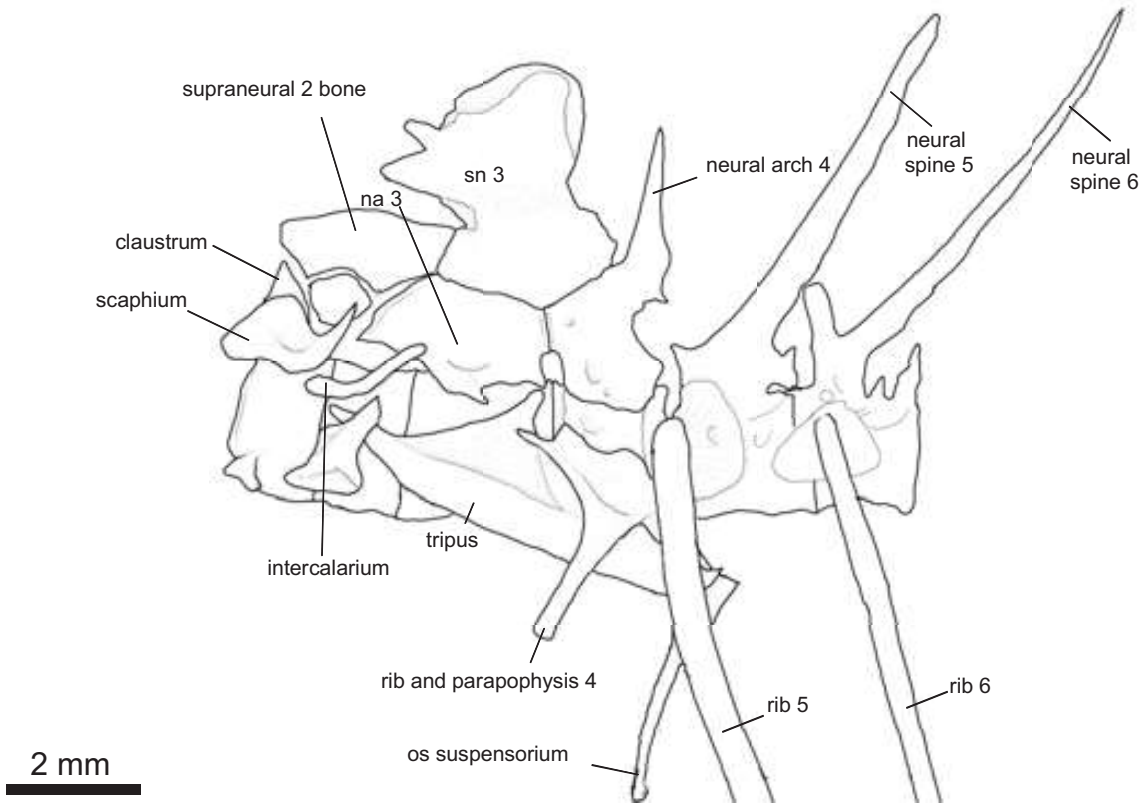
supraneural 2 bone
sn 3
na 3
neural arch 4
neural spine 5
neural spine 6
claustrum
scaphium
tripus
intercalarium
rib and parapophysis 4
rib 5
rib 6
os suspensorium
2 mm

Plate 12-9

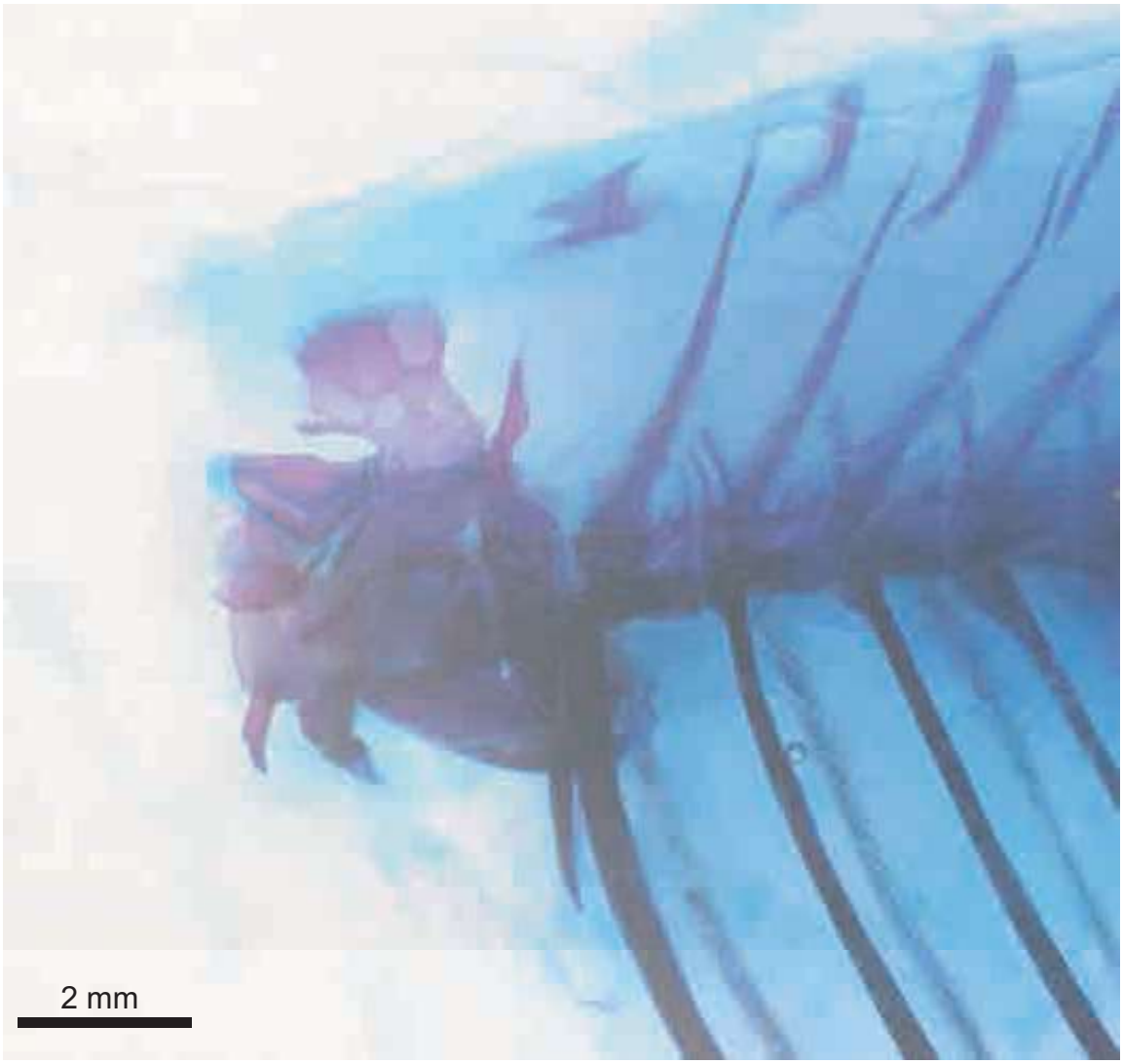
2 mm

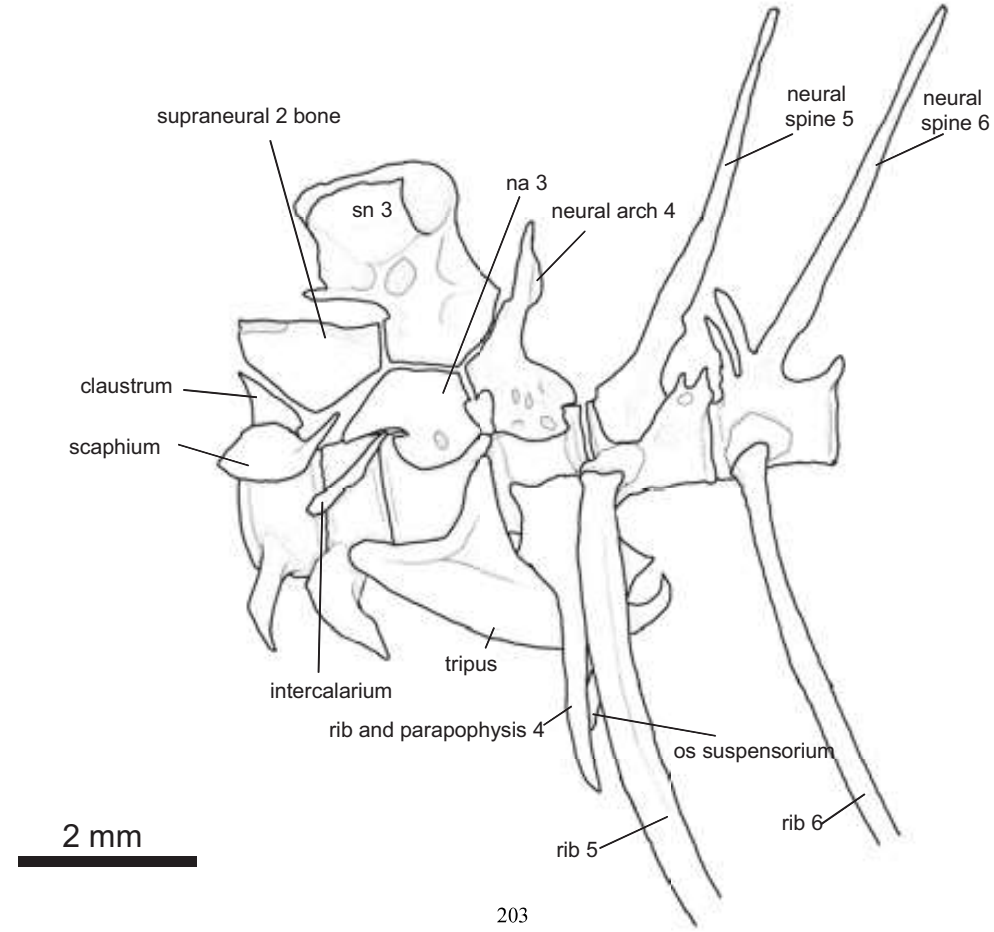
supraneural 2 bone
sn 3
na 3
neural arch 4
neural spine 5
neural spine 6
claustrum
scaphium
tripus
intercalarium
rib and parapophysis 4
os suspensorium
rib 6
rib 5
2 mm

Plate 13-1

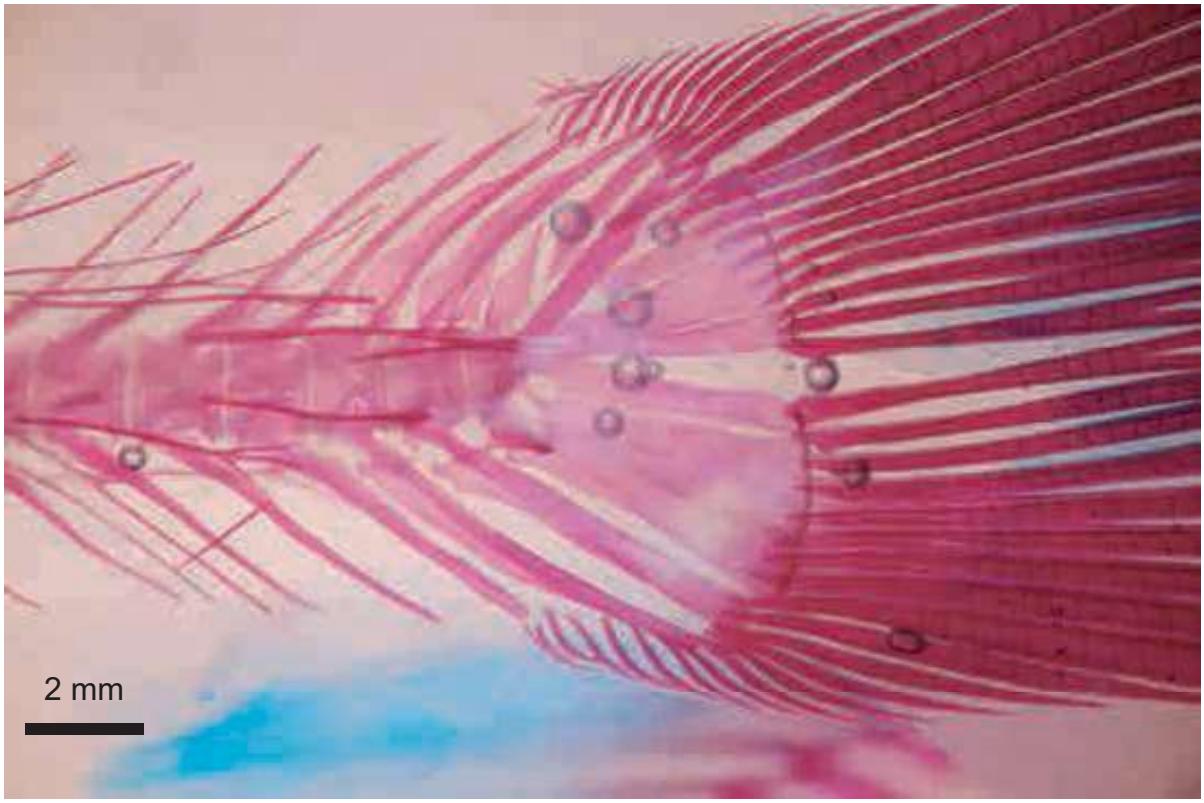
2 mm

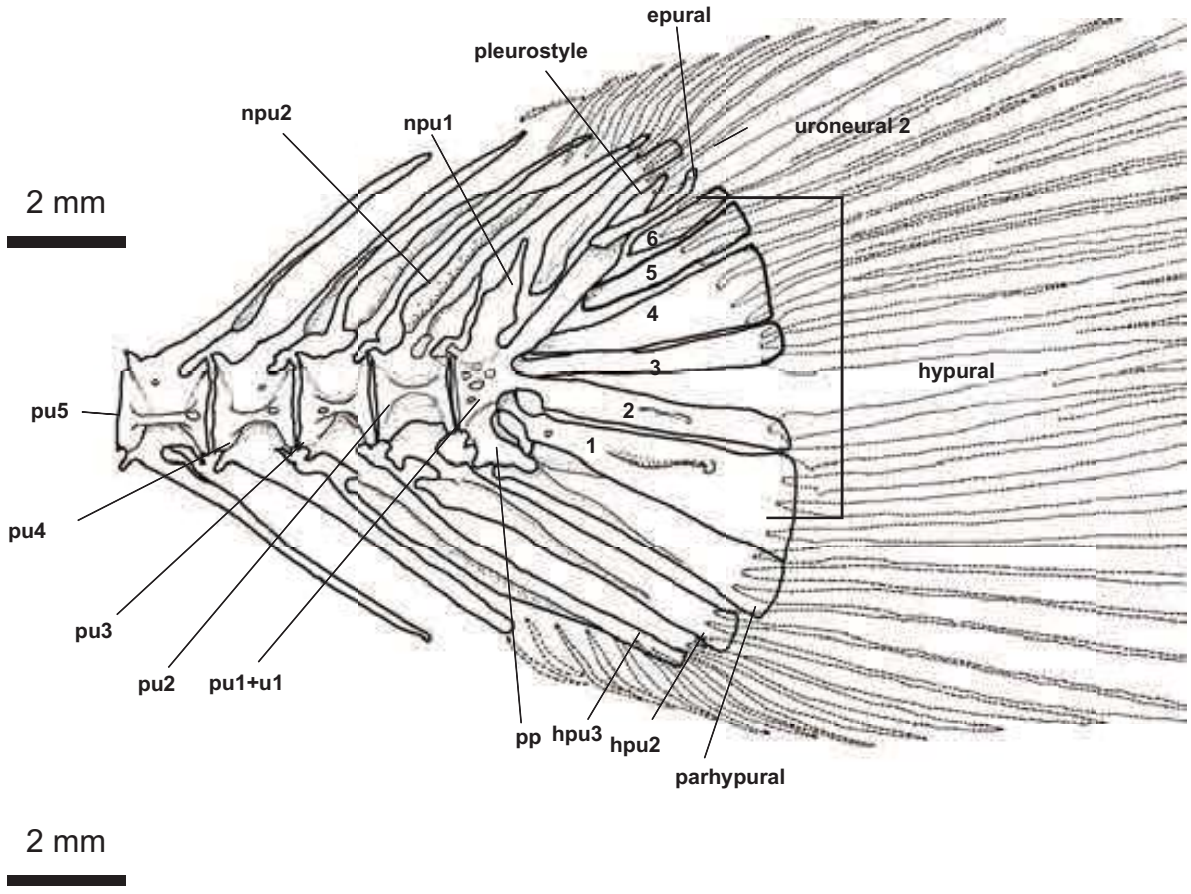
epural
pleurostyle
npu2
npu1
uroneural 2
2 mm
6
5
4
3
hypural
pu5
2
1
pu4
pu3
pu2
pu1+u1
pp
hpu3
hpu2
parhypural
2 mm

Plate 13-2

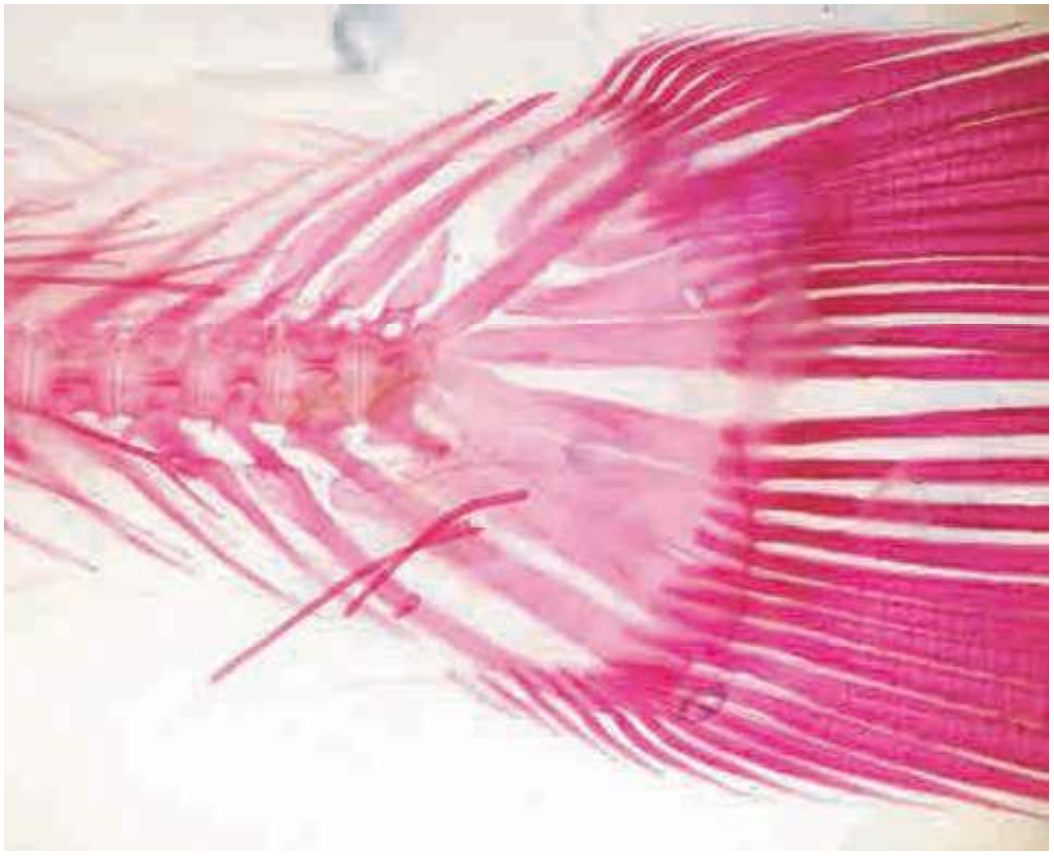

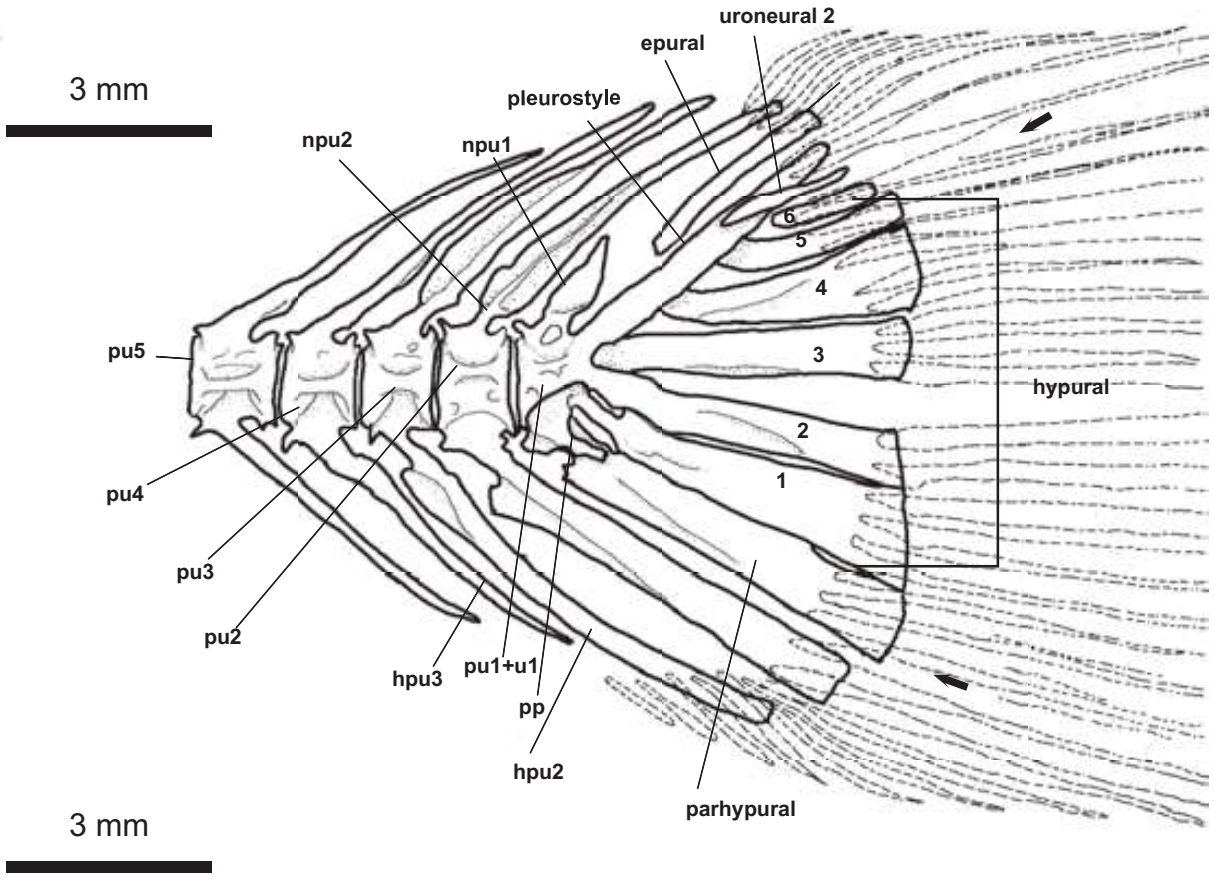
3 mm
uroneural 2
epural
pleurostyle
npu2
npu1
6
5
4
3
hypural
2
1
pu5
pu4
pu3
pu2
hpu3
pu1+u1
pp
hpu2
parhypural
3 mm

Plate 13-3

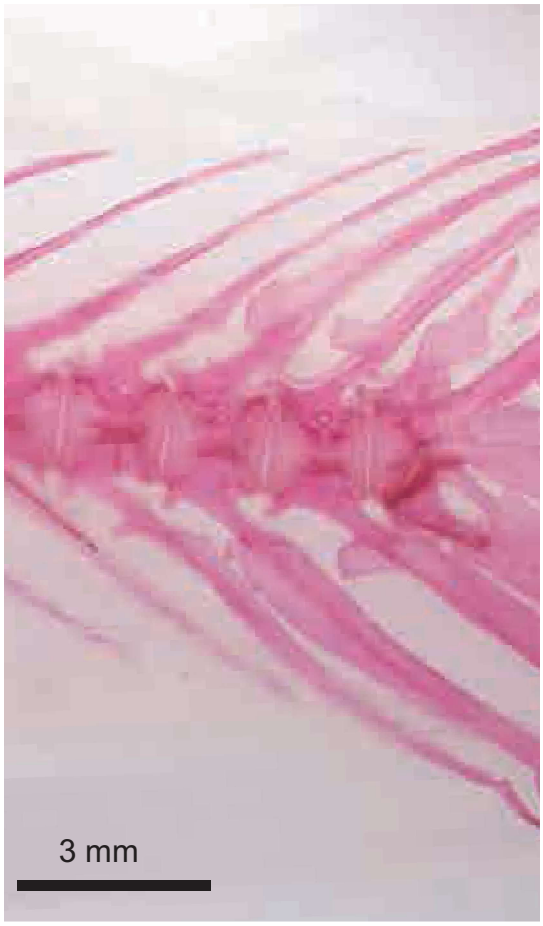
3 mm

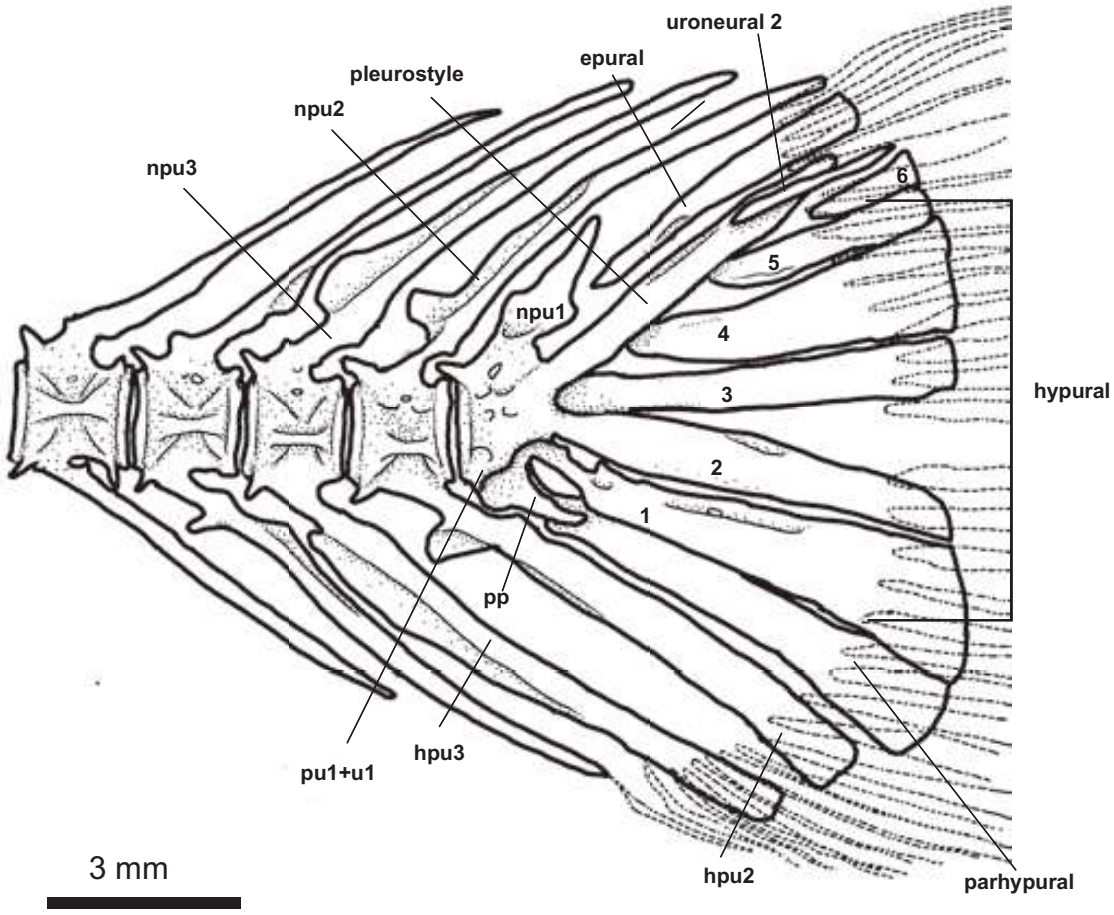
uroneural 2
epural
pleurostyle
npu2
npu3
6
5
npu1
4
3
hypural
2
1
pp
pu1+u1
hpu3
hpu2
parhypural
3 mm

Plate 13-4

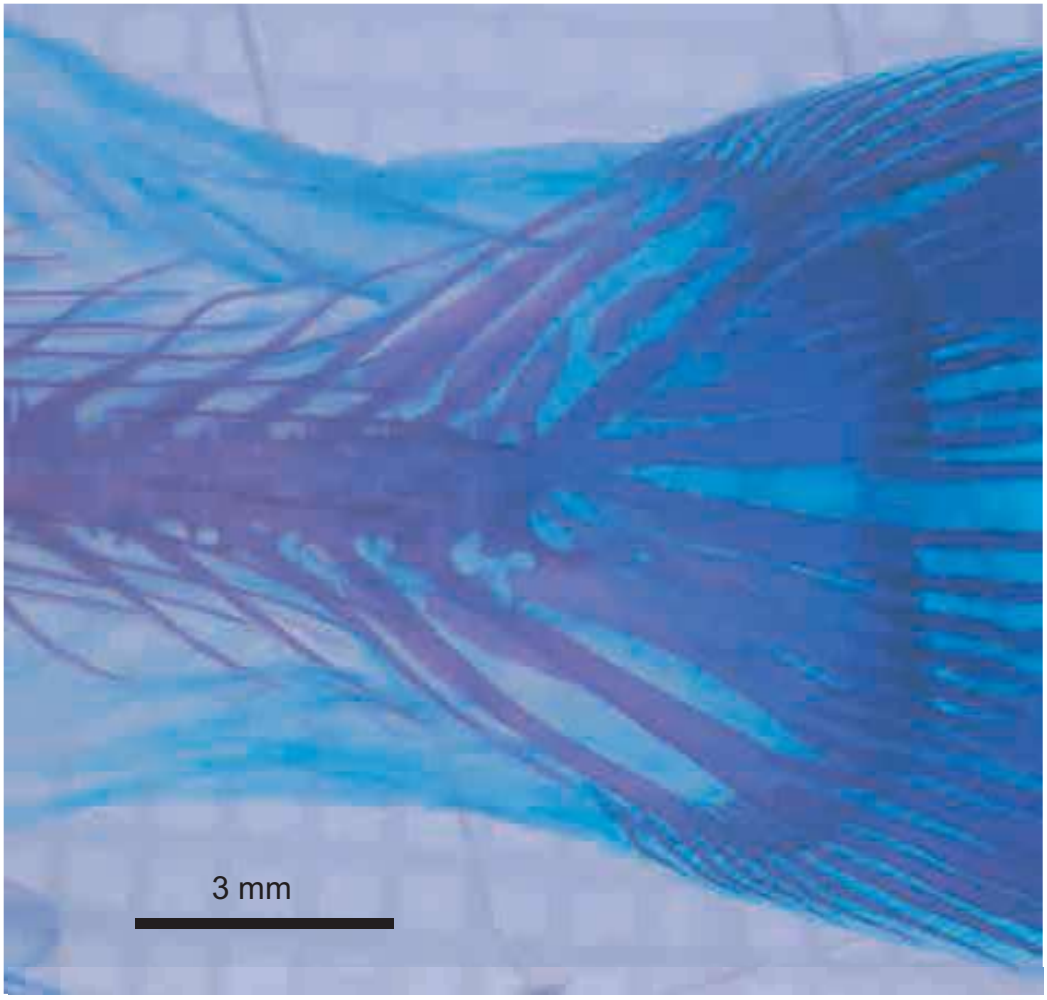
3 mm

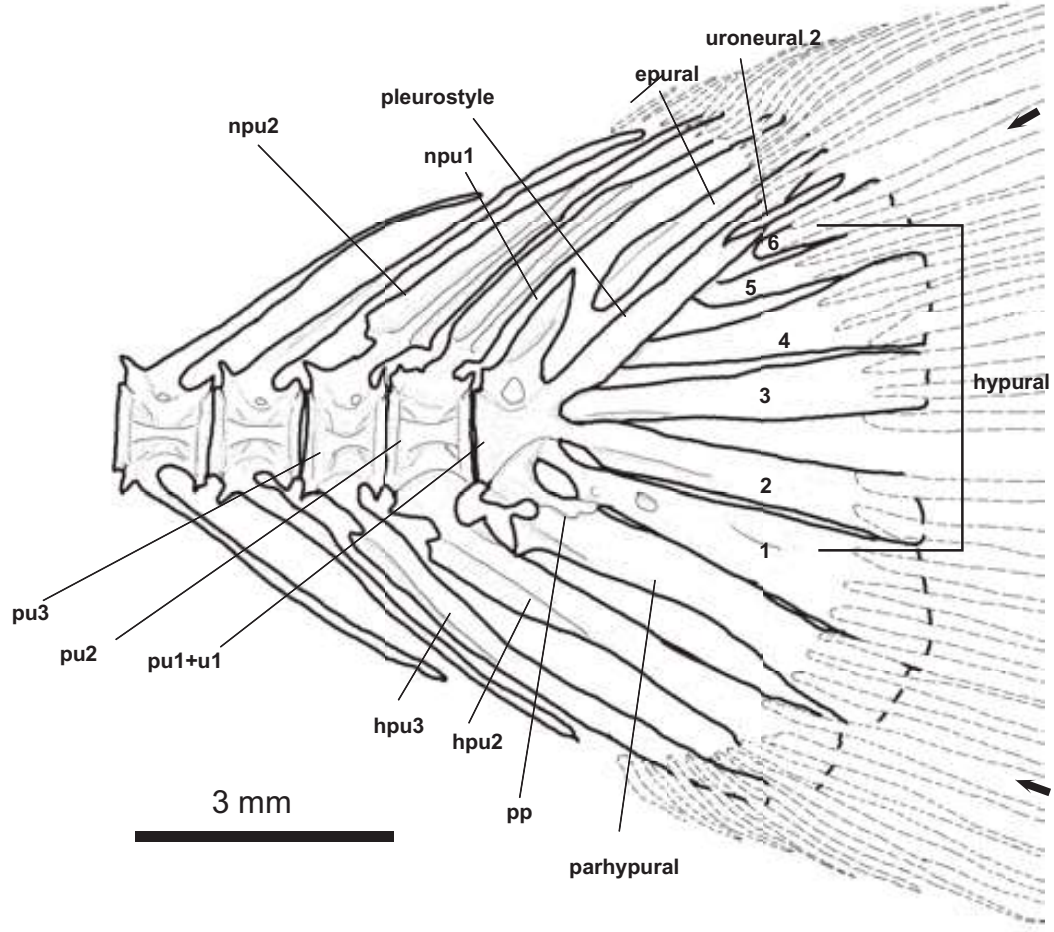
uroneural 2
epural
pleurostyle
npu2
npu1
6
5
4
3
2
1
hypural
pu3
pu2
pu1+u1
hpu3
hpu2
pp
parhypural
3 mm

Plate 13-5

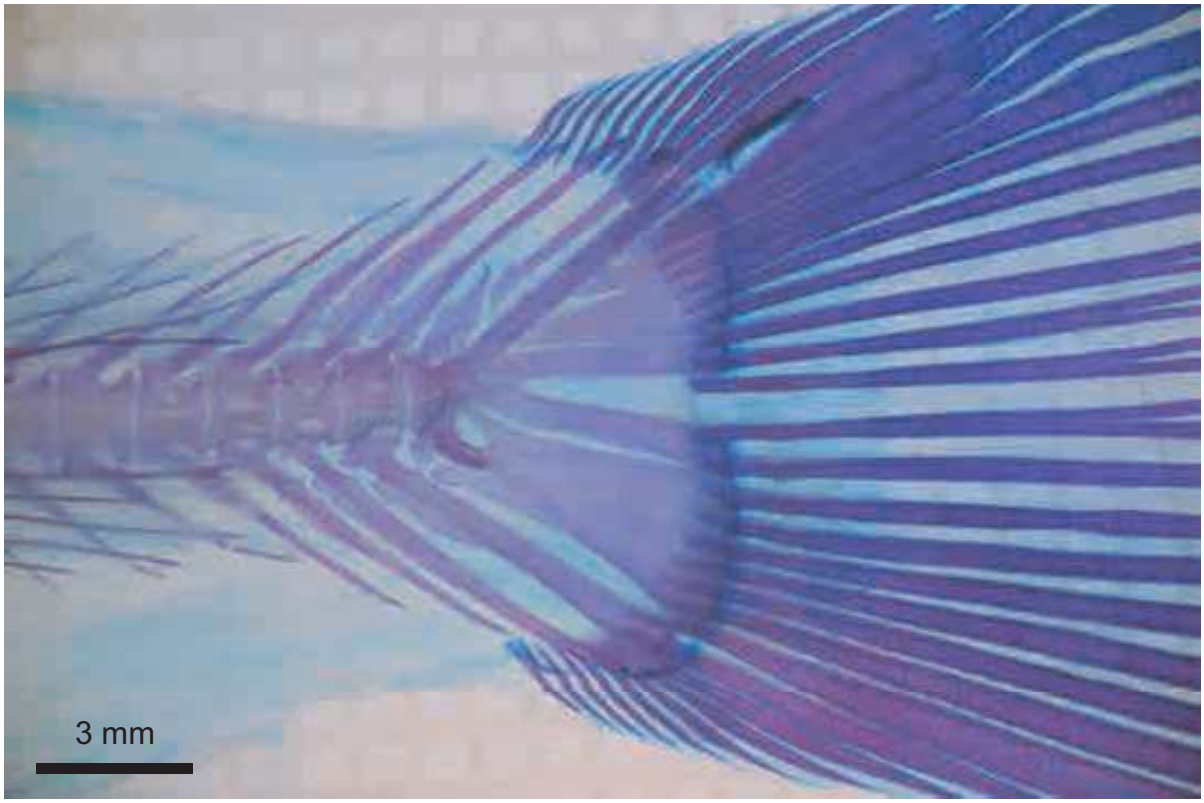
3 mm

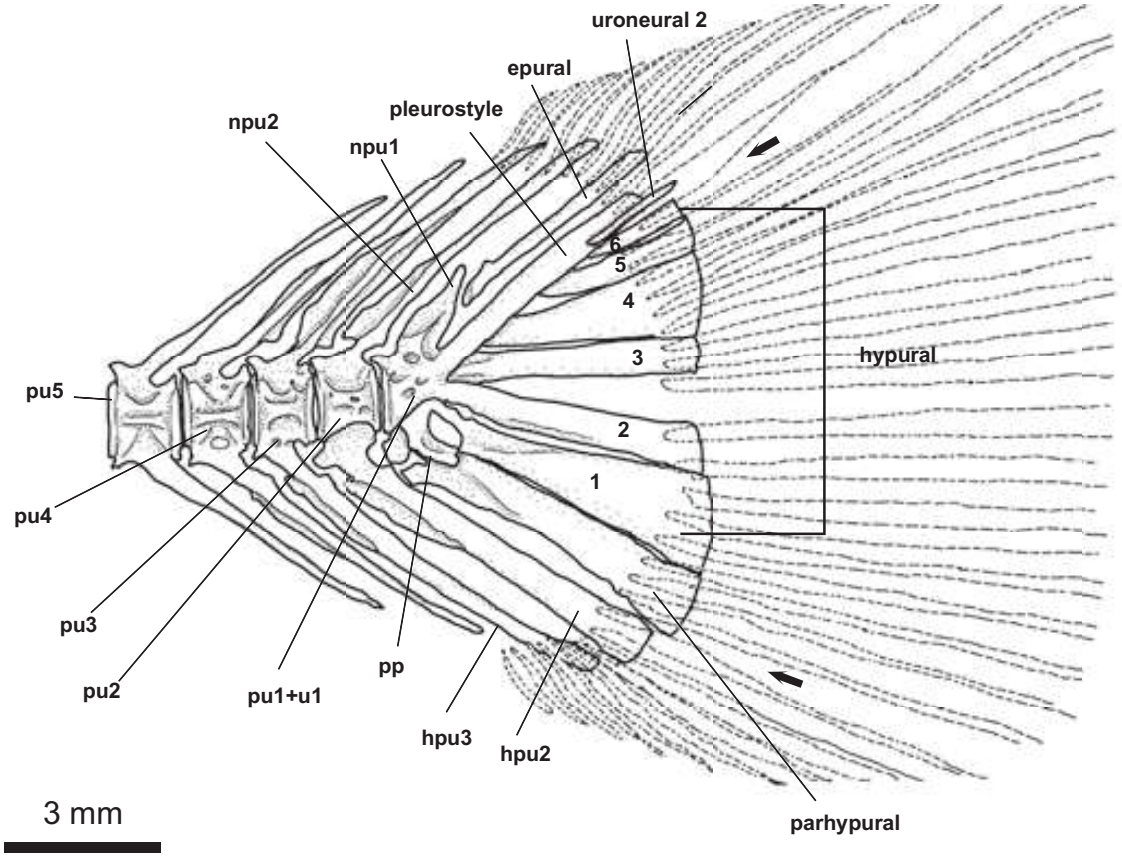
uroneural 2
epural
pleurostyle
npu2
npu1
6
5
4
3
2
1
hypural
pu5
pu4
pu3
pu2
pu1+u1
pp
hpu3
hpu2
parhypural
3 mm

Plate 13-6

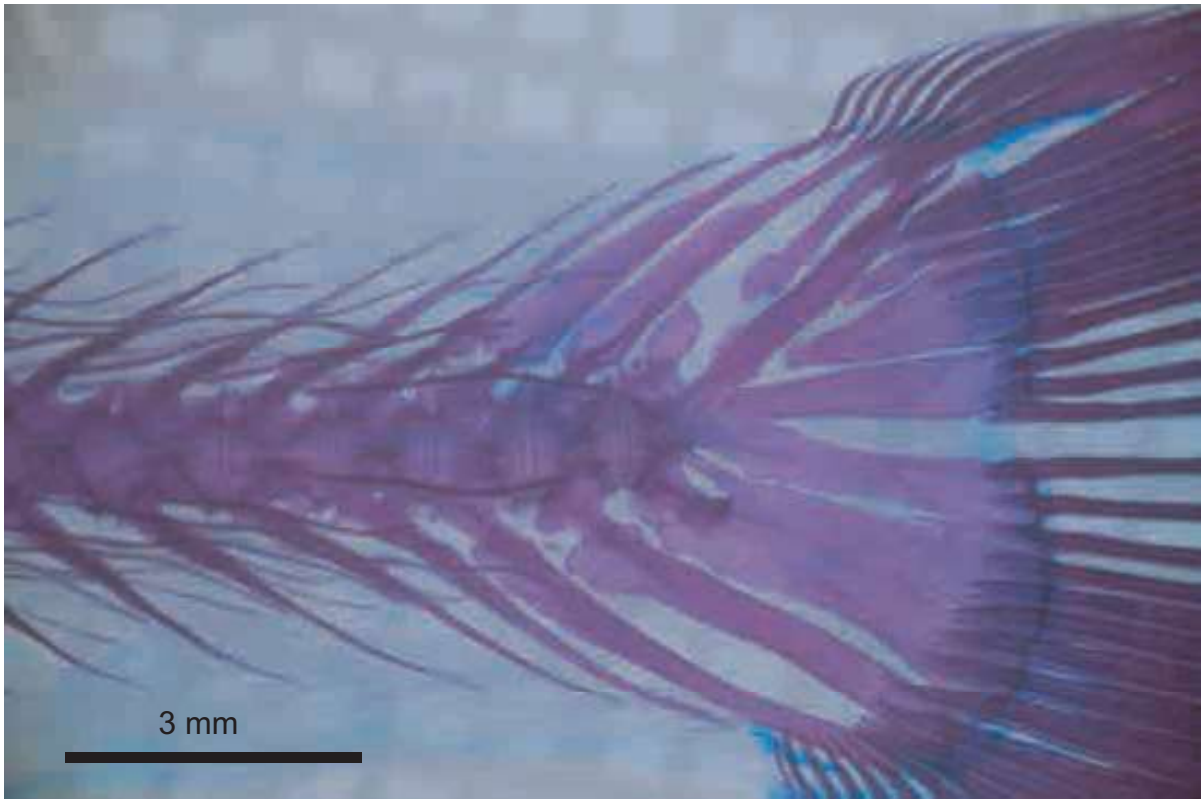
3 mm

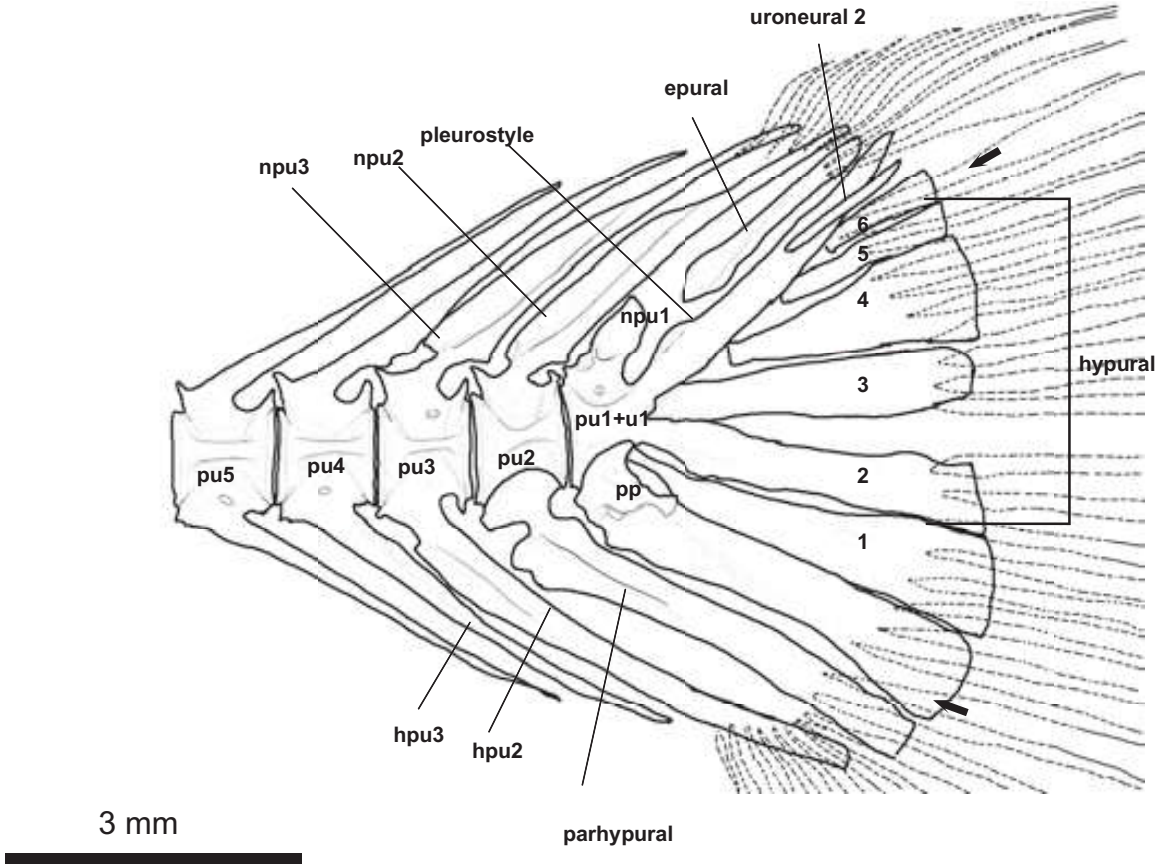
uroneural 2
epural
pleurostyle
npu3
npu2
npu1
6
5
4
hypural
3
pu1+u1
pu5
pu4
pu3
pu2
pp
2
1
hpu3
hpu2
parhypural
3 mm

Plate 13-7


3 mm

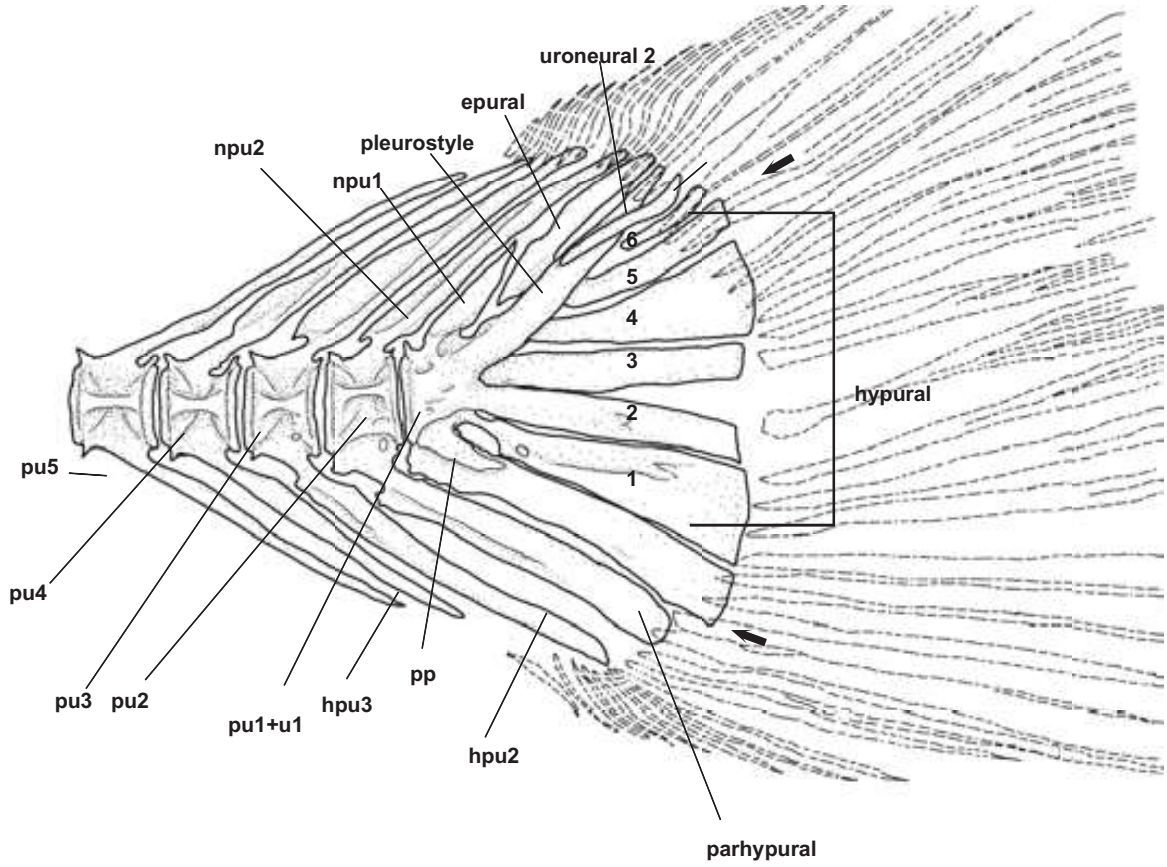
uroneural 2
epural
pleurostyle
npu2
npu1
7
6
5
4
3
2
1
hypural
pu5
pu4
pu3
pu2
pu1+u1
hpu3
pp
hpu2
parhypural
3 mm

Plate 13-8


3 mm

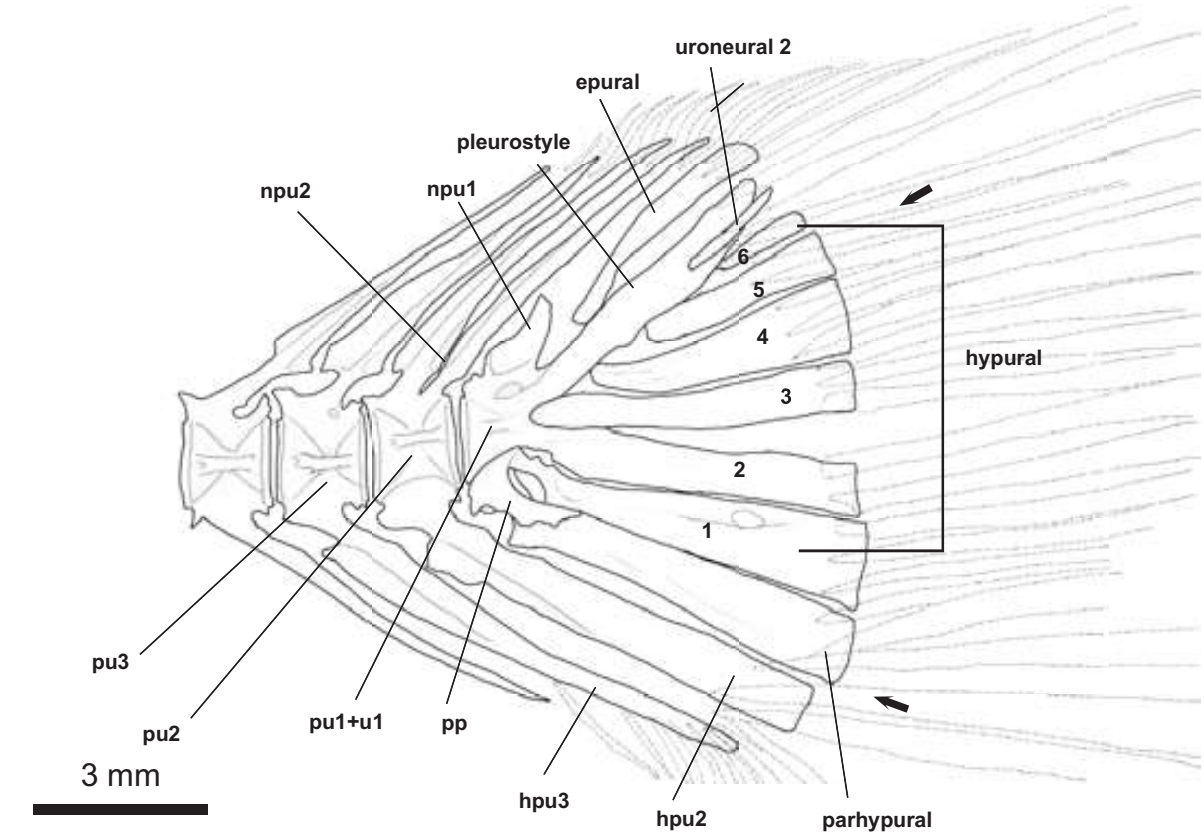
uroneural 2
epural
pleurostyle
npu2
npu1
6
5
4
3
2
1
hypural
pu3
pu2
pu1+u1
pp
hpu3
hpu2
parhypural
3 mm

Plate 12-9

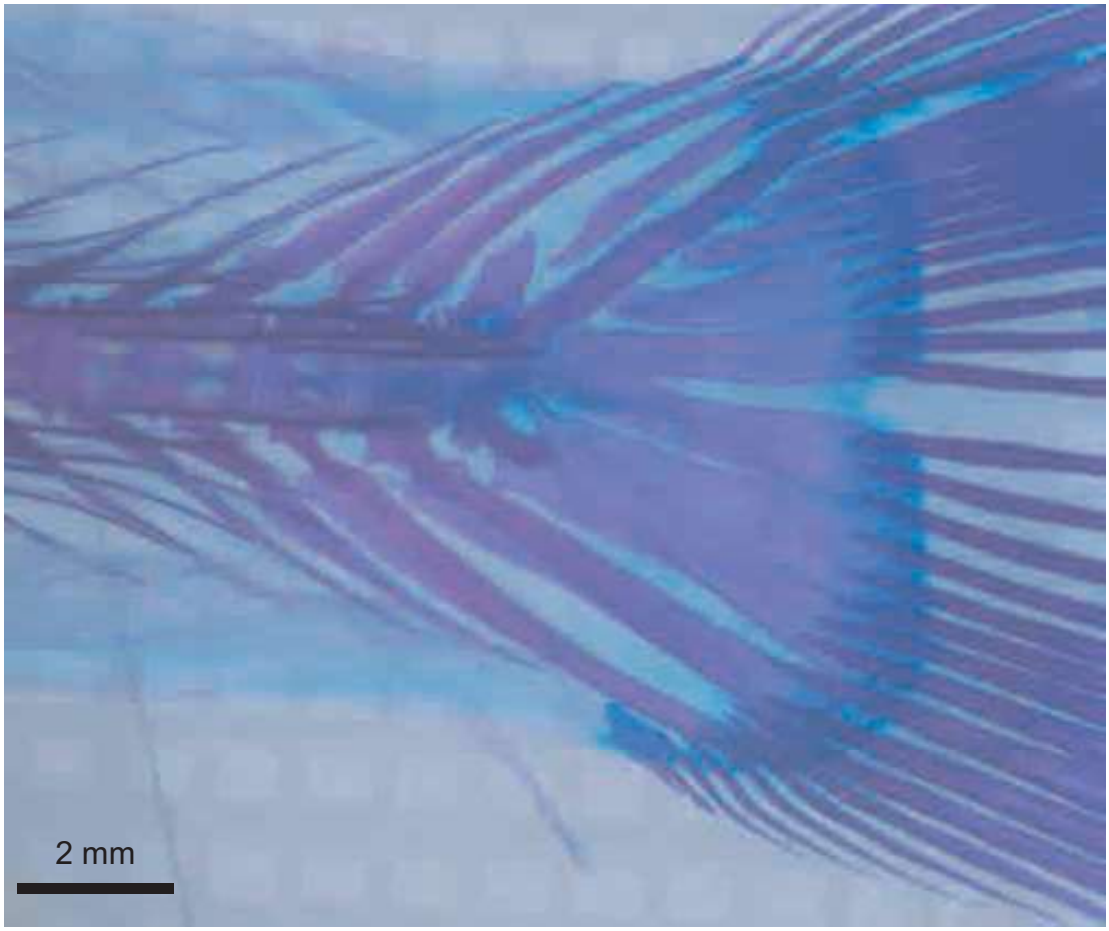
2 mm

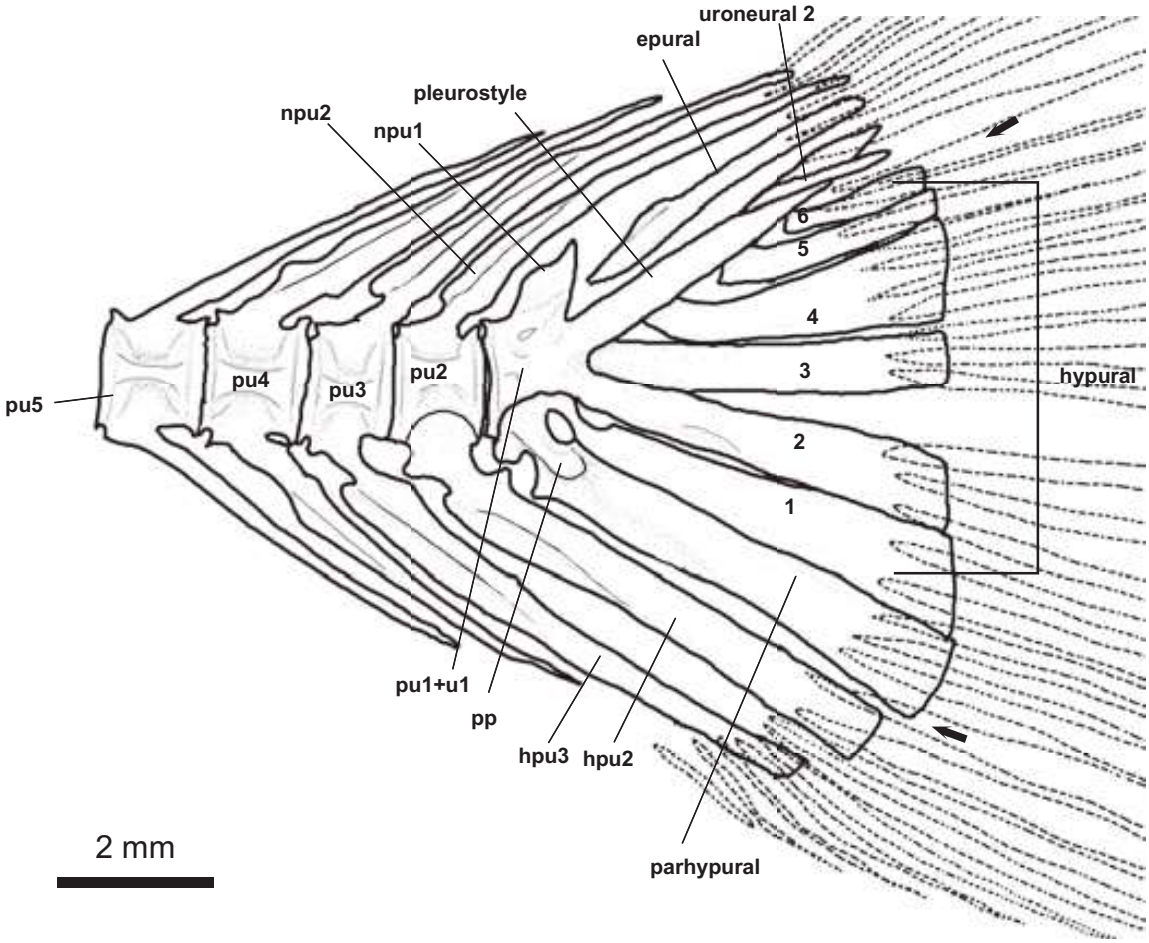
uroneural 2
epural
pleurostyle
npu2
npu1
6
5
4
3
2
1
hypural
pu5
pu4
pu3
pu2
pu1+u1
pp
hpu3
hpu2
parhypural
2 mm

Plate 14-1

supraneural bone

5 mm

Plate 14-2

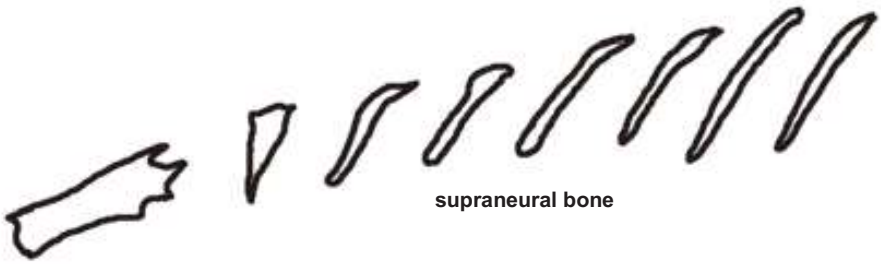

2 mm

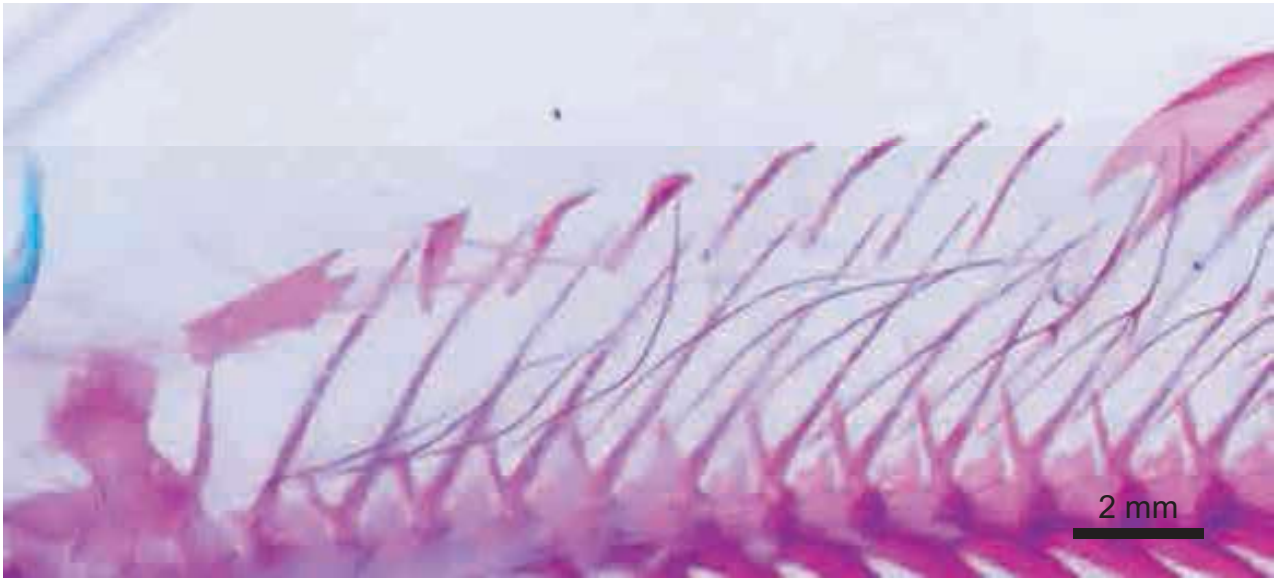

Plate 14-3

supraneural bone

3 mm

Plate 14-4

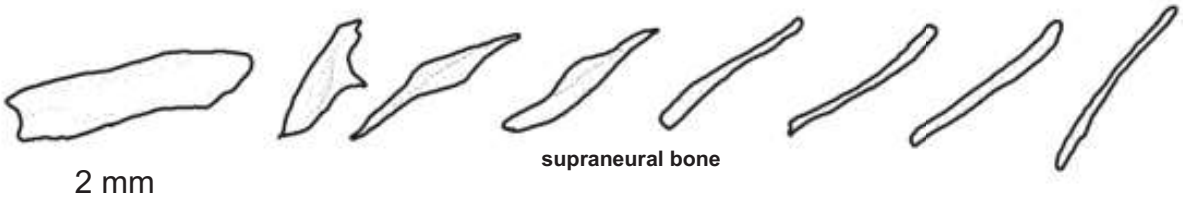

supraneural bone

2 mm

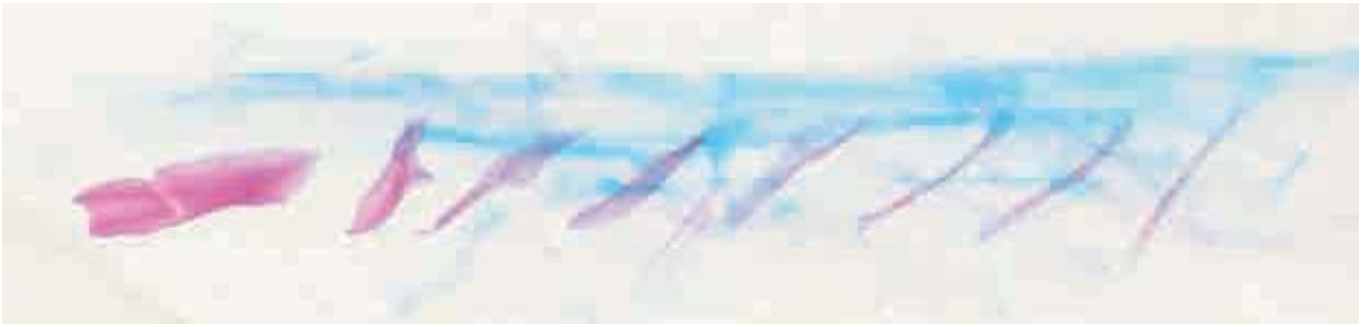

2 mm

Plate 14-5

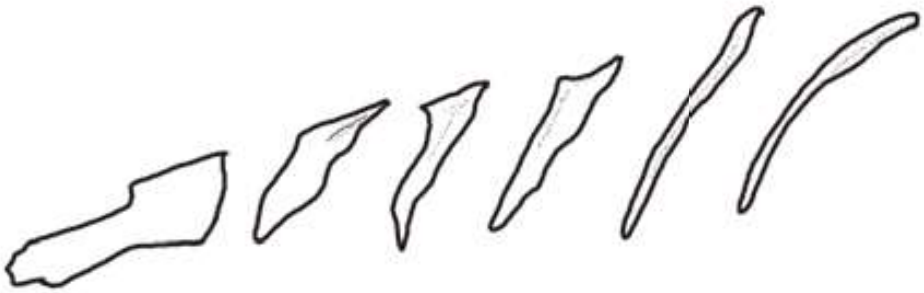

supraneural bone

2 mm

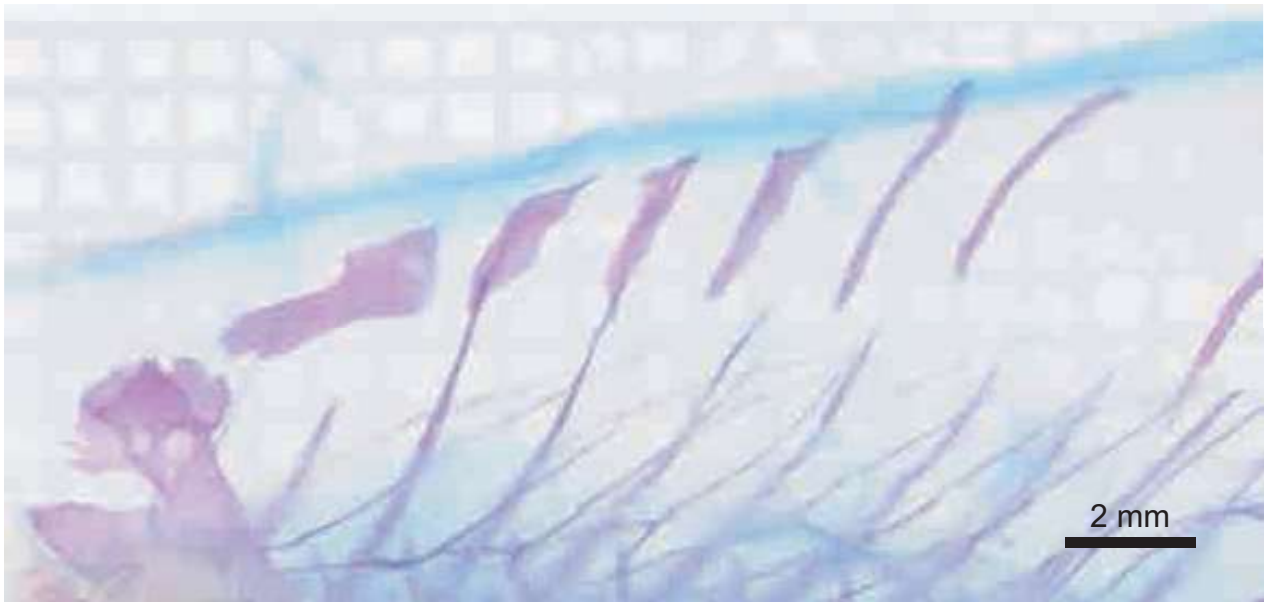

Plate 14-6

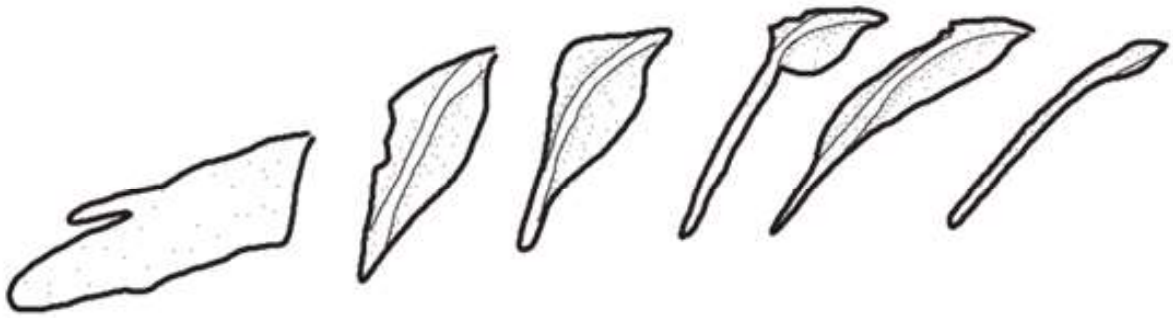

supraneural bone

2 mm

Plate 14-7

supraneural bone

1 cm

1 cm

Plate 14-8

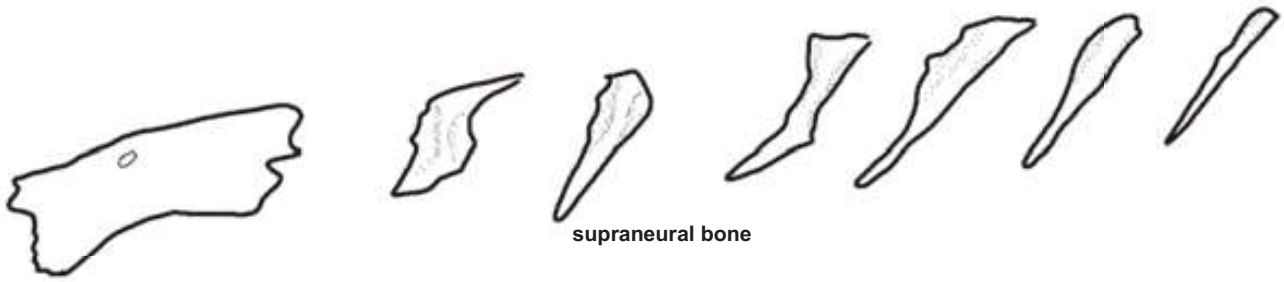

2 mm

2 mm

Plate 14-9

2 mm

supraneural bone

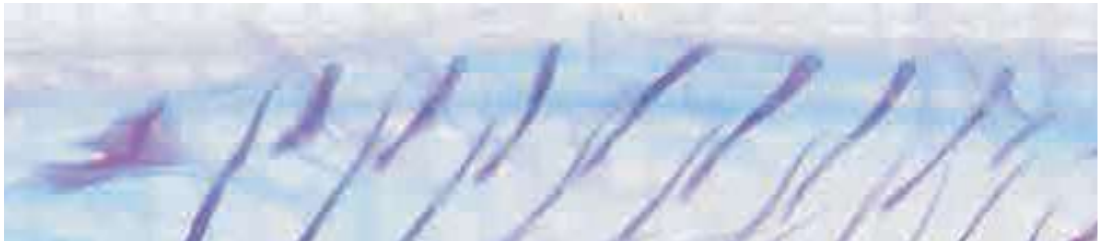

2 mm

Plate 15-1

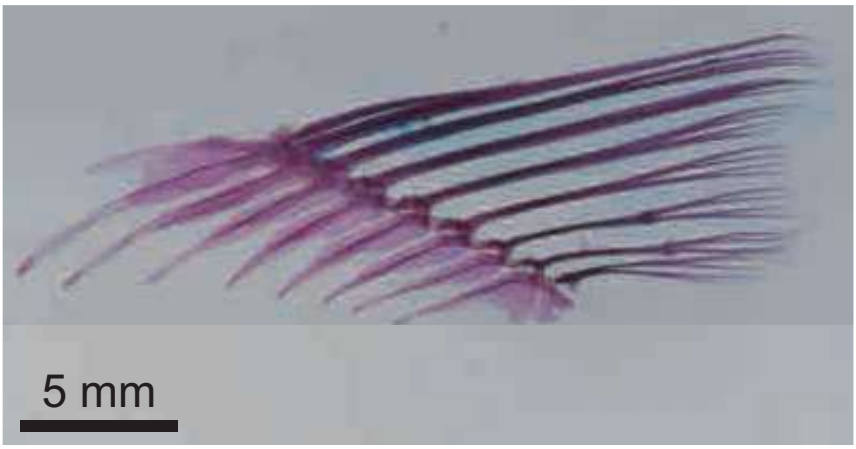
5 mm

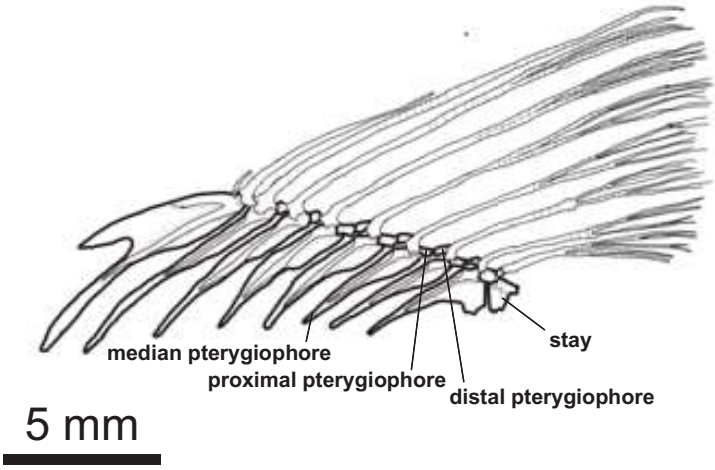
median pterygiophore
proximal pterygiophore
stay
distal pterygiophore
5 mm

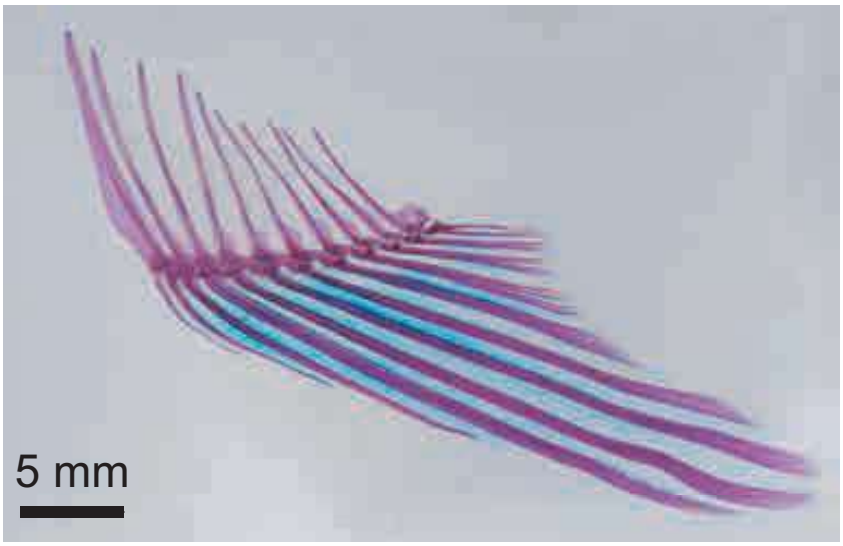
5 mm

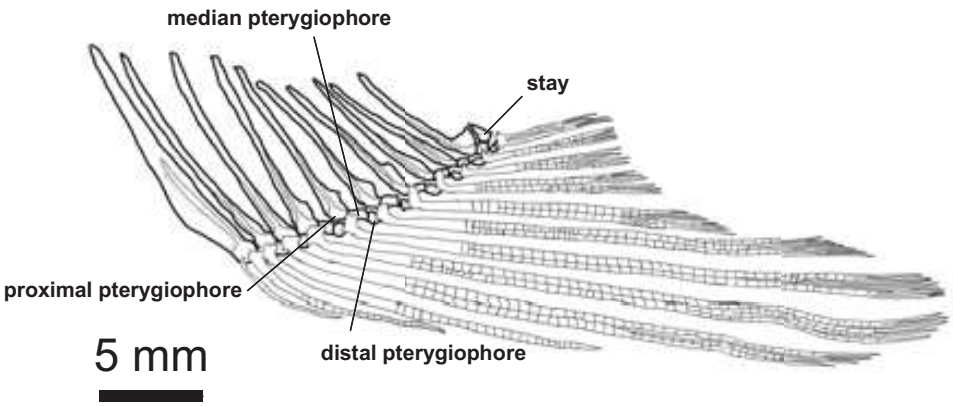
median pterygiophore
stay
proximal pterygiophore
distal pterygiophore
5 mm

Plate 15-2

A

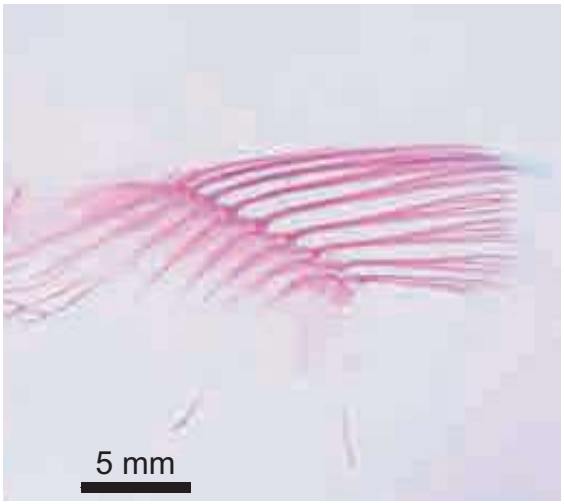

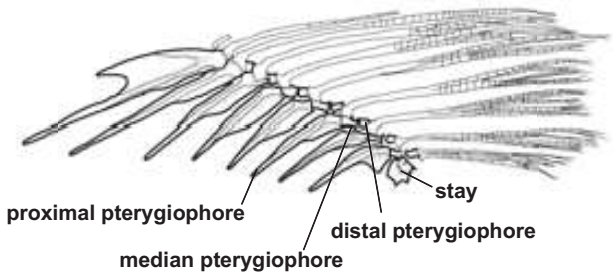

5 mm

B

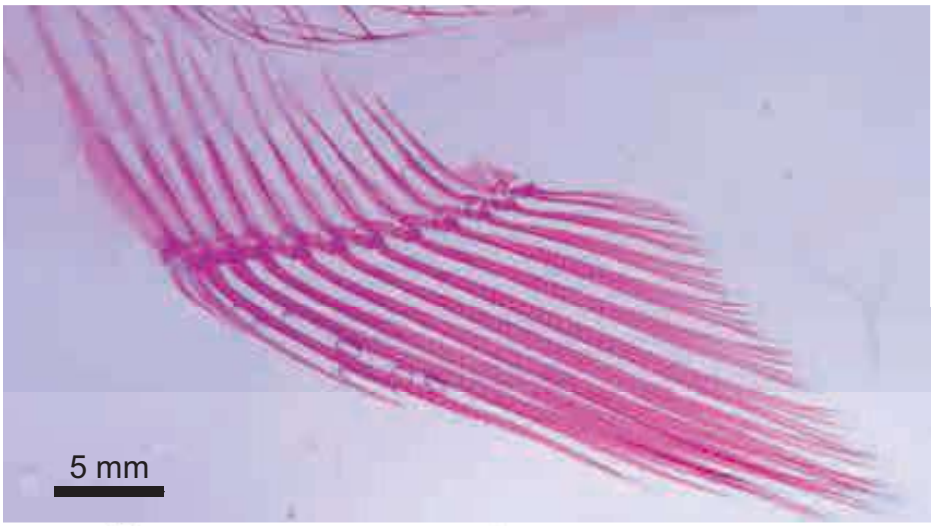

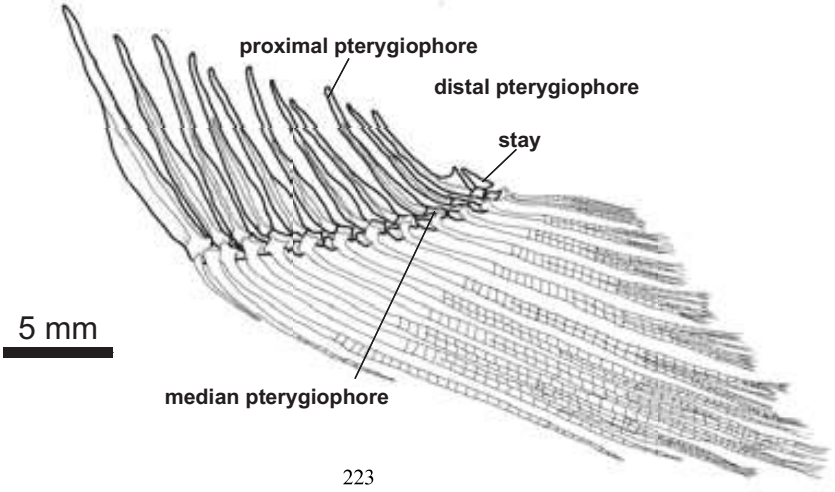

Plate 15-3

A

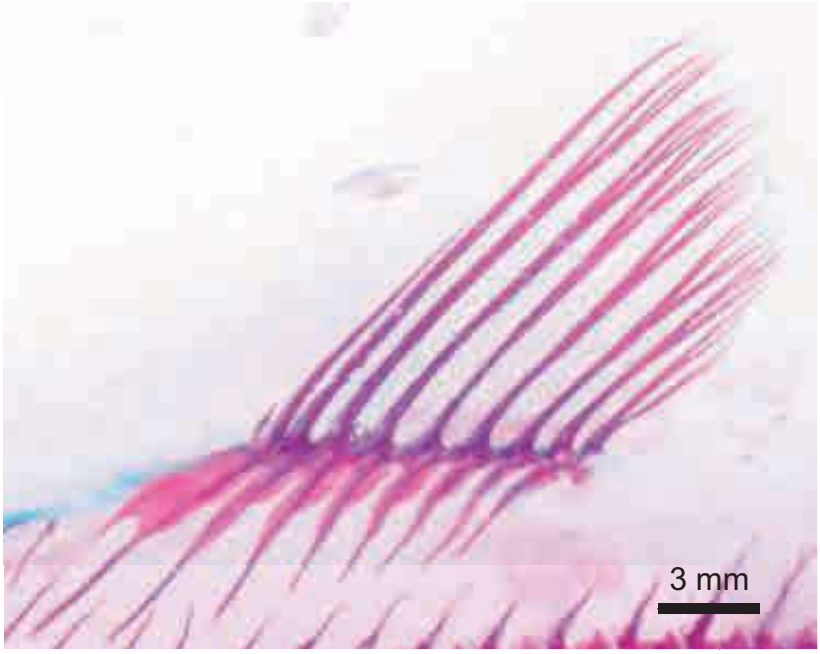
3 mm

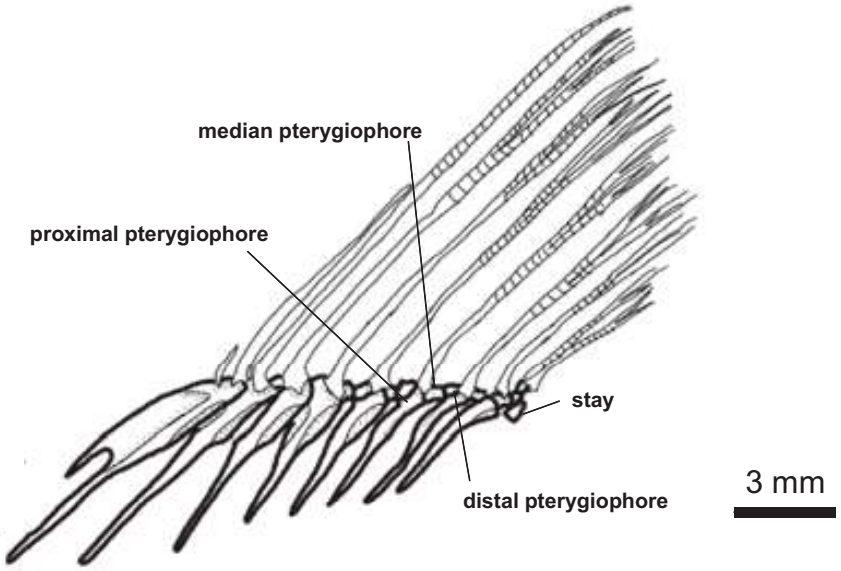
median pterygiophore
proximal pterygiophore
stay
distal pterygiophore
3 mm

B

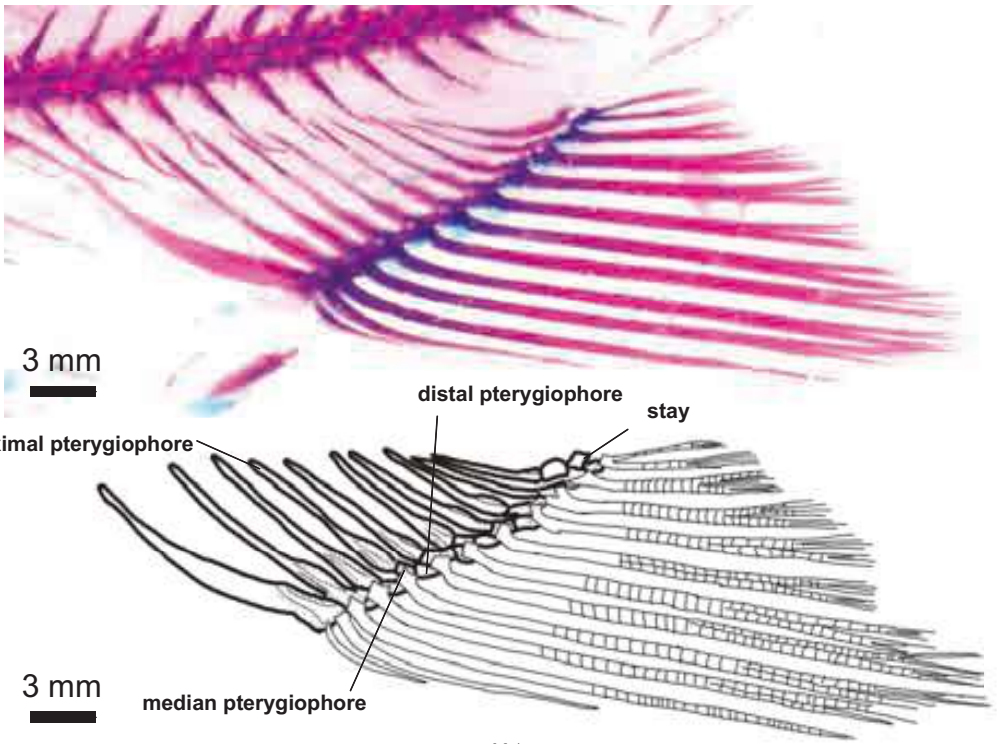
3 mm
distal pterygiophore
stay
proximal pterygiophore
3 mm
median pterygiophore

Plate 15-4

A

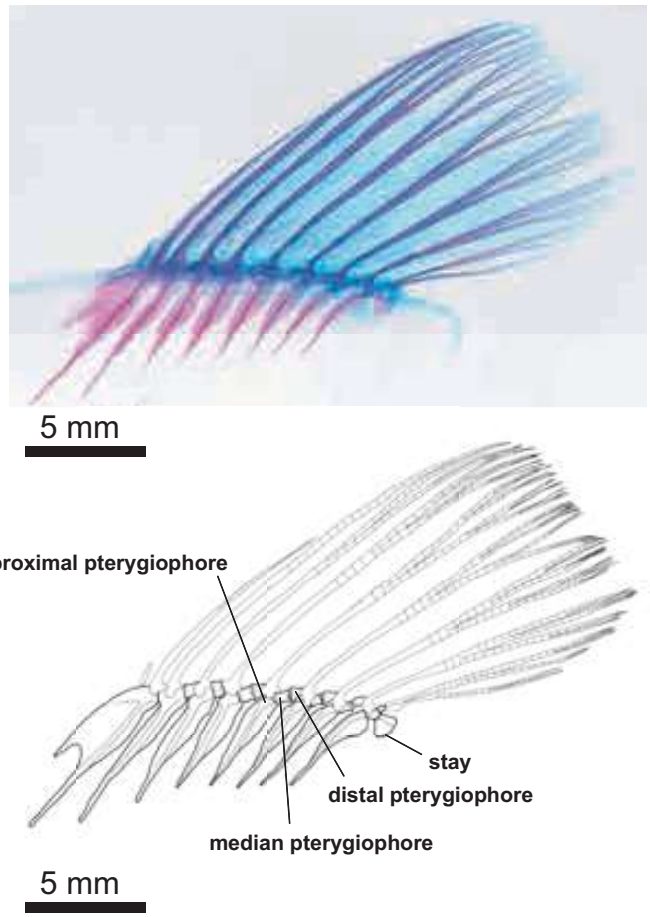
5 mm
proximal pterygiophore
stay
distal pterygiophore
median pterygiophore
5 mm

B

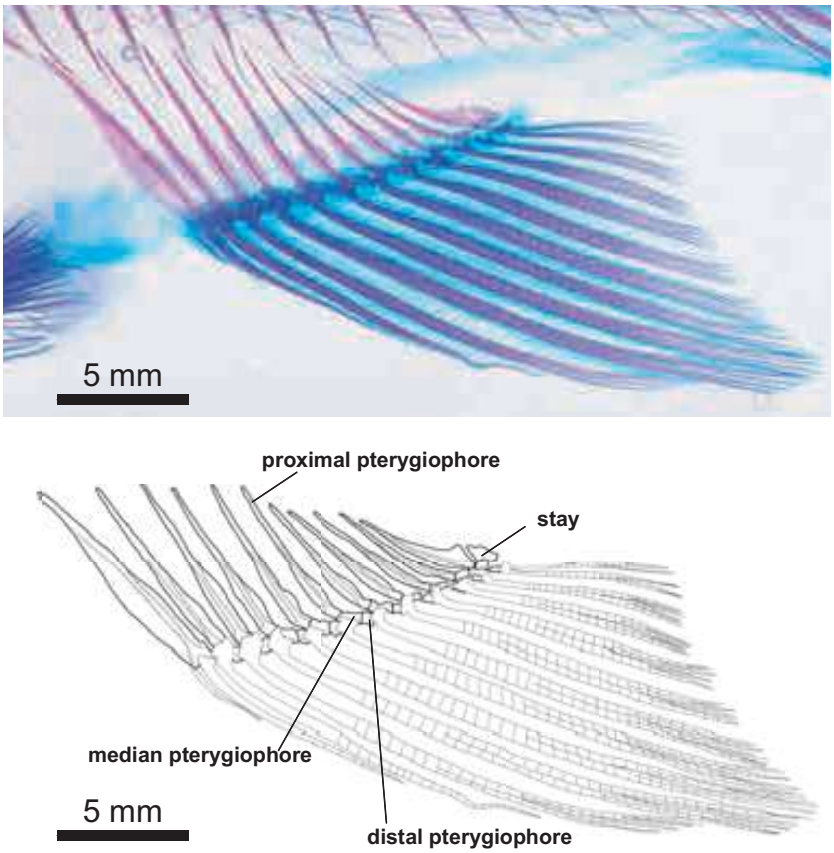
5 mm
proximal pterygiophore
stay
median pterygiophore
5 mm
distal pterygiophore

Plate 15-5

A

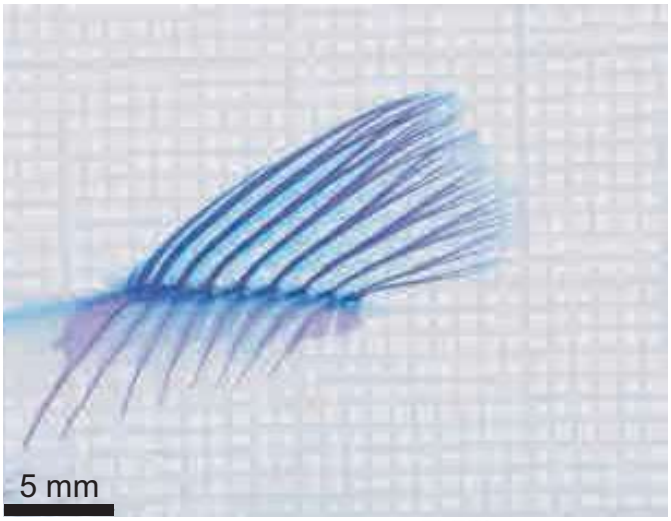
5 mm

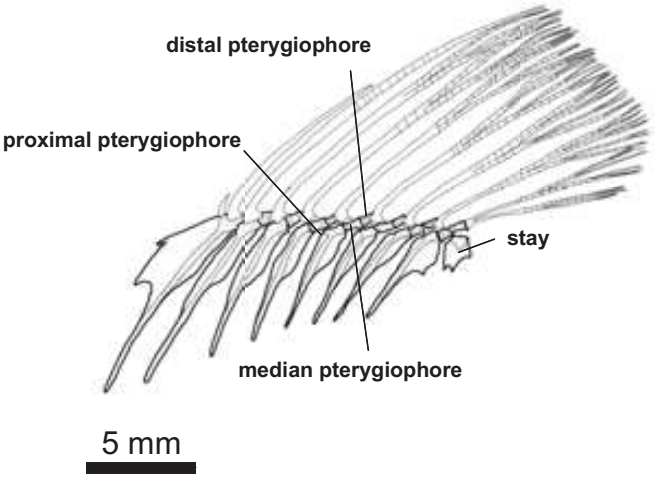
distal pterygiophore
proximal pterygiophore
stay
median pterygiophore
5 mm

B

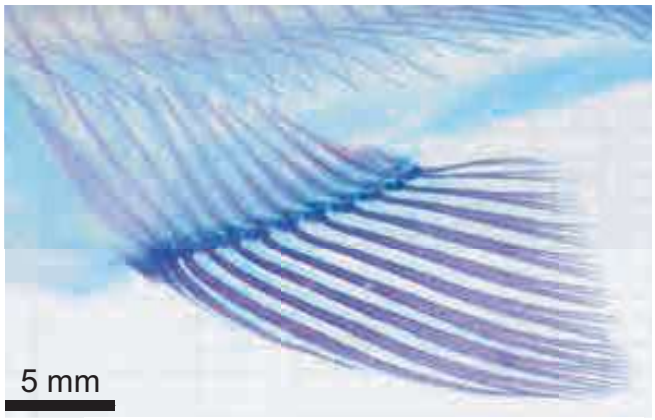
5 mm

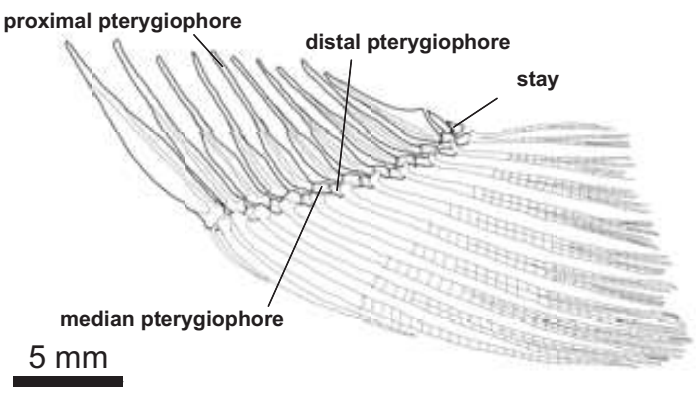
proximal pterygiophore
distal pterygiophore
stay
median pterygiophore
5 mm

Plate 15-6

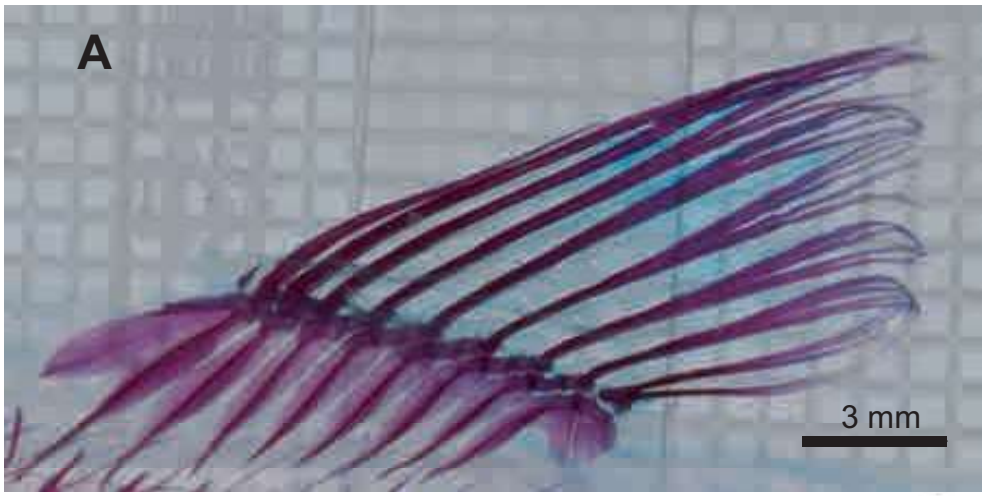
A
3 mm

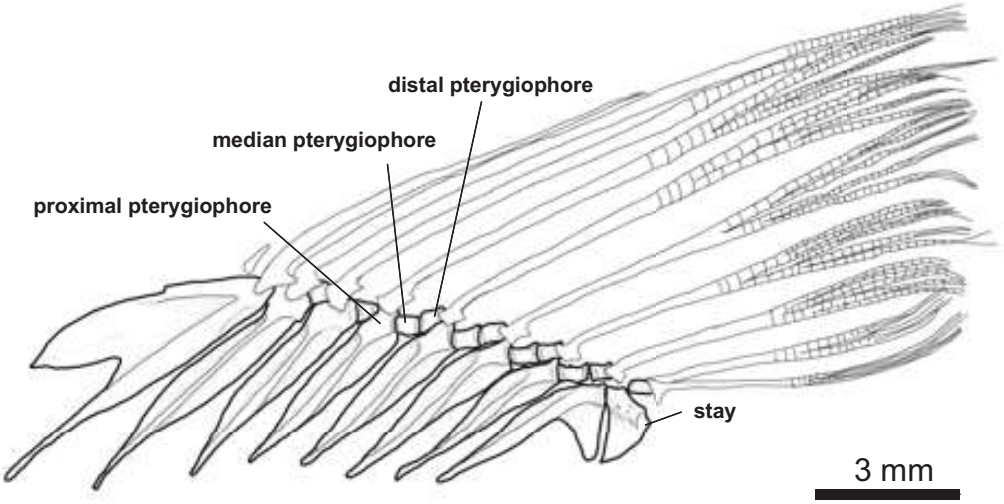
distal pterygiophore
median pterygiophore
proximal pterygiophore
stay
3 mm

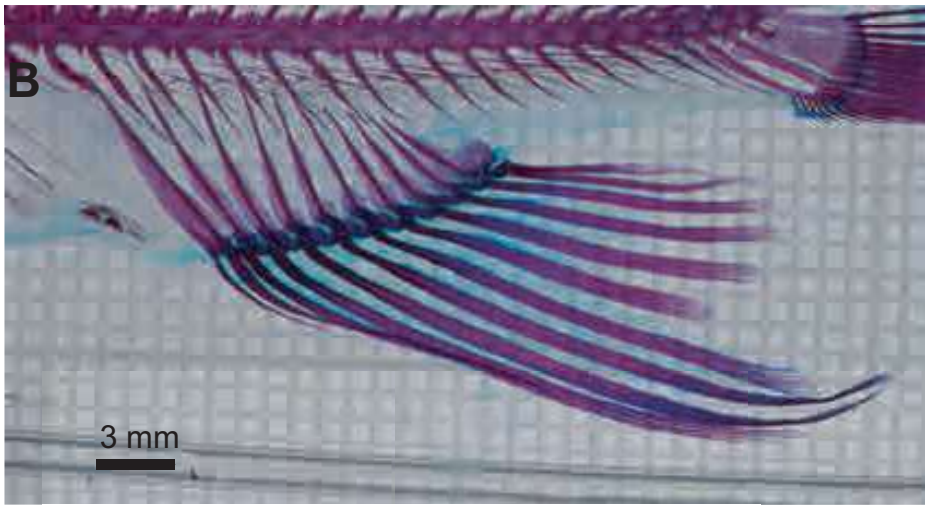
B
3 mm

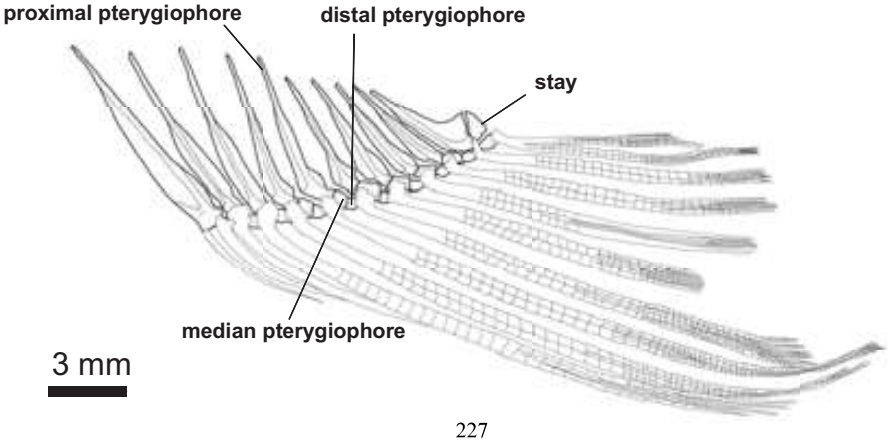
proximal pterygiophore
distal pterygiophore
stay
median pterygiophore
3 mm

Plate 15-7

A

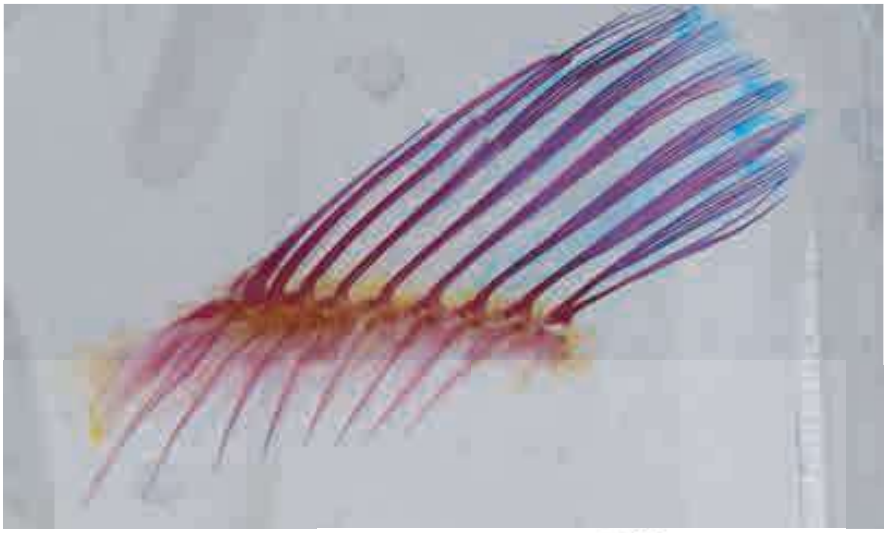

1 cm

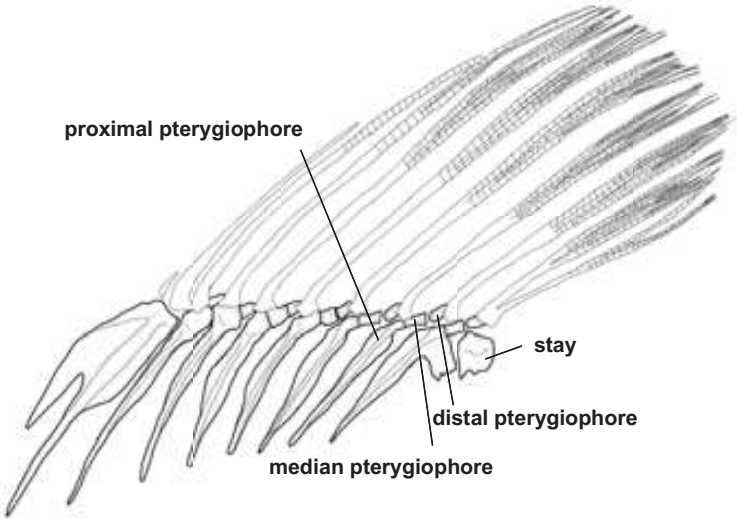

1 cm

B

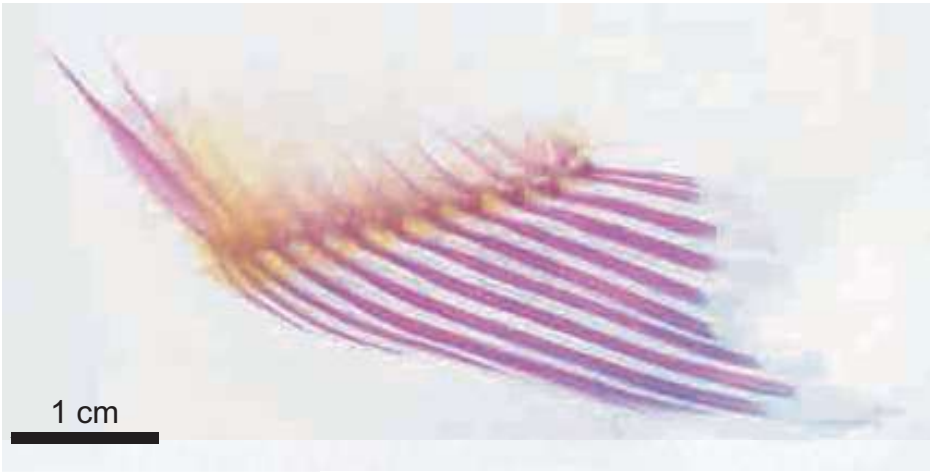

1 cm

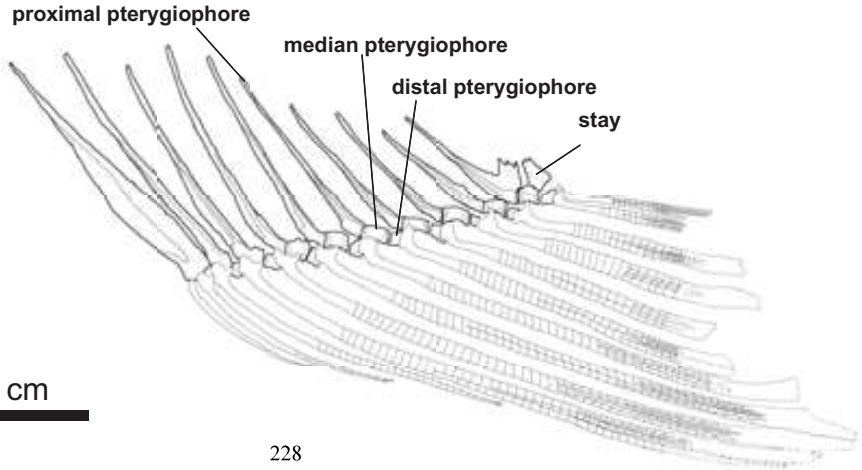

1 cm

Plate 15-8

A

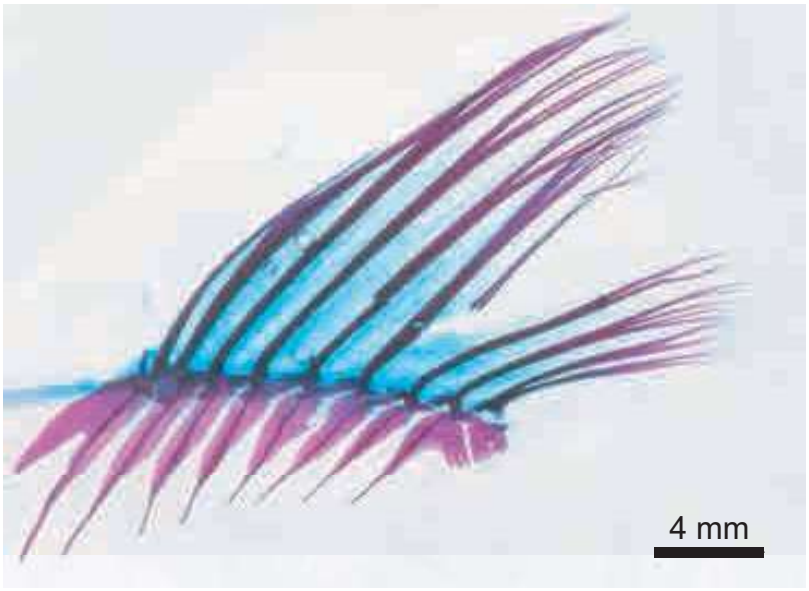
4 mm

B

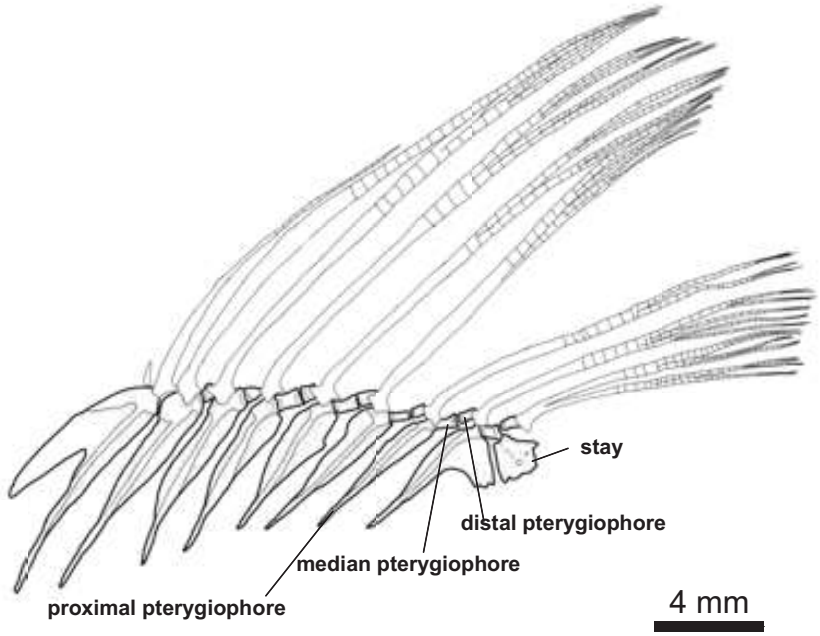
stay
distal pterygiophore
median pterygiophore
proximal pterygiophore
4 mm

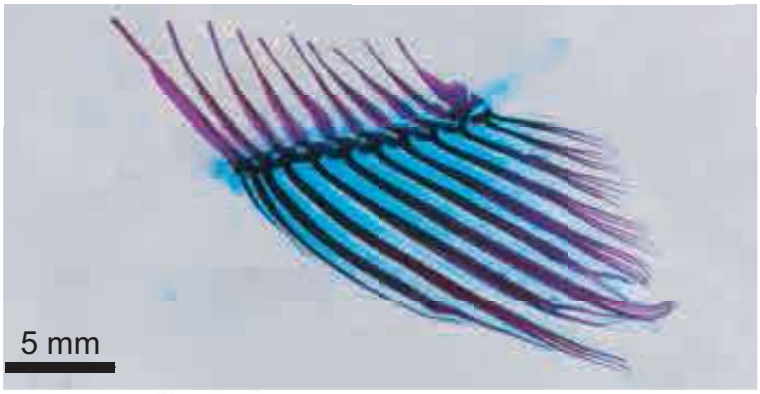
5 mm

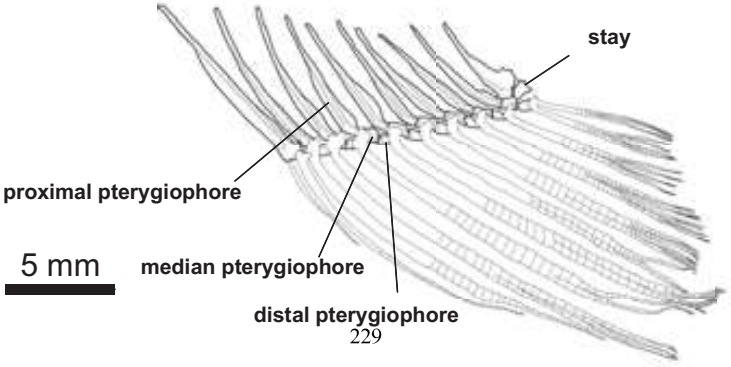
stay
proximal pterygiophore
5 mm
median pterygiophore
distal pterygiophore

Plate 15-9

A

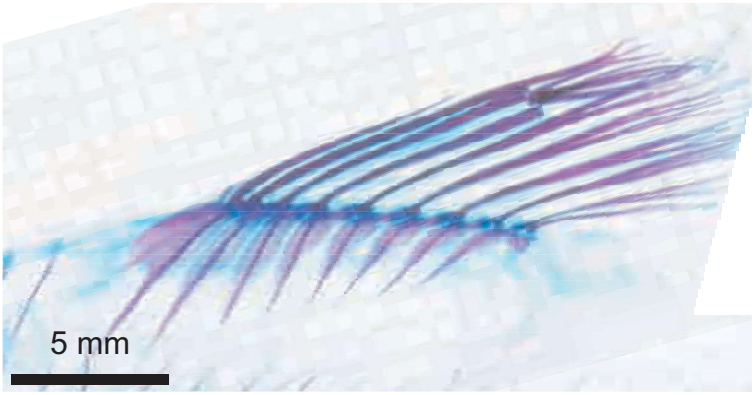
5 mm

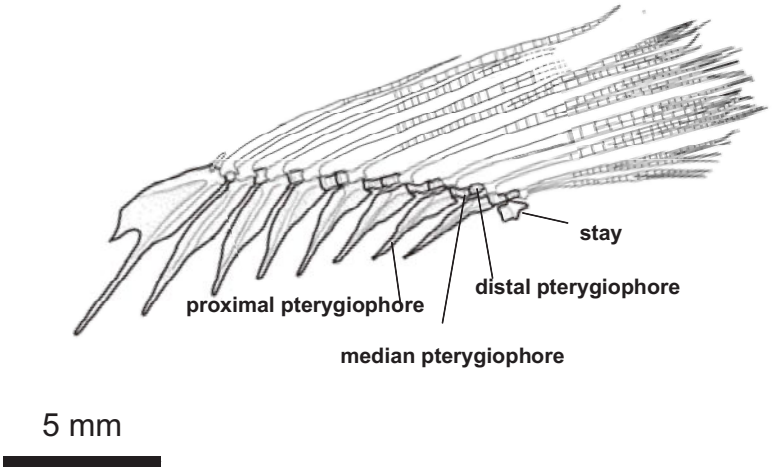
stay
distal pterygiophore
proximal pterygiophore
median pterygiophore
5 mm

B

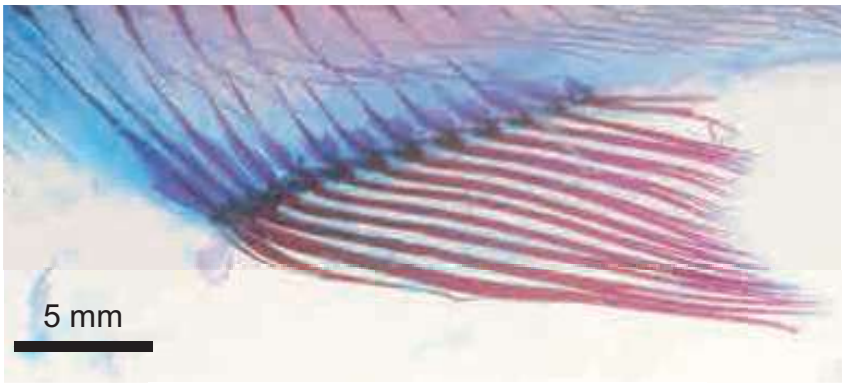
5 mm

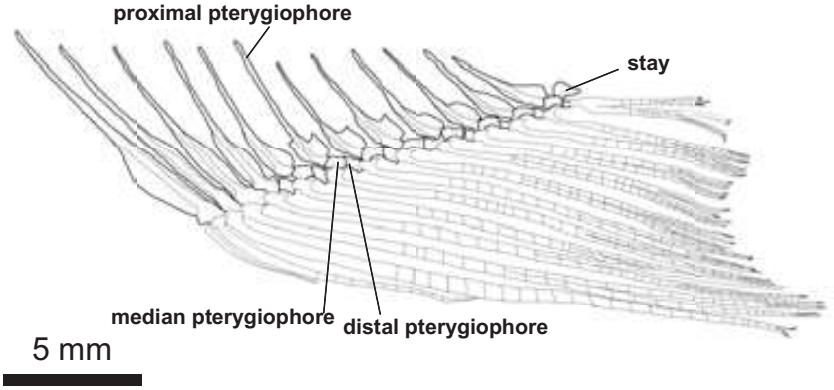
proximal pterygiophore
stay
median pterygiophore
distal pterygiophore
5 mm

Plate 16-1

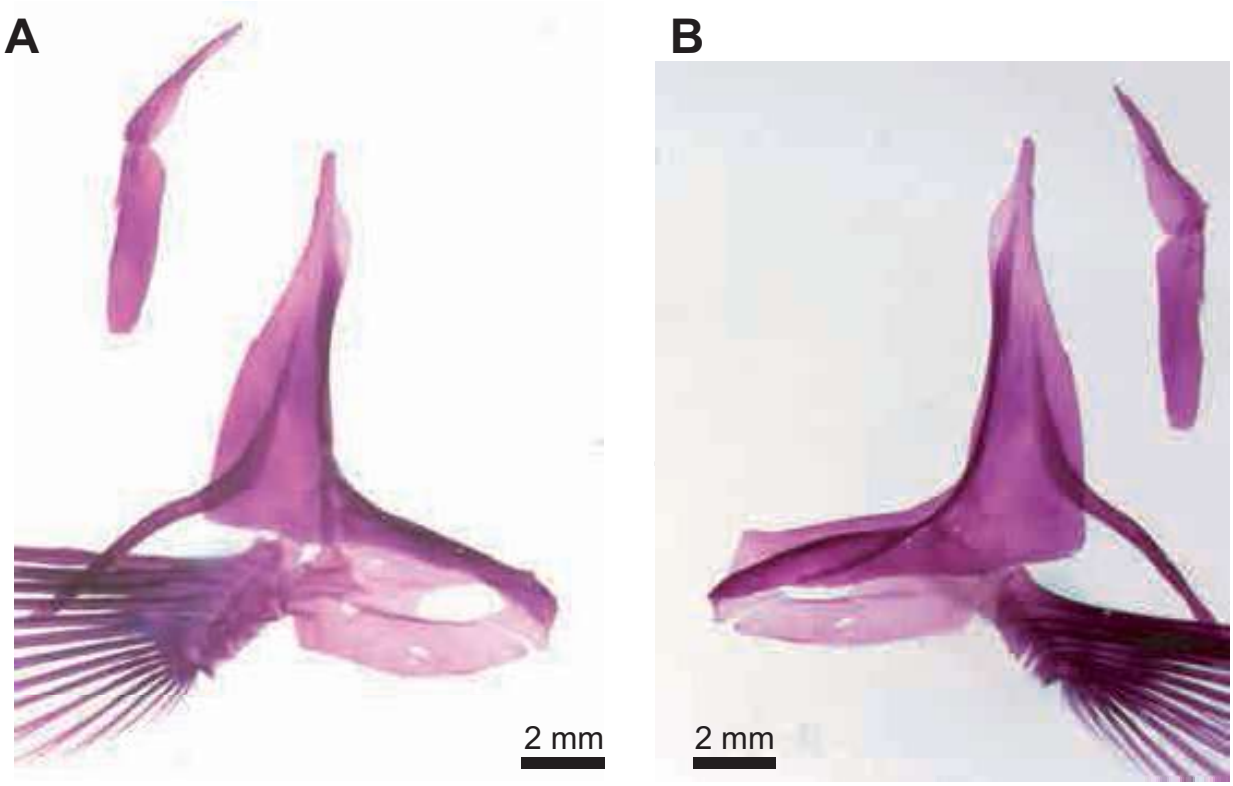
A
B
2 mm
2 mm

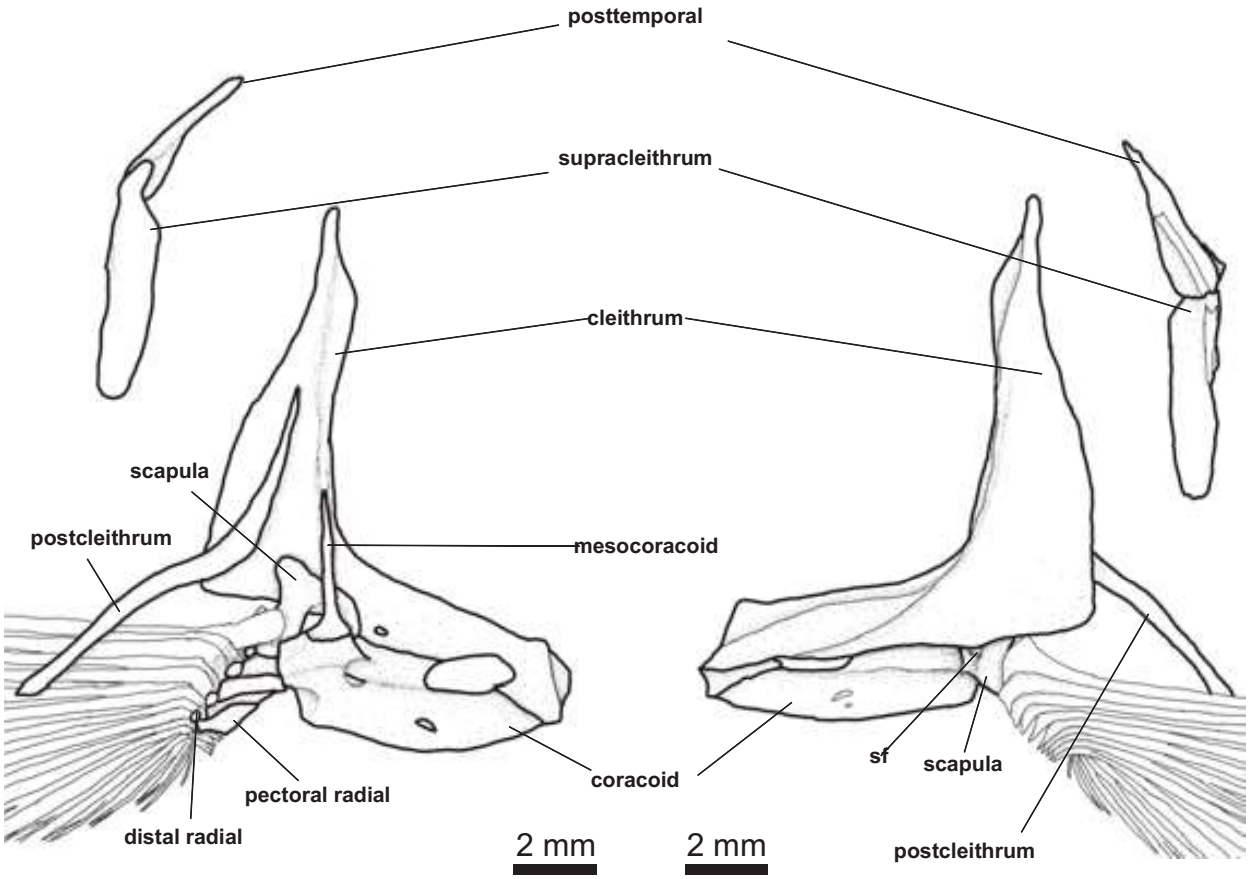
posttemporal
supracleithrum
cleithrum
scapula
postcleithrum
mesocoracoid
pectoral radial
distal radial
coracoid
sf
scapula
postcleithrum
2 mm
2 mm

Plate 16-2

A **B**

2 mm 2 mm

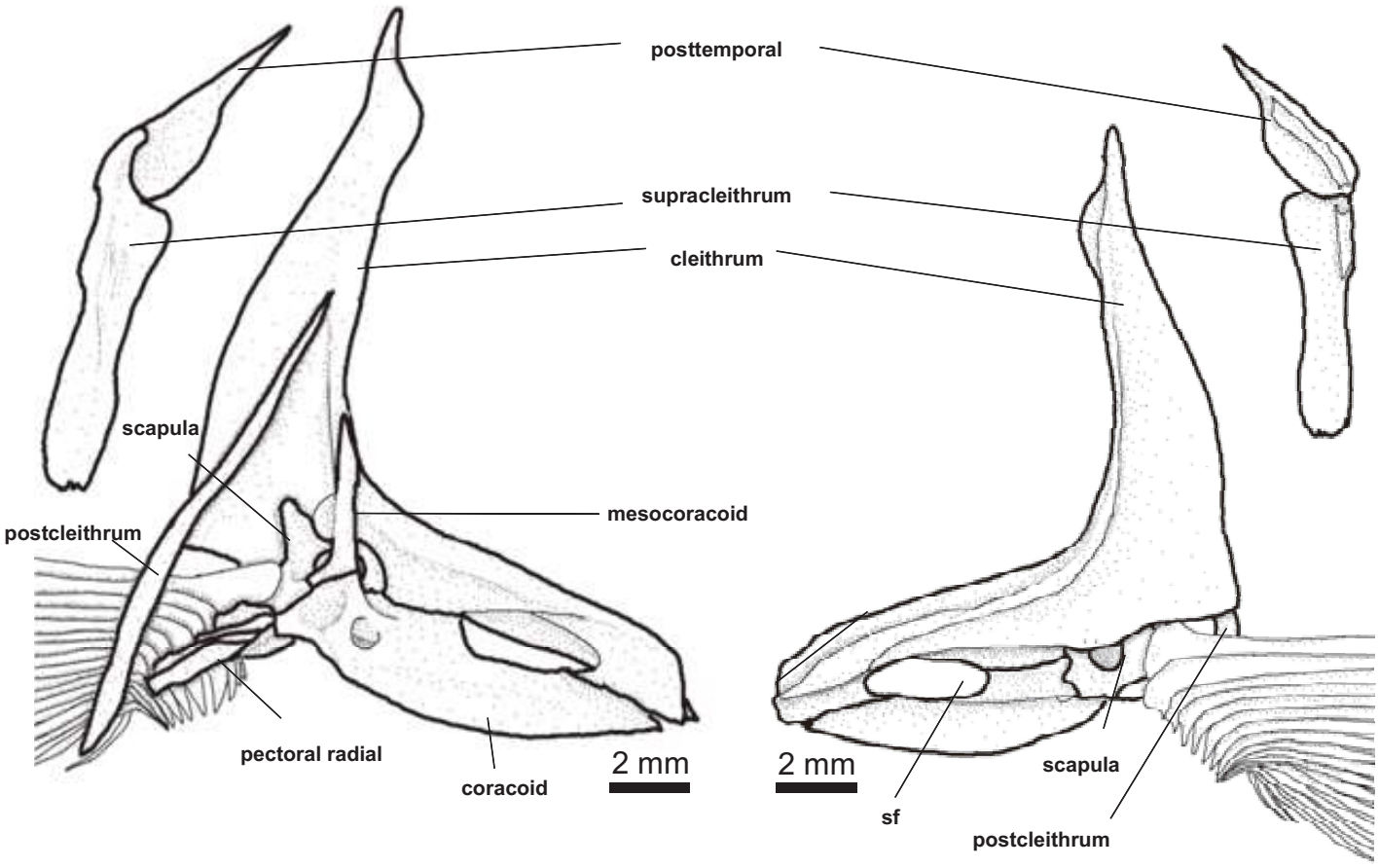

Plate 16-3

A **B**

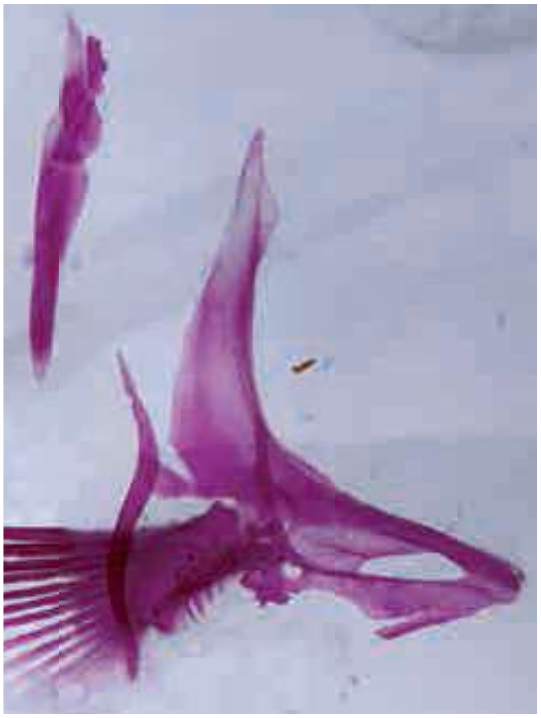

3 mm

3 mm

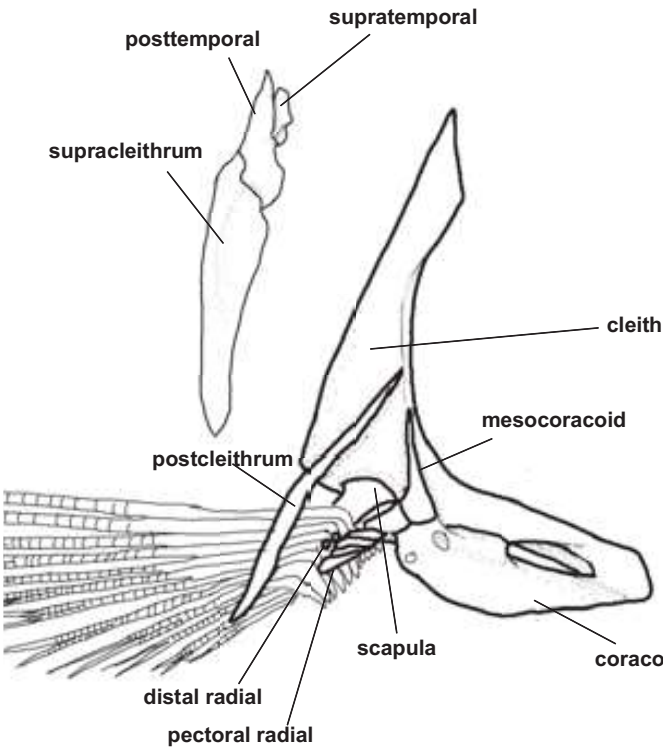

3 mm

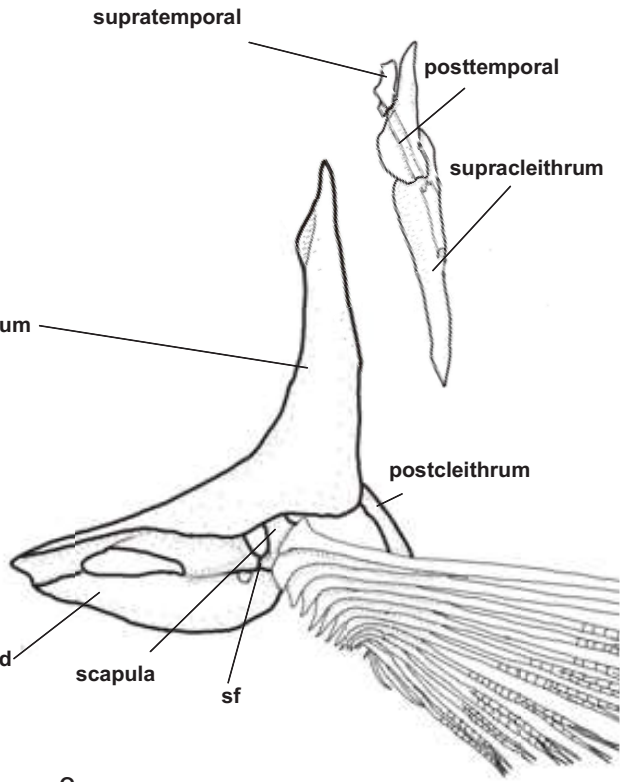

3 mm

Plate 16-4

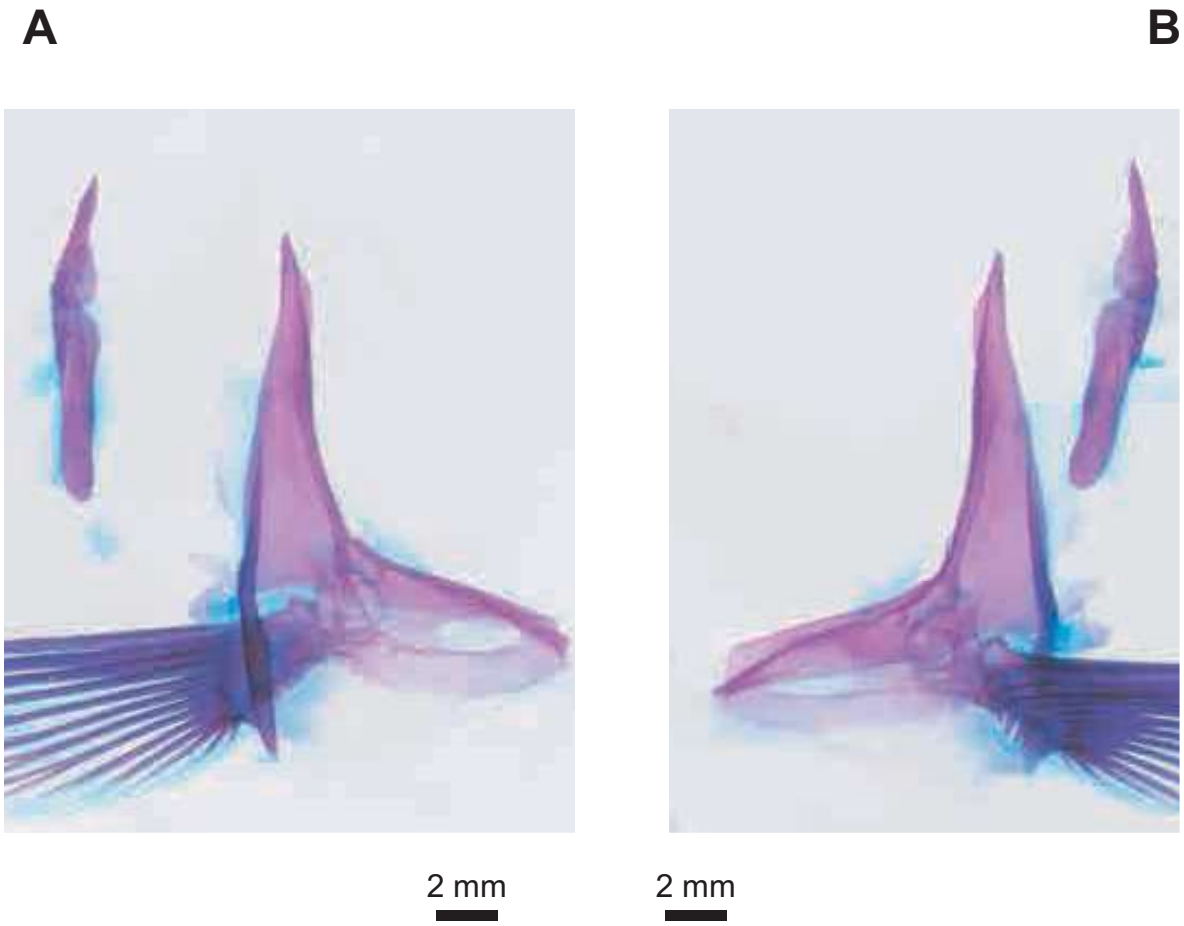
A
B
2 mm
2 mm

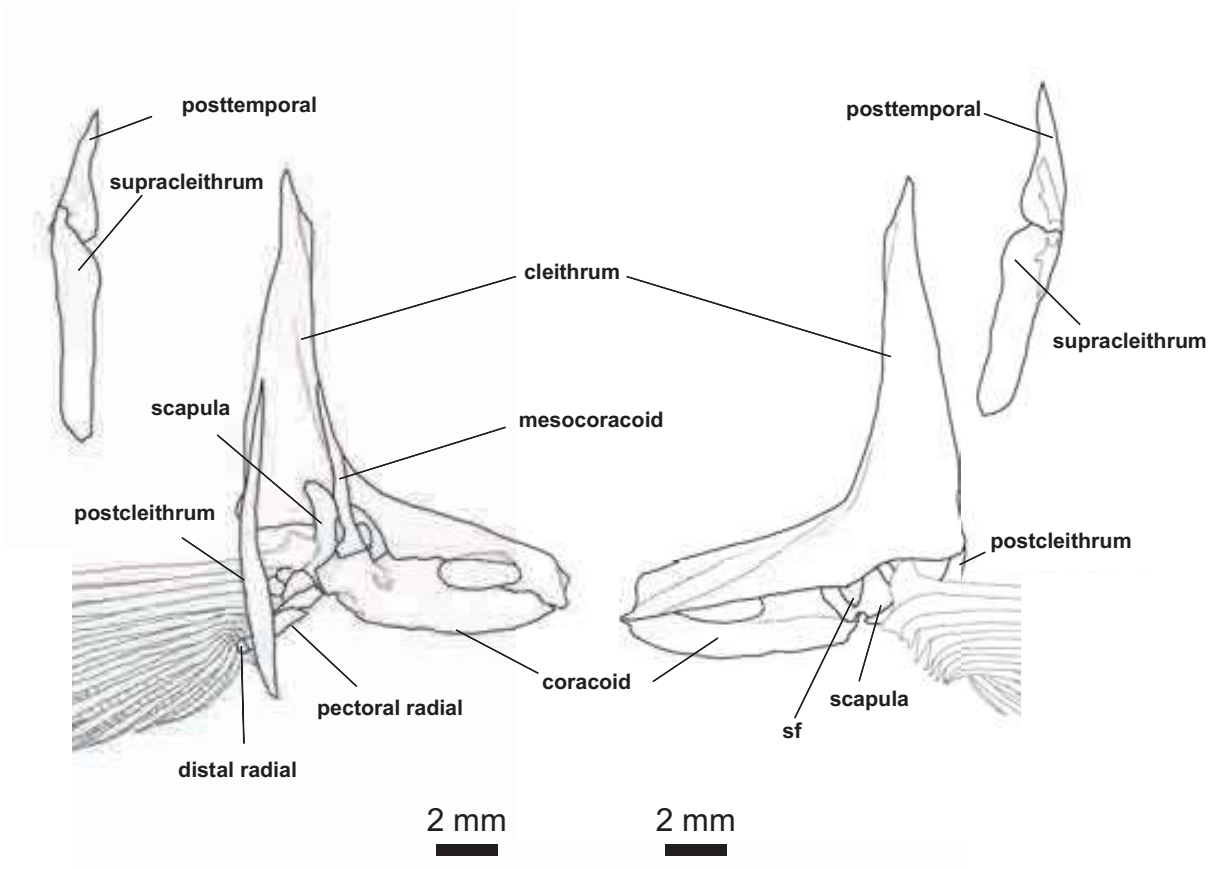
posttemporal
supracleithrum
cleithrum
scapula
mesocoracoid
postcleithrum
pectoral radial
distal radial
coracoid
posttemporal
supracleithrum
postcleithrum
scapula
sf
2 mm
2 mm

Plate 16-5

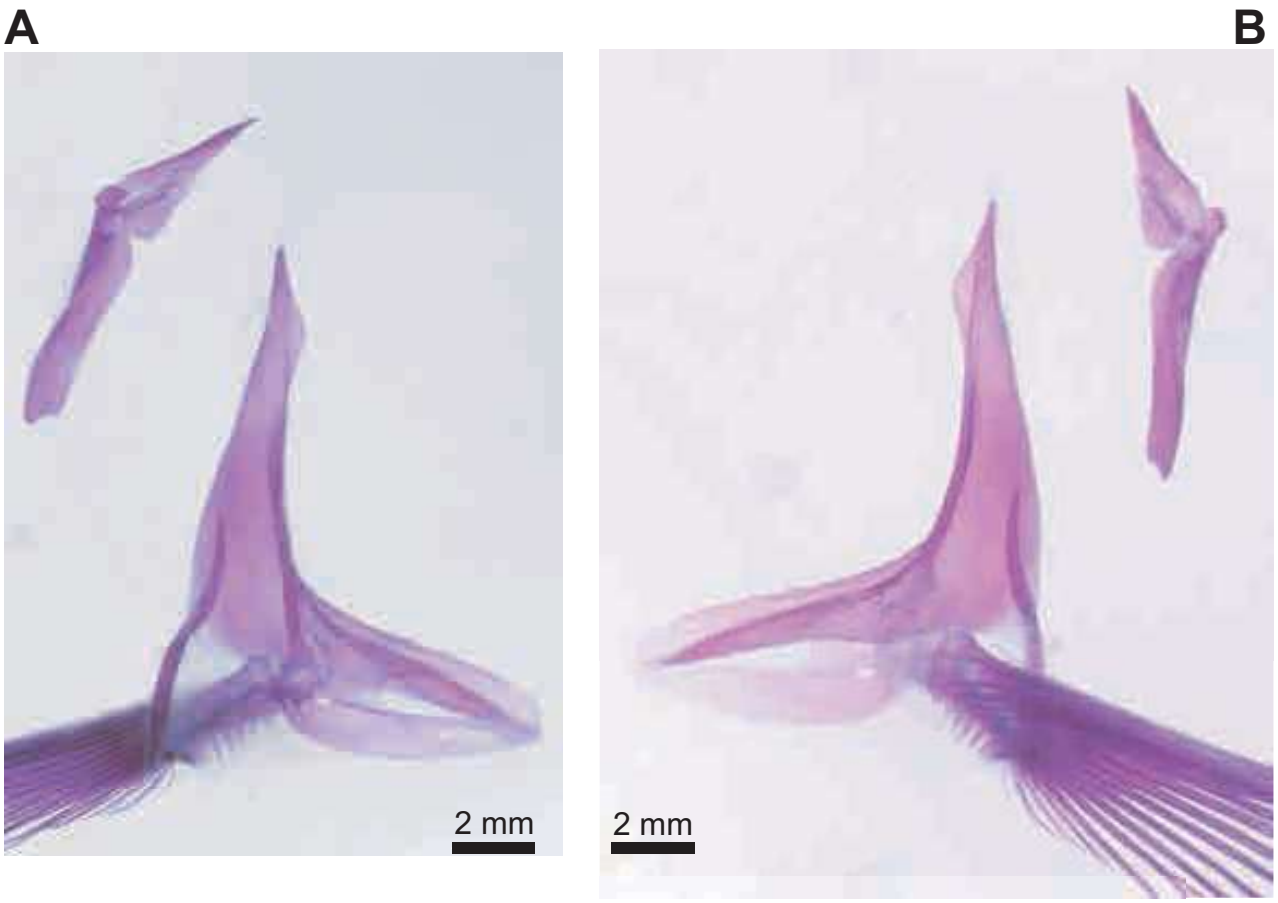
A
B
2 mm
2 mm

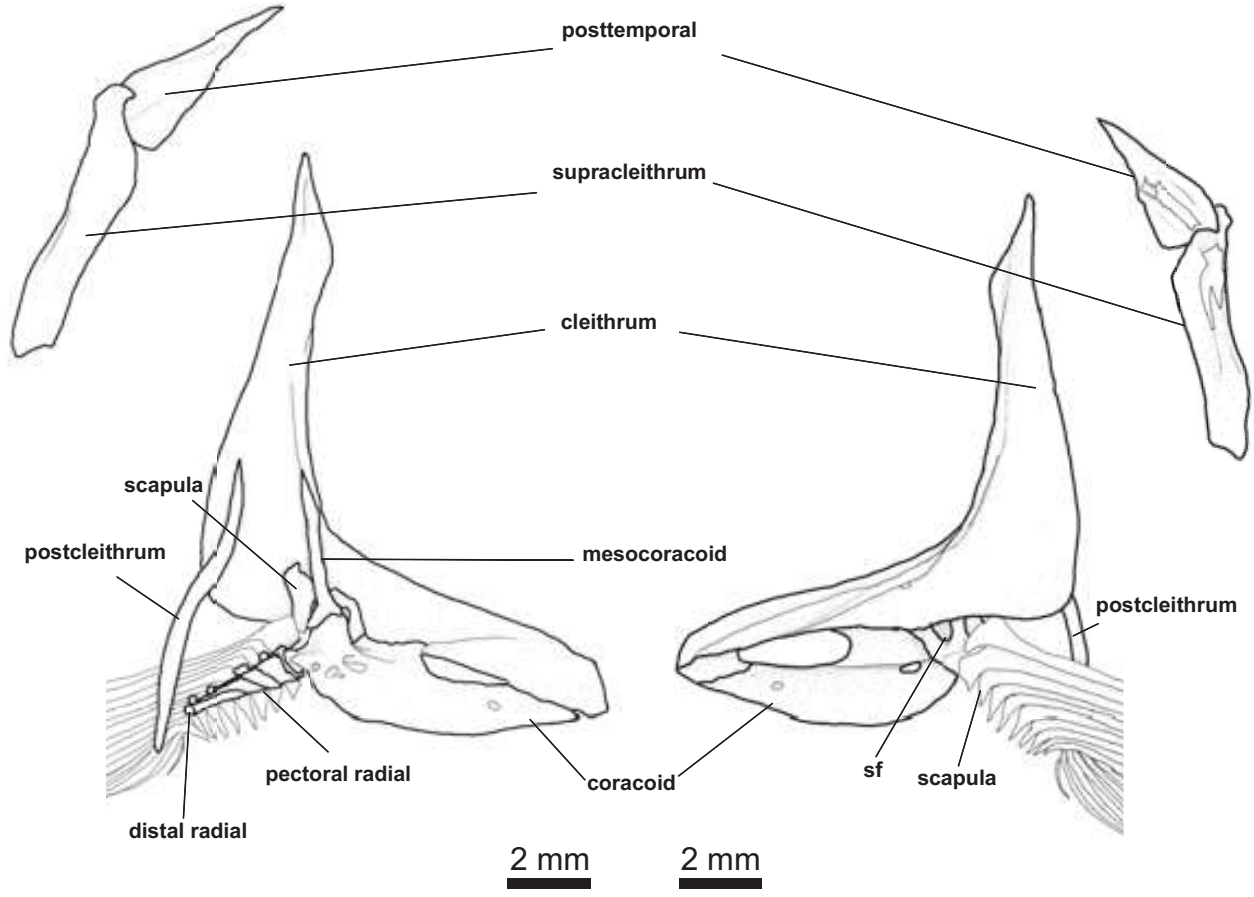
posttemporal
supracleithrum
cleithrum
scapula
postcleithrum
mesocoracoid
pectoral radial
distal radial
coracoid
sf
scapula
postcleithrum
2 mm
2 mm

Plate 16-6


A
2 mm

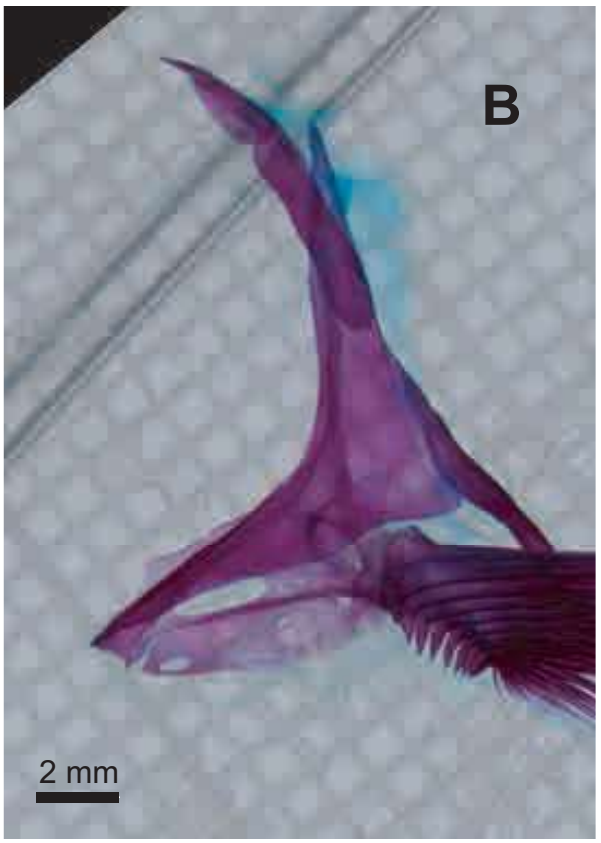
B
2 mm

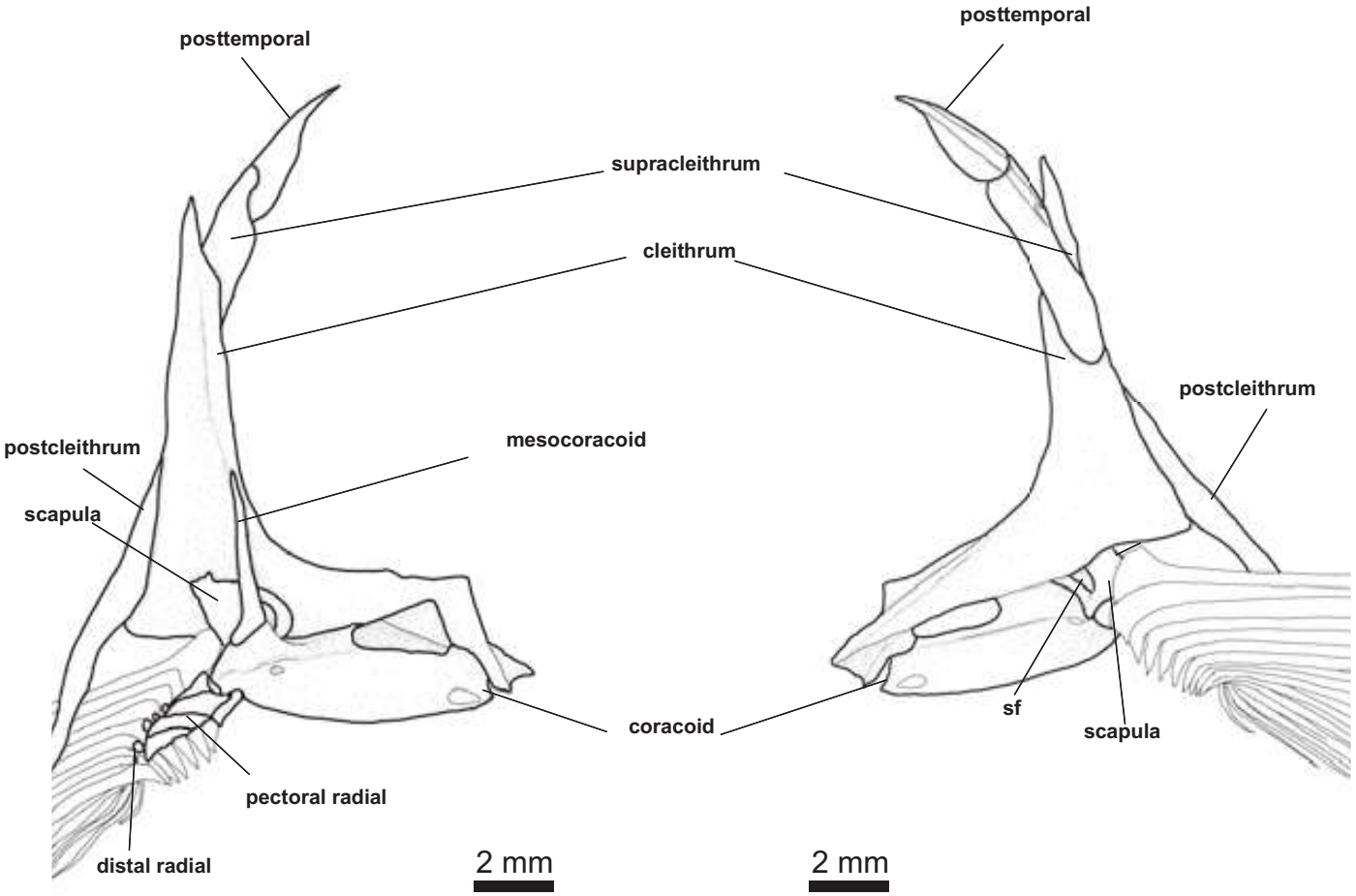
posttemporal
supracleithrum
cleithrum
postcleithrum
mesocoracoid
scapula
coracoid
pectoral radial
distal radial
2 mm
posttemporal
postcleithrum
sf
scapula
2 mm

Plate 16-7

A **B**


1 cm


1 cm

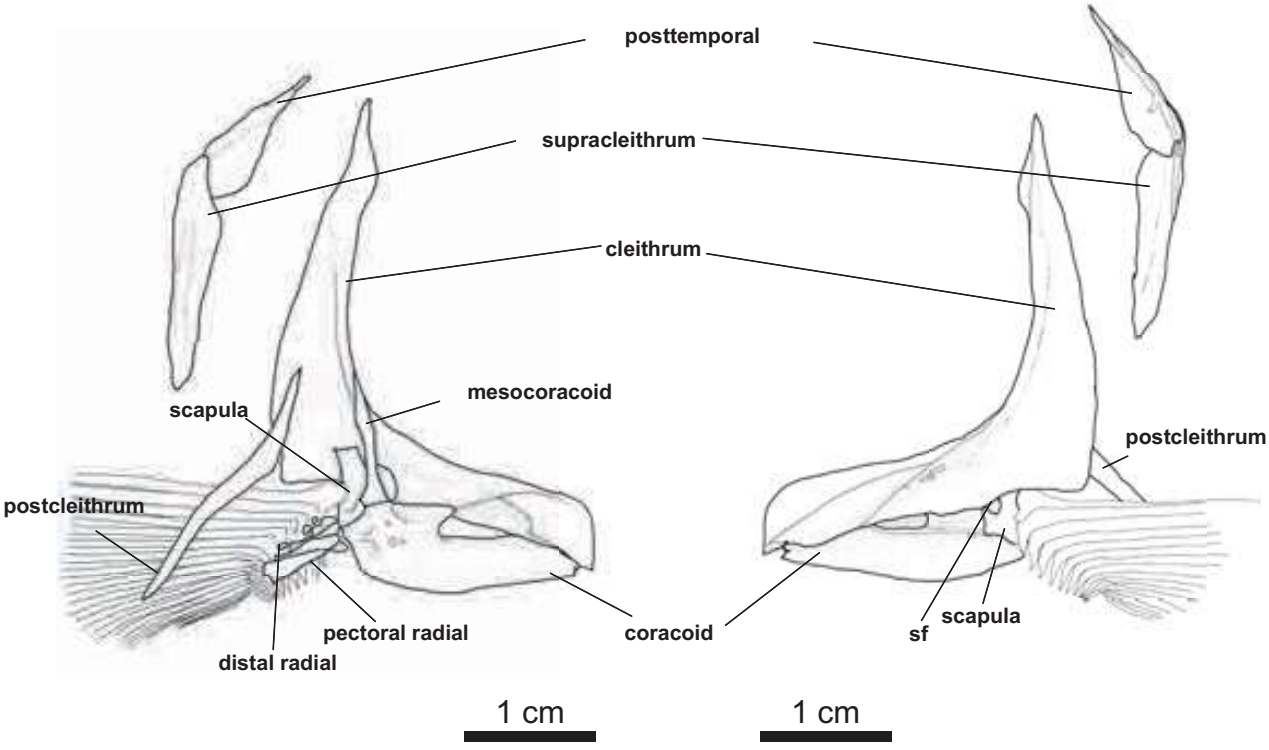
posttemporal
supracleithrum
cleithrum
mesocoracoid
scapula
postcleithrum
pectoral radial
distal radial
coracoid
sf
scapula
postcleithrum
1 cm
1 cm

Plate 16-8

A **B**


2 mm

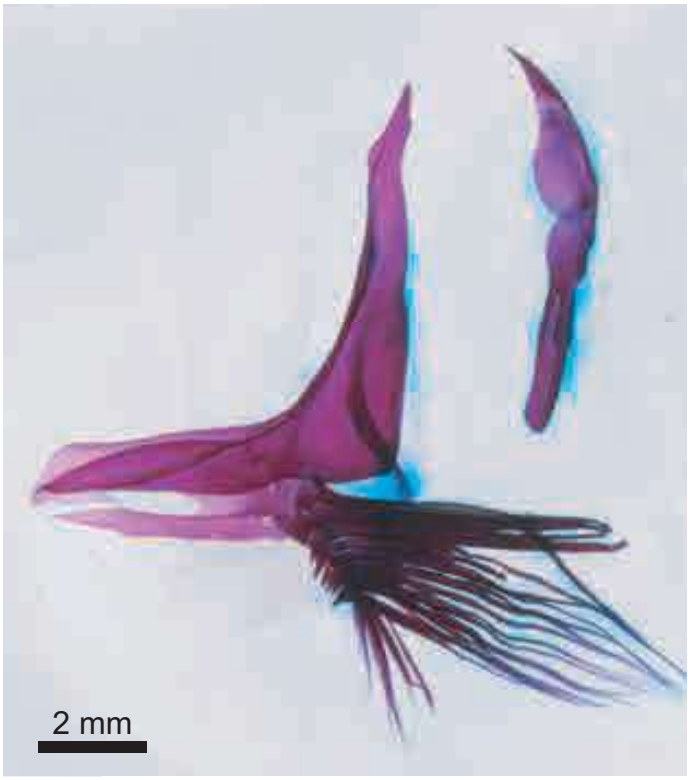
2 mm

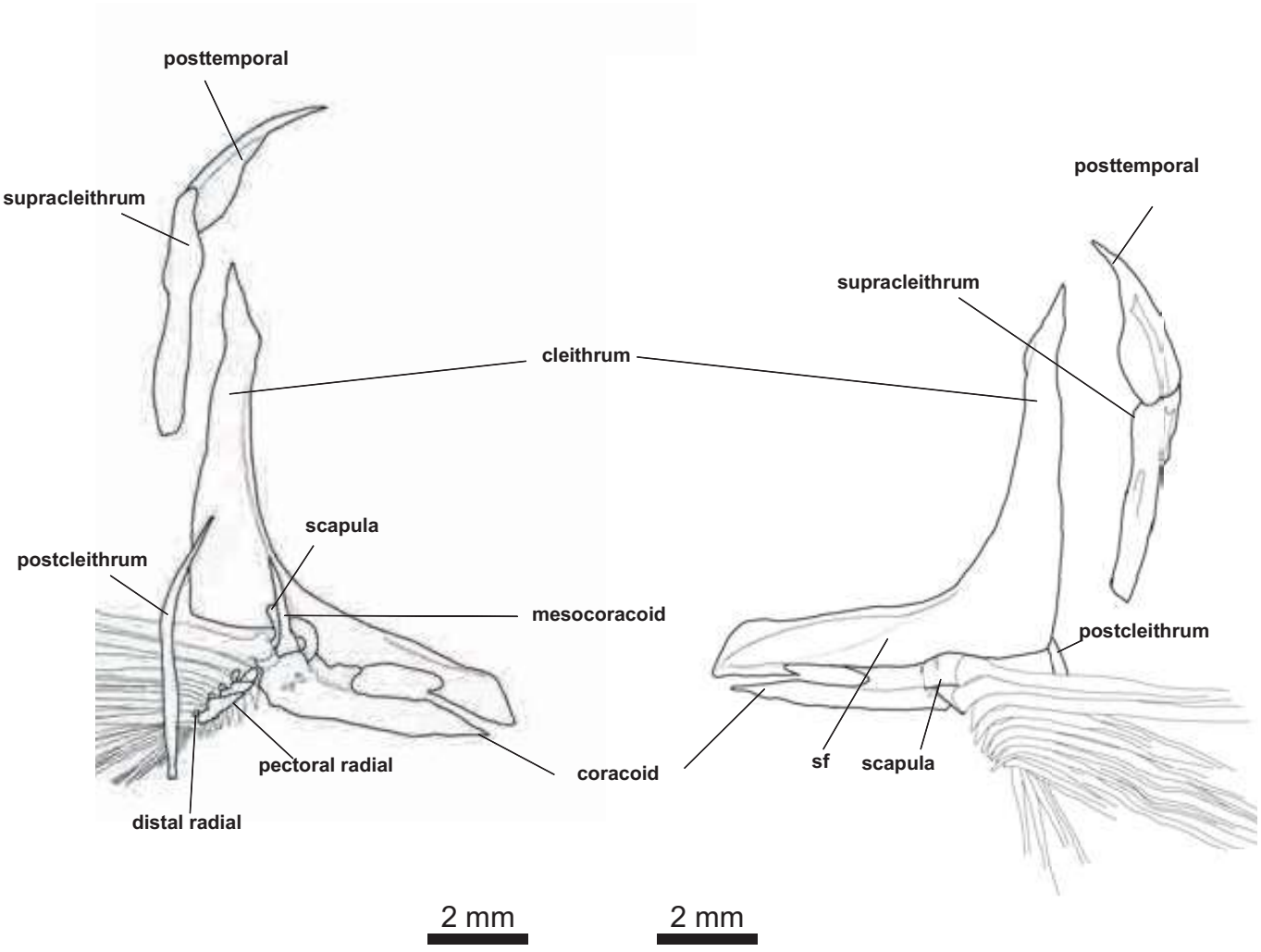
posttemporal
supracleithrum
cleithrum
scapula
postcleithrum
mesocoracoid
pectoral radial
distal radial
coracoid
2 mm
posttemporal
supracleithrum
postcleithrum
sf
scapula
2 mm

Plate 16-9

A **B**

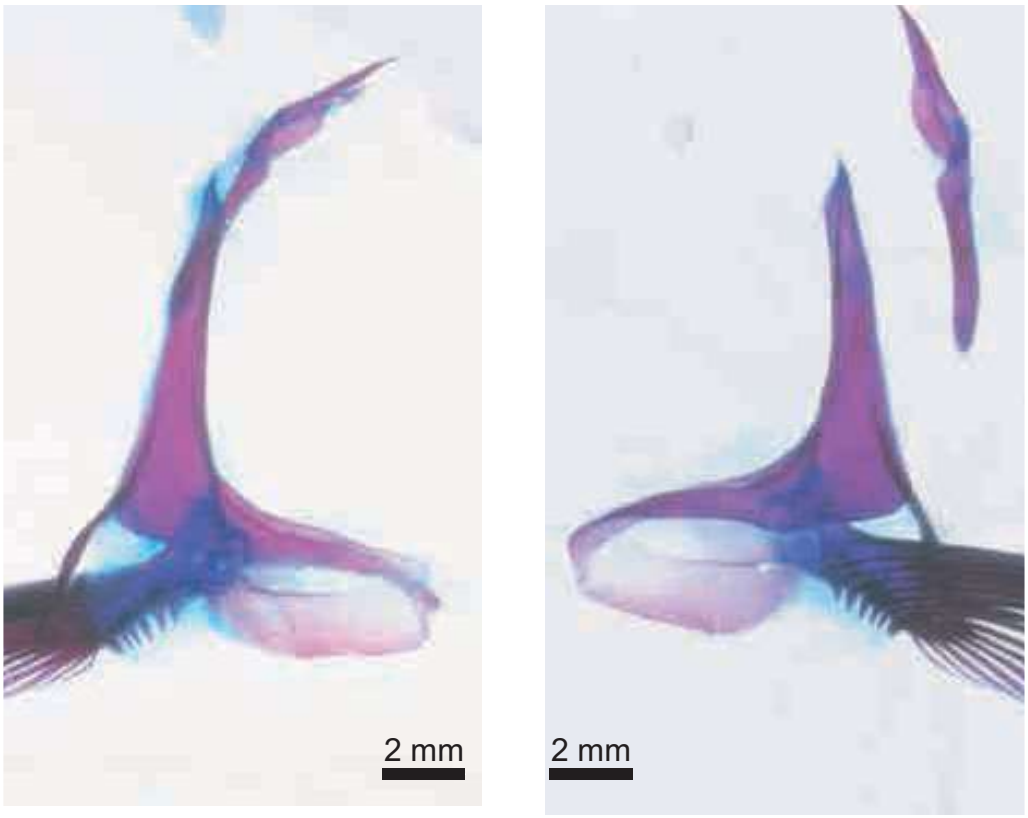
2 mm
2 mm

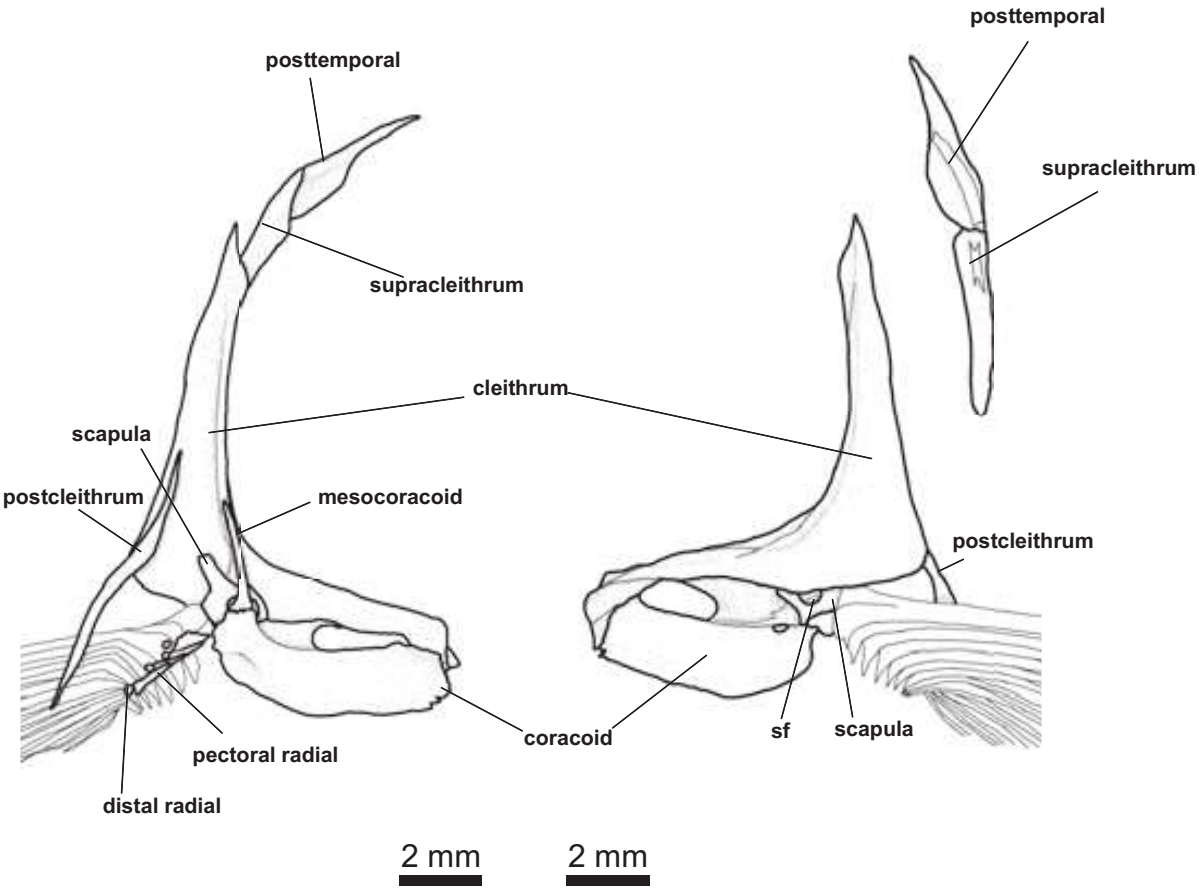
posttemporal
supracleithrum
cleithrum
scapula
postcleithrum
mesocoracoid
pectoral radial
distal radial
coracoid
posttemporal
supracleithrum
postcleithrum
sf
scapula
2 mm
2 mm

Plate 17-1

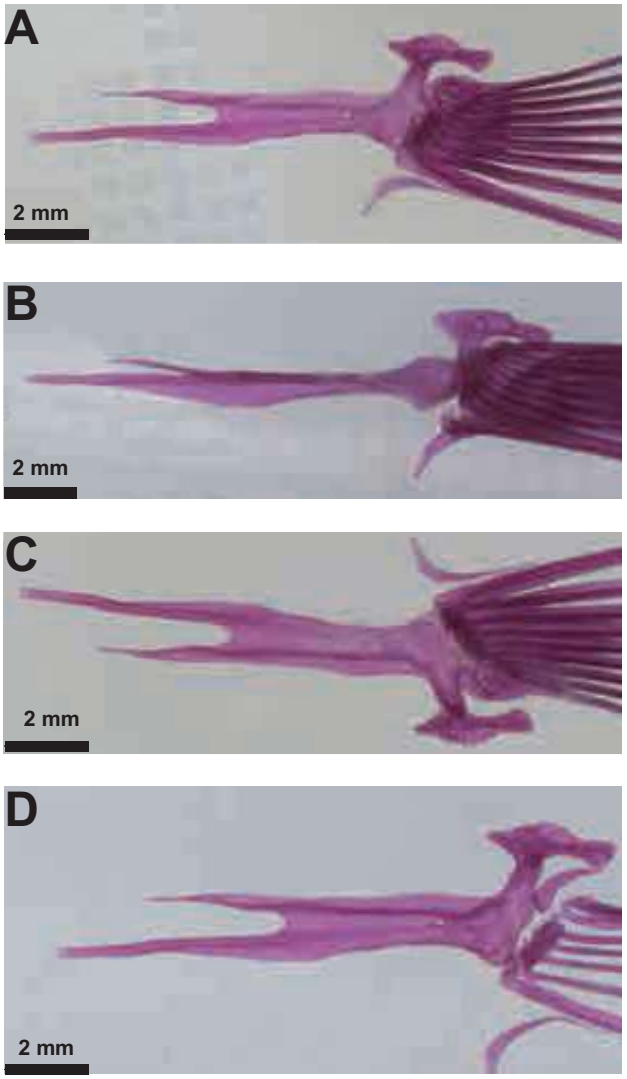
A
2 mm
B
2 mm
C
2 mm
D
2 mm

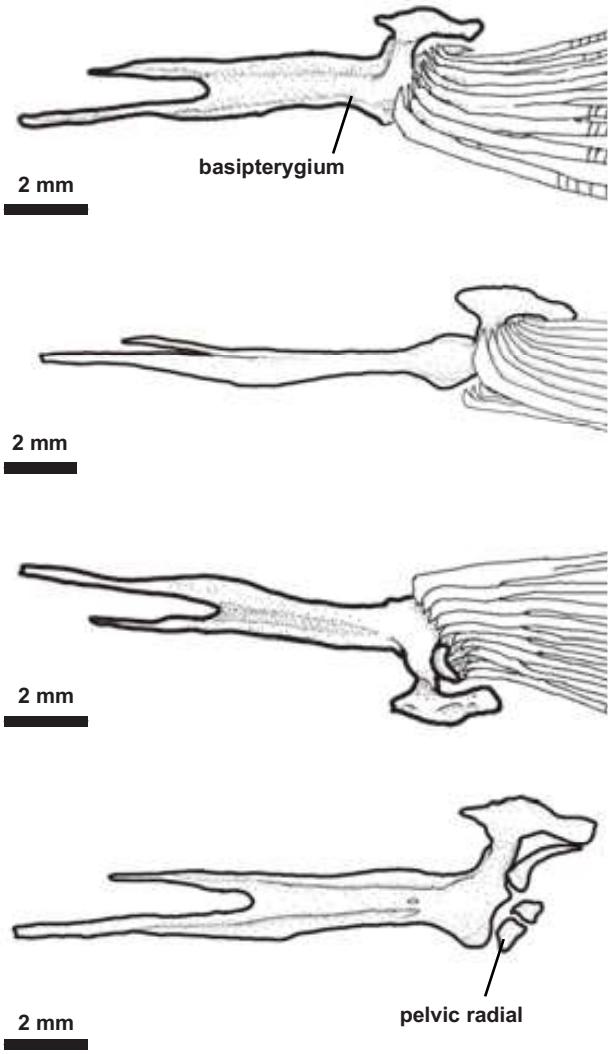
basipterygium
2 mm
2 mm
2 mm
pelvic radial
2 mm

Plate 17-2

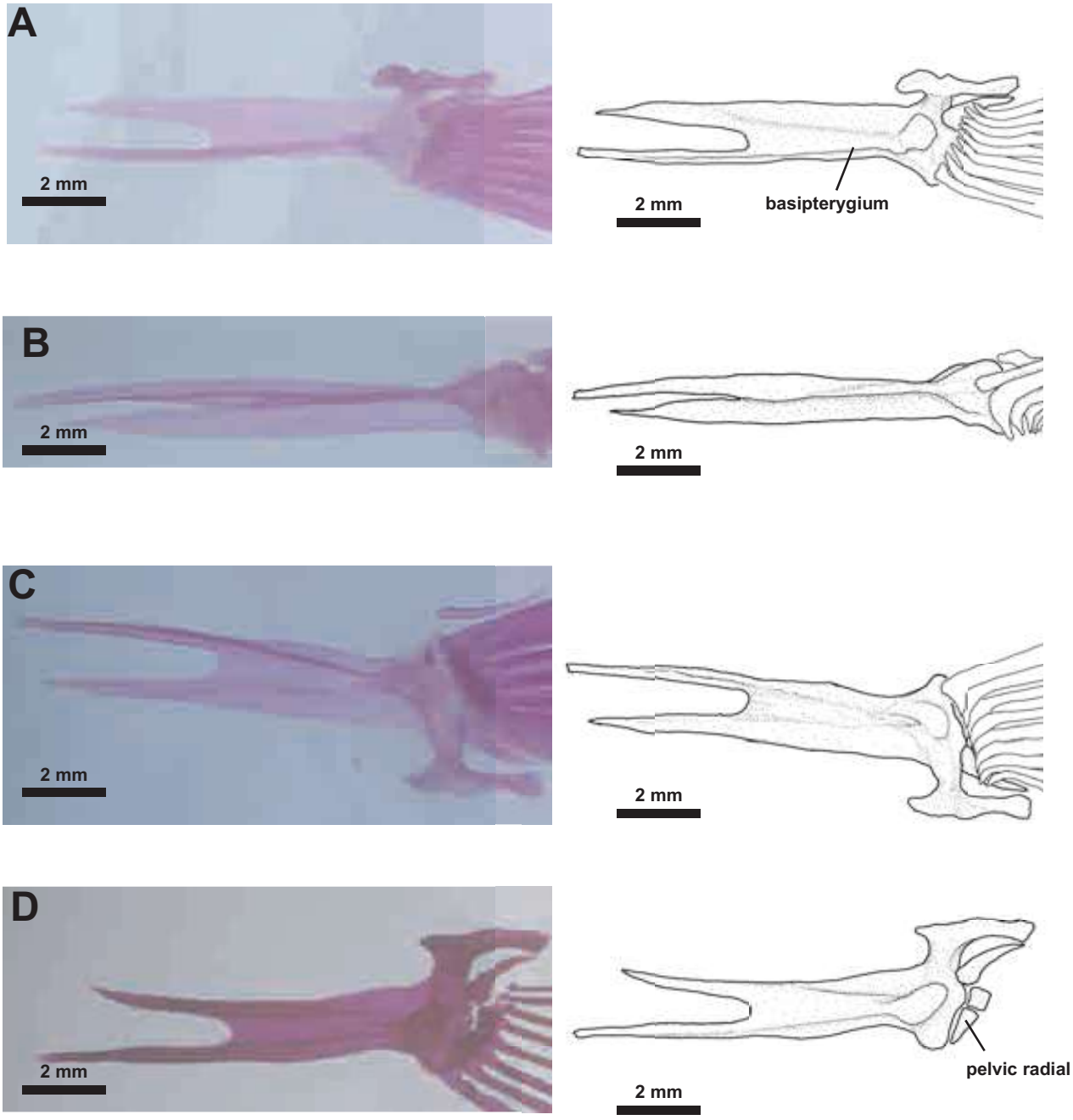
A
2 mm
2 mm
basipterygium
B
2 mm
2 mm
C
2 mm
2 mm
D
2 mm
2 mm
pelvic radial

Plate 17-3

A

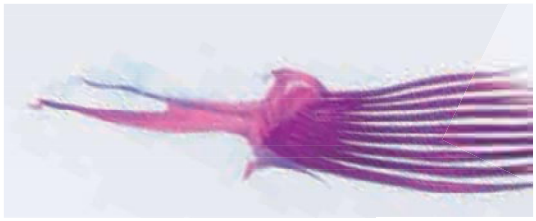

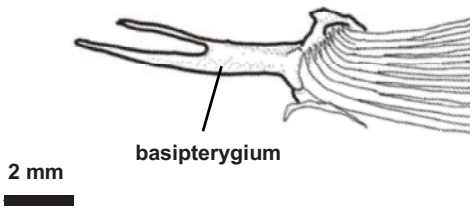

B

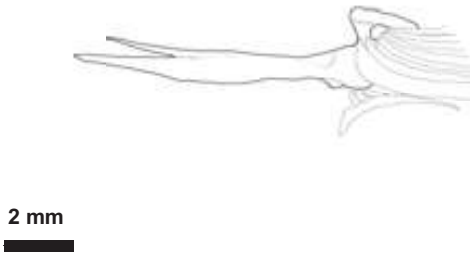

C

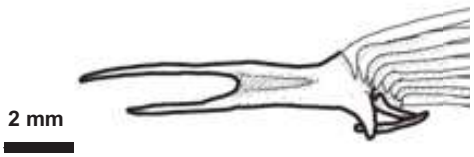

D

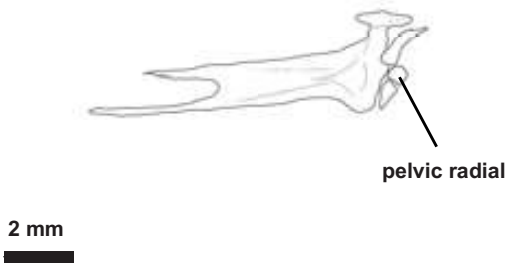

Plate 17-4

A

2 mm

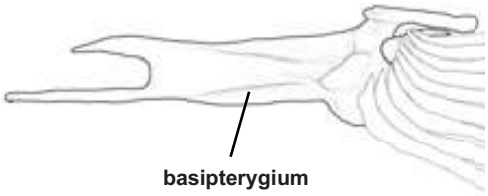

2 mm

B

2 mm

2 mm

C

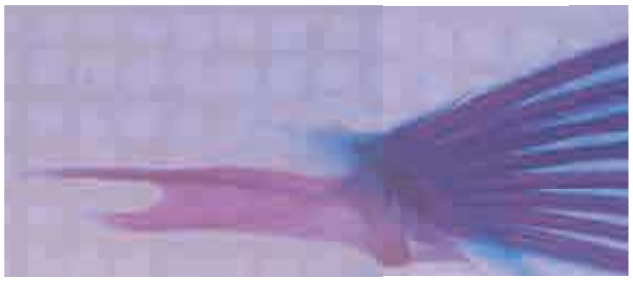

2 mm

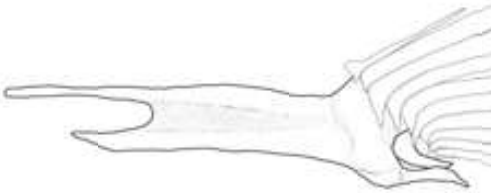

2 mm

D

2 mm

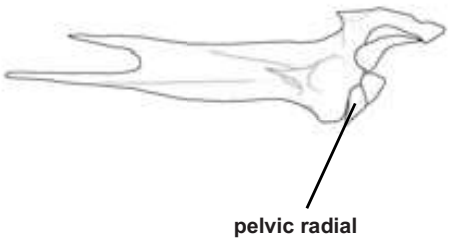

2 mm

Plate 17-5

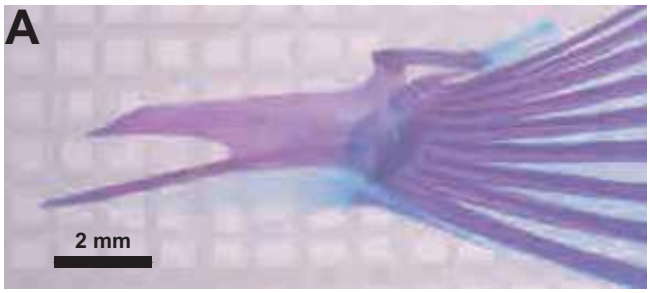
A
2 mm

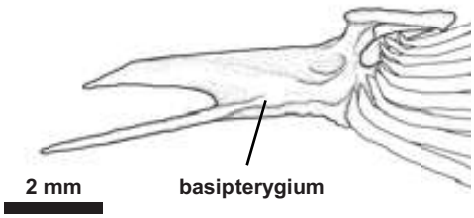
2 mm
basipterygium


B
2 mm


2 mm

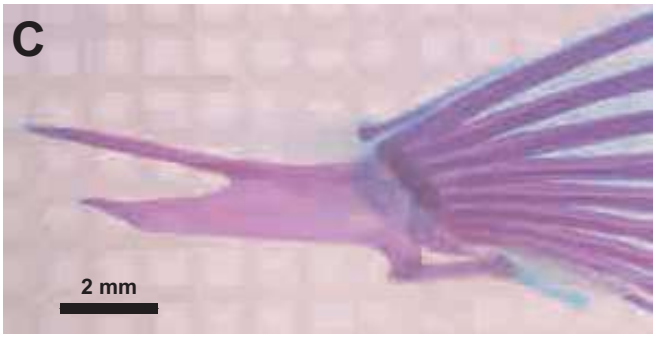
C
2 mm

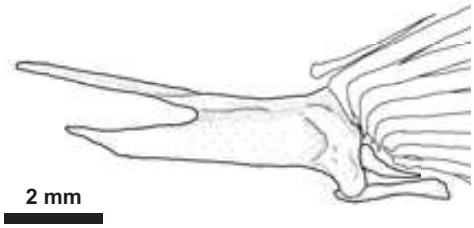
2 mm


D
2 mm

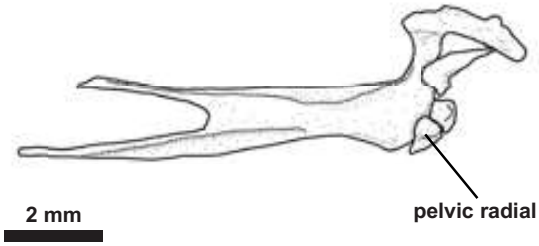
2 mm
pelvic radial

Plate 17-6

A

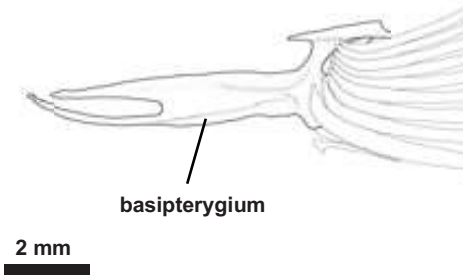

B

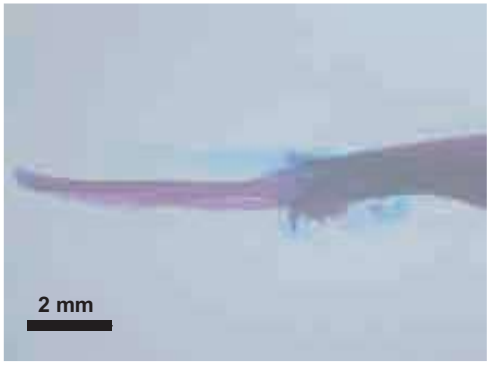

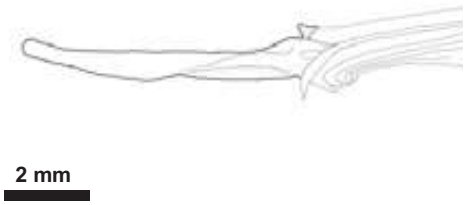

C

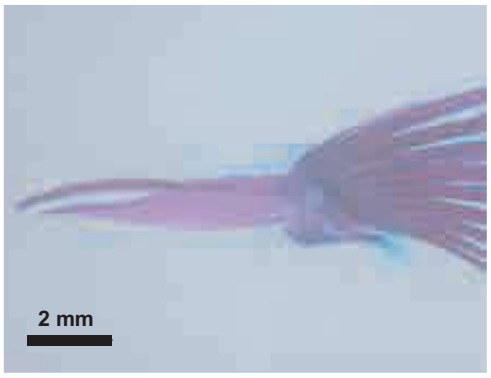

D

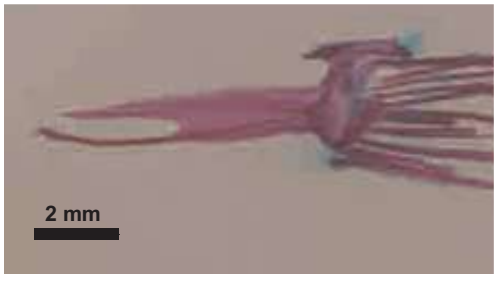

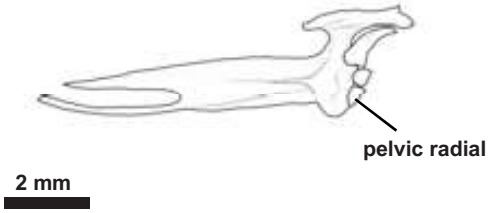

Plate 17-7

A

1 cm

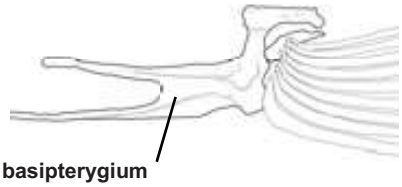

1 cm

B

1 cm

1 cm

C

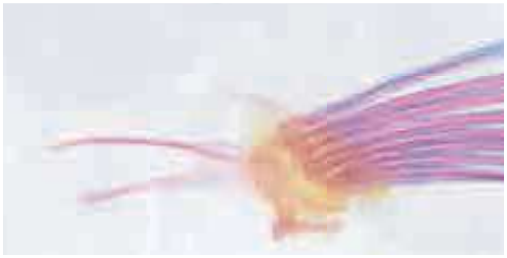

1 cm

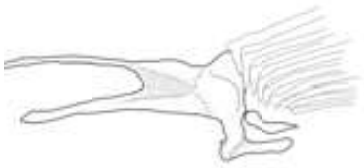

1 cm

D

1 cm

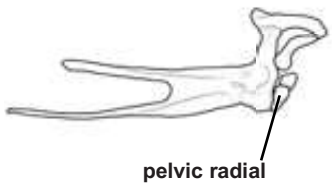

1 cm

Plate 17-8

A

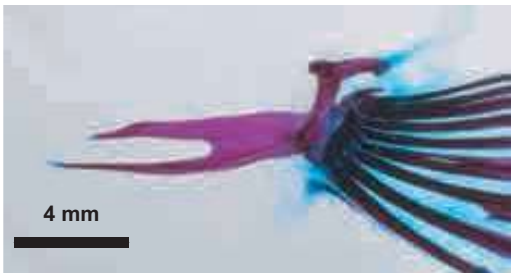

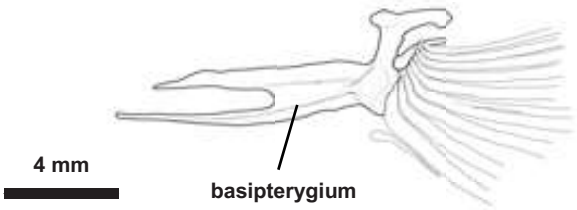

B

C

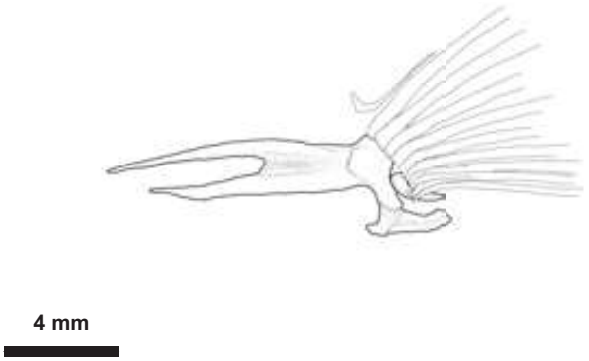

D

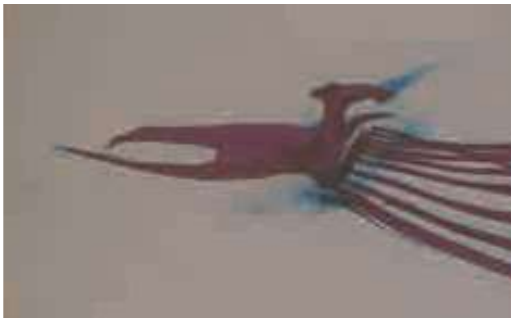

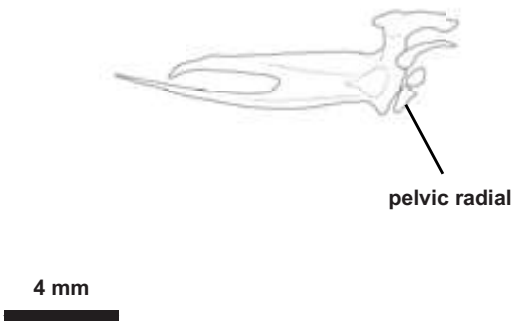

Plate 17-9

A

2 mm

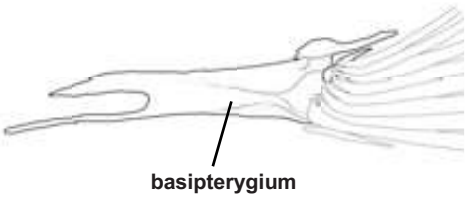

2 mm

B

2 mm

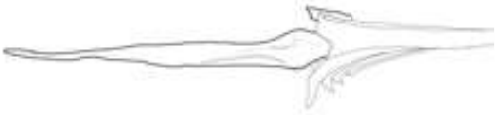

2 mm

C

2 mm

2 mm

D

2 mm

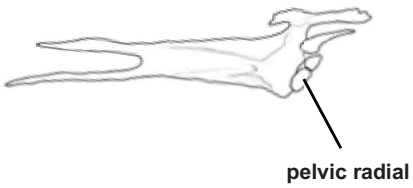

2 mm

早稲田大学　博士（理学）　学位申請　研究業績書

氏 名　　宮田 真也

（2014 年　2 月　現在）

種 類 別	題名、　発表・発行掲載誌名、　発表・発行年月、　連名者（申請者含む）
査読付き論文	○**宮田真也**・籔本美孝・平野弘道, 2011. コイ科魚類オイカワ *Zacco platypus* (Temminck and Schlegel, 1846)の骨学的研究. 北九州市立自然史・歴史博物館研究報告, A 類, (9), 137-155. ○**宮田真也**・籔本美孝・平野弘道, 2012. コイ科魚類タイワンアカハラ *Candidia barbatus* (Regan, 1908)の骨学的研究. 北九州市立自然史・歴史博物館研究報告, A 類, (10), 101-121.
学会発表	○**宮田真也**・籔本美孝・平野弘道, 2010. 日本産コイ科魚類オイカワ、カワムツ、ヌマムツの骨学的研究. 日本魚類学会 2010 年会, 三重文化会館, 津, 2010 年 9 月 23 日（木）～9 月 26 日（日）, 55p（ポスター） ○**宮田真也**・籔本美孝・平野弘道, 2011. コイ科魚類オイカワ属とその近縁種に関する骨学的研究. 日本魚類学会 2011 年会, 弘前大学文京町キャンパス, 弘前市, 2011 年 9 月 29 日（木）-10 月 2 日（日）, 53p.（ポスター） ○**宮田真也**・籔本美孝・平野弘道, 2012. 大分県中部更新統野上層産コイ科オイカワ属魚類化石の再検討. 第 161 回日本古生物学会例会, 群馬県富岡市生涯学習センター, 2012 年 1 月 20 日（金）～1 月 22 日（日）, 57p.（ポスター） **宮田真也**・籔本美孝・中島保寿・佐々木孟智・伊藤泰弘・平野弘道, 2012. 北海道産上部白亜系からのクロッソグナス目魚類 *Apsopelix miyazakii* の第 2 標本とその意義. 2012 年日本古生物学会年会, 名古屋大学, 2012 年 6 月 29 日（金）～ 7 月 1 日（日）, 55p.（ポスター） ○**Shinya Miyata**, Yoshitaka Yabumoto, and Hiromichi Hirano, 2013. Revision of a cyprinid fish, *Zacco* cf. *Zacco temminckii* from the Middle Pleistocene Nogami Formation, Kusu Basin, Oita Prefecture, Kyusyu, Japan. 9th Indo-Pacific Fish Conference 24- 28 June 2013, Okinawa, Japan. Naha, Okinawa, 24-28 June 2013, 198p.（poster） ○**Shinya Miyata**, Yoshitaka Yabumoto, and Hiromichi Hirano, 2013. Comparative study of the Pleistocene cyprinid fish of the genus *Zacco* from the Nogami Formation in Oita Prefecture, Japan and allied Recent taxa. Symposium on Systematics and Diversity of Fishes, National Museum of Nature and Science, Tokyo, July 6, 2013. P- 15.（poster）

早稲田大学　博士（理学）　学位申請　研究業績書

種 類 別	題名、　発表・発行掲載誌名、　発表・発行年月、　連名者（申請者含む）
その他 記事･報告	早稲田大学坪内逍遥博士記念演劇博物館（編），2013,「新耽奇会展―奇想天外コレクション」出品目録. 早稲田大学坪内逍遥博士記念演劇博物館, pp. 31 (分担執筆) **宮田真也**，　2011，G 班 常陸台地の第四系下総層群の層序と堆積システムの時空変化. 日本地質学会 News，14, (11)，19–20 **宮田真也**, 2011, 石油技術協会特別見学会に参加して. 石油技術協会誌, **76**, (6), 570. 中島 光治・宇都宮 正志・**宮田真也**，2010，堆積学スクール OTB2010「未固結変形構造と脱水構造」（2010 年 8 月，千葉）参加報告. 堆積学研究, **69**, (2)，99 – 103. **宮田真也**，2009，石油技術協会特別見学会に参加して. 石油技術協会誌，**74**，(6), 582–583. **宮田真也** 2008，箱根火山巡検に参加して. 日本地質学会 News, **11**, (6), 12.
書籍監修	洋泉社, 2013，地球と人類の 46 億年史 ： 地球創生から生命の進化、文明の誕生、そして現代まで. 洋泉社 MOOK，pp135.（部分監修）